Assessment of Fruit Growth Response to Water Stress in a Super-High-Density Olive Orchard: *monitoring, physiological mechanisms and potential use to schedule irrigation*

Rafael Dreux Miranda Fernandes

2018

TESIS DOCTORAL

Assessment of fruit growth response to water stress in a super-high-density olive orchard: monitoring, physiological mechanisms and potential use to schedule irrigation

Memoria que presenta

Rafael Dreux Miranda Fernandes

Para optar a título de Doctor por la Universidad de Sevilla

Sevilla, 7 de Septiembre 2018

Universidad de Sevilla
Departamento de Cristalografía, Mineralogía y Química Agrícola
Programa de Doctorado Recursos Naturales y Medio Ambiente
Instituto de Recursos Naturales y Agrobiología de Sevilla (IRNAS-CSIC)

Universidad de Sevilla
Departamento de Cristalografía, Mineralogía y Química Agrícola
Programa de Doctorado Recursos Naturales y Medio Ambiente
Tesis Doctoral

Assessment of fruit growth response to water stress in a super-high-density olive orchard: monitoring, physiological mechanisms and potential use to schedule irrigation

Tesis Doctoral presentada por Rafael Dreux Miranda Fernandes, en satisfacción de los requisitos necesários para optar al grado de Doctor en Ingeniería Agronómica, dirigida por Dr. María Victoria Cuevas Sánchez y Dr. Virginia Hernández Santana (Instituto de Recursos Naturales y Agrobiología de Sevilla) y tutorada por María Elena Fernández Boy (Dpto. Cristalografía, Mineralogía y Química Agrícola, Universidad de Sevilla).

LOS DIRECTORES

Dr. María Victoria Cuevas Sánchez

Dr. Virginia Hernández-Santana

EL TUTOR

María Elena Fernández Boy

EL DOCTORANDO

D. Rafael Dreux Miranda Fernandes

University of Seville
Department of Cristallography, Mineralogy and Agricultural Chemistry
Doctoral Program in Natural Resources and Environment
Ph.D. Thesis

Assessment of fruit growth response to water stress in a super-high-density olive orchard: monitoring, physiological mechanisms and potential use to schedule irrigation

Ph.D. Thesis presented by Rafael Dreux Miranda Fernandes to fulfill the necessary requirements of the Doctor of Philosophy degree of Agronomic Engineering under the supervision of Dr. María Victoria Cuevas Sánchez and Dr. Virginia Hernández Santana (Institute of Natural Resources and Agrobiology of Seville) and being advised by María Elena Fernández Boy (Department of Cristallography, Mineralogy and Agricultural Chemistry, University of Seville).

THESIS SUPERVISORS

Dr. María Victoria Cuevas Sánchez

Dr. Virginia Hernández-Santana

THESIS ADVISOR

María Elena Fernández Boy

Ph.D. CANDIDATE

D. Rafael Dreux Miranda Fernandes

FACULTAD DE QUÍMICA
Departamento de Cristalografía, Mineralogía y Química Agrícola

DRA. ISABEL GONZÁLEZ DÍEZ, DIRECTORA DEL PROGRAMA DE DOCTORADO EN RECURSOS NATURALES Y MEDIO AMBIENTE DE LA UNIVERSIDAD DE SEVILLA,

Certifica que la presente Memoria de Investigación titulada "Assessment of fruit growth response to water stress in a super-high-density olive orchard: monitoring, physiological mechanisms and potential use to schedule irrigation", presentada por Rafael Dreux Miranda Fernandes para optar al grado de Doctor por la Universidad de Sevilla, ha sido realizada en el marco del Programa de Doctorado en Recursos Naturales y Medio Ambiente del Departamento de Cristalografía, Mineralogía y Química A-grícola.

En Sevilla, a 7 de Septiembre de 2018.

DOCTOR JOSÉ ENRIQUE FERNÁNDEZ LUQUE, DIRECTOR DEL INSTITUTO DE RECURSOS NATURALES Y AGROBIOLOGÍA DE SEVILLA, DEL CONSEJO SUPERIOR DE INVESTIGACIONES CIENTÍFICAS,

Certifica: que la presente Memoria de Investigación titulada "Assessment of fruit growth response to water stress in a super-high-density olive orchard: monitoring, physiological mechanisms and potential use to schedule irrigation", presentada por Rafael Dreux Miranda Fernandes para optar al grado de Doctor por la Universidad de Sevilla, ha sido realizada en el Instituto de Recursos Naturales y Agrobiología de Sevilla (IRNAS-CSIC), bajo la dirección de las Drs. María Victoria Cuevas Sánchez y Virginia Hernández Santana, reuniendo todas las condiciones exigidas a los trabajos de Tesis Doctoral.

En Sevilla, a 7 de Septiembre de 2018.

LIST OF WORKS DERIVED FROM THIS Ph.D. THESIS

Fernandes, R.D.M., M.V. Cuevas, A. Diaz-Espejo and V. Hernandez-Santana (2018). "Effects of water stress on fruit growth and water relations between fruits and leaves in a hedgerow olive orchard". In: *Agricultural Water Management* 210, pp. 32-40.

Fernandes, R.D.M., M.V. Cuevas, V. Hernandez-Santana, C.M. Rodriguez-Dominguez, C.M. Padilla-Diaz and J.E. Fernández (2017). "Classification models for automatic identification of daily states from leaf turgor related measurements in olive". In: *Computers and Electronics in Agriculture* 142, pp. 181-189.

Hernandez-Santana, V., **R.D.M. Fernandes**, A. Perez-Arcoiza, J.E. Fernández, J.M. García and A. Diaz-Espejo (2018). "Relationships between fruit growth and oil accumulation with simulated seasonal dynamics of leaf gas exchange in the olive tree". In: *Agriculture and Forest Meteorology* 256-257, pp. 458-469.

OTHER WORKS PUBLISHED DURING THIS Ph.D.

Fernandes, R.D.M., J.A. Frizzone, J. Vieira José (2017). "Chicory (*Cichorium intybus* L.) yield under water stress and estimation of leaf area using allometric relations". In: *Australian Journal of Crop Science* 11, pp. 1547-1552.

Fernandes, R.D.M., J. Vieira José, W. Wolff and M.V. Folegatti (2016). "Daily maximum annual rainfall statistical regionalization in Andalusia". In: *X Congreso Internacional de la Asociación Española de Climatología*, Alicante, Spain.

Padilla-Díaz, C.M., **R.D.M. Fernandes**, A. Díaz-Espejo and J.E. Fernándes (2017). "Influence of vapour pressure deficit in leaf turgor pressure measured in olive shoots with and without fruits". In: *XIV MEDECOS & XIII AEET meeting*, Seville, Spain.

Padilla-Díaz, C.M., C.M. Rodriguez-Dominguez, V. Hernandez-Santana, A. Perez-Martin, **R.D.M. Fernandes**, A. Montero, J.M. García and J.E. Fernández (2018). "Water status, gas exchange and crop performance in a super high density olive orchard under deficit irrigation scheduled from leaf turgor measurements". In: *Agricultural Water Management* 202, pp. 241-252.

Wolff, W., S.N. Duarte, O.J. Soccol, L.N. Rodrigues and **R.D.M. Fernandes** (2017). "Methodology for rainwater reservoir dimensioning: a probabilistic approach". In: *Acta Scientiarum Agronomy* 39, pp. 283-289.

"Remember, a good attitude produces good results, a fair attitude fair results, a poor attitude poor results. We each shape our own life, and the shape of it is determined largely by our attitude."

M. Russell Ballard

Acknowledgments

Qué emocionante y al mismo tiempo aterrador es llegar a este momento de escribir los agradecimientos. Hay tanta gente para agradecer, tantos nombres que recordar. ¡A cuántos he conocido por el camino, en estos tres años que estuve en Sevilla, personas que ahora son parte de mi historia, de mi trayectoria hasta este mismo instante! ¡A cuántos tengo que recordar y agradecer entre los que ya no están aquí! ¡Cuánta gente a los que no quiero decir adiós! Y al mismo tiempo ¡cuánta gente he dejado en mi país y que extraño, y quiero verles!

No sé como expresarme muy bien en español, y aún menos al escribir. Me faltan palabras, pero principalmente me falta la traducción de la palabra "saudade". Esta palabra no existe en ningún otro idioma, solamente en portugués, y no hay una palabra o expresión en español que incluya todos los sentidos de la palabra "saudade". Se podría decir que significa "echar de menos" o "extrañar a alguien", pero creo que solamente aquellos que comprenden el significado de esta palabra desde su niñez son los que realmente saben qué es lo que significa. Les pido perdón a los que no hablan portugués, pero en mis agradecimientos usaré la palabra "saudade" para expresarme libremente.

Empiezo agradeciendo a mis directoras de tesis, **María Victoria Cuevas** y **Virginia Hernández Santana**, por la dirección paciente y constructiva que han hecho, al aportar conocimiento metodológico, ideas nuevas y cambios de punto de vista. Le agradezco también a José Enrique Fernández por haberme recibido como alumno de doctorado en el grupo REC, y por las tantas aportaciones en la tesis. Y cómo no agradecerle a **Luciano Mateo** (investigador del Instituto de Agricultura Sostenible – IAS, CSIC), por haberme recomendado a Enrique como alumno de doctorado.

Por todo lo que me han ayudado los componentes del grupo REC les agradezco a **María Dolores** y **Saray** por las incansables mañanas (o días) que han echado para limpiar y escanear las raíces. Agradezco a **Antonio Montero** por el gran trabajo que hace y por la ayuda que me dio tantas veces para medir crecimiento vegetativo, por ayudarme tantas veces en las medidas quincenales y en la cosecha final. Agradezco a **Saray** y a **Alfonso** por las tantas veces que me enseñaron a calibrar y usar el Licor. Agradezco también a **Antonio Díaz Espejo** por las grandes aportaciones metodológicas y por el gran trabajo que hizo para contestar a revisores de revistas científicas. Finalmente, pero no menos importante, le agradezco a **Carmen Padilla Díaz** por haberme enseñado tanto, mediciones con la cámara de Scholander, curvas presión-volumen, y por las veces que me dejó ayudarla en sus mediciones.

Quiero dedicar un apartado especial a las personas que han sufrido tanto o más que yo a lo largo de mi doctorado, y que han hecho posible que yo concluyera esta etapa de mi vida **¡Mis padres!** Gracias por el apoyo, consuelo y guía que han sido para mí

durante toda mi vida. A pesar de muchas veces no comprender lo que digo acerca de la ecofisiología del olivo, habéis sabido escucharme apoyarme y guiarme durante estos últimos tres años. Y por haberme ayudado tanto con lo que yo necesité. ¡Qué saudades tengo de casa! Gracias doy también a mi hermano (**Thomas Dreux**) por los consejos y por el apoyo.

También agradezco a las personas que ya no están aquí, pero que directa o indirectamente me han influenciado, apoyado y ayudado en momentos felices, difíciles y tristes. A mis abuelos, **Djalma Paranhos Miranda, Vera Dreux, Waldemar Martins Fernandes y Maria Del'Graça De Rosis Fernandes**, por el gran ejemplo que fueron para mí, por su perseverancia, buen humor y apoyo a los demás. ¡Cómo tengo saudades de ellos! Saudades de los buenos ratos que hemos vividos juntos.

Agradezco muchísimo a todos que me han ayudado tanto a acercarme más a Dios. Primeramente agradezco a **Jason Allred, Preston Catmull, Paul Earland Urzagaste and Jonathan McGarry**, por haber entrado inesperadamente en mi vida en el año de 2012, presentándome el Libro de Mormón y el Evangelio de Jesucristo. A ellos agradezco por guiarme a la *Iglesia de Jesucristo de los Santos de los Últimos Días*. En Sevilla pude conocer y cultivar grandes amistades, con **Gonzalo Saavedra Pinillos, Daniel Koh, Dante, Daniel García Millán, Silvia Casas, Enrique Escalante, Ismael Escalante** y tantos más. Pude conocer a misioneros consagrados como los Élderes **Hirst, Reseigh, Stewart, Walker, Wilding, Wilkins, Wilson, Mamani, Van Lewuen, Rembacz, Nyland, Bean, Wood, Jenkins, Maldonado, Owens** y tantos más.

Por último, y lo más importante, agradezco a mi *Dios* y a Su Hijo *Jesucristo*. Sé que Ellos viven, reconozco y agradezco Su ayuda y apoyo durante toda mi vida. Sin Su ayuda no podría haber llegado al final de esta tesis.

Contents

List of Figures

List of Tables

CHAPTER 1 - General Introduction.

1.1 Abstract

Olive fruit growth has an important effect on the final yield, and thus, it is important to study its response to water stress, and to know how olive fruits grow under no water restriction. The present PhD. Thesis centered on the fruit growth, and the factors that influence it, such as the root system distribution, the leaf gas exchange and the water relations between fruits and leaves as well as on the utility of continuous measurements of fruit diameter variations. Therefore, in Chapter 2 we assessed the influence of the increment of drip lines (from one to two drip lines per tree row) on the belowground and aboveground vegetative and on the fruit growth, during two irrigation seasons. We also estimated leaf stomatal conductance from sap flux measurements, and simulated photosynthesis (Chapter 3). From the simulated photosynthesis, we compared its accumulated values with growth, both vegetative growth (leaf area and number of internodes in current-year stems) and fruit growth (fruit dry weight and oil content). As fruit growth is not only influenced by photosynthesis, but also by the water relations, we assessed the influence of water stress on the water relations between fruits and leaves, and its influence on fruit growth (Chapter 4). Additionally, we performed pressure-volume curves with olive fruits from well irrigated and deficit irrigated treatments. Finally, we evaluated the usefulness of fruit dendrometers, and the indexes derived from its measurements, to assess tree water status and to schedule irrigation (Chapter 5). The results presented in this PhD. Thesis improve the knowledge on the factors involved in fruit growth and present a first step towards the use of fruit dendrometers in olive trees. Additionally, these results are important for the development of future studies on the olive fruit growth physiology.

1.2 Introduction

1.2.1 Olive production and challenges

Olive trees are cultivated throughout the Mediterranean region, both for table fruit and also for olive oil extraction. The world average harvested area for the 2012-2016 period was equal to 10,322,887 ha, being 47.7% of this area in Europe, and 24.1% in Spain (2,490,381 ha, 2012-2016 average), being the first country in harvested area of the world, according to FAO. Regarding harvested area, Spain is followed by Tunisia (16.5%) and Italy (11.1%). The global olive production is around 1.9 mi tones, being Europe responsible for approximately 60% of it, and Spain for around 31% of the global olive production (FAO, 2015).

For a long time, olive trees were cultivated under rainfed conditions at the Mediter-

ranean region (Fig. 1.1). However, Orgaz and Fereres (2008) have proven that the productivity could be improved with the application of irrigation. Some years ago, traditional or intensive orchards started to be substituted by new orchards with higher tree density per hectare, called super-high-density (SHD) olive orchards or hedgerow olive orchard, with plant densities equal to 1500 trees ha-1 and upwards, aiming olive oil production. This increase in trees density means an increase of leaf and root area by hectare, increasing the need to apply irrigation. The main objective of increasing the tree density per hectare is to increase productivity per hectare and enable the mechanical harvest of olive fruits, reducing costs and time in the harvesting (Fig. 1.2).

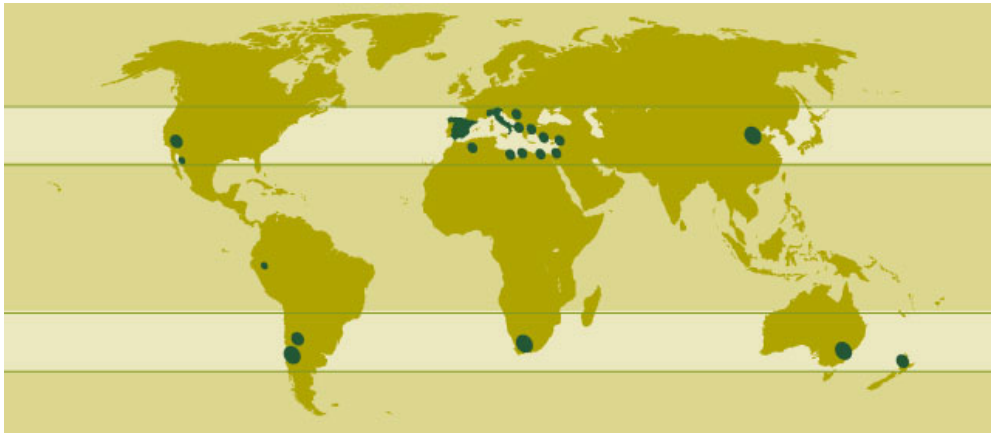

Figure 1.1: The distribution of main regions where olive trees are cultivated. Image taken from http://deoleo.com

Figure 1.2: Super-high-density olive orchard mechanical harvest in the study area (Sanabria orchard).

The perspective of global warming and climate change is increasing the need for good use of high quality water, as the forecast is for the precipitations to decrease and the temperature to increase in the Mediterranean region (Fig. 1.3, IPCC (2014)). This, added

to the fact of higher plant density in the SHD olive orchards, initiated the search for a better irrigation strategy for this kind of olive orchard. In this context, many studies have been performed on the response of olives to deficit irrigation strategies (Fernández et al., 2013; Fernández and Cuevas, 2011; Gómez-del-Campo, 2013; Gucci et al., 2007; Moriana et al., 2003). Some authors consider both sustained deficit irrigation (SDI) and regulated deficit irrigation (RDI) reliable for olive orchards (Iniesta et al., 2009; Moriana et al., 2003; Ramos and Santos, 2009). The SDI strategy comprehends applying a certain percentage of the crop evapotranspiration (ET_C) throughout the period when irrigation is needed. On the other hand, the RDI strategy focus on giving more or less water according to the phenological stage and its respective sensitivity for water stress (Fernández et al., 2013; Fernández et al., 2018c).

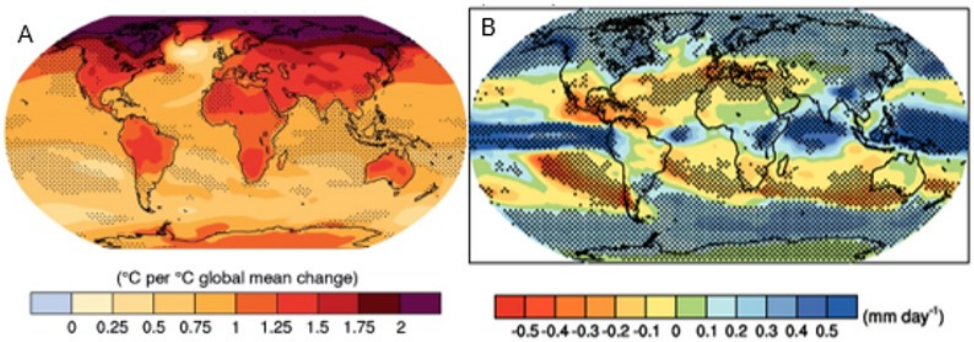

Figure 1.3: Projection of climate change regarding surface temperature (A) and precipitation (B), predictions from 2081 to 2100. Images from International Panel for Climate Change (IPCC, 2014).

The calculations of the irrigation needs (IN), both in the SDI and RDI strategies are usually performed by first calculating the crop evapotranspiration (ET_C) through the parametrized equation recommended by FAO (Allen et al., 1998). However, this method considers a crop coefficient, which should be obtained for every location and crop, which may imply some uncertainties in this coefficient calculation.

1.2.2 Plant-based methods to schedule irrigation

The correct application of RDI strategies can be improved and more precisely through the use of sensors to automatically and continuously monitor changes in water status (Fernández, 2017). These sensors may monitor soil water, atmospheric demand and plant water status, being the last ones advantageous for using the plant as a biosensor, integrating soil water, atmospheric demand and the plant response to the water availability (Fernández, 2017). In the last decade many studies have been published on the use of plant sensors to assess plant water status and the need to increase or decrease irrigation amount (IA).

One of the sensors more evaluated to schedule deficit irrigation are **trunk dendrometers**. Indeed, many researchers have performed experiments on the use of trunk den-

drometry to monitor the daily patterns of micrometric variations in trunk diameter (e.g. Corell et al. (2017), Cuevas et al. (2010), Cuevas et al. (2013), Fernández et al. (2011b), Girón et al. (2015b), and Girón et al. (2015c), using some indexes derived from the trunk dendrometers measurements to assess olive tree water status. Fernández and Cuevas (2010) performed a review of the published articles at the moment on the use of trunk dendrometers and standardized most of these indexes through the graph presented here in Figure 1.4.

Trunk dendrometers and the indexes derived from their measurements are useful to schedule irrigation as they respond early to water stress. However, the maximum daily shrinkage (MDS, Fig. 1.4) in olive trees presents an increase in its values as the leaf water potential (Ψ) decreases to a certain value, after this Ψ value MDS decreases as Ψ continues to decrease (Ortuño et al., 2010). Additional difficulties occur on the data processing and interpretation of these values (Fernández, 2017; Fernández and Cuevas, 2010).

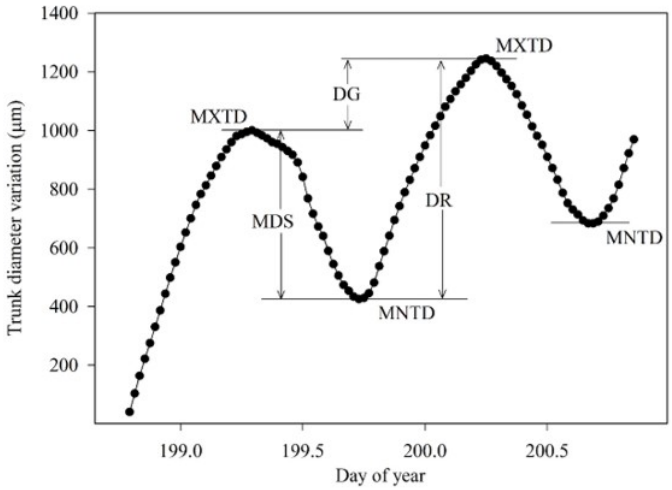

MXTD = maximum trunk diameter

MNTD = minimum trunk diameter

MDS_{DOY} = maximum daily shrinkage = $MXTD_{DOY} - MNTD_{DOY}$

DR_{DOY} = daily recovery = $MXTD_{DOY} - MNTD_{DOY-1}$

DG_{DOY} = daily growth = $MXTD_{DOY+1} - MXTD_{DOY}$

TGR_{DOY} = trunk growth rate = DG for N days = $MXTD_{DOY+1} - MXTD_{DOY-N}$

CG = cumulative growth, for N days = $\sum_{DOY-N}^{DOY} DG$

Figure 1.4: Trunk diameter variation derived indices. The plot data were recorded with an LVDT sensor installed in the trunk of a 37-year-old 'Manzanilla de Sevilla' olive tree. DOY = day of year. After (Fernández and Cuevas, 2010).

Another useful measurement that is possible to automatize is the **sap flux density**, which allows the estimative of the whole plant water consumption. There are three main groups of methods, all of them using heat to estimate sap flux density or sap flow di-

rectly: heat-pulse compensation (Huber, 1932; Marshall, 1958), constant heat (Granier, 1987; Nadezhdina et al., 1998) and heat balance (Daum, 1967). Different authors have used these methods to estimate the water use by olive trees (Moreno et al., 1996; Cuevas et al., 2013; Fernández et al., 2006; Fernández et al., 2012) and tried to use them to schedule irrigation (Fernández et al., 2008a; Fernández et al., 2008b). However, most approaches for scheduling irrigation from sap flow related measurements requires high training for installing and maintaining the system, and considerable data processing (Fernández, 2014a), curtailing their use in commercial orchards.

New approaches, however, opened recently the possibility to a wider use of sap flow-related measurements. This is the case of a new method proposed by (Hernandez-Santana et al., 2016b) to estimate stomatal conductance (g_s) directly from sap flux density (J_s) values normalized by vapor pressure deficit (D). In this approach estimations of g_s are based on the control that stomata exert on transpiration, and thus, on sap flux density (J_s) under conditions of high coupling to the atmosphere, which is the case for olive (Moreno et al., 1996; Tognetti et al., 2009). This approach is sensitive enough to allow the evaluation of the g_s response to the two main driving variables of transpiration under water stress: atmospheric and soil water deficit. Thus, it allows, for the first time, the automated estimation of g_s in olive orchards, which has a great potential to schedule irrigation. Similarly, based on the tight coupling of g_s and photosynthesis (A_N), (López-Bernal et al., 2015) derived an approach to estimate the canopy A_N in olive trees from sap flow related measurements.

Yet under the perspective of a search for better plant sensors and aiming at getting a better knowledge of the water status of individual leaves, Zimmermann et al. (2008) developed a new probe, called **leaf patch clamp pressure probe or LPCP probe**. This probe has been studied thoroughly in olive orchards, mainly after Ehrenberger et al. (2012) and Fernández et al. (2011a) established some leaf turgor states for olive trees, based in the shape of the output pressure retrieved from the LPCP probes (P_p). For example, Padilla-Díaz et al. (2016) and Padilla-Díaz et al. (2018) performed a two-year experiment using the commercial version of the LPCP probes, called ZIM probes. These authors increased or decreased the irrigation amount according to the leaf water state retrieved from the ZIM probes, in periods when olive trees are more sensitive to water stress. This probe has also been studied and validated by Marino et al. (2016), in olive orchards in south Italy. This kind of probe has proven useful for irrigation scheduling, through the use of the leaf turgor states derived from the P_p daily curves. However, little is known about the importance, relevance and significance of the absolute values of P_p and, even with the use of the leaf turgor states to schedule irrigation, at the present moment it is a time-consuming task and requires an experienced user, as its identification is performed visually.

These three sensors mentioned above (trunk dendrometers, sap flux density probes and LPCP probes), among other plant-based sensors, constitute a try to continuously and automatically monitor tree water status. These sensors are normally compared with the widely and traditionally used measurements of leaf water potential (Ψ_{leaf}), daily maximum leaf stomatal conductance (g_s) and daily maximum net photosynthesis rate (A_N) (Fernández, 2017).

All these sensors have advantages and disadvantages as mentioned, but all of them are centered in the tree water status, not taking into account what is most important to the final yield, which is the fruit. Therefore, it would be interesting to study a sensor that could integrate the tree water status and the fruit growth, which could help to predict the yield according to the applied irrigation in the future. A sensor like this would enable us to know when the deficit irrigation is causing a severe reduction in the fruit size and how the fruits respond to an increase in the irrigation dose.

1.2.3 Olive root system and irrigation practices

Since the beginning of the expansion of super-high-density (SHD) olive orchards, the most common irrigation method has been by localized irrigation (Fernández, 2014b), with only one line of drip emitters per row of trees, applying irrigation to one side of the trees (Diaz-Espejo et al., 2012; Fernández et al., 2013; Gómez-del-Campo et al., 2008; Padilla-Díaz et al., 2016; Padilla-Díaz et al., 2018). However, in the work by (Diaz-Espejo et al., 2012), in a SHD olive orchard, simulated results from the use of models (Sperry et al., 2002; Buckley et al., 2003) indicated that the main limitation of water use by olive trees was due to the limited root zone in comparison to the leaf area (Fig. 1.5). In other words, the transpiration was limited by the high leaf-root ratio, being too many transpiring leaves for a small amount of roots absorbing water, imposing a great hydraulic limitation.

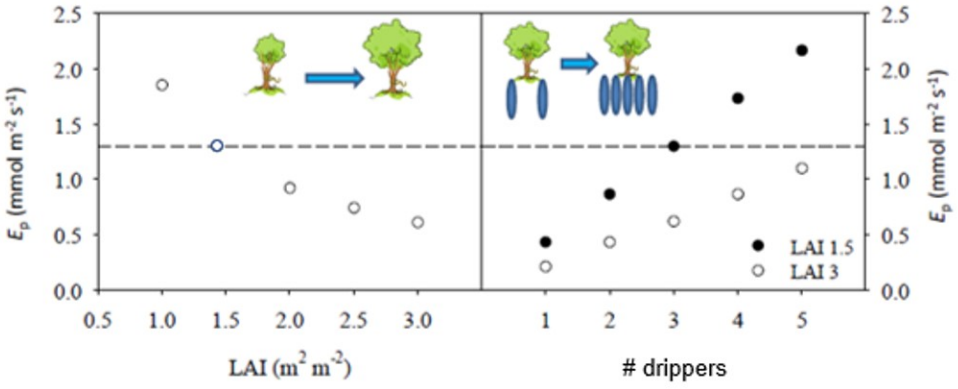

Figure 1.5: Relations between transpiration (E_p) and leaf area index (LAI) and between transpiration and number of drippers per tree. Graph obtained by Diaz-Espejo et al. (2012) by applying the Sperry et al. (2002) model to a super-high-density olive orchard.

A probable explanation for the results obtained by Diaz-Espejo et al. (2012) is the distribution of fine active roots obtained by Fernández et al. (1991) and Searles et al. (2009), which observed greater root length density of these active roots in the wetted soil volume, closer to the drippers for the irrigated olive trees. Contrary to that, rainfed olive trees concentrate their active roots closer to the trunk (<0.6 m) and between 0.15 and 1 m in depth, presenting a greater effort to explore deeper layers of soil, searching for water (Abd el Rahman et al., 1966; Fernández et al., 1991).

Accordingly to Diaz-Espejo et al. (2012), a recent work conducted by Espadafor et al. (2018) assessed the influence of the increase in wetted soil volume on physiological variables and growth of young almond trees. These authors obtained greater plant transpiration and growth when the wetted soil volume increased. In a similar study, Gispert et al. (2013) tested the influence of wetted soil volume on the olive fruit and olive oil production, obtaining higher final yield for the treatment which had a greater soil volume wetted by irrigation.

The works by Fernández et al. (1991), Gispert et al. (2013), and Searles et al. (2009) were performed in olive orchards with trees widely spaced, with tree density lower than 1,000 trees ha^{-1}. However, a relevant study has been recently made public by García-Tejera et al. (2018) on the root distribution of SHD olive orchards under deficit and full irrigation. These authors obtained results that show greater growth of roots with low diameter in the wet bulb when regulated deficit irrigation is applied (García-Tejera et al., 2018). However, we still do not know the influence of increasing the number of drip emitters in the vegetative and fruit growth in super-high-density olive orchards, which could be really useful to avoid transpiration limitation produced by the high leaf-root ratio, according to the hypothesis of Diaz-Espejo et al. (2012) is correct.

The study of the fruit growth and oil accumulation under two irrigation treatments with different distribution of the applied water would be interesting to evaluate if the transpiration limitation mentioned above affect the fruit growth and oil accumulation.

1.2.4 Olive fruit botany and growth

From the botanical point of view, the olive fruit is a drupe, characterized by a thin exocarp, a pulpy mesocarp and a hard, stony endocarp which protects the seed (King, 1938; Rallo and Rapoport, 2001). The endocarp of olive fruit starts to grow from the flower fertilization (ca. May for the northern hemisphere) and grows in size during the next two months (Rapoport, 2008). The mesocarp also starts to develop from the fertilization, but differently from the fruit endocarp which stops growing after two months, it continues to grow until fruit maturation. The mesocarp cells are parenchymatic, little differentiated but with a great growing potential. During the mesocarp development the parenchymatic cells present a great increase in size (Rapoport, 2008). The oil accumula-

tion occurs in the vacuoles of the mesocarp parenchymatic cells (King, 1938). During the first period of the mesocarp growth, which goes from fertilization until 6 to 8 weeks after full bloom (WAFB), both processes of cell division and expansion occur concomitantly. From the 6^{th} to 8^{th} WAFB, the mesocarp growth is only due to cell expansion (Rallo and Rapoport, 2001). Depending on the environmental conditions and specially on the tree water status, this process may be continuous or discontinuous (Rapoport, 2008).

Regarding the growth behavior of olive fruits, Hartmann (1949) and Lavee (1986) described a characteristic drupe double sigmoid growth curve for variables such as fruit diameter, volume, fresh weight and dry weight. The results obtained in the studies performed by Rallo and Rapoport (2001) confirmed this same growing pattern for other variables such as mesocarp width and cell size.

Fruit growth involves biochemical and biophysical processes which lead to increase in fruit fresh and dry weight, depending on the biomass and water accumulation. Xylem and phloem inflows are responsible for accumulation of water, carbohydrates and minerals in the fruits (Morandi et al., 2016). Two features influence the fruit xylem flow, the water potential gradients ($\Delta\Psi$) and the fruit xylem pathway hydraulic conductance (K). Fruits can also loose water by the epidermal transpiration (Greenspan et al., 1996; Morandi et al., 2016) and, theoretically, by xylem backflows (Kozlowski, 1968; Kozlowski, 1972; Jarvis, 1975). Fruit transpiration occurs due to both fruit characteristics (fruit surface conductance, g_c) and the environmental conditions (i.e. vapor pressure deficit – D) (Greenspan et al., 1996).

Regarding the mentioned possibility of xylem backflows from fruits to leaves, it is based in the idea that the fruits may serve as a water reservoir in the tree and would supply water to transpiring leaves during periods of high evaporative demand (Kozlowski, 1968; Kozlowski, 1972; Jarvis, 1975). For the backflow to occur, the water potential gradient between the stem (or leaves) and fruits ($\Delta\Psi_{\text{leaf-fruit}} = \Psi_{\text{leaf}} - \Psi_{\text{fruit}}$) would need to be negative, in other words, leaves presenting more negative Ψ than fruits. However, studies such as the one of Greenspan et al. (1996) challenged this idea, demonstrating that the grape berries presented relevant contraction to when $\Delta\Psi_{\text{leaf-fruit}}$ was positive. These authors hypothesized that this fact could be explained by the xylem inflow being lower than the fruit transpiration rate, causing the fruit contraction. More recently, other works (Higuchi and Sakuratani, 2006; Clearwater et al., 2009; Clearwater et al., 2012) found similar results and hypothesized that back flows only occur as transient morning reversal of flow or under severe water stress.

1.2.5 Fruit diameter variations to assess water status

Other drupes have shown great fruit diameter variations in response to atmospheric variables and irrigation doses (Greenspan et al., 1996; Morandi et al., 2014a), and as

fruit growth is directly associated to the final yield in case of olives, an alternative to assess the plant water status could be the use of **fruit dendrometers** to automatically monitor daily fruit diameter variations (Fig. 1.6). Fruit dendrometers have been used in many experiments to calculate the water and sap flow into and water flow out of the fruits, mainly in fruits with big diameter as in kiwifruit (Morandi et al., 2010a; Torres-Ruiz et al., 2016); apple (Morandi et al., 2011c; Zibordi et al., 2009), pear (Morandi et al., 2014b) and peach (Morandi et al., 2007b; Morandi et al., 2010b; Morandi and Corelli Grappadelli, 2009). The study by Greenspan et al. (1996) was the only one, as far as we know, that performed experiments with the use of fruit dendrometers in small fruits (grape berries) and under water stress conditions.

Figure 1.6: Fruit dendrometer installed in an olive fruit in the study area (Sanabria orchard).

Olive fruits are known to present a thick cuticle, with few stomas in the epidermis (Rapoport, 2008), possibly presenting reduced fruit transpiration. According to the findings reported by Morandi et al. (2016), fruits with high surface conductance tend to be characterized by high xylem conductance. These fruits grow due to the high rates of water exchange through the xylem and transpiration, when transpiration rate is greater than water inflow (sunny hours) fruit shrinkage occurs. On the contrary, fruits with thicker cuticles and consequently lower surface conductance are characterized by low water exchanges by transpiration and by xylem, presenting no fruit daily shrinkage. However, this hypothesis has not yet been assessed in olive.

To the best of our knowledge, the study by Greenspan et al. (1996) was the only one to present concomitant measurements of daily fruit diameter variations and water potential gradient between fruits and stem. However, none of these authors have performed an analysis of the usefulness of the fruit dendrometers to monitor the plant water status

or to schedule irrigation. Monitoring fruit diameter variations could be useful to assess tree water status as it provides valuable information on the water available for the fruit growth. Additionally, there is no record in the literature regarding the daily variations of olive fruit diameter.

1.3 Objectives

The main purpose of this Ph.D. thesis was to study the relationship between olive fruit growth and tree water status, considering the water relations between fruits and leaves and the competition with vegetative growth for photoassimilates and water and to explore the use of fruit diameter variations to assess tree water status and to schedule irrigation. We began with the study of the influence of the increment of wetted soil volume on the vegetative and fruit growth (Chapter 2), we followed with the study of the relationship between photosynthesis rate and fruit growth compared to vegetative growth (Chapter 3) and of the water relations between leaves and fruits (Chapter 4). Finally, we applied all this knowledge to explore the usefulness of fruit dendrometers to assess the plant water stress and to schedule irrigation (Chapter 5). To accomplish these objectives we focused on the following specific objectives:

- To assess the response of vegetative and fruit growth to the increase of the number of drippers per tree in a super-high-density olive orchard (cv. Arbequina). The vegetative growth was measured both aboveground (i.e. leaf area and number of internodes per current year shoots'), and belowground (i.e. root length density per unit volume and root surface area per unit volume).

- To calibrate and validate an approach to simulate AN based on the estimation of g_s from continuous sap flow measurements in olive trees to assess the use of simulated AN to study the fruit growth and the vegetative growth of a super-high-density olive orchard in response to water stress.

- To explore the effect of water relations between leaves and fruits on fruit growth in well-watered and water-stressed olive trees during an entire irrigation season. We performed an experiment with frequent measurements of leaf and fruit water potential at two moments of the day (predawn and midday) and the continuous measurement of fruit diameter with the use of fruit dendrometers.

- To evaluate the fruit dendrometers usefulness to assess water stress and appraising its use to schedule regulated deficit irrigation in olive orchards. Therefore, we compared the fruit dendrometers with other plant sensors (i.e. trunk dendrometers and leaf patch clamp pressure probes) and with traditional measurements of

physiological variables (i.e. midday leaf water potential and daily maximum leaf stomatal conductance).

References

Abd el Rahman, A. A., A.F. Shalaby, and M.S. Balegh (1966). "Water economy of olive under desert conditions". In: *Flora oder Allgemeine botanische Zeitung. Abt. A, Physiologie und Biochemie* 156.2, pp. 202–219. DOI: 10.1016/S0367-1836(17)30254-9.

Allen, R., L. S. Pereira, D. Raes, and M. Smith (1998). *Crop evapotranspiration - Guidelines for computing crop water requirements*. Rome: FAO Irrigation and Drainage, p. 15.

Buckley, T. N., K. A. Mott, and G. D. Farquhar (2003). "A hydromechanical and biochemical model of stomatal conductance". In: *Plant, Cell and Environment* 26.10, pp. 1767–1785. DOI: 10.1046/j.1365-3040.2003.01094.x.

Clearwater, Michael J., Zhiwei Luo, Mariarosaria Mazzeo, and Bartolomeo Dichio (2009). "An external heat pulse method for measurement of sap flow through fruit pedicels, leaf petioles and other small-diameter stems". In: *Plant, Cell and Environment* 32.12, pp. 1652–1663. DOI: 10.1111/j.1365-3040.2009.02026.x.

Clearwater, Michael J., Zhiwei Luo, Sam Eng Chye Ong, Peter Blattmann, and T. Grant Thorp (2012). "Vascular functioning and the water balance of ripening kiwifruit (Actinidia chinensis) berries". In: *Journal of Experimental Botany* 63.5, pp. 1835–1847. DOI: 10.1093/jxb/err352.

Corell, M., M. J. Martín-Palomo, D. Pérez-López, A. Centeno, I. Girón, F. Moreno, A. Torrecillas, and A. Moriana (2017). "Approach for using trunk growth rate (TGR) in the irrigation scheduling of table olive orchards". In: *Agricultural Water Management* 192, pp. 12–20. DOI: 10.1016/j.agwat.2017.06.020.

Cuevas, M.V., J. M. Torres-Ruiz, R. Álvarez, M. D. Jiménez, J. Cuerva, and J.E. Fernández (2010). "Assessment of trunk diameter variation derived indices as water stress indicators in mature olive trees". In: *Agricultural Water Management* 97.9, pp. 1293–1302. DOI: 10.1016/j.agwat.2010.03.011.

Cuevas, M.V., M.J. Martín-Palomo, Antonio Diaz-Espejo, J.M. Torres-Ruiz, C.M. Rodriguez-Dominguez, A. Perez-Martin, R. Pino-Mejías, and J.E. Fernández (2013). "Assessing water stress in a hedgerow olive orchard from sap flow and trunk diameter measurements". In: *Irrigation Science* 31.4, pp. 729–746. DOI: 10.1007/s00271-012-0357-x.

Daum, C. R. (1967). "A Method for Determining Water Transport in Trees". In: *Ecology* 48.3, pp. 425–431. DOI: 10.2307/1932677.

Diaz-Espejo, Antonio, T.N. Buckley, J.S. Sperry, M.V. Cuevas, A. de Cires, S. Elsayed-Farag, M.J. Martin-Palomo, J.L. Muriel, A. Perez-Martin, C.M. Rodriguez-

Dominguez, A.E. Rubio-Casal, J.M. Torres-Ruiz, and J.E. Fernández (2012). "Steps toward an improvement in process-based models of water use by fruit trees: A case study in olive". In: *Agricultural Water Management* 114, pp. 37–49. DOI: 10.1016/j.agwat.2012.06.027.

Ehrenberger, W., S. Rüger, C.M. Rodriguez-Dominguez, Antonio Diaz-Espejo, J.E. Fernández, J. Moreno, D. Zimmermann, V. L. Sukhorukov, and U. Zimmermann (2012). "Leaf patch clamp pressure probe measurements on olive leaves in a nearly turgorless state". In: *Plant Biology* 14.4, pp. 666–674. DOI: 10.1111/j.1438-8677.2011.00545.x.

Espadafor, M., F. Orgaz, L. Testi, I. J. Lorite, O. García-Tejera, F. J. Villalobos, and E. Fereres (2018). "Almond tree response to a change in wetted soil volume under drip irrigation". In: *Agricultural Water Management* 202.September 2017, pp. 57–65. DOI: 10.1016/j.agwat.2018.01.026.

FAO (2015). *FAOSTAT*.

Fernández, J.E. (2014a). "Plant-based sensing to monitor water stress: Applicability to commercial orchards". In: *Agricultural Water Management* 142, pp. 99–109. DOI: 10.1016/j.agwat.2014.04.017.

— (2014b). "Understanding olive adaptation to abiotic stresses as a tool to increase crop performance". In: *Environmental and Experimental Botany* 103, pp. 158–179. DOI: 10.1016/j.envexpbot.2013.12.003.

— (2017). "Plant-Based Methods for Irrigation Scheduling of Woody Crops". In: *Horticulturae* 3.2, p. 35. DOI: 10.3390/horticulturae3020035.

Fernández, J.E. and M.V. Cuevas (2010). "Irrigation scheduling from stem diameter variations: A review". In: *Agricultural and Forest Meteorology* 150.2, pp. 135–151. DOI: 10.1016/j.agrformet.2009.11.006.

— (2011). "Using plant-based indicators to schedule irrigation in olive". In: *Acta Horticulturae* 888, pp. 207–214. DOI: 10.17660/ActaHortic.2011.888.23.

Fernández, J.E., F. Moreno, F. Cabrera, J. L. Arrue, and J. Martín-Aranda (1991). "Drip irrigation, soil characteristics and the root distribution and root activity of olive trees". In: *Plant and Soil* 133.2, pp. 239–251. DOI: 10.1007/BF00009196.

Fernández, J.E., P.J. Durán, M.J. Palomo, Antonio Diaz-Espejo, V. Chamorro, and I. F. Girón (2006). "Calibration of sap flow estimated by the compensation heat pulse method in olive, plum and orange trees: Relationships with xylem anatomy". In: *Tree Physiology* 26.6, pp. 719–728. DOI: 10.1093/treephys/26.6.719.

Fernández, J.E., Antonio Diaz-Espejo, Riccardo D'Andria, Luca Sebastiani, and Roberto Tognetti (2008a). "Potential and limitations of improving olive orchard design and management through modelling". In: *Plant Biosystems* 142.1, pp. 130–137. DOI: 10.1080/11263500701872853.

Fernández, J.E., S.R. Green, H. W. Caspari, Antonio Diaz-Espejo, and M.V. Cuevas (2008b). "The use of sap flow measurements for scheduling irrigation in olive, apple and Asian pear trees and in grapevines". In: *Plant and Soil* 305.1-2, pp. 91–104. DOI: 10.1007/s11104-007-9348-8.

Fernández, J.E., Celia M. Rodriguez-Dominguez, Alfonso Perez-Martin, U. Zimmermann, S. Rüger, M.J. Martín-Palomo, J.M. Torres-Ruiz, M.V. Cuevas, C. Sann, W. Ehrenberger, and Antonio Diaz-Espejo (2011a). "Online-monitoring of tree water stress in a hedgerow olive orchard using the leaf patch clamp pressure probe". In: *Agricultural Water Management* 100.1, pp. 25–35. DOI: 10.1016/j.agwat.2011.08.015.

Fernández, J.E., J.M. Torres-Ruiz, Antonio Diaz-Espejo, Antonio Montero, R. Álvarez, M.D. Jiménez, J. Cuerva, and M.V. Cuevas (2011b). "Use of maximum trunk diameter measurements to detect water stress in mature 'Arbequina' olive trees under deficit irrigation". In: *Agricultural Water Management* 98.12, pp. 1813–1821. DOI: 10.1016/j.agwat.2011.06.011.

Fernández, J.E., M.V. Cuevas, C.M. Rodriguez-Dominguez, A. Perez-Martin, J.M. Torres-Ruiz, S. Elsayed-Farag, Antonio Diaz-Espejo, and M. J. Martín-Palomo (2012). "Sap flow response to olive water stress: A comparative study with trunk diameter variations and leaf turgor pressure". In: *Acta Horticulturae* 951, pp. 101–110.

Fernández, J.E., Alfonso Perez-Martin, José M. Torres-Ruiz, María V. Cuevas, Celia M. Rodriguez-Dominguez, Sheren Elsayed-Farag, Ana Morales-Sillero, José M. García, Virginia Hernandez-Santana, and Antonio Diaz-Espejo (2013). "A regulated deficit irrigation strategy for hedgerow olive orchards with high plant density". In: *Plant and Soil* 372.1-2, pp. 279–295. DOI: 10.1007/s11104-013-1704-2.

Fernández, José E., Antonio Diaz-Espejo, Rafael Romero, Virginia Hernandez-Santana, José M. García, Carmen M. Padilla-Díaz, and María V. Cuevas (2018c). "Precision Irrigation in Olive (Olea europaea L.) Tree Orchards". In: *Water Scarcity and Sustainable Agriculture in Semiarid Environment*. Elsevier, pp. 179–217. DOI: 10.1016/B978-0-12-813164-0.00009-0.

García-Tejera, Omar, Álvaro López-Bernal, Francisco Orgaz, Luca Testi, and Francisco J. Villalobos (2018). "Are olive root systems optimal for deficit irrigation?" In: *European Journal of Agronomy* 99.June, pp. 72–79. DOI: 10.1016/j.eja.2018.06.012.

Girón, I.F., M. Corell, M.J. Martín-Palomo, A. Galindo, A. Torrecillas, F. Moreno, and A. Moriana (2015b). "Feasibility of trunk diameter fluctuations in the scheduling of regulated deficit irrigation for table olive trees without reference trees". In: *Agricultural Water Management* 161, pp. 114–126. DOI: 10.1016/j.agwat.2015.07.014.

— (2015c). "Limitations and usefulness of maximum daily shrinkage (MDS) and trunk growth rate (TGR) indicators in the irrigation scheduling of table olive trees". In: *Agricultural Water Management* 2010. DOI: 10.1016/j.agwat.2015.09.014.

Gispert, J.R., F. Ramírez de Cartagena, J.M. Villar, and J. Girona (2013). "Wet soil volume and strategy effects on drip-irrigated olive trees (cv. 'Arbequina')". In: *Irrigation Science* 31.3, pp. 479–489. DOI: 10.1007/s00271-012-0325-5.

Gómez-del-Campo, María (2013). "Summer deficit-irrigation strategies in a hedgerow olive orchard cv. 'Arbequina': effect on fruit characteristics and yield". In: *Irrigation Science* 31.3, pp. 259–269. DOI: 10.1007/s00271-011-0299-8.

Gómez-del-Campo, María, A. Leal, and C. Pezuela (2008). "Relationship of stem water potential and leaf conductance to vegetative growth of young olive trees in a hedgerow orchard". In: *Australian Journal of Agricultural Research* 59.3, p. 270. DOI: 10.1071/AR07200.

Granier, A. (1987). "Evaluation of transpiration in a Douglas-fir stand by means of sap flow measurements". In: *Tree Physiology* 3.4, pp. 309–320. DOI: 10.1093/treephys/3.4.309.

Greenspan, Mark D., Hans R. Schultz, and Mark A. Matthews (1996). "Field evaluation of water transport in grape berries during water deficits". In: *Physiologia Plantarum* 97, pp. 55–62.

Gucci, R., E. Lodolini, and H. F. Rapoport (2007). "Productivity of olive trees with different water status and crop load". In: *Journal of Horticultural Science and Biotechnology* 82.4, pp. 648–656.

Hartmann, H. T. (1949). "Growth of the olive fruit". In: *American Society Horticultural Science* 54, pp. 86–94.

Hernandez-Santana, Virginia, J.E. Fernández, Celia M. Rodriguez-Dominguez, R. Romero, and Antonio Diaz-Espejo (2016b). "The dynamics of radial sap flux density reflects changes in stomatal conductance in response to soil and air water deficit". In: *Agricultural and Forest Meteorology* 218-219, pp. 92–101. DOI: 10.1016/j.agrformet.2015.11.013.

Higuchi, Hirokazu and Tetsuo Sakuratani (2006). "Water Dynamics in Mango (Mangifera indica L.) Fruit during the Young and Mature Fruit Seasons as Measured by the Stem Heat Balance Method". In: *Journal of the Japanese Society for Horticultural Science* 75.1, pp. 11–19. DOI: 10.2503/jjshs.75.11.

Huber, Bruno (1932). "Beobachtung und Messung pflanzlicher saftstrome". In: *Ber. deutsch. Bot. Ges.* 50, pp. 89–109.

Iniesta, F., L. Testi, F. Orgaz, and F. J. Villalobos (2009). "The effects of regulated and continuous deficit irrigation on the water use, growth and yield of olive trees". In: *European Journal of Agronomy* 30.4, pp. 258–265. DOI: 10.1016/j.eja.2008.12.004.

IPCC (2014). *Climate Change 2014: Synthesis Report. Contribution of Working Groups I, II and III to the Fifth Assessment Report of the Intergovernmental Panel on Climate Change*. Ed.

by Core Writing Team, R.K. Pachauri, and L.A. Meyer. Geneva, Switzerland: IPCC, p. 151.

Jarvis, P.G. (1975). "Water transfer in plants". In: *Heat and Mass Transfer in the Environment of Vegetation*. Ed. by D.A. de Vries. Washington, DC: Scripta, pp. 369–394.

King, J. R. (1938). "Morphological development of the fruit of the olive". In: *Hilgardia* 11.8, pp. 343–424.

Kozlowski, T. T. (1968). "Diurnal Changes in Diameters of Fruits and Tree Stems of Montmorency Cherry". In: *Journal of Horticultural Science* 43.1, pp. 1–15. DOI: 10.1080/00221589.1968.11514227.

Kozlowski, T.T. (1972). "Shrinking and swelling of plant tissues". In: *Plant Responses and Control of Water Balance*. Elsevier. Chap. 1, pp. 1–64. DOI: 10.1016/B978-0-12-424153-4.50007-2.

Lavee, Shimon (1986). "Olive". In: *Handbook of fruit set and development*. Ed. by S. P. Monselise. 1st. Boca Raton, Florida, USA: CRC Press Inc., pp. 261–276.

López-Bernal, Álvaro, Omar García-Tejera, Victorino A. Vega, Juan C. Hidalgo, Luca Testi, Francisco Orgaz, and Francisco J. Villalobos (2015). "Using sap flow measurements to estimate net assimilation in olive trees under different irrigation regimes". In: *Irrigation Science* 33.5, pp. 357–366. DOI: 10.1007/s00271-015-0471-7.

Marino, Giulia, Fulvio Pernice, Francesco Paolo Marra, and Tiziano Caruso (2016). "Validation of an online system for the continuous monitoring of tree water status for sustainable irrigation managements in olive (Olea europaea L.)" In: *Agricultural Water Management* 177, pp. 298–307. DOI: 10.1016/j.agwat.2016.08.010.

Marshall, D. C. (1958). "Measurement of Sap Flow in Conifers by Heat Transport". In: *Plant Physiology* 33.6, pp. 385–396.

Morandi, Brunella and L. Corelli Grappadelli (2009). "Source and sink limitations in vascular flows in peach fruit". In: *The Journal of Horticultural Science and Biotechnology* 84.6, pp. 150–156. DOI: 10.1080/14620316.2009.11512613.

Morandi, Brunella, Mark Rieger, and Luca Corelli-Grappadelli (2007b). "Vascular flows and transpiration affect peach (Prunus persica Batsch.) fruit daily growth". In: *Journal of Experimental Botany* 58.14, pp. 3941–3947. DOI: 10.1093/jxb/erm248.

Morandi, Brunella, Luigi Manfrini, Pasquale Losciale, Marco Zibordi, and Luca Corelli Grappadelli (2010a). "Changes in vascular and transpiration flows affect the seasonal and daily growth of kiwifruit (Actinidia deliciosa) berry". In: *Annals of Botany* 105.6, pp. 913–923. DOI: 10.1093/aob/mcq070.

Morandi, Brunella, Luigi Manfrini, Pasquale Losciale, Marco Zibordi, and Luca Corelli-Grappadelli (2010b). "The positive effect of skin transpiration in peach fruit growth". In: *Journal of Plant Physiology* 167.13, pp. 1033–1037. DOI: 10.1016/j.jplph.2010.02.015.

Morandi, Brunella, Marco Zibordi, Pasquale Losciale, Luigi Manfrini, Emanuele Pierpaoli, and Luca Corelli-Grappadelli (2011c). "Shading decreases the growth rate of young apple fruit by reducing their phloem import". In: *Scientia Horticulturae* 127.3, pp. 347–352. DOI: 10.1016/j.scienta.2010.11.002.

Morandi, Brunella, Pasquale Losciale, Luigi Manfrini, Marco Zibordi, Stefano Anconelli, Fabio Galli, Emanuele Pierpaoli, and Luca Corelli Grappadelli (2014a). "Increasing water stress negatively affects pear fruit growth by reducing first its xylem and then its phloem inflow". In: *Journal of Plant Physiology* 171.16, pp. 1500–1509. DOI: 10.1016/j.jplph.2014.07.005.

Morandi, Brunella, Pasquale Losciale, Luigi Manfrini, Marco Zibordi, Stefano Anconelli, Emanuele Pierpaoli, and Luca Corelli Grappadelli (2014b). "Leaf gas exchanges and water relations affect the daily patterns of fruit growth and vascular flows in Abbé Fétel pear (Pyrus communis L.) trees". In: *Scientia Horticulturae* 178, pp. 106–113. DOI: 10.1016/j.scienta.2014.08.009.

Morandi, Brunella, Luigi Manfrini, Marco Zibordi, Luca Corelli-Grappadelli, and Pasquale Losciale (2016). "From fruit anatomical features to fruit growth strategy: is there a relationship?" In: *Acta Horticulturae* 1130.1130, pp. 185–192. DOI: 10.17660/ActaHortic.2016.1130.27.

Moreno, Félix, J.E. Fernández, Brent E. Clothier, and Steven R. Green (1996). "Transpiration and root water uptake by olive trees". In: *Plant and Soil* 184.1, pp. 85–96. DOI: 10.1007/BF00029277.

Moriana, Alfonso, Francisco Orgaz, Miguel Pastor, and Elias Fereres (2003). "Yield responses of a mature olive orchard to water deficits". In: *Journal of the American Society for Horticultural Science* 128.3, pp. 425–431.

Nadezhdina, N., J. Cemark, and V. Nadezhdin (1998). "Heat field deformation method for sap flow measurements". In: *Measuring sap flow in intact plants. Proceedings of 4th International Workshop*. Židlochovice, Czech Republic: IUFRO Publ. Brno, Czech Republic: Mendel University, pp. 72–92.

Orgaz, Francisco and Elías Fereres (2008). "Riego". In: *El cultivo del olivo*. Ed. by D. Barranco, R Fernández-Escobar, and L. Rallo. 6th. Coedition Mundi-Prensa and Junta de Andalucía, pp. 337–362.

Ortuño, M. F., W. Conejero, F. Moreno, A. Moriana, D. S. Intrigliolo, C. Biel, C. D. Mellisho, A. Pérez-Pastor, R. Domingo, M. C. Ruiz-Sánchez, J. Casadesus, J. Bonany, and A. Torrecillas (2010). "Could trunk diameter sensors be used in woody crops for irrigation scheduling? A review of current knowledge and future perspectives". In: *Agricultural Water Management* 97.1, pp. 1–11. DOI: 10.1016/j.agwat.2009.09.008.

Padilla-Díaz, Carmen M., Celia M. Rodriguez-Dominguez, Virginia Hernandez-Santana, Alfonso Perez-Martin, Rafael D.M. Fernandes, Antonio Montero, J.M. García, and J.E.

Fernández (2018). "Water status, gas exchange and crop performance in a super high density olive orchard under deficit irrigation scheduled from leaf turgor measurements". In: *Agricultural Water Management* 202.January, pp. 241–252. DOI: 10.1016/j.agwat.2018.01.011.

Padilla-Díaz, C.M., Celia M. Rodriguez-Dominguez, Virginia Hernandez-Santana, Alfonso Perez-Martin, and J.E. Fernández (2016). "Scheduling regulated deficit irrigation in a hedgerow olive orchard from leaf turgor pressure related measurements". In: *Agricultural Water Management* 164, pp. 28–37. DOI: 10.1016/j.agwat.2015.08.002.

Rallo, Pilar and Hava Rapoport (2001). "Early growth and development of the olive fruit mesocarp". In: *The Journal of Horticultural Science and Biotechnology* 76.4, pp. 408–412. DOI: 10.1080/14620316.2001.11511385.

Ramos, Alice F. and Francisco L. Santos (2009). "Water use, transpiration, and crop coefficients for olives (cv. Cordovil), grown in orchards in Southern Portugal". In: *Biosystems Engineering* 102.3, pp. 321–333. DOI: 10.1016/j.biosystemseng.2008.12.006.

Rapoport, Hava F (2008). "Botánica y morfología". In: *El cultivo del olivo*. Ed. by D. Barranco. 6th. Mundi-Prensa. Chap. 2, pp. 37–62.

Searles, Peter S., Diego A. Saravia, and M. Cecilia Rousseaux (2009). "Root length density and soil water distribution in drip-irrigated olive orchards in Argentina under arid conditions". In: *Crop and Pasture Science* 60.3, p. 280. DOI: 10.1071/CP08135.

Sperry, J. S., U. G. Hacke, R. Oren, and J. P. Comstock (2002). "Water deficits and hydraulic limits to leaf water supply". In: *Plant, Cell and Environment* 25.2, pp. 251–263. DOI: 10.1046/j.0016-8025.2001.00799.x.

Tognetti, Roberto, Alessio Giovannelli, Antonella Lavini, Giovanni Morelli, Fulvio Fragnito, and Riccardo D'Andria (2009). "Assessing environmental controls over conductances through the soil-plant-atmosphere continuum in an experimental olive tree plantation of southern Italy". In: *Agricultural and Forest Meteorology* 149.8, pp. 1229–1243. DOI: 10.1016/j.agrformet.2009.02.008.

Torres-Ruiz, José M., Giulio Demetrio Perulli, Luigi Manfrini, Marco Zibordi, Gerardo Lopez Velascoo, Stefano Anconelli, Emanuele Pierpaoli, Luca Corelli-Grappadelli, and Brunella Morandi (2016). "Time of irrigation affects vine water relations and the daily patterns of leaf gas exchanges and vascular flows to kiwifruit (Actinidia deliciosa Chev.)" In: *Agricultural Water Management* 166, pp. 101–110. DOI: 10.1016/j.agwat.2015.12.012.

Zibordi, Marco, Sara Domingos, and Luca Corelli Grappadelli (2009). "Thinning apples via shading: an appraisal under field conditions". In: *The Journal of Horticultural Science and Biotechnology* 84.6, pp. 138–144. DOI: 10.1080/14620316.2009.11512611.

Zimmermann, D., R. Reuss, M. Westhoff, P. Geßner, W. Bauer, E. Bamberg, F. W. Bentrup, and U. Zimmermann (2008). "A novel, non-invasive, online-monitoring, versatile and easy plant-based probe for measuring leaf water status". In: *Journal of Experimental Botany* 59.11, pp. 3157–3167. DOI: 10.1093/jxb/ern171.

CHAPTER 2

Response of vegetative and fruit growth to the soil volume affected by irrigation in a super-high-density olive orchard.

Abstract

Olive root growth is known to be greatly influenced by the soil volume wetted by irrigation. We studied the effect of one (1L) and two (2L) drip line per tree row on root, vegetative and fruit growth, and tree water status, under full and deficit irrigation, for two years. Greater root length density and root surface area per unit volume were obtained close to the new wetted soil volume (2L treatments), mainly in the deficit irrigated treatment. This greater root growth closer to the new drip line influenced somewhat the physiological variables related to water status (leaf water potential at predawn and midday and daily maximum leaf stomatal conductance), the two drip line deficit irrigated treatment presented slightly better water status in comparison to the one drip line deficit irrigated treatment. Aboveground vegetative growth during 2017 irrigation season was greatly influenced by the new drip line in the two drip line deficit irrigated treatment, both for leaf area and current-year shoots' number of internodes. Our data also revealed greater influence of the irrigation treatments on vegetative growth than on fruit growth, mainly fruit dry weight, which presented statistically similar results for all irrigation treatments for the great majority of the irrigation seasons. This confirms that the fruits are a priority to the trees, even during water stressed periods. Unfortunately, our data on olive fruit and virgin olive oil yield presented great variability, within and between the experimental plots.

2.1 Introduction

Hedgerow olive orchards with plant densities over 1500 trees ha^{-1}, also called super-high-density (SHD) orchards, are becoming increasingly popular (Rius and Lacarte, 2010). This is explained by this management system being among the most profitable ones for olive production. SHD orchards, however, are technically demanding and, in most cases, require irrigation. More precisely, and both because of the low water availability in olive growing areas and the need to avoid excessive growth, deficit irrigation strategies are often the best option in SHD olive orchards. Concerning the irrigation system, those with one line of drippers per tree row are commonly used in SHD olive orchards (Diaz-Espejo et al., 2012; Fernández et al., 2013; Gómez-del-Campo et al., 2008; Padilla-Díaz et al., 2016; Padilla-Díaz et al., 2018). However, in the study performed by (Diaz-Espejo et al., 2012), in which the mechanistic models of Buckley et al. (2003) and of Sperry et al. (2002) were used to assess the performance of main physiological traits, results led to the conclusion that a reduced root zone volume wetted by irrigation can highly limit transpiration in SHD olive orchards. These authors concluded, in fact, that the low root to leaf ratio determined both by the high plant density and by the localized irrigation,

imposed a large hydraulic limitation to transpiration.

Root distribution has been studied in main woody crops, such as apple (Sokalska et al., 2009), avocado (Michelakis et al., 1993) and grapevine (Stevens and Douglas, 1994), among others. In olive, just a few studies are found in the literature on the relation between irrigation and root distribution (Deng et al., 2017; Fernández, 2017; Searles et al., 2009), and a fraction only refers to SHD olive orchards (Diaz-Espejo et al., 2012; García-Tejera et al., 2018). Fernández et al. (1991) performed a study on the root distribution of mature 'Manzanilla de Sevilla' trees planted at 7 x 7 m. Two orchards were considered, one irrigated from orchard planting and the other from 12 years after planting. Drip irrigation was applied in both cases. These authors demonstrated that root distribution was highly dependent on both the location of the drippers and on adaptive traits of the species to drought. For instance, the high concentration of young, active roots near the trunk, which are effective for taking up the rainfall water collected by the canopy (Gómez et al., 2001), persisted even after eight years of irrigation. Regarding the wetted soil volume by irrigation, (Searles et al., 2009), studied the root distribution in 'Manzanilla fina' and 'Manzanilla reina' olive orchards in Argentina, with 312 and 250 trees ha^{-1}, and with two and four drippers per tree. They found greater root length in the trees irrigated with four drippers, as compared to those with two drippers only. Pastor et al. (2005) irrigated mature 'Picual' olive trees with the same amount of water but with increasing number of drippers, which resulted on increasing fractions of the root zone wetted by irrigation. They found that yield increased with increasingly wetted soil volumes. This agrees with results reported by Gispert et al. (2013) for 'Arbequina' trees. Recently, Espadafor et al. (2018) conducted a work in which the influence of the increased wetted soil volume on physiological aspects and growth of young almond trees was assessed. They reported greater growth and plant transpiration when the wetted volume increased. Modeling exercises, such as that made by García-Tejera et al. (2017a), have confirmed that transpiration of drip-irrigated olive trees is likely to be limited by a reduced fraction of the soil volume wetted by irrigation, and added that the degree of such limitation depends on the atmospheric demand and the ratio of root area vs. leaf area. García-Tejera et al. (2018) performed root samplings with augers in a 'Arbequina' SHD olive orchard (1667 trees ha^{-1}) with trees under full irrigation and under regulated deficit irrigation (RDI). Their results show that the reduction of irrigation volume in RDI induced a change in the root growing pattern, promoting root elongation in the alley between tree rows. Their simulation exercises indicated that the root system of trees under deficit irrigation shows an active response to the water patches created by the drippers, leading to an increase in photosynthetic assimilation (A_N), particularly when the available water in the soil is low.

Based on the findings reported above, we hypothesized that, for the same irrigation

amounts, an increase in the soil volume wetted by irrigation determined by a greater number of drippers per tree, will increase the root zone volume and the root length and total root surface area per tree. As a consequence, this improvement in water uptake conditions would improve the tree water status, with a positive impact on growth and production. To the best of our knowledge, no previous studies have been performed in SHD olive orchards on the increase of drip emitters per tree and its influence on vegetative and fruit growth. Thus, the main objective of this study was to assess the impact on tree performance of installing a second irrigation line per tree row in a SHD 'Arbequina' orchard. More precisely, we worked with two irrigation strategies, full irrigation and regulated deficit irrigation. In both cases we used one (1L) and two single dripper lines (2L) per tree row. For the 2L trees each irrigation event lasted half of the time, for keeping the same irrigation amounts in all trees of each irrigation strategy. We analyzed the effect of each irrigation treatment on leaf water potential and stomatal conductance, as well as on root growth, canopy growth and fruit growth. Root growth was assessed from root length and root surface area measurements, while the number of internodes of current-year shoots and leaf area measurements were used to assess canopy growth. Fruit growth was assessed from fruit dry weight, fruit volume and water content measurements.

2.2 Material and Methods

2.2.1 Experimental orchard and irrigation treatments

The experiments were performed in a super-high-density (SHD) olive orchard (Olea europaea L., cv. Arbequina) at 25 km to the south-east of Seville, Spain (37°15′ N, −5°48′ W, 60 m a.s.l.). Measurements were made mainly in the irrigation season of 2016 (from June 4th, day of the year –DOY– 156, to November 3rd, DOY 308) and 2017 (from May 31st, DOY 151, to October 25th, DOY 298). The orchard, which was 10-year-old in 2016, had 'Arbequina" trees at 4.5 m x 1.5 m (1667 trees ha^{-1}), planted at the top of 0.4 m high ridges with a N-NE to S-SW orientation. The average annual precipitation (P) and potential evapotranspiration (ET_o) in the area were 516.4 mm and 1528.5 mm, respectively (period 2002-2017). Meteorological variables were recorded by a Campbell weather station (Campbell Scientific Ltd., Shepshed, UK) located in the center of the area covered by the experimental plots, with the meteorological sensors located above the canopies. The station recorded 30 min average radiation (R_s), air temperature (T_{air}), relative humidity (RH) of the air, and total P. The air vapor pressure deficit (D) was derived from the recorded T_{air} and RH values.

In 2016 we had two full irrigation treatments (control treatments) aimed to supply 100% of the irrigation needs (IN). The difference between both treatments is that in one

of them (treatment 100C-1L) we used one drip line per tree row with a 2 $L\,h^{-1}$ dripper every 0.5 m, next to the tree trunks, while in the other one (treatment 100C-2L) we used two drip lines per tree row, one on each side of the trunks and separated 0.5 m. With that distance, and according to the study on hydraulic characteristics of the soil orchard made by Egea et al. (2016), the wetted soil volume per tree was about double in 100C-2L than in 100C-1L. We also had two sustained deficit irrigation (SDI) treatments, aimed to supply 45% of the irrigation needs throughout the irrigation period. As in the control treatments, we had trees with one drip line (treatment 45SDI-1L) and with two drip lines (treatment 45SDI-2L). In the 2L plots, the irrigation time was scheduled to be half of that in the 1L plots, so that the trees received the same volume of water despite having double number of drippers. In all treatments irrigation was applied daily, from the beginning (DOY 156) to the end of the irrigation season (DOY 308). The irrigation needs were calculated on a daily basis as IN = ET_c - P_e, with ET_c being the potential crop evapotranspiration calculated with the single crop coefficient approach (Allen et al., 1998), and P_e the effective precipitation which, according to Orgaz and Fereres (2008), was assumed to be 75% of the precipitation recorded in the orchard. For the calculation of ET_c we used values of the drop coefficient adjusted for the orchard, and meteorological records from a nearby standard weather station belonging to the network of agroclimatic weather stations of the local government. This approach to calculate ET_c has proven satisfactory, as reported elsewhere (Diaz-Espejo et al., 2012; Fernández et al., 2013; Egea et al., 2016). An irrigation controller (Agronic 2000, Sistemes Electrònics PROGRÉS,S.A., Lleida, Spain) was used to apply the calculated irrigation amounts (IA). The second line of drippers of the 2L treatments was installed on May 17th, 2016. Both in 2016 and 2017, we used a complete randomized design, with four plots (replicates) per treatment. Each plot consisted of 8 central trees surrounded by 16 border trees.

In 2017 we also had two full irrigation treatments, 100C-1L and 100C-2L, with the same design and management than in 2016. In this second experimental year, however, the irrigation needs were calculated daily from a simplified version of the stomatal conductance (g_s) model tested for the orchard conditions by Diaz-Espejo et al. (2012). Our soil water measurements (Section 2.2) confirmed that in the 100C-1L and 100C-2L trees, irrigation amounts were enough to keep the soil volumes wetted by irrigation close to field capacity conditions all along the irrigation season (from DOY 151 to DOY 298). Under these non-limiting soil water conditions and according to the model evaluated by Diaz-Espejo et al. (2012), g_s is a function of D, R_s and tree leaf area. Vapor pressure deficit hourly values were predicted for the three following days according to the weather forecast for the studied area provided by Meteogrid (Madrid, Spain). Tree leaf area was estimated as described in Section 2.4. The percentage of sunny to total leaf area, estimated after Diaz-Espejo et al. (2002) and Fernández et al. (2008b), was assumed to

be 0.35. Assuming a perfect coupling between canopy and atmosphere (the olive tree has small leaves), tree water consumption (E_p) was calculated as $E_p = D \cdot (g_{s,sun} \cdot A_{sun} + g_{s,shade} \cdot A_{shade})$, where D is the vapour pressure deficit, $g_{s,sun}$ and $g_{s,shade}$ are stomatal conductance of new, sun-exposed leaves and old, shaded leaves, respectively; A_{sun} and A_{shade} are the corresponding leaf areas of sun and shade leaves, respectively. Soil evaporation (E_s) was estimated according to Orgaz et al. (2006). Finally, the irrigation requirements (IN) were estimated as $E_p + E_s$ (see Fernandes et al. (2018), for further details). In addition to the control treatments, in 2017 we had two regulated deficit irrigation (RDI) treatments, aimed to supply a total amount of water in the whole irrigation period equal to 45% of IN. The RDI treatments, named 45RDI-1L and 45RDI-2L, received the same amounts of water but supplied with one or two drip lines, respectively, as described for the 2016 treatments. A main difference between the SDI strategy applied in 2016 and the RDI strategy applied in 2017 is that, in the latter, both the irrigation dose and the frequency of irrigation changed depending on the phenological stages. More precisely, we applied the 45RDI strategy first described in Fernández et al. (2013) and perfectioned by Fernández (2017). Basically, the 45RDI strategy consisted on applying daily irrigation to replace the crop water needs in the so-called period 1 (from the last stages of floral development to full bloom; second fortnight of April, in our case), period 2 (from the 6 to the 10 weeks after bloom; June) and period 3 (three weeks prior to ripening, after the midsummer period of high atmospheric demand; from late August to mid-September). For the rest of the time, just one to three irrigation events per week were applied. In our case, in the periods 1, 2 and 3 the 45RDI trees were irrigated daily to supply approximately 80% of the IN. Between periods 2 and 3 (from DOY 185 to 238), irrigation was applied twice per week only, amounting to a total of ca. 20% IN for that period. From the end of period 3 to harvesting (DOY 262 to 308) we applied two or three irrigation events per week, supplying a total of some 40% of IN.

2.2.2 Soil water status

We assessed the soil volumetric water content (θ, $m^3\ m^{-3}$) with a Profile probe (Delta-T Devices Ltd., Cambridge, UK) calibrated in situ (Fernández and Cuevas, 2011) and two access tubes in each plot, at 0.1 and 0.4 m from the drippers and at 0.5 m from the tree trunk. We measured 1-2 times per week, all throughout the irrigation seasons, and occasionally from a couple of months before the irrigation seasons. Measurements were performed at the time of maximum g_s (ca. 9.00 GMT), at the depths of 0.1, 0.2, 0.3, 0.4, 0.6 and 1.0 m. Since the maximum rooting depth in the orchard was 0.4 m (Diaz-Espejo et al., 2012), for the calculations of average θ for each treatment we used θ records from 0.1 to 0.4 m only. Those were weighted by the percentage of roots, and then a simple average of the averages obtained for each plot.

2.2.3 Root growth

Roots were sampled with a soil sampling auger of 8 cm of diameter and 10 cm of length (502.6 cm^3). Soils samples were taken at the beginning of the 2016 irrigation season (May-June) and again in February-March 2017, before the start of the irrigation season. In 2016 the samples were taken from one plot per treatment only, until the depth of 40 cm. In 2017 we sampled three plots per treatment. Both in 2016 and 2017, the samples were taken at two locations in the 1L treatments, close to the only drip line (In1) and at 0.4 m from the drip line (Out). For the 2L treatments, samples were taken at three locations, close to the original drip line (In1), close to the additional drip line (In2) and at 0.4 m from the drip lines (Out).

The soil samples were washed out in the laboratory and the roots separated from the soil with the use of sieves of different sizes. They were then separated into roots of diameter $\varnothing$<2 mm and $\varnothing$>2 mm. From the group of roots thinner than 2 mm, roots were randomly sampled and scanned with a regular office scanner, and the image treated with the WinRHIZO system (Regent Instruments, Québec, Canada). From these images, we assessed root length density per unit volume (L_v, $cm\,cm^{-3}$) and root surface area per unit volume (S_v, $cm^2\,cm^{-3}$). All roots were then dried at 65°C for 48 hours, to obtain the root dry weight of the roots.

2.2.4 Plant water status

Leaf water potential was measured with a Scholander-type pressure chamber (PMS Instrument Company, Albany, Oregon, USA). Measurements were made every two weeks between July 7th (DOY 189) and November 3rd (DOY 308) in 2016, and between May 17th (DOY 137) and October 23rd (DOY 296) in 2017. Measurements were performed both at predawn ($\Psi_{l,pd}$) and at midday (ca. 11.00 GMT, $\Psi_{l,md}$). Measurements of $\Psi_{l,pd}$ and $\Psi_{l,md}$ were made in two leaves per plot, in three out of the four plots per treatment (n = 3), one per tree, sampled from current-year shoots from the outer part of the canopy. The sampled leaves were stored in plastic bags with humid filter paper until its measurement at the laboratory, in the afternoon of the sampling days. A portion of the leaf blade was cut to allow the insertion of the leaf petiole into the pressure chamber.

Maximum leaf stomatal conductance ($g_{s,max}$) was also measured every two weeks, on the same days when $\Psi_{l,pd}$ and $\Psi_{l,md}$ measurements were performed. We used a Licor LI-6400 portable photosynthesis system (Li-cor, Lincoln NE, USA), with a 2 x 3 cm standard chamber, at 08.00–09.00 GMT, the time for maximum daily stomatal conductance in olive (Fernández et al., 1997). We measured $g_{s,max}$ in two young but fully developed leaves per tree, in two central trees per plot and in three out of the four plots per treatment (n = 3).

2.2.5 Shoot and fruit growth

Aboveground growth was assessed through leaf area, number of internodes of current year shoots and fruit growth (fruit dry weight, fruit volume and fruit water content). Measurements of leaf area (LA) were made every two weeks, from June 17th to November 3rd in the 2016 irrigation season, and from May 17th to October 23rd in the 2017 irrigation season. We used a LAI-2200 Plant Canopy Analyzer (Li-Cor, Inc., Lincoln, NE, USA) and followed the measurement procedure described by Villalobos et al. (1995) for olive orchards. In brief, eight measurements were made in each plot per treatment, four underneath the tree canopies where leaf area index (LAI) is maximum (LAI_{max}), and the other four at the midpoint between two tree rows, where LAI is minimum (LAI_{min}). The average (LAI_{avg}) was calculated using the fraction of ground cover (GC) as weighting factor ($LAI_{avg} = LAI_{max} \cdot GC + LAI_{min} \cdot (1\text{-}GC)$). The average LA was calculated as LAI_{avg} multiplied by the ground area per plot and dividing by the number of trees in the plot. In May 2016 and April 2017, four current year shoots were selected and tagged in two central trees per plot, totaling eight and 32 current year shoots per plot and per treatment, respectively. Their growth was assessed by counting the number of internodes every two weeks, from June 13th to October 31st in 2016 and from May 2nd until October 10th in 2017. To assess fruit growth, six fruits per plot were sampled every two weeks, from May 30th to November 3rd in 2016 and from May 17th to October 23rd in 2017. These fruit samples were stored in plastic bags with wet filter paper inside and refrigerated. At the afternoon of the same day, we weighted (fresh weight, FFW) and measured the longitudinal and equatorial diameters (D_L and D_E, mm) of each fruit. These data were used to estimate the fruit volume (FV, cm^3), through the following equation:

$$FV = \frac{\pi}{6} D_E D_L$$

Finally, the fruits were dried at 65°C for 48 hours, to obtain its dry weight (FDW). From the fruit fresh and dry weights, we estimated fruit water content (FWC).

2.2.6 Fruit and oil production

Final yield as fruit and virgin olive oil (VOO) yields were obtained by manually harvesting three trees from the central trees of each of the four plots per treatment. Harvesting was performed on November 3rd, 2016 (DOY 308) and on October 25th, 2017 (DOY 298). The entire fruit production of each tree was weighted individually. We took a random sample of 2 kg of fruits from each plot for the VOO physical extraction with the Abencor method (Comercial Abengoa S.A., Seville, Spain) (Martinez et al., 1975).

2.2.7 Statistical analysis

Predawn and midday leaf water potentials, fruit dry weight, fruit volume and fruit water content were analyzed using linear mixed models, with the experimental plots and leaves or fruits as random factors. Values of maximum stomatal conductance, number of internodes in current-year shoots and fruit yield were analyzed using linear mixed models with the experimental plots and trees as random factors. Finally, data on leaf area, soil water content and VOO yield were analyzed using the linear mixed models without the use of random factors, as we only had one measurement per plot. All the data analyses were performed with the R 3.2.2® software (R Core Team, 2015), through the package "nlme" (Pinheiro et al., 2017). The Tukey test for linear mixed models was performed as a Post-hoc test, with the use of the "multcomp" package (Hothorn et al., 2008).

Graphs on root length and root surface area measured in 2016 do not present error bars because we sampled one plot per treatment only. Graphs for the 2017 data show an error bar relative to the standard error of the mean, as each column represent the average of three plots per treatment. The 2017 root data were tested with linear mixed models, and the Tukey test was applied as a Post-hoc test with the "multcomp" package when significant differences were detected. No random factor was used to analyze belowground growth in 2017 as we had only one sample per plot.

The rest of the graphs present the treatment average and standard error obtained from the average of the three plots of each treatment. In the graphs, differences between treatments are indicated by letters. Different letters indicate significant differences between treatments (p <0.05).

2.3 Results

2.3.1 Weather and soil water conditions

High average temperature occurred throughout both experimental years (2016 and 2017), with maximum temperature above 35°C for 58 days in 2016 irrigation season (Fig. 2.1A) and for 64 days in 2017 (Fig. 2.1B). The maximum air temperature was 45.3°C on DOY 249 (September 5th, 2016) and 42.7°C on DOY 204 (July 23rd, 2017). The daily average potential evapotranspiration (ET_o) for the 2016 irrigation season was 6.17 mm (Fig. 2.1C). Maximum daily ET_o values were recorded in July and August. From DOY 250 to the end of the 2016 irrigation season ET_o values showed a decreasing trend. For the 2017 irrigation season, the daily average ET_o was 5.20 mm, with a decreasing trend from DOY 225 (Fig. 1D). The highest daily total solar radiation (R_s) values were recorded at the beginning of both irrigation seasons. The average daily R_s value from DOY 122

to DOY 240 was 26.21 kJ m^{-2} in 2016 and 27.52 kJ m^{-2} in 2017 (Figs. 1E and 1F). After DOY 240, the average daily R_s was 15.97 kJ m^{-2} in 2016 and 19.79 kJ m^{-2} in 2017. For the whole irrigation season, the average values were 21.66 and 24.69 kJ m^{-2} in 2016 and 2017, respectively. In both years the trend of R_s de creased after mid-July (ca. DOY 200).

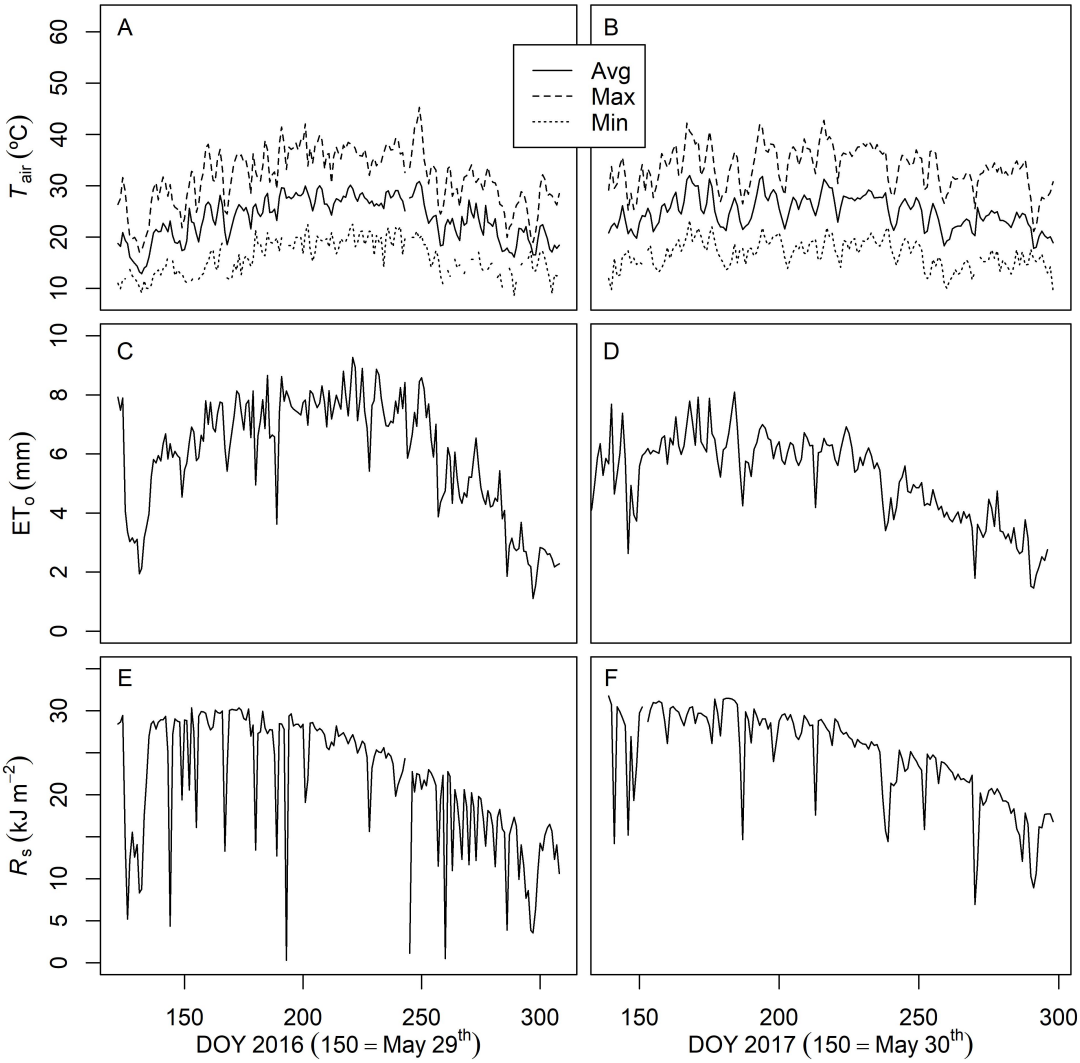

Figure 2.1: Weather conditions during the 2016 and 2017 irrigation seasons. T_{air} = air temperature; ET_o = FAO56 Penman-Monteith potential evapotranspiration; R_s = daily total solar radiation.

Both the irrigation amounts (IA, mm) for each treatment and the precipitation (P) recorded in the orchard are shown in Figs. 2.2A (2016) and 2.2B (2017). Also shown are the irrigation needs (IN) calculated with the crop coefficient approach (2016) and derived from estimated values of maximum daily stomatal conductance (2017) (Section 2.1). Total IA per treatment and year are shown in Table 2.1. Irrigation was reasonably well managed, in the sense that the agreement between the applied irrigation amounts and the calculated irrigation needs was reasonably good (Figs. 2.2A,B). The total IA in 2017 was lower than in 2016 (Table 2.1). First, because of the lower atmospheric demand (Figs. 2.2C,D). Second, because of the method to calculate IN. Thus, the method

used in 2017, based on stomatal conductance (g_s) values lead to an average IA of 3752.95 $m^3\,ha^{-1}$ for the 100C treatments (Table 2.1), while the IN value calculated with the crop coefficient approach on that year (not shown in Table 2.1) amounted to 4595.27 $m^3\,ha^{-1}$. In other words, the IA values applied in 2017 with the g_s approach were 81.7% only of the IN values calculated with the crop coefficient approach. The precipitation recorded within the irrigation season amounted to 77.01 mm in 2016 and to 20.39 mm in 2017. In 2016, non-significant differences on θ were found among treatments, not even between the 100C and the 45SDI treatments, apart from the first measurement day when the soil water regimes were not established yet (Fig. 2.2C). This could be due to the high variability shown by the θ values, as indicated by the large error bars found for this variable in 2016. As expected, both in 2016 and 2017 the θ values in the 100C treatments where close to field capacity (0.28 $cm^3\,cm^{-3}$), suggesting non-limiting soil water conditions for the 100C trees. Concerning the 45SDI treatments applied in 2016, we expected decreasing θ values along the irrigation season, but data in Fig. 2.2C show the contrary, both for 45SDI-1L and 45SDI-2L. This can be partly explained by the rainfall events recorded at the end of the 2016 irrigation season (Fig. 2.2A). In 2017, the seasonal θ courses were as expected. Thus, they were relatively constant and close to field capacity for the 100C trees, and quite variable for the 45RDI trees, echoing changes in the irrigation amounts established by the applied RDI strategy.

Table 2.1: Irrigation amounts ($m^3\,ha^{-1}$) supplied to each treatment. Numbers between parentheses are the applied amounts expressed as a percentage of the calculated irrigation needs for full irrigation.

Treatment	2016	2017
100C-1L	4368.22 (98.87%)	3748.10 (81.56%)
100C-2L	4353.85 (98.54%)	3757.80 (81.77%)
45SDI-1L	1911.27 (43.26%)	-
45SDI-2L	1850.28 (41.88%)	-
45RDI-1L	-	1689.00 (36.76%)
45RDI-2L	-	1671.63 (36.38%)

2.3.2 Belowground growth

Data on root length density per unit volume (L_v, $cm\,cm^{-3}$) for each treatment, sampling time and sampling location (Out, In1, In2) are shown in Figure 2.3. Considering that the sampling of roots was made in May-June 2016 and again in February-March 2017, data in Fig. 2.3 refers to the 100C and 45SDI tr ees only, since the 45RDI strategy was applied after root sampling in 2017. Results show that L_v values were always lower in the soil volumes non-affected by irrigation (Out) than within the soil volumes wetted

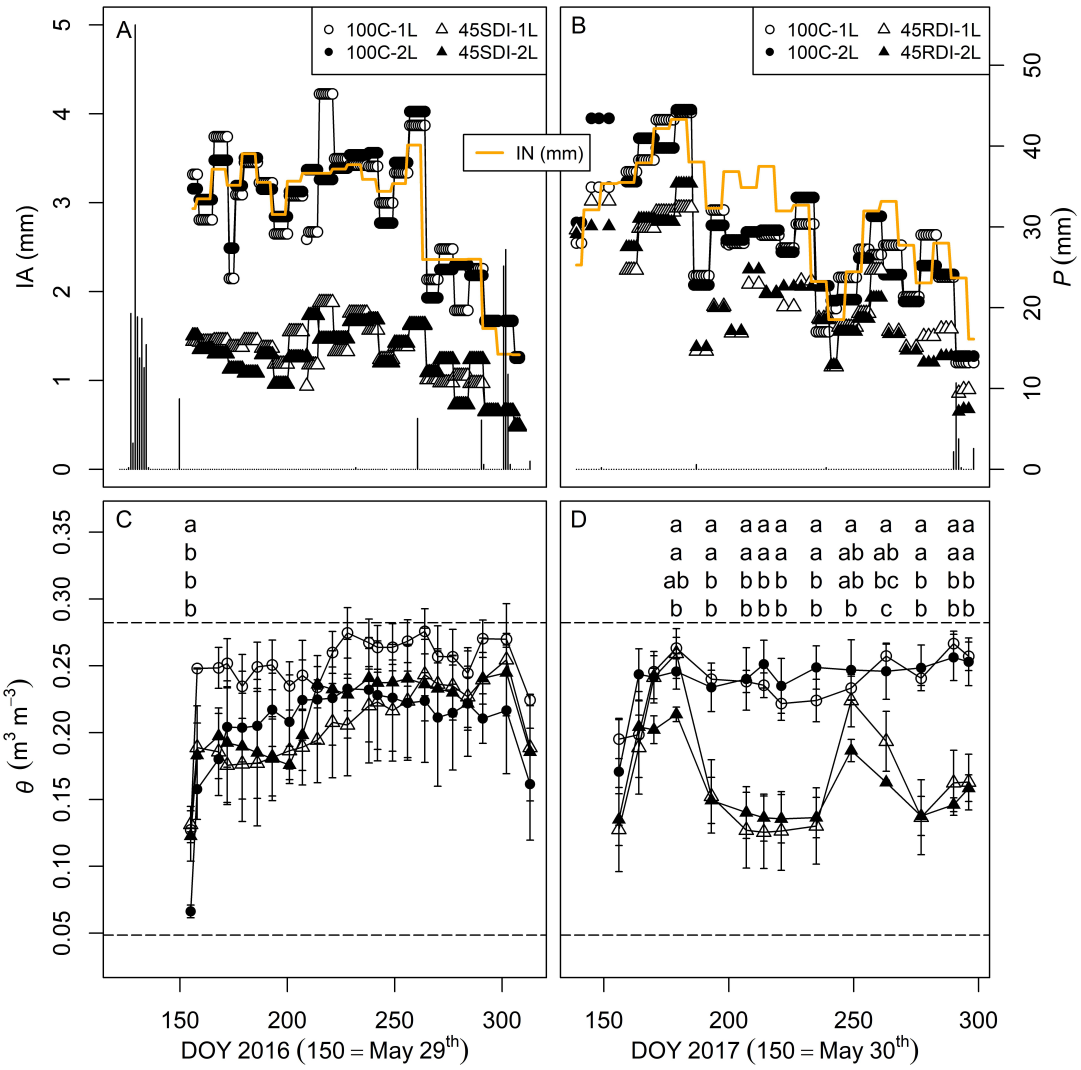

Figure 2.2: Top graphs show the irrigation amounts (IA) supplied to each treatment, and the precipitation (P) recorded in the orchard in 2016 (graph A) and 2017 (graph B). The calculated irrigation needs (IN) to replace 100% of the crop water needs are also shown. Bottom graphs show the seasonal courses of the average soil water content (θ) in 2016 (graph C) and 2017 (graph D). Each data point of the bottom graphs represents the average of three plots, with vertical bars representing the standard error of the mean. Different letters show significant differences (p <0.05). The horizontal dashed lines in graphs C and D represents θ values at field capacity (0.28 $m^3\ m^{-3}$) and at the driest soil conditions measured during the experimental period (0.049 $m^3\ m^{-3}$).

by irrigation (In1 and In2), although differences were not always significant. Also, L_v values were generally greater in In1 than in In2. This was expected, since in ln2 each tree had double volume of soil wetted by irrigation. The greatest L_v values were recorded in the In1 locations of the 45SDI-2L trees. This occurred even in May-June 2016, i.e. prior to the beginning of the irrigation season. Therefore, it cannot be attributed to an effect of the additional drip line. For all sampling locations, L_v values were greater in 2017 than in 2016. This was also expected, since data form 2017 accounts for root growth during the whole 2016 irrigation season plus most of the 2016-2017 rainy season, which went from October 22nd, 2016 (DOY 296) to May 12th, 2017 (DOY 132). At both sampling dates, the

45SDI trees presented higher L_v values at In1 and In2 in comparison to the 100C trees. Likely, the reduced soil volume affected by irrigation in the 45SDI trees, as compared to the 100C trees, caused a greater root concentration in the irrigation bulbs. Also, the 2L treatments presented higher values of root length at both In1 and In2 when compared to the respective 1L treatments. Again, the 2L trees had smaller irrigation bulbs than the 1L trees, which likely led to greater root densities in the wetted soil volume. No significant differences were found between treatments at the 2017 measurements (data not shown). However, In1 presented significantly higher root length for the 100C-2L and 45RDI-1L treatments, in comparison to the other sampling locations (Out and In2). For the 45RDI-2L the In1 presented significantly higher root length in comparison to Out, but no significant difference was found between In2 and In1 and between In2 and Out (Fig. 2.3B). For the 100C-1L treatment, no significant difference was found between In1 and Out.

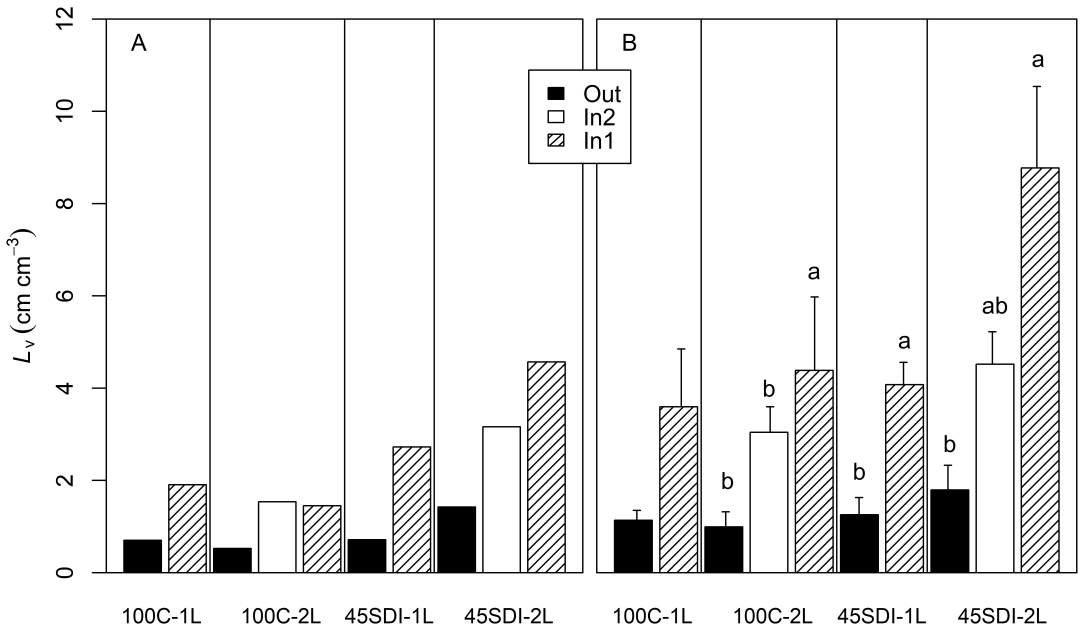

Figure 2.3: Root length density per unit volume (L_v) measured in May-June 2016 (A) and February-March 2017 (B). Data are average values for the 0 to 40 cm depth. In 2016 each column represents one plot per treatment. In 2017 each column represents the average of three plots per treatment. Vertical bars represent the standard error of the mean. Different letters indicate significant difference within the irrigation treatments in 2017 (p <0.05).

Data regarding root surface area per unit volume (S_v, cm^2 cm^{-3}) (Fig. 2.4), agree with those of L_v (Fig. 2.3), with the exception of data from the Out location of the 45RDS-2L treatment sampled in 2016.

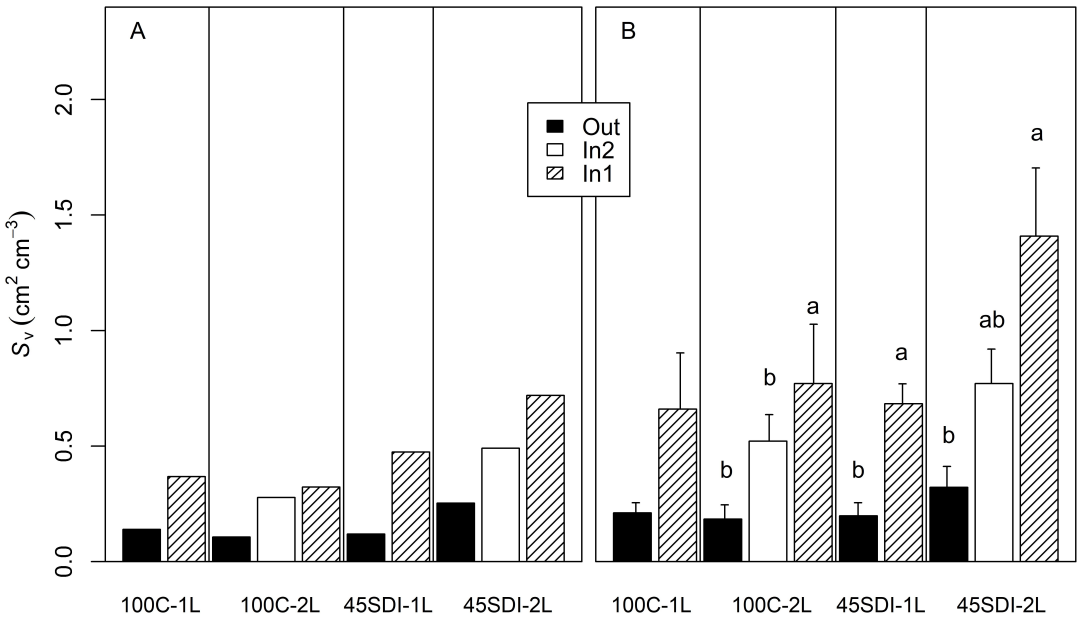

Figure 2.4: Root surface area per unit volume (S_v) measured in May-June 2016 (A) and February-March 2017 (B). Data are average values for the 0 to 40 cm depth. In 2016 each column represents one plot per treatment. In 2017 each column represents the average of three plots per treatment. Vertical bars represent the standard error of the mean. Different letters indicate significant difference within the irrigation treatments in 2017 (p <0.05).

2.3.3 Tree water status and gas exchange

In 2016, predawn leaf water potential ($\Psi_{l,pd}$) values recorded in 100C trees were generally close to -0.5 MPa (Fig. 2.5A), a threshold $\Psi_{l,pd}$ value for water stress in olive (Fernández and Moreno, 1999), which is in agreement with the non-limiting soil water conditions commented on the prior section. That year, differences in $\Psi_{l,pd}$ between the 100C and the 45SDI treatments were significant on DOY 208 and 224 only. For the rest of the season, no significant differences between the 100C and the 45SDI treatments were found. The low values recorded around DOY 250, in all the irrigation treatments (Fig. 2.5A), were probably due to the high ET_o values recorded on that period (Fig. 2.1A).

In 2017, the $\Psi_{l,pd}$ values in the 100C trees showed decreasing values from ca. DOY 180 (Fig. 2.5B), becoming lower than -0.5 MPa. The decreasing trends of $\Psi_{l,pd}$ in the 100C treatments are in agreement with the decreasing trends of IA (Fig. 2.2B), although not with the θ values (Fig. 2.2D). Concerning the 45RDI treatments, the $\Psi_{l,pd}$ seasonal courses were in agreement with both the seasonal courses of IA and θ. Minimum $\Psi_{l,pd}$ values were recorded in the 45RDI trees at the end of the mid-summer period, just before the recovering period 3 (Fig. 2.5B).

Concerning differences between the 1L and 2L treatments, those were non-significant for the 100C treatments, both in 2016 and 2017 (Fig. 2.5). The same can be said for the deficit irrigation treatments, with the exception of DOY 207 in 2017, which corresponds

to the beginning of the period with deficit irrigation between periods 2 and 3. On that day, the 45RDI-2L trees presented $\Psi_{l,pd}$ values significantly higher than those recorded in 45RDI-1L trees. Values recorded in the 45RDI-2L trees were, in fact, similar to those of the 100C trees.

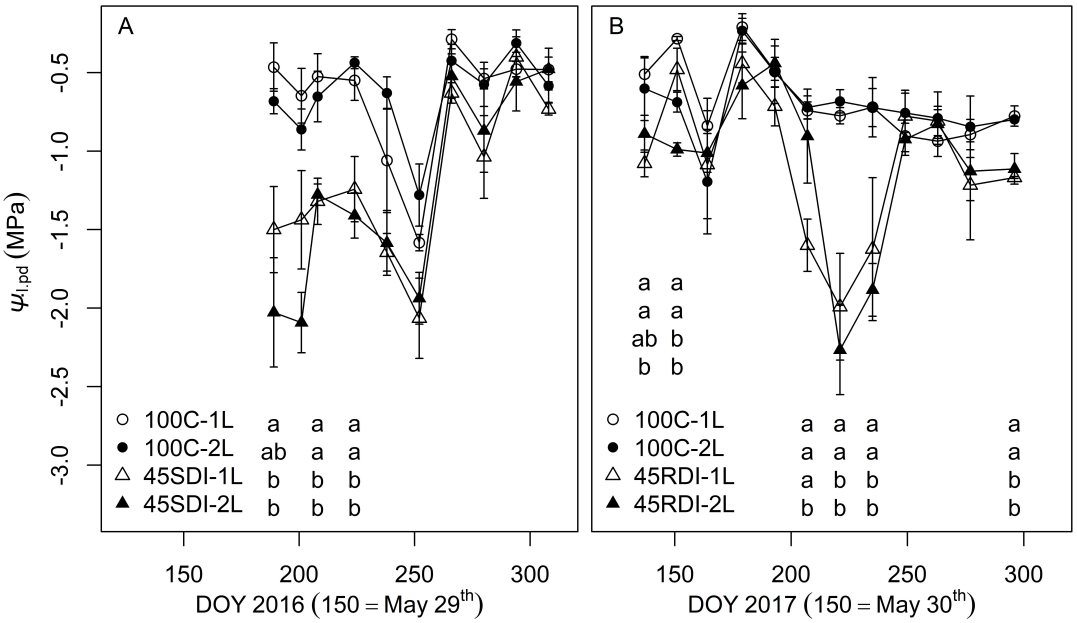

Figure 2.5: Seasonal courses of predawn leaf water potential ($\Psi_{l,pd}$) measured in trees of all treatments in 2016 (A) and 2017 (B). Each data point is the average of three plots, with two measurements per plot. Vertical bars represent the standard error of the mean. Different letters show significant differences (p <0.05).

In 2016, midday leaf water potential ($\Psi_{l,md}$) in 100C trees was higher than -1.4 MPa for most of the irrigation season (Fig. 2.6A). $\Psi_{l,md}$ = -1.4 MPa is a threshold for water stress in olive (Moriana et al., 2012). We registered values greater than -1.5 MPa at the beginning of the season only. On DOY 201 the 100C treatments presented significantly higher $\Psi_{l,md}$ values in comparison to the 45SDI treatments, and on DOY 294 the 45SDI-2L presented significantly lower values in comparison to the other irrigation treatments. For the rest of the irrigation season, the recorded differences among treatments were not significant. In both the 100C and the 45SDI treatments, the seasonal courses of $\Psi_{l,md}$ agreed with those of soil water content (Fig. 2.2C). In 2017, $\Psi_{l,md}$ for the 100C treatments was above -1.4 MPa for most of the irrigation season (Fig. 2.6B). Only at the end of the season values lower than -1.4 MPa were registered. For the 45RDI treatments, $\Psi_{l,md}$ values were lower at the periods of low soil water content, reaching values below -3 MPa at the end of August, i.e. immediately before the recovering period 3. Between periods 2 and 3 (from DOY 185 to 238), the 45RDI-2L trees presented a slower decrease in $\Psi_{l,md}$, in comparison to the 45RDI-1L trees.

The time courses of the daily maximum leaf stomatal conductance ($g_{s,max}$) (Fig. 2.7) were, somehow, similar to those of $\Psi_{l,md}$. In 2016 $g_{s,max}$ values measured in 100C trees

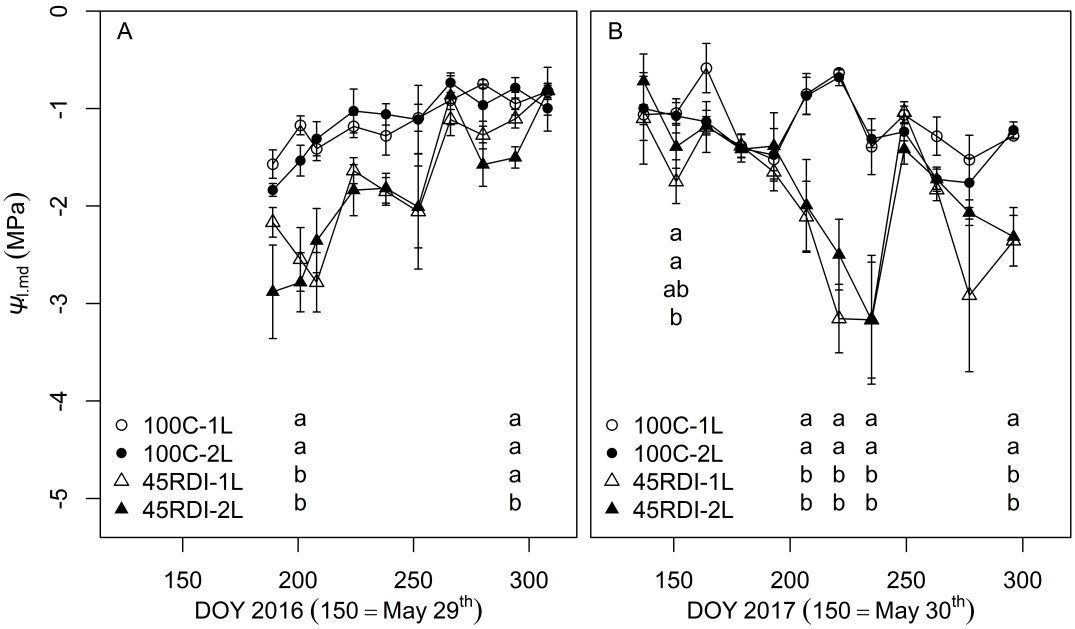

Figure 2.6: Seasonal courses of the midday leaf water potential ($\Psi_{l,md}$) measured in trees of all treatments in 2016 (A) and 2017 (B). Each data point is the average of three plots, with two measurements per plot. Vertical bars represent the standard error of the mean. Different letters show significant differences (p <0.05).

were generally greater than those from the 45SDI trees for most of the season, until DOY 280. On DOY 252 and 266, however, no significant differences were found. Likely, the high ET_o values recorded in that period (Fig. 2.1A) induced stomatal closure even in the 100C trees. This year we observed no differences between the 1L and 2L trees, for either treatment. As in 2016, seasonal courses of $g_{s,max}$ recorded in 2017 agreed with those of $\Psi_{l,pd}$, $\Psi_{l,md}$ and θ. Thus, the 45RDI trees presented significantly lower $g_{s,max}$ values than the 100C trees when deficit irrigation was applied, i.e. in between periods 2 and 3 and after period 3 (Fig. 2.7B). The 100C trees showed $g_{s,max}$ values close or above 0.2 mol m^{-2} s^{-1} for most of the irrigation season, with peak values of 0.33 mol m^{-2} s^{-1} on DOY 207, In the 45RDI trees, however, $g_{s,max}$ values were usually lower than 0.1 mol m^{-2} s^{-1}, with minimum values of 0.03 at the end of August (DOY 235). No significant differences were found between 1L and 2L for either treatment, although there was a trend for the 2L trees to show higher $g_{s,max}$ values.

2.3.4 Aboveground growth

According to the number of internodes in current year shoots (Fig. 2.8A), shoot growth in 2016 was greeter in the 100C-2L trees than in the 100C-1L trees, with the greater differences at the end of the season (Fig. 2.8A). Shoot growth in the 45SDI trees, was negligible, both in 1L and 2L trees. Shoot growth in 2017 was greater in the 100C trees than in the 45RDI trees, although this year no differences between 100C-1L and

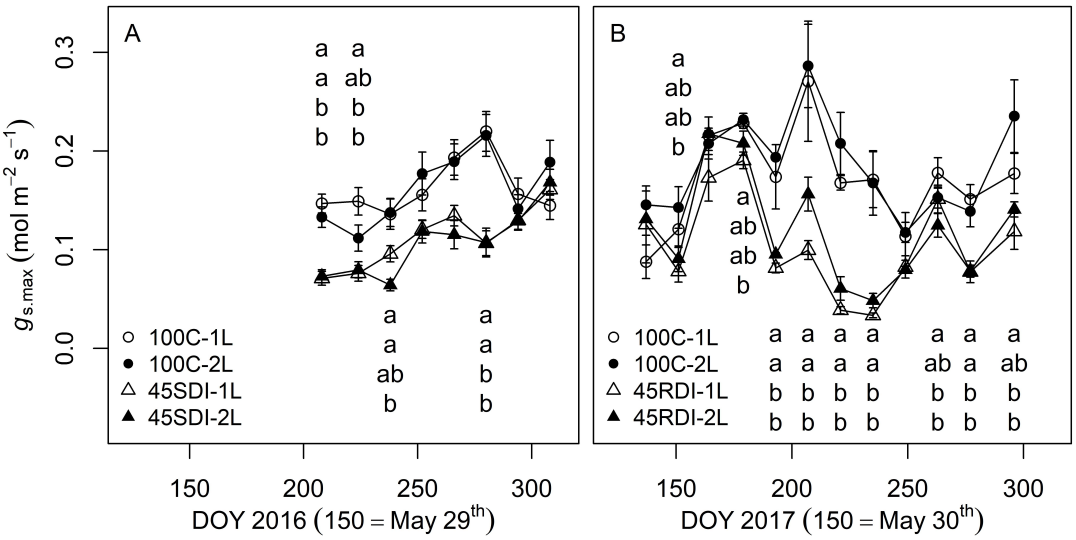

Figure 2.7: Seasonal courses of daily maximum leaf stomatal conductance ($g_{s,max}$) measured in trees of all treatments in 2016 (A) and 2017 (B). Each data point is the average of three plots, with four measurements per plot. Vertical bars represent the standard error of the mean. Different letters show significant differences (p <0.05).

100C-2L were found. Shoot growth was also observed in the 45RDI trees, although to a lesser extent (Fig. 2.8B). No significant differences were found between 45RDI-1L and 45RDI-2L trees, although the number of internodes was usually greater in the latter. In fact, no significant differences were found between 100C and 45RDI-2L, while differences between 100C and 45RDI-1L were significant since DOY 193.

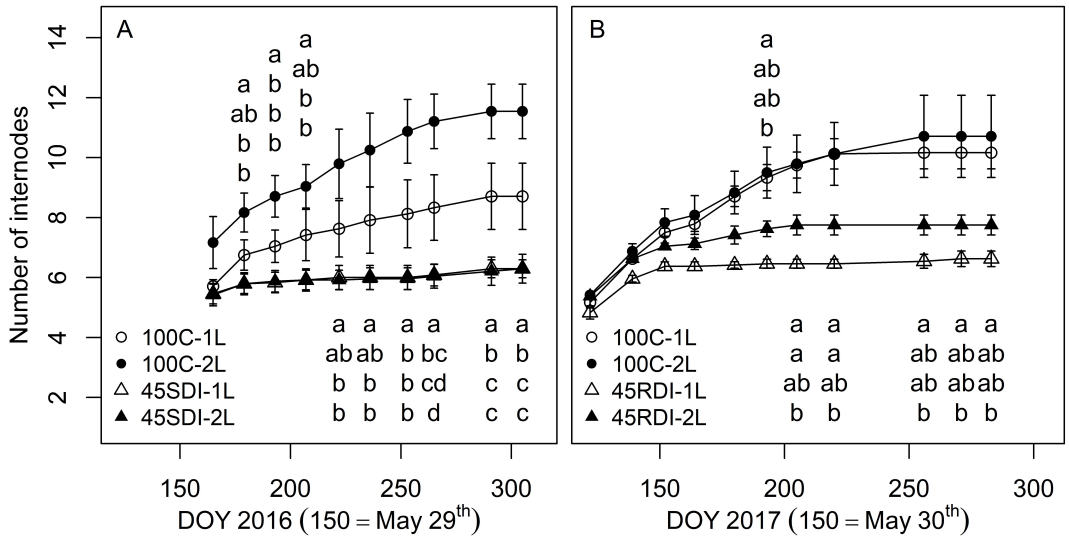

Figure 2.8: Seasonal courses of the number of internodes of current year shoots measured in trees of all treatments in 2016 (A) and 2017 (B). Each data point is the average of three plots, with eight measurements per plot. Vertical bars represent the standard error of the mean. Different letters show significant differences (p <0.05).

In 2016, the seasonal courses of leaf area (LA) revealed greater growth in the 100C

trees than in the 45SDI trees, from DOY 208 (Fig. 2.9A). Although the figure shows differences between the 45SDI-1L and the 45SDI-2L trees, these could be explained by differences in the initial value. Therefore, and considering that the slopes of the seasonal courses of both 45SDI-1L and 45SDI-2L were about horizontal, our data show that no significant LA increase was recorded along the irrigation season in those treatments. Results in LA (Fig. 2.9A) agree with those in the number of internodes in the current year shoots (Fig. 2.8A), in the sense that both variables indicate negligible growth in the 45SDI trees. No significant differences in LA were found between 100C-1L and 100C-2L either, although in these treatments LA increased along the season, as mentioned above. Differences in the number of internodes recorded between the 100C treatments did not have an effect on LA.

In 2017, the 100C trees were again those showing greater increases in LA during the irrigation season, with no difference between 100C-1L and 100C-2L (Fig. 2.9B). Some increase in LA was also recorded in the 45RDI trees, although less than in the 100C trees. Still, the statistical analysis showed no differences between the 100C trees and the 45RDI-2L trees, and greater increase in LA in the 45RDI-2L trees than in the 45RDI-1L trees.

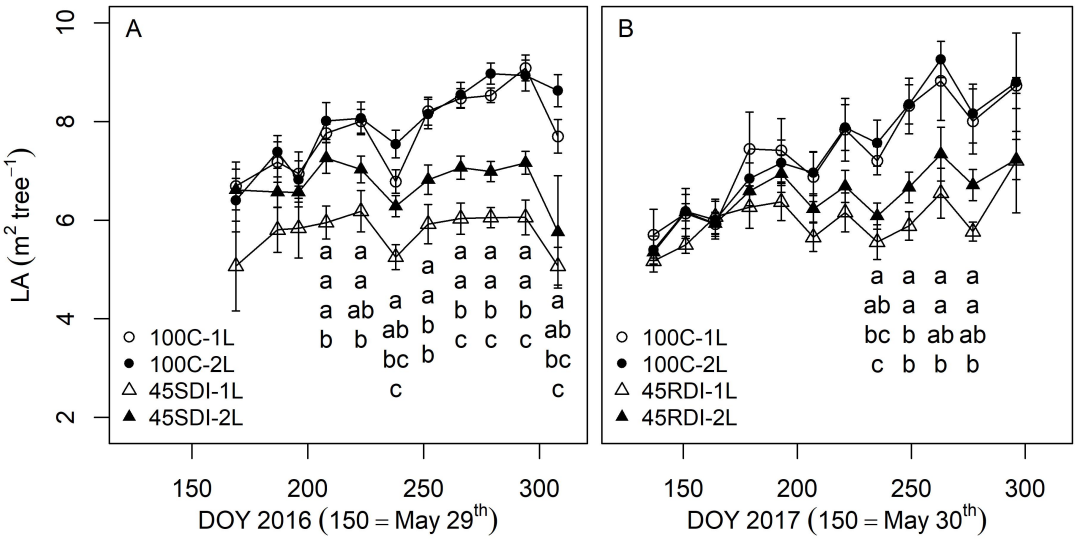

Figure 2.9: Seasonal courses of canopy leaf area measured in trees of all treatments in 2016 (A) and 2017 (B). Each data point is the average of three plots. Vertical bars represent the standard error of the mean. Different letters show significant differences (p <0.05).

Data on fruit dry weight (FDW) collected along the two irrigation seasons revealed practically no significant differences between treatments (Fig. 2.10). From the end of July (ca. DOY 210) to the end of the season, lower FDW values were recorded in the 45SDI (2016) and 45RDI (2017) trees, but differences with the 100C trees were not significant. In 2016 no differences were appreciated between the two 45SDI treatments. In 2017 the lowest FDW values were recorded in fruits from the 45RDI-1L trees. But, again,

differences were not significant. Both in 2016 and 2017, the slope of the FDW seasonal courses was greater before than after the end of July.

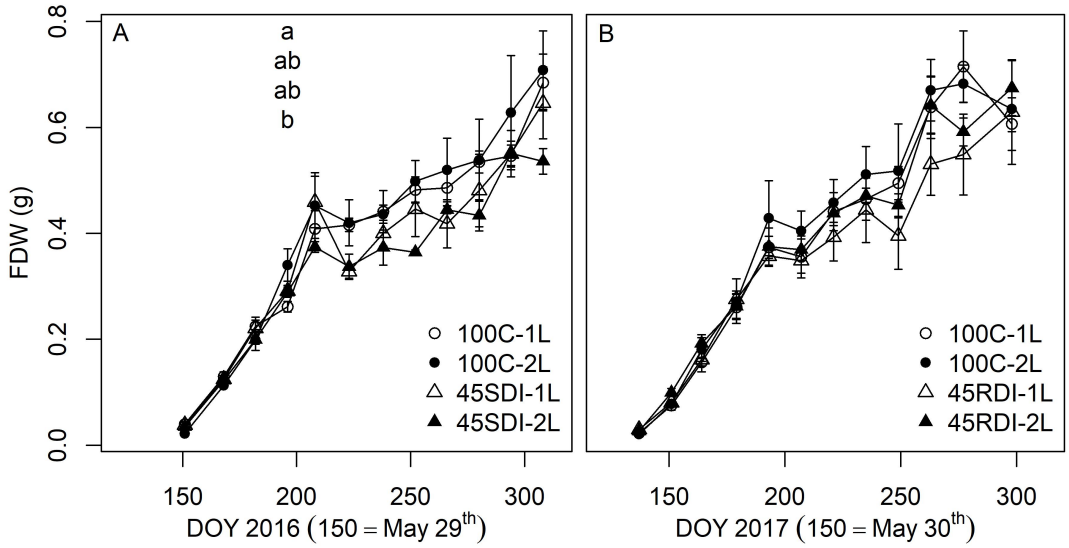

Figure 2.10: Seasonal courses of fruit dry weight measured in trees of all treatments in 2016 (A) and 2017 (B). Each data point is the average of three plots. Vertical bars represent the standard error of the mean. Different letters show significant differences (p <0.05).

Contrarily to fruit dry weight, significant differences between the full irrigation and deficit irrigation treatments were found in fruit volume (FV), both in 2016 and 2017 (Fig. 2.11). In both years, fruits from the 100C trees showed greater FV values from the end of July to the end of the season, although differences with the 45SDI (2016) and 45RDI (2017) trees were not always significant. In 2016, significant differences were recorded in August and September only (Fig. 2.11A). Form the end of September (ca. DOY 270) to harvesting, the 45SDI trees showed lower FV values than the 100C trees, but differences were not significant. In 2017, the dynamics of the FV seasonal courses were similar than in 2016, although differences between the control and the deficit irrigated trees remained until later in the season in 2017 than in 2016. At the end of the season of both years, FV values were lower for the deficit irrigated trees than for the fully irrigated trees, although with not statistical difference. Maximum FV values reached at the end of the season were greater in 2016 than in 2017. Changes in the slope of the FV time courses recorded both in 2016 and 2017 show lower increase rate of FV in midsummer, when the stress was high, than in June and July (Fig. 2.11). During the recovery period 3, from the end of August (ca. DOY 240) to mid-September (ca. DOY 260), the rate of FV vs. time increased again. At the end of the irrigation season, FV increases quicker in 2016 than in 2017, likely because of the greater precipitation recorded in 2016 at that time of the year (Figs. 2.2A,B).

In 2016, values of fruit water content (FWC) from all treatments decreased markedly from mid-June (ca. DOY 165) to the end of July (ca. DOY 210), and remained low un-

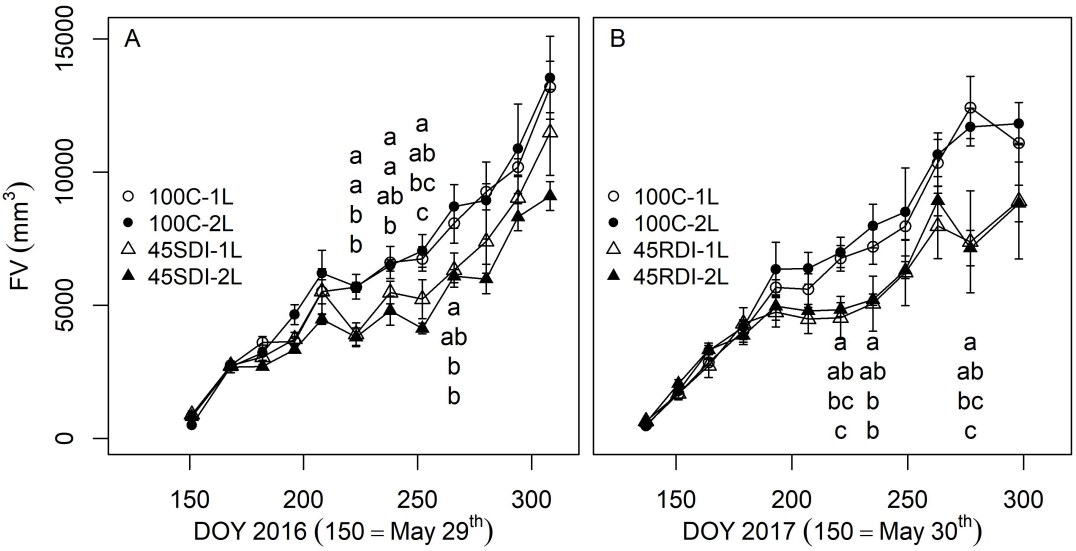

Figure 2.11: Seasonal courses of fruit volume in measured in trees of all treatments in 2016 (A) and 2017 (B). Each data point is the average of three plots, with six fruits per plot. Vertical bars represent the standard error of the mean. Different letters show significant differences (p <0.05).

til early September (ca. DOY 210) (Fig. 2.12A). From then to harvesting FWC values increased, in agreement with a less demanding atmospheric demand (Fig. 1) and the autumn rainfall (Fig. 2). In general, FWC measured in 2016 were always lower for the 45SDI trees than for the 100C trees, all along the irrigation season. Differences, however, were significant between the 100C fruits and the 45SDI-2L fruits only, from DOY 182 until the last measurement day (DOY 308). From DOY 238 until DOY 280, there were no significant differences between the 45SDI-1L and both 100C treatments. In 2017, FWC data showed significant differences between the 100C and the 45RDI treatments between period 2 and period 3, i.e. along the mid-summer period of increasing water stress in the 45RDI trees (Fig. 2.12B). During period 3, when those trees recovered from water stress, no differences in FWC were found between the 45RDI and the 100C trees. After period 3, when the 45RDI trees were again under deficit irrigation, new differences in FWC appear between the fully irrigated and the deficit irrigated trees. No significant differences were found between 1L and 2L, either for the 100C trees or for the 45RDI trees.

2.3.5 Crop production

Final yield was assessed through measurements of fruit and virgin olive oil (VOO) yields. No significant differences were identified by the linear mixed models either for fruit or VOO yield, on both 2016 and 2017 harvests (Table 2.2). The high variability of the yields, inside and in between plots, partly explain the lack of differences among treatments. Both for fruit and VOO, the yields obtained in 2017 were considerably lower than those obtained in 2016. Likely, this was due to a severe pruning that was performed between in December 2016.

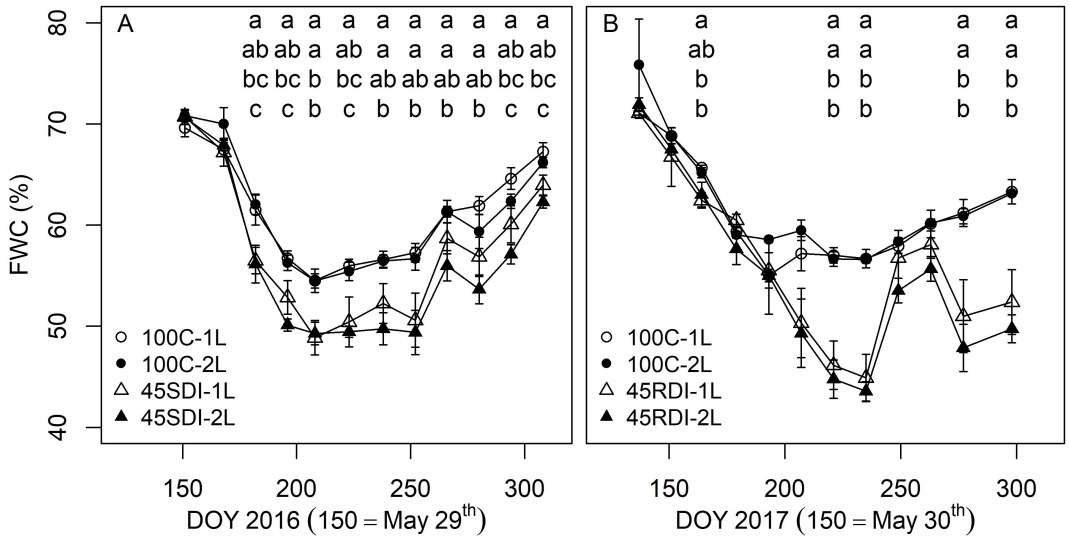

Figure 2.12: Seasonal courses of fruit water content measured in trees of all treatments in 2016 (A) and 2017 (B). Each data point is the average of three plots, with six fruits per plot. Vertical bars represent the standard error of the mean. Different letters show significant differences (p <0.05).

Table 2.2: Final fruit yield per hectare and virgin olive oil (VOO) yield averaged per each treatment. No significant differences were found between irrigation treatments for each year.

	2016		2017	
Treatment	Fruit (kg ha^{-1})	VOO (kg ha^{-1})	Fruit (kg ha^{-1})	VOO (kg ha^{-1})
100C-1L	16,817.7±915.4	1,062.2±122.3	12,633.1±3,448	1,076.5±378.8
100C-2L	17,835.5±1,082.5	1,356.6±110	8,392±372.4	621.5±211.54
45SDI-1L	16,062.9±931.7	1,372±69.7	—	—
45SDI-2L	14,042.4±832.7	1,250.5±109	—	—
45RDI-1L	—	—	7,398.7±276.1	777.1±98.4
45RDI-2L	—	—	7,593.2±994.2	915.7±133.3

2.4 Discussion

2.4.1 Irrigation supplies and soil water status

Although the aim of this study was not to evaluate differences between the irrigation scheduling approaches applied in 2016 (the K_c approach) and 2017 (the g_s approach), our results show that the aimed irrigation supplies to each treatment were accomplished reasonable well (Table 2.1, Fig. 2.2B). On the other hand, the total irrigation amounts in 2017, i.e. estimated from the g_s approach, were ca. 82% lower than the irrigation needs (IN) estimated from the K_c approach (Table 2.1). We are confident on the IN values estimated from the K_c approach, since we calibrated it and tested it widely for the orchard

conditions (Fernández et al., 2013; Fernández et al., 2018c). Still, every Monday we calculated the IN for the starting week based on the ET_o values recorded on the previous week. With the g_s approach, however, we rely on a 3-day weather forecast prediction (Section 2.1). On the other hand, the g_s approach computes estimations of leaf area index (LAI) and of the g_s in the orchard trees. For estimating LAI we used a method (Section 2.4) that have proven to be useful for the orchard conditions (Fernández et al., 2013; Padilla-Díaz et al., 2018). Concerning the estimated g_s, Hernandez-Santana et al. (2016b) compared $g_{s,sun}$ results calculated as described in Section 2.1 with the field measurements of $g_{s,max}$ (Section 2.4), and Hernandez-Santana et al. (2018) compared the g_s simulated through sap flow related measurements and the field measurements of $g_{s,max}$.

In the sustained deficit irrigation treatments (2016), the soil water contents remained above the level of soil water depletion which may limit water uptake in olive (Fig. 2.2C). Thus, the readily available water for olive is considered to be between 60 and 75% of the available soil water (Orgaz et al., 2006; Cuevas et al., 2010), and Fig. 2.2C shows that the average soil water content for the 0.0-0.4 m soil layer was always above that limit. Concerning the regulated deficit irrigation treatments (2017), the soil water status (Fig. 2.2D) changed according to the dynamics of water supply (Fig. 2.2B). In mid-summer, i.e. between periods 2 and 3, soil water contents were below the readily available water level. Late in the 2017 season, during the deficit irrigation applied after period 3, the soil water content in the 45RDI trees was much lower than the values recorded for the 45SDI trees on that period, in 2016. This can be explained by both the greater rainfall and lower ET_o recorded in 2016.

2.4.2 Treatment effects on the root system

The root sampling methodology used in this study, based on the use of an auger able to take soil samples of big volume, has been successfully used in olive orchards (Deng et al., 2017; Fernández et al., 1991; García-Tejera et al., 2018; Searles et al., 2009). Other authors have obtained reliable data with the trench method (Fernández et al., 1991; Michelakis et al., 1993; Diaz-Espejo et al., 2012). In our case, however, the large variability on root distribution found in the orchard hampered the identification of significant differences among treatments. Also, both the lack of replicas in the 2016 root sampling, and differences on the root sampling times between 2016 and 2017, curtailed the detection of any possible differences on the annual root growth due to the irrigation treatment. Still, the collected data gave us reliable information on the development of new roots closer to the additional drip line, from its installation before the irrigation season of 2016 to the beginning of the spring in 2017. Thus, and according to our initial hypothesis, the increase in number of drip lines per tree row from the 1L to 2L treatments, and the consequent increase in the fraction of the rhizosphere wetted by irrigation, led to

greater root length density (L_v) and root surface area per unit volume (S_v) (Figs. 2.3 and 2.4, respectively). The greater increases in these two variables were found in the 45SDI-2L trees. These increases in L_v and S_v found in the 2L treatments agree with the results reported by Fernández et al. (1991) and Searles et al. (2009), who obtained the greatest root length densities of fine, active roots, closer to the drippers, i.e. within wetted soil volumes. Close to the additional drip line (In2), L_v and S_v values were lower than at the In1 locations, likely because the plant had had less time for the development of new roots in those soil volumes. Our data suggest that the non-limiting soil water conditions kept all along the irrigation season in the fraction of the rhizosphere affected by irrigation in the 100C-1L trees, allowed for enough water uptake, such that the installation of the additional drip line in the 100C-2L trees did not led to a great increase either in L_v or S_v.

2.4.3 Treatment effects on water status, gas exchange and growth

For all the considered variables related to water status, gas exchange and shoot and fruit growth, the 100C treatments showed a better performance than the deficit irrigated treatments. This was expected, since previous work in the orchard showed an effect of the 45RDI treatments on those variables (Fernández et al., 2013; Padilla-Díaz et al., 2016; Padilla-Díaz et al., 2018). Concerning the 45SDI treatments, 2016 was the first year in which a sustained deficit irrigation strategy was applied to the orchard. For the physiological variables ($\Psi_{l,pd}$, $\Psi_{l,md}$ and $g_{s,max}$), no marked differences were found between the 1L and 2L treatments, either in 100C, 45SDI and 45RDI strategies, with the exception of some days in 2017 in which $\Psi_{l,pd}$, $\Psi_{l,md}$ and $g_{s,max}$ data showed less stress in the 45RDI-2L trees than in the 45RDI-1L trees (Figs. 2.5B, 2.6B and 2.7B, respectively). Below we discuss about the effect of this in growth and production. The $\Psi_{l,pd}$ and $\Psi_{l,pd}$ data show increasing water stress in the 100C trees, along the irrigation season. Data on $g_{s,max}$ (Fig. 2.7B) were also below 0.2 mol m^{-2} s^{-1} from ca. DOY 225 to ca. DOY 270, which also suggest moderate water stress. The applied irrigation amounts in 2017 were ca. 15% lower than the irrigation needs calculated with the crop coefficient approach (Table 2.1), but we cannot say that this was enough to explain the increasing seasonal water stress, because data on soil water content (Fig. 2.2B) do not show increasing water depletion. Still, this is a warning on the irrigation needs estimated with the g_s approach to be rather low. For the 45 deficit irrigation treatments, $\Psi_{l,pd}$, $\Psi_{l,md}$ and $g_{s,max}$ data show that, at the end of the season, the 45SDI trees (2016) were less stressed than the 45RDI trees (2017). This, however, cannot be attributed to the irrigation treatments only, but also to weather differences between the two years (Figs. 2.1 and 2.2).

Data on the number of internodes show greater growth in the 100C trees than in the deficit irrigated trees, both in 2016 and 2017 (Fig. 2.8). It is striking that, in 2016,

these differences were quite high despite of the lack of differences in soil water content (Fig. 2.2C). Thus, no growth was detected along the irrigation season in the 45SDI trees, while in the 100C trees, especially the 100C-2L, growth of the current-year shoots was remarkable (Fig. 2.8A). This advises for caution when interpreting soil water content measurements. In this case, the greater soil volume wetted in the 2L trees, as compared to the 1L trees, should have account for a greater water availability for the 2L trees. It is known, in fact, that the amount of water that a plant can take up from the soil depends not only on the average soil water content, but also on the total soil volume wetted by irrigation. In 2017 we also observed greater growth in the 100C trees than in the 45RDI trees. This year we recorded some growth in the 45RDI trees, especially in the 45RDI-2L trees. This agrees with the greater L_v and S_v values recorded on those trees (Figs. 2.3 and 2.4, respectively). As expected, our data on leaf area (LA, Fig. 2.9) shows the same growth trends than the data on the number of internodes in shoots of the current year, with the difference that similar LA values were found in 2016 in the two 100C-1L and 100C-2L treatments. Differences between the two 45SDI treatments were likely due to differences in the initial LA of the measured trees, so they must not be attributed to an effect of the 1L vs. 2L treatments. In 2017, both the number of internodes and LA measurements show growth in the 45RDI trees along the irrigation season. Differences between the 45RDI-1L and the 45RDI-2L suggests that the reduced root zone volumes of the 45RDI-1L trees, together with the reduced soil water contents due to the deficit irrigation applied to those trees, clearly limited growth in the 45RDI treatments as compared to the 100C treatments. These results are in accordance with those obtained by Ismail and Almarshadi (2013), which obtained greater current-year shoots growth of jujube fruit trees when irrigated with more drip emitters per tree. Espadafor et al. (2018) also reported greater growth in young almond trunk diameter with the increase of wetted soil volume. It is known that growth is highly sensitive to water stress (Connor and Fereres, 2005; Fernández, 2014b) so, despite the lack of differences between 1L and 2L treatments in $\Psi_{l,pd}$, $\Psi_{l,pd}$ and $g_{s,max}$, our data on shoot and leaf area growth suggest, in summary, less water stress in the 2L plants.

Contrarily to vegetative aboveground growth, fruit growth in terms of fruit dry weight (FDW) (Fig. 2.10) was not affected by the additional drip line. These results agree with those obtained by Ismail and Almarshadi (2013) in jujube fruits. They worked with trees irrigated with different number of emitters and drip emitters of different flow rates, although maintaining the same total flow rate per tree. Their findings show significant differences between treatments in shoots' growth but similar FDW. This can be explained by fruit development being a priority for plants, as compared to vegetative growth. Recently, Hernandez-Santana et al. (2018) showed data from our orchard, for 2016, for which they reported, for the first time, the lack of differences in FDW despite

of differences in shoot growth. Our data of 2017 confirms that tendency (Fig. 2.10). The fruit volume (Fig. 2.11) revealed some differences during the irrigation season, which are in agreement with data regarding fruit water content (Fig. 2.12). Fruit water content was greatly influenced by precipitation, irrigation and atmospheric demand. Despite no significant differences were found between 45RDI-1L and 45RDI-2L, the 45RDI-1L treatment presented lower values of fruit water content (Fig. 2.12). Other authors have already reported that the oil content is less influenced by deficit irrigation than shoot growth (Gómez-del-Campo, 2013; Hernandez-Santana et al., 2018), fruit water content and fruit size (Gómez-del-Campo et al., 2014). This agrees with our results, as the oil content is reflected in the fruit dry weight which did not present significant differences between irrigation treatments.

Data from 2017 on the number of internodes in current-year shoots (Fig. 2.8) and fruit volume (Fig. 2.11) agree with the fact that midday leaf water potentials (Fig. 2.6) were somehow greater in 45SDI-2L trees than in the 45RDI-1L trees. As mentioned in the Results section, differences were not significant, but the fact that water stress was less severe in the 45RDI-2L trees than in the 45RDI-1L trees is supported by the greater canopy growth of the 45RDI-2L trees (Figs. 2.8B and 2.9B). Likely, during 2017 these trees would already have more active roots in the new wet bulb, probably increasing its water uptake.

The fact that no differences in fruit dry weight (FDW) were detected despite of differences in fruit water content and fruit volume illustrates the fact that fruits are a priority in terms of carbon allocation for the plant. This was recently addressed by Hernandez-Santana et al. (2018), who reported that neither oil synthetization nor fruit growth and development were affected by the 2016 treatments in the orchard. The change in the FDW slope at the beginning of July both in 2016 and 2017 (Fig. 2.10), for all treatments, indicate the influence of the endocarp sclerification that happens at some 6-10 weeks after bloom, a period when most of cell division occurs and when the approximate final number of cells per fruit is established (Hammami et al., 2011; Hammami et al., 2013).

Although increments in root surface area compared to leaf area has been suggested to contribute to the improvement of plant hydraulic efficiency (Magnani et al., 2002), increase transpiration (Diaz-Espejo et al., 2012) and reduce belowground hydraulic conductance decline with soil drying (Johnson et al., 2018) we did not observe a clear better plant water status in the 2L trees as compared to the 1L trees. García-Tejera et al. (2018) used the soil plant atmosphere continuum model (SPAC model) developed by García-Tejera et al. (2017b) to simulate the response of photosynthesis to a change in root density. These authors obtained results that revealed an increase of about 10% of net assimilation in olive trees when the root density was increased 25% on the soil volume affected by localized irrigation.

In general, our data suggest that the 100C treatment with one single drip line had rooting conditions good enough to allow for maximum tree growth, such that they did not suffer hydraulic limitation to transpiration. This may explain the lack of differences between 100C-1L and 100C-2L.

To the best of our knowledge, this is the first experiment concerning changes in wetted soil volume on olive orchards under full irrigation and under sustained and regulated deficit irrigation.

2.4.4 Treatment effects on crop production

Unfortunately, our data on production (Table 2.2) are far from conclusive. First, because of the high variability we found, which suggest that the three sampled trees per plot were not representative enough. On the other hand, it seems that the severe pruning made in December 2016, among other factors perhaps, markedly reduced the production of 2017, which hampered the evaluation of the impact of the irrigation treatments on production. Our data from the prior section shows clear differences in growth and leaf area between the control and the deficit irrigated trees, so differences in production of fruit and oil should have been detected. Our data in Table 2.2, however, shows that the irrigation treatments had no effect on production. But, as mentioned above, both the high variability and the possible effect of the severe pruning advices for not taking into account data in Table 2.2 when interpreting the effect of the irrigation treatments on production.

2.5 Conclusions

Considering the results obtained and the experimental conditions, we may conclude that the increment of an extra drip line per tree row in the 2L treatments influenced positively the root growth closer to the new wetted soil volume, on both root length density (L_v) and root surface area per unit volume (S_v), mainly in the deficit irrigated treatments. This, together with the greater fraction of the rhizosphere wetted by irrigation, contributed to lower water stress levels in the 2L trees as compared to the 1L trees, especially when being under the deficit irrigation approaches tested in this work. Our data on fruit development and production did not allow us to detect differences among treatments, likely because of the great variability found in the field and because of severe pruning before the 2017 growing cycle. Doubt remains on whether the observed benefits of installing a second drip line will pay the grower for the cost of installing and maintaining that line. The second irrigation line affected root and canopy growth, two variables that have an impact on crop performance in the medium and long term. Therefore, a longer experiment is needed for a rigorous evaluation of the benefits of installing

a second dripper line in hedgerow olive orchards with high plant densities.

References

Allen, R., L. S. Pereira, D. Raes, and M. Smith (1998). *Crop evapotranspiration - Guidelines for computing crop water requirements*. Rome: FAO Irrigation and Drainage, p. 15.

Buckley, T. N., K. A. Mott, and G. D. Farquhar (2003). "A hydromechanical and biochemical model of stomatal conductance". In: *Plant, Cell and Environment* 26.10, pp. 1767–1785. DOI: 10.1046/j.1365-3040.2003.01094.x.

Connor, David J and E. Fereres (2005). "The physiology of adaptation and yield expression in olive". In: *Horticultural reviews* 31, pp. 155–229.

Cuevas, M.V., J. M. Torres-Ruiz, R. Álvarez, M. D. Jiménez, J. Cuerva, and J.E. Fernández (2010). "Assessment of trunk diameter variation derived indices as water stress indicators in mature olive trees". In: *Agricultural Water Management* 97.9, pp. 1293–1302. DOI: 10.1016/j.agwat.2010.03.011.

Deng, Shixin, Qun Yin, Shanshan Zhang, Kankan Shi, Zhongkui Jia, and Luyi Ma (2017). "Drip Irrigation Affects the Morphology and Distribution of Olive Roots". In: *HortScience* 52.9, pp. 1298–1306. DOI: 10.21273/HORTSCI11997-17.

Diaz-Espejo, Antonio, B. Hafidi, J.E. Fernandez, M.J. Palomo, and H. Sinoquet (2002). "Transpiration and photosynthesis of olive tree: a model approach". In: *Acta Horticulturae* 586, pp. 457–460. DOI: 10.17660/ActaHortic.2002.586.94.

Diaz-Espejo, Antonio, T.N. Buckley, J.S. Sperry, M.V. Cuevas, A. de Cires, S. Elsayed-Farag, M.J. Martin-Palomo, J.L. Muriel, A. Perez-Martin, C.M. Rodriguez-Dominguez, A.E. Rubio-Casal, J.M. Torres-Ruiz, and J.E. Fernández (2012). "Steps toward an improvement in process-based models of water use by fruit trees: A case study in olive". In: *Agricultural Water Management* 114, pp. 37–49. DOI: 10.1016/j.agwat.2012.06.027.

Egea, Gregorio, Antonio Diaz-Espejo, and José E. Fernández (2016). "Soil moisture dynamics in a hedgerow olive orchard under well-watered and deficit irrigation regimes: Assessment, prediction and scenario analysis". In: *Agricultural Water Management* 164, pp. 197–211. DOI: 10.1016/j.agwat.2015.10.034.

Espadafor, M., F. Orgaz, L. Testi, I. J. Lorite, O. García-Tejera, F. J. Villalobos, and E. Fereres (2018). "Almond tree response to a change in wetted soil volume under drip irrigation". In: *Agricultural Water Management* 202.September 2017, pp. 57–65. DOI: 10.1016/j.agwat.2018.01.026.

Fernandes, Rafael Dreux Miranda, Maria Victoria Cuevas, Antonio Diaz-Espejo, and Virginia Hernandez-Santana (2018). "Effects of water stress on fruit growth and water

relations between fruits and leaves in a hedgerow olive orchard". In: *Agricultural Water Management* 210.April, pp. 32–40. DOI: 10.1016/j.agwat.2018.07.028.

Fernández, J.E. (2014b). "Understanding olive adaptation to abiotic stresses as a tool to increase crop performance". In: *Environmental and Experimental Botany* 103, pp. 158–179. DOI: 10.1016/j.envexpbot.2013.12.003.

— (2017). "Plant-Based Methods for Irrigation Scheduling of Woody Crops". In: *Horticulturae* 3.2, p. 35. DOI: 10.3390/horticulturae3020035.

Fernández, J.E. and M.V. Cuevas (2011). "Using plant-based indicators to schedule irrigation in olive". In: *Acta Horticulturae* 888, pp. 207–214. DOI: 10.17660/ActaHortic.2011.888.23.

Fernández, J.E. and F. Moreno (1999). *Water use by the olive tree*.

Fernández, J.E., F. Moreno, F. Cabrera, J. L. Arrue, and J. Martín-Aranda (1991). "Drip irrigation, soil characteristics and the root distribution and root activity of olive trees". In: *Plant and Soil* 133.2, pp. 239–251. DOI: 10.1007/BF00009196.

Fernández, J.E., F. Moreno, I. F. Girón, and O. M. Blázquez (1997). "Stomatal control of water use in olive tree leaves". In: *Plant and Soil* 190.2, pp. 179–192. DOI: 10.1023/A:1004293026973.

Fernández, J.E., S.R. Green, H. W. Caspari, Antonio Diaz-Espejo, and M.V. Cuevas (2008b). "The use of sap flow measurements for scheduling irrigation in olive, apple and Asian pear trees and in grapevines". In: *Plant and Soil* 305.1-2, pp. 91–104. DOI: 10.1007/s11104-007-9348-8.

Fernández, J.E., Alfonso Perez-Martin, José M. Torres-Ruiz, María V. Cuevas, Celia M. Rodriguez-Dominguez, Sheren Elsayed-Farag, Ana Morales-Sillero, José M. García, Virginia Hernandez-Santana, and Antonio Diaz-Espejo (2013). "A regulated deficit irrigation strategy for hedgerow olive orchards with high plant density". In: *Plant and Soil* 372.1-2, pp. 279–295. DOI: 10.1007/s11104-013-1704-2.

Fernández, José E., Antonio Diaz-Espejo, Rafael Romero, Virginia Hernandez-Santana, José M. García, Carmen M. Padilla-Díaz, and María V. Cuevas (2018c). "Precision Irrigation in Olive (Olea europaea L.) Tree Orchards". In: *Water Scarcity and Sustainable Agriculture in Semiarid Environment*. Elsevier, pp. 179–217. DOI: 10.1016/B978-0-12-813164-0.00009-0.

García-Tejera, Omar, Álvaro López-Bernal, Francisco Orgaz, Luca Testi, and Francisco J. Villalobos (2017a). "Analysing the combined effect of wetted area and irrigation volume on olive tree transpiration using a SPAC model with a multi-compartment soil solution". In: *Irrigation Science* 35.5, pp. 409–423. DOI: 10.1007/s00271-017-0549-5.

García-Tejera, Omar, Álvaro López-Bernal, Luca Testi, and Francisco J. Villalobos (2017b). "Erratum to: A soil-plant-atmosphere continuum (SPAC) model for simu-

lating tree transpiration with a soil multi-compartment solution". In: *Plant and Soil* 418.1-2, p. 581. DOI: 10.1007/s11104-017-3273-2.

García-Tejera, Omar, Álvaro López-Bernal, Francisco Orgaz, Luca Testi, and Francisco J. Villalobos (2018). "Are olive root systems optimal for deficit irrigation?" In: *European Journal of Agronomy* 99.June, pp. 72–79. DOI: 10.1016/j.eja.2018.06.012.

Gispert, J.R., F. Ramírez de Cartagena, J.M. Villar, and J. Girona (2013). "Wet soil volume and strategy effects on drip-irrigated olive trees (cv. 'Arbequina')". In: *Irrigation Science* 31.3, pp. 479–489. DOI: 10.1007/s00271-012-0325-5.

Gómez, J.A., J.V. Giráldez, and E. Fereres (2001). "Rainfall interception by olive trees in relation to leaf area". In: *Agricultural Water Management* 49.1, pp. 65–76. DOI: 10.1016/S0378-3774(00)00116-5.

Gómez-del-Campo, María (2013). "Summer deficit-irrigation strategies in a hedgerow olive orchard cv. 'Arbequina': effect on fruit characteristics and yield". In: *Irrigation Science* 31.3, pp. 259–269. DOI: 10.1007/s00271-011-0299-8.

Gómez-del-Campo, María, A. Leal, and C. Pezuela (2008). "Relationship of stem water potential and leaf conductance to vegetative growth of young olive trees in a hedgerow orchard". In: *Australian Journal of Agricultural Research* 59.3, p. 270. DOI: 10.1071/AR07200.

Gómez-del-Campo, María, María Ángeles Pérez-Expósito, Sofiene B.M. Hammami, Ana Centeno, and Hava F. Rapoport (2014). "Effect of varied summer deficit irrigation on components of olive fruit growth and development". In: *Agricultural Water Management* 137, pp. 84–91. DOI: 10.1016/j.agwat.2014.02.009.

Hammami, Sofiene B M, Trinidad Manrique, and Hava F. Rapoport (2011). "Cultivar-based fruit size in olive depends on different tissue and cellular processes throughout growth". In: *Scientia Horticulturae* 130.2, pp. 445–451. DOI: 10.1016/j.scienta.2011.07.018.

Hammami, Sofiene B M, Giacomo Costagli, and Hava F. Rapoport (2013). "Cell and tissue dynamics of olive endocarp sclerification vary according to water availability". In: *Physiologia Plantarum* 149.4, pp. 571–582. DOI: 10.1111/ppl.12097.

Hernandez-Santana, Virginia, J.E. Fernández, Celia M. Rodriguez-Dominguez, R. Romero, and Antonio Diaz-Espejo (2016b). "The dynamics of radial sap flux density reflects changes in stomatal conductance in response to soil and air water deficit". In: *Agricultural and Forest Meteorology* 218-219, pp. 92–101. DOI: 10.1016/j.agrformet.2015.11.013.

Hernandez-Santana, Virginia, Rafael D.M. Fernandes, A. Perez-Arcoiza, J.E. Fernández, J.M. Garcia, and Antonio Diaz-Espejo (2018). "Relationships between fruit growth and oil accumulation with simulated seasonal dynamics of leaf gas exchange in the

olive tree". In: *Agricultural and Forest Meteorology* 256-257.March, pp. 458–469. DOI: 10.1016/j.agrformet.2018.03.019.

Hothorn, Torsten, Frank Bretz, and Peter Westfall (2008). "Simultaneous Inference in General Parametric Models". In: *Biometrical Journal* 50.3, pp. 346–363. DOI: 10.1002/bimj.200810425.

Ismail, S M and M H S Almarshadi (2013). "Effect of water distribution patterns on productivity, fruit quality and water use efficiency of Ziziphus jujuba in arid regions under drip irrigation system". In: *Journal of Food Agriculture & Environment* 11.1, pp. 373–378.

Johnson, Daniel M., Jean Christophe Domec, Z. Carter Berry, Amanda M. Schwantes, Katherine A. McCulloh, David R. Woodruff, H. Wayne Polley, Remí Wortemann, Jennifer J. Swenson, D. Scott Mackay, Nate G. McDowell, and Robert B. Jackson (2018). "Co-occurring woody species have diverse hydraulic strategies and mortality rates during an extreme drought". In: *Plant Cell and Environment* 41.3, pp. 576–588. DOI: 10.1111/pce.13121.

Magnani, F, J Grace, and Marco Borghetti (2002). "Acclimation of coniferous tree structure to the environment under hydraulic constraints." In: *Functional Ecology* 16, pp. 385–393.

Martinez, J.M., E. Muñoz, J. Alba, and A. Lanzón (1975). "Report about the use of the "Abencor" analyzer". In: *Grasas y aceites* 26, pp. 379–385.

Michelakis, N., E. Vougioucalou, and G. Clapaki (1993). "Water use, wetted soil volume, root distribution and yield of avocado under drip irrigation". In: *Agricultural Water Management* 24.2, pp. 119–131. DOI: 10.1016/0378-3774(93)90003-S.

Moriana, A., D. Pérez-López, M. H. Prieto, M. Ramírez-Santa-Pau, and J.M. Pérez-Rodriguez (2012). "Midday stem water potential as a useful tool for estimating irrigation requirements in olive trees". In: *Agricultural Water Management* 112, pp. 43–54. DOI: 10.1016/j.agwat.2012.06.003.

Orgaz, F., L. Testi, F.J. Villalobos, and E. Fereres (2006). "Water requirements of olive orchards–II: determination of crop coefficients for irrigation scheduling". In: *Irrigation Science* 24.2, pp. 77–84. DOI: 10.1007/s00271-005-0012-x.

Orgaz, Francisco and Elías Fereres (2008). "Riego". In: *El cultivo del olivo*. Ed. by D. Barranco, R Fernández-Escobar, and L. Rallo. 6th. Coedition Mundi-Prensa and Junta de Andalucía, pp. 337–362.

Padilla-Díaz, Carmen M., Celia M. Rodriguez-Dominguez, Virginia Hernandez-Santana, Alfonso Perez-Martin, Rafael D.M. Fernandes, Antonio Montero, J.M. García, and J.E. Fernández (2018). "Water status, gas exchange and crop performance in a super high density olive orchard under deficit irrigation scheduled from leaf turgor measure-

ments". In: *Agricultural Water Management* 202.January, pp. 241–252. DOI: 10.1016/j.agwat.2018.01.011.

Padilla-Díaz, C.M., Celia M. Rodriguez-Dominguez, Virginia Hernandez-Santana, Alfonso Perez-Martin, and J.E. Fernández (2016). "Scheduling regulated deficit irrigation in a hedgerow olive orchard from leaf turgor pressure related measurements". In: *Agricultural Water Management* 164, pp. 28–37. DOI: 10.1016/j.agwat.2015.08.002.

Pastor, M, V Vega, and J C Hidalgo (2005). "Ensayos en plantaciones de olivar superintesivas e intesivas". In: *Vida Rural* November 2005, pp. 30–40.

Pinheiro, José, Douglas Bates, Saikat DebRoy, Deepayan Sarkar, and R Core Team (2017). *nlme: Linear and Nonlinear Mixed Effects Models*.

R Core Team (2015). *R: A Language and Environment for Statistical Computing*. Vienna, Austria.

Rius, X. and J.M. Lacarte (2010). *La revolución del olivar: El cultivo en seto*. Barcelona, p. 340.

Searles, Peter S., Diego A. Saravia, and M. Cecilia Rousseaux (2009). "Root length density and soil water distribution in drip-irrigated olive orchards in Argentina under arid conditions". In: *Crop and Pasture Science* 60.3, p. 280. DOI: 10.1071/CP08135.

Sokalska, D. I., D. Z. Haman, A. Szewczuk, J. Sobota, and D. Dereń (2009). "Spatial root distribution of mature apple trees under drip irrigation system". In: *Agricultural Water Management* 96.6, pp. 917–924. DOI: 10.1016/j.agwat.2008.12.003.

Sperry, J. S., U. G. Hacke, R. Oren, and J. P. Comstock (2002). "Water deficits and hydraulic limits to leaf water supply". In: *Plant, Cell and Environment* 25.2, pp. 251–263. DOI: 10.1046/j.0016-8025.2001.00799.x.

Stevens, Rob M. and Tim Douglas (1994). "Distribution of grapevine roots and salt under drip and full-ground cover microjet irrigation systems". In: *Irrigation Science* 15.4, pp. 147–152. DOI: 10.1007/BF00193681.

Villalobos, F.J., F. Orgaz, and L. Mateos (1995). "Non-destructive measurement of leaf area in olive (Olea europaea L.) trees using a gap inversion method". In: *Agricultural and Forest Meteorology* 73.1-2, pp. 29–42. DOI: 10.1016/0168-1923(94)02175-J.

CHAPTER 3

Relationships between fruit growth and oil accumulation with simulated seasonal dynamics of leaf gas exchange in the olive tree.

Published as: Hernandez-Santana, V., R.D.M. Fernandes, A. Perez-Arcoiza, J.E. Fernández, J.M. Garcia, and A. Diaz-Espejo (2018). "Relationships between fruit growth and oil accumulation with simulated seasonal dynamics of leaf gas exchange in the olive tree". In: Agricultural and Forest Meteorology 256-257.March, pp. 458–469. DOI: 10.1016/j.agrformet.2018.03.019.

Abstract

Carbohydrates availability, which are directly related to photosynthesis (A_N), and turgor are the main de- terminants of fruit growth. Since stomatal conductance (g_s) is the main limiting factor of A_N in fruit trees in most environments, and is strongly regulated by turgor, its measurement is pivotal to understanding fruit growth dynamics. Despite its relevance, the use of g_s to estimate A_N faces the major limitation of being difficult to measure in an automated and continuous manner. Based on these observations, and considering the control that the stomata exert on transpiration, and thus on sap flux density (J_s) under conditions of high coupling to the atmosphere, we conducted a multi-faceted experiment in olive trees. The main objective was to assess the use of continuously modeled A_N, derived using a simulated g_s, as a tool to study fruit growth and oil accumulation and other components of vegetative above-ground growth (leaf area and number of shoot internodes) in a super-high-density olive orchard under different irrigation levels. Sixteen olive trees under four different irrigation treatments (two control and two deficit irrigated, with one and two drip lines each) were continuously monitored with J_s sensors from May to November 2016. Gas exchange, fruit growth, number of shoot internodes and leaf area were measured periodically. Stomatal conductance was empirically simulated through J_s, and A_N was modeled using previously simulated g_s and a biochemical model of photosynthesis. Results showed that A_N can be accurately modeled from simulated g_s, obtained in turn from J_s measurements divided by pressure deficit. Moreover, the approach was shown to be sensitive enough to infer the response of g_s and A_N to soil water content and vapour pressure deficit. Interestingly, accumulated A_N was significantly related to fruit growth and oil content for all the irrigation treatments which determine the slope of these relations. In contrast, the relationship with leaf area was only significant for the control irrigation treatments, where the number of shoot internodes increased significantly more than in the water-stressed trees. Our results show that under water stress conditions trees prioritize fruit growth and oil content accumulation over vegetative growth, suggesting a higher sink strength for reproductive growth than for vegetative growth. We conclude that the use of sap flow and the proposed approach provides reliable g_s and A_N data, and allows the modeling of the relations between carbon assimilation and allocation, which are helpful to estimate fruit growth.

3.1 Introduction

Water is an increasingly scarce resource, but central to achieve a more productive agricultural output to feed the growing world population (Foley et al., 2011; Mueller et

al., 2012). Plants require water for growth and tissue expansion, with water absorbed by plants through their roots being lost through the stomata while CO_2 is taken up for photosynthesis. Stomatal opening is the main factor determining CO_2 uptake, and therefore, the synthesis of photoassimilates in the plant (Flexas and Medrano, 2002). Furthermore, stomatal closure is one of the earliest responses to water deficit (Martin-StPaul et al., 2017), markedly affecting water uptake and water movement through the plant. Stomatal conductance (g_s) is, therefore, a sensitive water stress indicator, directly related to plant function, shoot and fruit growth and, eventually, to yield (Jones and Tardieu, 1998). In addition to affecting the amount of carbohydrate available for the fruit, stomatal regulation ultimately determines the fruit water status through its effect on both leaf and fruit water potential (Ho et al., 1987; Fishman and Génard, 1998; Lechaudel et al., 2007).

Despite it being important to know g_s for ecophysiological studies and agricultural applications such as irrigation scheduling, its continuous and automated recording is not yet possible. However, new approaches have been recently proposed to conduct g_s estimations continuously, either by modifying the inverted equation of Penman-Monteith (Kučera et al., 2017), or by using its simplified version (McNaughton and Jarvis, 1983; Jarvis and McNaughton, 1986) as proposed by Hernandez-Santana et al. (2016b). Specifically, Hernandez-Santana et al. (2016b) proposed simulating g_s from sap flux density (J_s) values measured in the trunks of trees, divided by the air vapour pressure deficit (D). This avoids the uncertainty derived from upscaling from single point measurements of J_s in the trunk to the whole tree transpiration (Swanson, 1994; Lopez-Bernal et al., 2010; Hernandez-Santana et al., 2015; Berdanier et al., 2016). The automated estimation of g_s opens the possibility of using it both as a reliable water stress indicator and as an input in photosynthesis models which, when applied to fruit tree orchards, could help to predict yield. The mechanistic model of photosynthesis by Farquhar et al. (1980) has proven to be robust and easily applicable to many species and environments (Farquhar, 2001; Caemmerer, 2013). This model has been parameterised for many species of high agronomic interest (Diaz-Espejo et al., 2006; Egea et al., 2011; Greer and Weedon, 2012; Kattge and Knorr, 2007). After a correct parametrization, the main difficulty to its application rests in the estimation of g_s. However, once we have a value for g_s, A_N can be estimated from environmental variables, such that we can predict which region of the $A_N - g_s$ relationship our crop is in at any given moment. Considering the close analogy between the $A_N - g_s$ relationship and yield-transpiration (Flexas et al., 2010; Medrano, 2002; Morison et al., 2008; Parry et al., 2005), i.e., the two relations can be considered equivalent, the combination of sap flux density measurements and Farquhar et al.'s photosynthesis model may overcome the difficulty of applying a target level of water stress in deficit irrigated trees. For example, the known hyperbolic curve usually found between A_N and g_s justifies the maintenance of g_s values below the plateau region in which A_N hardly

increases, but g_s, and thus tree water use, still grows significantly, thereby decreasing water use efficiency (Parry et al., 2005).

However, there is no straightforward relationship between A_N and yield. Indeed, the fraction of photoassimilates going to each organ of the plant depends on a series of complex rules. Carbon allocation partitioning links source and sink plant organs through various regulations and interactions among different plant processes related to carbon metabolism (Génard et al., 2008). When A_N is limited by low soil water availability, the allocation partitioning patterns can change based on priority rules. These allocation patterns have been widely studied (Le Roux et al., 2001), although they are not easy to implement in agriculture because the mechanisms by which dry matter is distributed among organs are not fully understood (Marcelis, 1996). Nevertheless, biomass allocation patterns have been manipulated in agricultural species for years to achieve a gain in productivity by increasing the plant harvest index (the ratio of grain/fruit weight to total plant weight), which reflects the partitioning of photoassimilates between the grain/fruit and the rest of the plant (Sinclair, 1998; Morison et al., 2008). Indeed, the plant harvest index can be increased by using deficit irrigation strategies (Morison et al., 2008). In addition to saving water, deficit irrigation strategies can reduce vegetative growth without decreasing yield, i.e., they are effective in decreasing the carbon spent on vegetative growth without decreasing fruit growth as shown previously in olive (Iniesta et al., 2009; Dag et al., 2010; Hernandez-Santana et al., 2017). Thus, under limited available water, fruits augment their already strong carbohydrate sink capacity and have higher priority for assimilates than vegetative organs, leading to a reduced vegetative growth of roots, stem and leaves (Génard et al., 2008; Hacket-Pain et al., 2017). Therefore, knowing the irrigation strategy that can modify the growth patterns of a plant to enhance the biomass allocation to fruits rather than to vegetative organs, would allow us to control excessive vegetative growth with a reduced impact on fruit growth. In addition, this would lead to a net water saving in agriculture. Recent results indicate that 30–45% of the irrigation needs of a super-high-density olive orchard could be useful for this purpose (Hernandez-Santana et al., 2017). However, these results were based on values obtained at the end of the irrigation season of different years, and did not provide information about the dynamics during the fruit growth period.

In this work, we simulated the dynamics of g_s and A_N continuously over an irrigation season (late May to early November) in a hedgerow olive orchard with high plant density. Fruit size, oil content, leaf area and number of shoot internodes were frequently measured, to derive the correlation between accumulated A_N and fruit development. We followed the approach described in Hernandez-Santana et al. (2016b) to simulate g_s from continuous and automated J_s/D measurements, and then used the photosynthesis model by Farquhar et al. (Farquhar et al., 1980) to estimate A_N. Our hypothesis was that

this approach would allow the estimation of the temporal dynamics of fruit size and oil content since g_s is highly sensitive to water stress, the main limiting factor of A_N and a major regulator of the incoming and outgoing water fluxes of the fruit. We further hypothesized that knowing the dynamics of accumulated A_N would allow the dynamics of fruit growth, oil accumulation, leaf area and the number of shoot internodes to be simulated over the course of the season. Finally, we hypothesized that vegetative growth would be more affected by deficit irrigation than fruit growth. Thus, our specific aims were (1) to calibrate and validate an approach to simulate g_s and A_N based on automated J_s measurements, and (2) to assess the use of continuously simulated A_N as a tool to study fruit growth, oil accumulation and other components of vegetative aboveground growth (leaf area and shoot length) in a super-high-density olive orchard under different levels of irrigation.

3.2 Material and Methods

3.2.1 Orchard and climate characteristics

The experiment was conducted along the irrigation season (late May to early November) of 2016, in a commercial super-high-density orchard near Seville (Spain) (37°15′ N, −5°48′ W). At that time, the 'Arbequina' olive trees used were 10years old. They were planted in a 4 by 1.5 m formation (1667 trees ha^{-1}), in rows oriented N-NE to S-SW. The trees, with a single trunk and shoots from 0.6 to 0.7m above the ground, were pruned in December-January each year. The orchard soil (Arenic Albaqualf, USDA 2010) had a sandy loam top layer and a sandy clay layer underneath. The trees were planted at the top of 0.4m-high ridges. The amount of fertilizer was changed every month to match the crop needs (Troncoso et al., 2001). Further details on the orchard characteristics can be found in Fernández et al. (2013).

The area has a Mediterranean climate with hot and dry weather from May to September, being mild and wet for the rest of the year. Most of the annual rainfall occurs between late September and May. Average values in the area of potential evapotranspiration (ET_o) and precipitation (p) were 1531mm and 509mm, respectively, for the 2002–2016 period. For that period, average maximum and minimum air temperature values were 25.3°C and 10.9°C, respectively. The hottest months are July and August.

We applied four irrigation treatments: two control treatments, in which irrigation fulfilled tree water demand, with one (100C-1L) or two (100C-2L) dripper lines, and two sustained deficit irrigation treatments (SDI) in which 45% of the water added to control was applied along the whole irrigation season, with one (45SDI-1L) or two (45SDI-2L) dripper lines. The objective of these sub-treatments is to alter the equilibrium between root and leaf area with localized irrigation by drippers which have an important effect

on transpiration as shown preliminarily in (Diaz-Espejo et al., 2012). However, this aim is beyond the scope of this work. Moreover, the dripper lines were doubled in 2016 and thus, no effect was observed between the treatments with one and two dripper lines in this work. All lines were close to the trunk and each line had a 2 $L\,h^{-1}$ dripper placed every 0.5 m. We used a complete randomized design, with four plots (replicates) per treatment. Each plot consisted of 8 central trees surrounded by 16 border trees. For the 100C treatment, the trees were irrigated daily to replace 100% of the irrigation needs (IN). These were calculated on a daily basis as $IN = ET_C - P_e$, with ET_C being the maximum potential crop evapotranspiration calculated with the single crop coefficient approach (Allen et al., 1998) and P_e, the effective precipitation which, according to Orgaz and Fereres (1997), was calculated as 75% of the precipitation recorded in the orchard. Estimation of ET_C in this orchard has proven satisfactory in several studies (Diaz-Espejo et al., 2012; Fernández et al., 2013; Egea et al., 2016). The 45SDI treatments were aimed to replace 45% of IN. In the 2L plots, the irrigation time was scheduled to be half that of the 1L plots, so that the trees received the same volume of water despite having double the number of drippers. An irrigation controller (Agronic 2000, Sistemes Electrònics PROGRÉS,S.A., Lleida, Spain) was used to apply the calculated irrigation amounts (IA).

3.2.2 Meteorological measurements

Thirty-minute average values of main meteorological variables were recorded by a weather station (Campbell Scientific Ltd., Shepshed, UK) located in the centre of the area covered by the experimental plots. All meteorological sensors were located just above the tree canopies. The station recorded 30 min average values of air temperature (T_{air}), air humidity (RH) and photosynthetically active radiation (PAR), among other variables. Vapour pressure deficit (D) was calculated as a function of T_{air} and RH.

3.2.3 Measurement of predawn leaf water potential

Measurements of predawn leaf water potential ($\Psi_{l,pd}$, MPa) were conducted before dawn every other week from July to the beginning of November, with a Scholander-type pressure chamber (PMS Instrument Company, Albany, Oregon, USA). On each measurement day we sampled two leaves per tree of four trees per irrigation treatment. These values were used as a proxy of soil water potential.

3.2.4 Sap flux density measurements

The Compensation Heat Pulse (CHP) method (Green et al., 2003) was used to derive sap flux density (J_s, mm h^{-1}) values in the sapwood of sampled trees (Tranzflo NZ Ltd.,

Palmerston North, New Zealand). CHP consists of measuring the time for the temperature difference registered by two temperature probes located 10mm downstream and 5mm upstream of a heater probe to become 0 after the release of a heat pulse. Details on the calibration and testing of the technique for the olive tree, as well as on data analysis, are given in Fernández et al. (2001) and Fernández et al. (2006). One or two central trees per plot, in three plots per treatment, were monitored with one sap flow probe set on the east-facing side of trunks, 0.3–0.4m above-ground; four trees were used per treatment to give a total of 16. Each temperature probe measured J_s at a depth 5mm below the cambium, given that we observed in a previous study (Hernandez-Santana et al., 2016b) that J_s measured at this depth was strongly related to g_s measured in new, sun-exposed leaves. Measurements were made every 30min by releasing heat pulses (60J; 60W over 1s) at that frequency for the entire experimental period (from May 29 to November 8, 2016). A CR1000 datalogger connected to a AM25T multiplexer (Campbell, Campbell Scientific Ltd., Shepshed, UK) was used to release the heat pulses and to collect probe outputs.

3.2.5 Gas exchange measurement and modeling

Stomatal conductance was simulated after Hernandez-Santana et al. (2016b), i.e. from the collected J_s/D values and measured g_s. The simulated g_s values were the input of the model by Farquhar et al. (Farquhar et al., 1980) to estimate A_N. Briefly, we established regressions between g_s measured in new, sun-exposed leaves, and J_s measured in the trunk of the same tree, divided by D values calculated from the weather station at the orchard. The J_s/D vs. g_s calibration equations were established using 10–23 data points from each instrumented tree (Table 3.1).

The stomatal conductance values used for the equations were obtained from measurements of g_s and A_N, which were conducted on four clear days from May to August, every 30–60min from dawn to noon, in three sun-exposed current-year leaves per instrumented tree. The sampled leaves were on the SE-facing side of the canopy, i.e. on the sun-exposed side. In addition, we used a dataset obtained from measuring maximum g_s and A_N ($g_{s,max}$ and $A_{N,max}$) in two leaves per tree, conducted every other week in every tree instrumented with sap flow probes, from mid-July to the beginning of October, at 8:00-9:00 GMT, this being the time for maximum stomatal opening in olive leaves (Fernández et al., 1997). Data from five randomly selected days from this last dataset were not included in the calibration but, instead, were used to validate the calibration g_s equations. We used two portable photosynthesis systems (Li-cor 6400-XT, LI-COR, Lincoln NE, USA), with a 2cm x 3cm standard chamber, at ambient light and CO_2 conditions for these measurements.

A_N was modelled from the simulated g_s values following the procedure described

Table 3.1: Calibration equations descriptors to estimate stomatal conductance from the ratio between sap flux density and air vapour pressure deficit (slope, intercept, coefficient of determination (R^2), probability value (P) and calibrations points (N)) and validation statistical parameters (root mean squared error (RMSE), mean absolute error (MAE) and mean bias error (MBE)).

Treatment	Tree	Slope	Intercept	R^2	p	n	RMSE	MAE	MBE
								$mol\,m^{-2}\,s^{-1}$	
100C-1L	1	0.017	-0.138	0.834	<0.001	12	0.039	<0.001	-0.005
100C-1L	2	0.020	0.014	0.594	0.006	10	0.051	0.038	0.038
100C-1L	3	0.009	0.080	0.573	0.002	12	0.035	0.009	0.009
100C-1L	4	0.028	-0.055	0.514	0.009	11	0.038	0.032	0.032
100C-2L	1	0.018	0.035	0.534	0.007	11	0.041	0.012	0.012
100C-2L	2	0.007	0.047	0.499	0.008	12	0.042	0.019	0.019
100C-2L	3	0.013	0.037	0.758	<0.001	19	0.051	0.034	0.034
100C-2L	4	0.008	0.086	0.690	<0.001	12	0.062	<0.001	-0.025
45SDI-1L	1	0.010	0.028	0.669	<0.001	12	0.017	0.009	0.009
45SDI-1L	2	0.010	0.037	0.479	0.012	12	0.036	<0.001	-0.001
45SDI-1L	3	0.006	0.015	0.858	<0.001	19	0.031	<0.001	-0.004
45SDI-1L	4	0.007	-0.012	0.688	<0.001	15	0.035	<0.001	-0.014
45SDI-2L	1	0.009	0.030	0.502	0.010	11	0.015	0.007	0.007
45SDI-2L	2	0.004	0.015	0.844	<0.001	23	0.037	0.010	0.010
45SDI-2L	3	0.007	0.051	0.737	<0.001	18	0.025	<0.001	-0.005
45SDI-2L	4	0.013	0.059	0.634	<0.001	18	0.041	<0.001	-0.036

in the Section 3.6. The specific temperature responses for olive were taken from Diaz-Espejo et al. (2006). The maximum rate of ribulose bisphosphate (RuBP) carboxylation (V_{cmax}), maximum rate of electron transport (J_{max}) and mesophyll conductance to CO_2 (gm) were determined from five $A_N - C_i$ response curves measured in the instrumented trees of the 100C and 45SDI plots, regardless of the number of dripper lines. The curves were measured between 09:00 and 13:00 GMT during the experimental period (June 14th, 15th, 21st and 23rd) using two LI-6400 portable photosynthesis systems (LI-COR, Lincoln, NE, USA) at ambient temperature, saturating photosynthetic photon flux density (1600 $\mu mol\,m^{-2}\,s^{-1}$) and an ambient CO_2 concentration (C_a) of between 50 and 1500 $\mu mol\,mol^{-1}$ as described in Hernandez-Santana et al. (2016a). After steady-state photosynthesis was achieved, the response of A_N to varying C_i was measured by lowering C_a stepwise from 390 to 50 $\mu mol\,mol^{-1}$, returning to 390 $\mu mol\,mol^{-1}$ and then increasing C_a stepwise from 390 to 1500 $\mu mol\,mol^{-1}$. Each $A - C_i$ curve comprised 16 measurements, each made after at least 3min at each C_a. Maximum carboxylation rate (V_{cmax}) was estimated by the curve-fitting method proposed by Ethier and Livingston (2004). Diffusion

leaks were corrected following the procedure by Flexas et al. (2007). Rubisco kinetic parameters were taken from Bernacchi et al. (2002). The validation of the Farquhar et al. (Farquhar et al., 1980) equation to simulate A_N was conducted with the measured dataset as described above. Accumulated A_N is calculated summing up the quantity of simulated A_N every 30 minutes until the moment the value is showed.

3.2.6 Leaf area measurements

Measurements of leaf area were made at dawn every other week from June to October, with a LAI-2200 Plant Canopy Analyzer (Li-cor, Lincoln, NE, USA). We followed the approach proposed by Villalobos et al. (1995) for olive orchards. In this way, measurements were taken at eight locations per plot with the LAI-2200 Plant Canopy Analyzer, in each of the four plots per irrigation treatment (100C-1L, 100C-2L, 45SDI-1L, 45SDI-2L). Four of those locations per plot were just underneath the two central tree rows of the plot, providing the maximum leaf area index (LAI_{max}). The other four locations were in-between the two central rows of each plot, where LAI is minimum (LAI_{min}). The fraction of groundcover (GC) was used as a weighting factor to calculate the average leaf area index (LAI_{avg}) as $LAI_{avg} = LAI_{max}GC + LAI_{min}(1 - GC)$. Finally, the average tree leaf area per plot was calculated by multiplying LAI_{avg} by the ground area per plot, and dividing this by the number of trees in the plot.

3.2.7 Shoot growth

Shoot growth was assessed by measuring the number of internodes of four current-year shoots per tree, each from a cardinal point of the canopy and randomly selected in two trees per plot in each treatment (n=32). Measurements were made every 15 days from June 13 to October 31.

3.2.8 Fruit growth and yield determination

Fruit growth was determined from fruit dry weight and fruit diameter measurements. For fruit weight we randomly sampled six fruits per plot for each treatment; these were oven-dried for 48h and then weighed on a digital balance (XS105 Dual Range, Mettler Toledo, Greifensee, Switzerland). Fruit weight was measured from the beginning (May 30th) to the end of the irrigation season (November 9th) every other week.

In addition, in one tree from each of the 100C-2L and 45SDI-2L treatments we installed two fruit dendrometers (FI-XSSF, Solfranc, Tarragona, Spain) to monitor the seasonal courses of fruit equatorial diameter, logging these every 5min. The fruit dendrometers were connected directly to CR1000 dataloggers (Campbell Scientific Ltd., Shepshed, UK). When the diameters of the fruits were close to the maximum range of mea-

surement of the fruit dendrometers, an offset was added to the fruit dendrometer, by changing the position of one of its ends. The fruit dendrometers were installed on August 17th (day of year (DOY) 230) and were removed from the experimental plots a few days before harvesting (November 9th, DOY 313). Calculations of accumulated daily fruit equatorial diameter increment and A_N were started the day the fruit dendrometers were installed. To better understand the seasonal dynamics of fruit growth in relation to A_N, we also calculated the accumulation of the two variables over a period of three days; this value was divided by the number of days to obtain the rate per day such that fruit growth reflects the effect of a previously fixed carbon. Three days was assumed to be a reasonable period of time to integrate/translate the accumulated A_N into fruit growth.

Four central trees were also manually harvested at the end of the irrigation season (November 9th) to determine total fruit yield in each experimental plot. Samples were oven-dried and weighed separately to determine the dry fruit weight. The number of fruits was calculated from the total fruit yield and dry fruit weight.

3.2.9 Oil accumulation

Oil accumulated in the fruits was determined from June to November, both in 2014 and 2015. We manually collected around 100 fruits from a height of ca. 1.5 m for five out of the eight central trees of each plot (the three remaining trees were used to determine yield, as described above). After grinding the fruits ca. 20 g of fresh paste was obtained, which was dehydrated at 105°C. The oil of the dehydrated paste was chemically extracted by using hexane as a solvent during 4 h (Soxhlet's method, García et al. (2013)). Results were expressed as percentage of oil per fruit dry weight.

3.2.10 Statistical analyses

Relationships, coefficient of determination (R^2) and probability values (p) were determined using SigmaPlot (version 12.0, Systat Software Inc., San Jose, California, USA). Estimation accuracy was determined by the calculation of root mean square error (RMSE) and mean absolute error (MAE). We also calculated the mean bias error (MBE) to estimate the deviation of the predicted g_s. The closer that R^2 is to 1 and that RMSE and MAE are to 0, the better is the agreement between measured and calculated g_s values. The sign of MBE indicates whether simulated g_s is being underestimated (negative) or overestimated (positive). More details on the formulas used here and their meaning can be found in Abbas et al. (2011) and Walther and Moore (2005).

We used linear mixed models (LMM) with Tukey's post-hoc comparisons to analyze the effects of irrigation treatment (fixed factor) on mean fruit number and yield as dependent variables at p <0.05. No random factor was necessary as only one measure-

ment was made per plot. When no normal or heteroscedastic residuals were obtained, appropriate transformation of the variable was used. We also used analysis of covariance (ANCOVA) including the interaction term (accumulated A_N* irrigation treatment) to test whether the slopes of the regression lines for fruit weight, leaf area, oil content and number of shoot internodes were significantly different. For these analyses, we considered that the variables were linearly related even though for dry fruit weight and oil content a linear relation did not provide the best fit. This same analysis was conducted when comparing measured and modeled g_s and A_N to detect any effect of irrigation treatment. These analyses were conducted with R software (R Core Team, 2015) using R packages "nlmeR" (Pinheiro et al., 2017) and "multcompR" (Hothorn et al., 2008).

3.3 Results

3.3.1 Simulation of stomatal conductance and net photosynthesis rate

The J_s/D vs. g_s relationships derived from each instrumented tree all had high R^2 values (between 0.48 and 0.86, with the majority of trees being over 0.6) and were highly significant (all p values were $<$0.01 except for one, which was 0.012) (Table 3.1). The validation results confirmed the good agreement between measured and simulated g_s values calculated with the calibration equations. Moreover, the observed RMSE and MAE values were small and close to 0 for every instrumented tree, while MBE did not show any under- or overestimating bias for g_s. The validation of the simulated g_s and A_N, calculated by treatment, also showed good agreement with measured g_s and A_N (Fig. 3.1). The high R^2 (0.7), the slopes close to 1, and the y-intercepts close to zero in both cases, indicated a good level of accuracy between observed and simulated g_s and A_N. No bias produced by the irrigation treatments was detected.

3.3.2 Automated and continuous simulation of stomatal conductance and net photosynthesis rate

Once the strong correlation between the dynamics of J_s measured in the outer xylem of the trunk and that of g_s in new, sun-exposed leaves in the canopy was confirmed, and after validating the Farquhar et al. model to estimate A_N in the monitored olive trees, we inferred the time dynamics of g_s and A_N for 170 days at 30min intervals. The simulated daily values of maximum stomatal conductance ($g_{s,max}$, Fig. 3.2a) and net photosynthesis rate ($A_{N,max}$, Fig. 3.2b) showed that the seasonal dynamics of these variables were mainly driven by D and the irrigation treatment, i.e. $g_{s,max}$ and $A_{N,max}$ decreased as D increased (Fig. 3.2c), but they decreased with soil water potential (predawn leaf water potential, $\Psi_{l,pd}$, was used as a proxy). Thus, lower $g_{s,max}$ and $A_{N,max}$ values were simu-

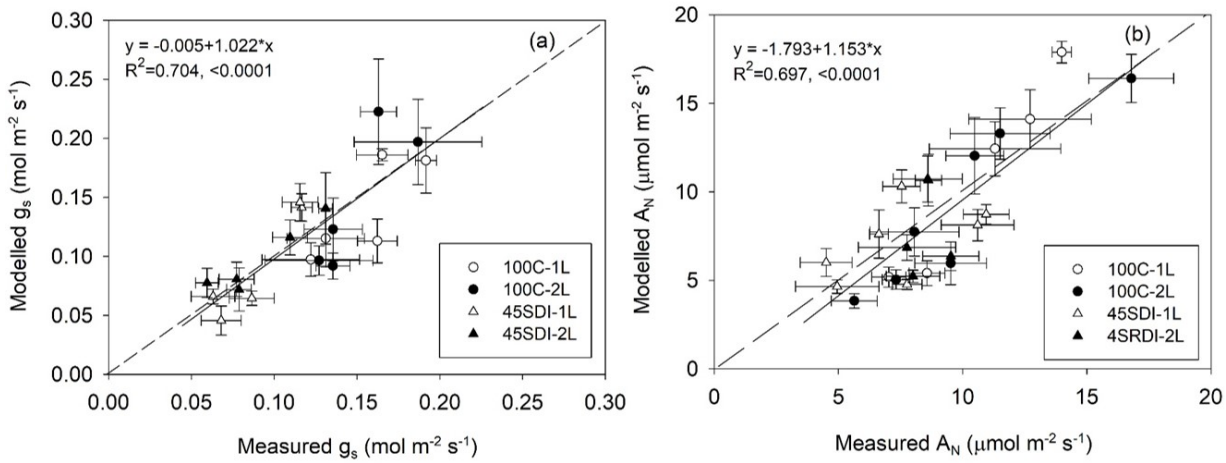

Figure 3.1: Comparisons of simulated (a) stomatal conductance (g_s) and measured g_s and (b) net photosynthesis rate (A_N). Measurements used to calculate the g_s calibration equations were not used in the validation results. Each point represents the average of four trees per treatment. Black symbols are control trees (100C), irrigated with one drip line (1L, circles), and two drip lines (2L, triangles). White symbols represent trees under deficit irrigation (45SDI) with one drip line (circles) and two drip lines (triangles). Dashed line represents the 1:1 relationship and the solid line the linear relationship between modeled and measured g_s. Bars are $\pm$ 1 SE.

lated in the 45SDI trees than in the 100C trees (Fig. 3.2d). The number of drip lines had no effect on these results.

3.3.3 Relationship between accumulated net photosynthesis and growth

Accumulated A_N was linearly related to the measured variables associated with vegetative growth, i.e. with leaf area (Fig. 3.3a) and number of shoot internodes (Fig. 3.3b). As mentioned in the Material and Methods section, accumulated A_N was calculated for the condition where the first day of measurement of fruit growth was taken as the baseline (A_N=0). The relationships between accumulated A_N and leaf area for the control irrigation treatments were strong and significant (100C-1L: R^2=0.95, p=0.002; 100C-2L: R^2=0.84, p=0.0002), but they were not for water-stressed trees (45SDI). The number of shoot internodes correlated well with A_N (100C-1L: R^2=0.95, p <0.0001; 100C-2L: R^2=0.98, p <0.0001; 45SDI-1L: R^2=0.76, p= 0.001; 45SDI-2L: R^2=0.91, p <0.0001), although in the case of 45SDI trees the slopes of the equations were very small despite the significant relationship (0.01–0.02 in 45SDI trees versus 0.04 in 100C).

On the other hand, the relationships between both dry fruit weight and oil content with A_N were strong and highly significant for all treatments, with power relationships providing the best fit (R^2=0.92–0.99, p <0.0001). However, the rate of increase in dry fruit weight was steeper at the beginning of the measurement period (Fig. 3.3c) than at the end, in contrast to the opposite holding true for oil accumulation (Fig. 3.3d).

An analysis of the regression equations suggests that the rate of increase of number

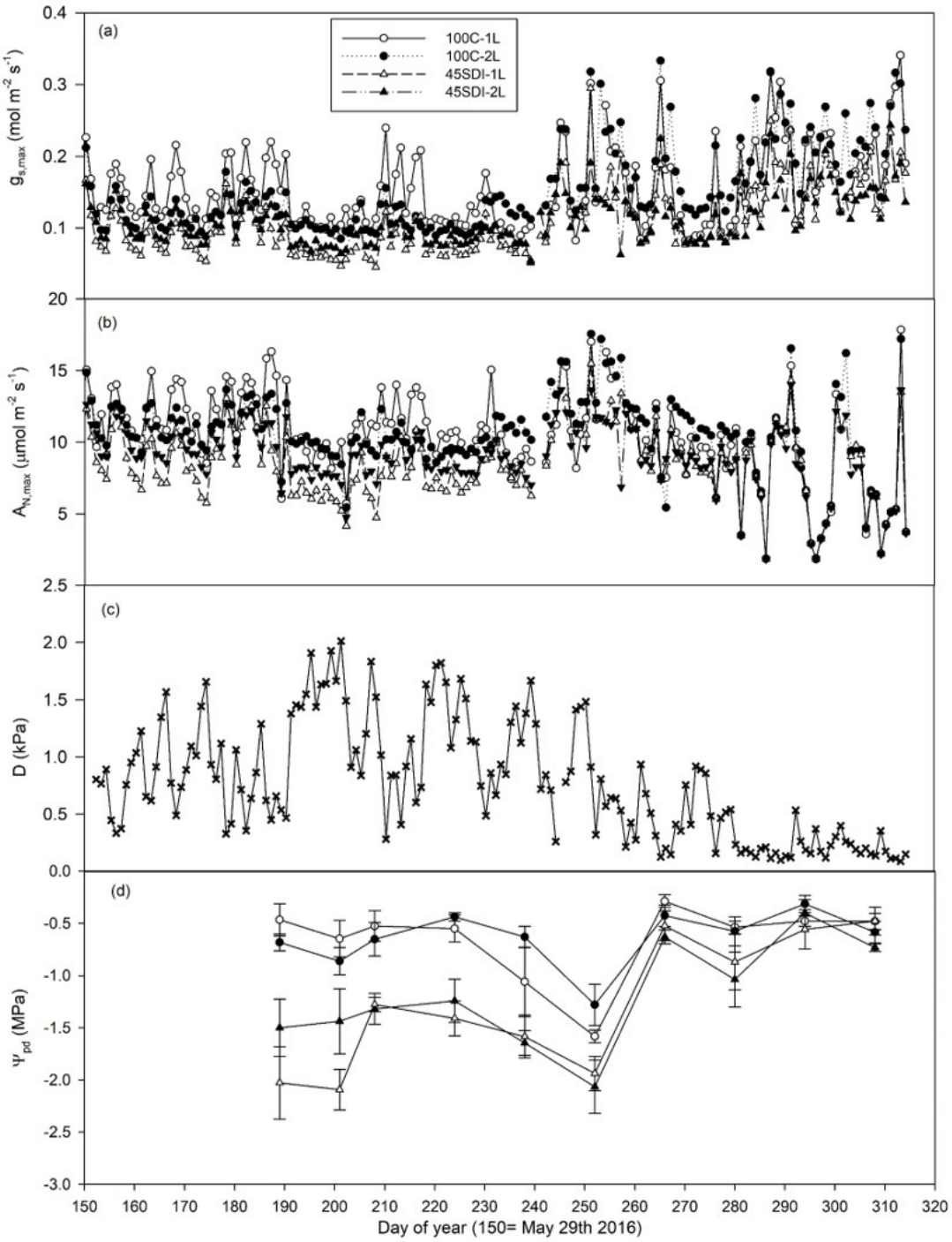

Figure 3.2: Temporal variation of (a) simulated daily maximum stomatal conductance ($g_{s,max}$), (b) simulated daily maximum photosynthesis rate ($A_{N,max}$), (c) vapor pressure deficit (D) measured at $g_{s,max}$ and $A_{N,max}$, (d) predawn leaf water potential ($\Psi_{l,pd}$) in the four irrigation treatments at the Sanabria experimental orchard. Symbols as in Fig. 3.1. Each point is the average of four trees; error bars are not shown for clarity purposes.

of shoot internodes (Fig. 3.3b) and olive oil accumulation were statistically different between 100C trees and 45SDI trees (different slopes), with either one or two dripper lines. In contrast, the slopes of the regression curves between dry fruit weight and accumulated A_N (Fig. 3.3c) were similar for all treatments, indicating a similar growth rate for

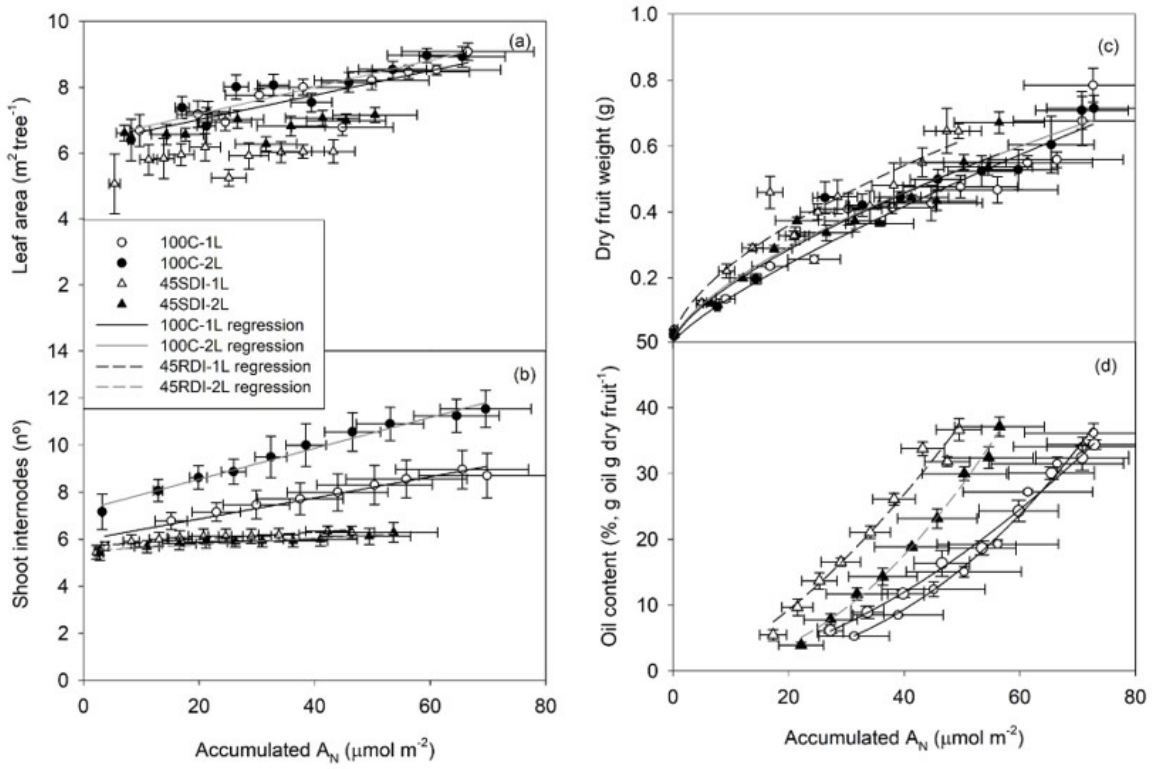

Figure 3.3: Relationship between accumulated net photosynthesis (A_N) and (a) leaf area, (b) number of shoot internodes, (c) dry fruit weight and (d) oil content. Symbols as in Fig. 3.1. Solid black and gray line are well-irrigated trees (100C) with one and two drip lines, respectively and dashed black and gray represent deficit irrigated trees (45SDI) with one and two drip lines, respectively. Each point for leaf area and internodes shoots is the average of four plots per treatment. Fruit weight symbols represent the average of 3-5 fruits. The calculation of accumulated A_N started on the first day that dry fruit weight was measured. Error bars are $\pm$ 1 SE.

fruits, regardless of the irrigation treatment.

Overall, and for all treatments, we observed a good agreement between accumulated A_N and both the number of shoot internodes and leaf area. However, the final fruit weight and the oil content were very similar despite the final accumulated A_N being different for the different treatments (Fig. 3). No statistical differences were found when comparing the number of fruits or the yield among treatments (Table 3.2), although the average yield reduction for the 45SDI treatments was 14% compared to the 100C yield.

Table 3.2: Final fruit number per plot, and yield averaged for each treatment. No significant differences were found among the irrigation treatments.

	100C-1L	100C-2L	45SDI-1L	45SDI-2L
Number of fruits (10^6)	22.3±2.32	25.5±2.97	25±1.73	20.9±8.6
Yield (kg ha^{-1})	16,817.7± 915.4	17,835.5± 1,082.5	16,062.9± 931.7	14,042.4± 832.7

The accumulated increase in fruit diameter measured with fruit dendrometers followed the seasonal dynamics of A_N (Fig. 3.4), with the increase in fruit diameter being

slightly higher in plot 9 tree (45SDI-2L) than in plot 15 tree (100C-2L), despite A_N being higher in the latter tree than in the former. The average fruit diameter was higher in the 100C-2L tree (7.966mm) than in the 45SDI tree (7.598mm) on DOY 231, at the beginning of the measurement period. However, the temporal dynamics of the fruit diameter increment were closely related to the rate of A_N accumulation in the two monitored trees for each irrigation treatment (Fig. 3.5).

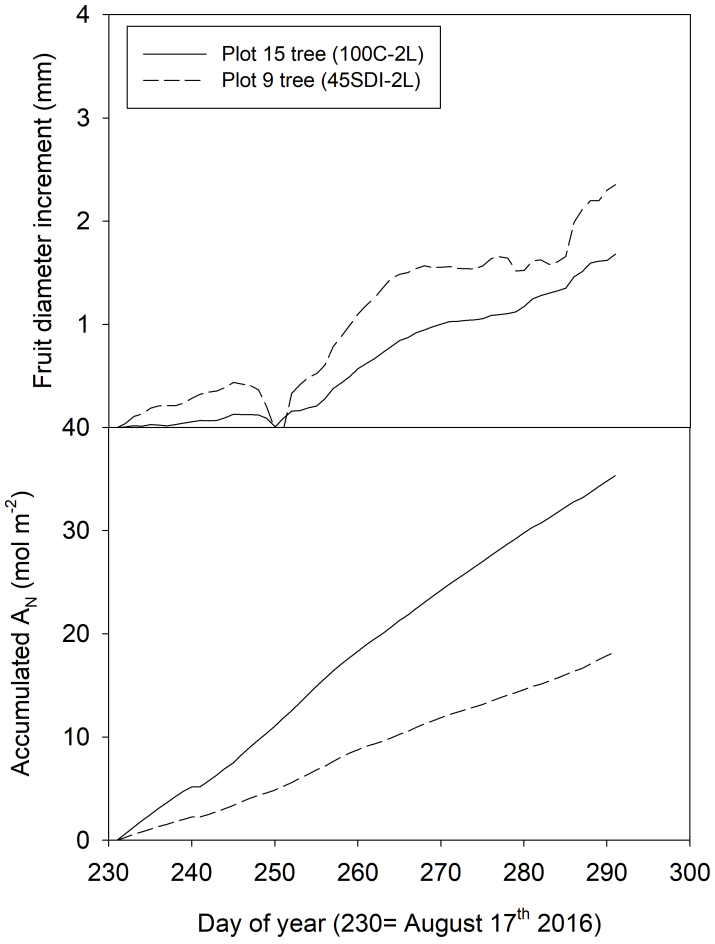

Figure 3.4: Fruit diameter increment and temporal dynamics of accumulated net photosynthesis (A_N) measured in two trees, one well-irrigated (plot 15 tree, 100C-2L) and one deficit-irrigated (plot 9 tree, 45SDI-2L). The lines of fruit diameter correspond to the average of two fruits; standard errors not shown for clarity purposes. Initial diameter was 7.966 and 7.598 mm on average for the two fruits measured in 100C-2L and 45SDI-2L trees, respectively.

3.4 Discussion

3.4.1 Automated simulation of leaf gas exchange

This study builds on the g_s simulation method reported in Hernandez-Santana et al. (2016b) and presents a new, simplified approach for tracking gas exchange in a continu-

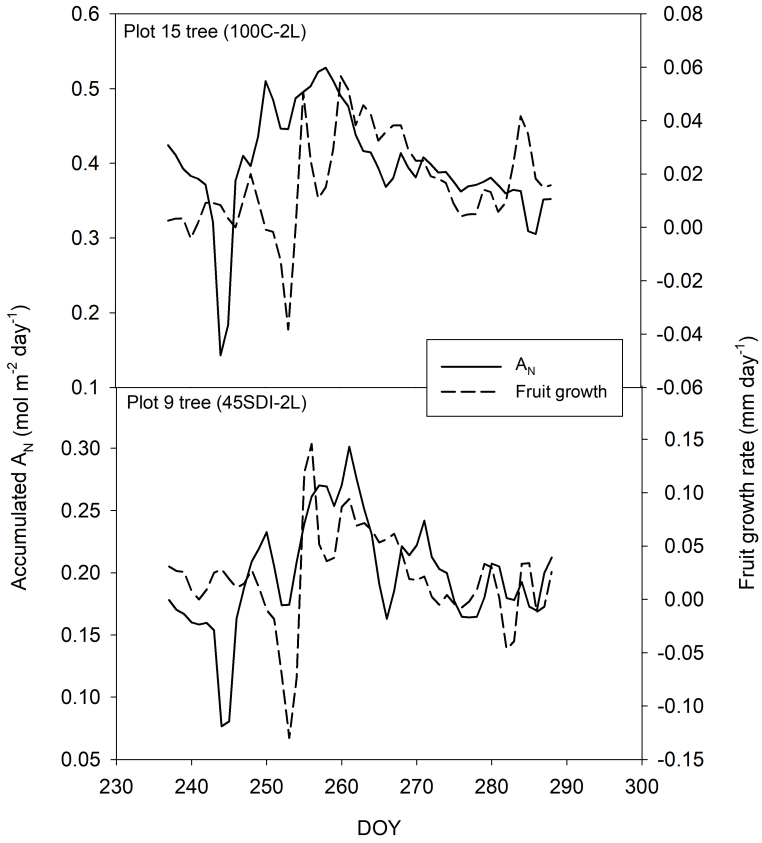

Figure 3.5: Increase in rate per day of net photosynthesis (A_N) and fruit diameter calculated as the sum of each variable for three days, divided by that number of days. The measurements were conducted in two fruits of two trees exposed to different irrigation treatments: the plot 9 tree is under deficit irrigation with two drip lines (45SDI-2L), while the plot 15 tree is well-irrigated with two drip lines (100C-2L).

ous manner and for studying its relationship with leaf area, number of shoot internodes, fruit growth and oil accumulation in olive trees. These results open the gate to develop a novel approach to manage the level of stress of the plant by irrigation, although still some uncertainties must be explored like the determination of photoassimilates partitioning to fruits vs other plant organs under a range of water stress levels, the effect of xylem-fruit water potential gradients on fruit growth or how to scale-up from fruit growth to yield considering different crop loads. Stomatal conductance was simulated from sap flow-related measurements and easy-to-record meteorological values. The proposed approach is sensitive enough to infer stomatal response to soil water availability and to D, and to quantify their impact on A_N (Fig. 3.2). The approach can be fully automated and provides values representative of the whole canopy (thereby avoiding errors derived from the natural variability among leaves). Importantly, it does not require any upscaling, or for any assumptions to be made about any parameter. Moreover, it does not require the measurement of total leaf area or environmental variables other than D in contrast to other approaches using sap flow data to simulate gas exchange at the canopy level (Granier et al., 2000; David et al., 2007; López-Bernal et al., 2015;

Kučera et al., 2017). Using direct measurements of J_s allows the use of sap flow probes with a single temperature sensor, which makes the method cheaper, as demonstrated by López-Bernal et al. (2017). In addition, the number of sensors required to assess the level of water stress is also reduced as it is not necessary to apply the signal intensity concept, in which measurements should be made both in treatment and in reference trees (Goldhamer and Fereres, 2004).

If used for scheduling irrigation, the described approach has two potential advantages: it is based on absolute values of $g_{s,max}$, which have a solid physiological meaning in relation to plant water stress (Medrano, 2002), and allows quantification of the A_N limitation imposed by deficit irrigation, which is an indicator of yield (Hernandez-Santana et al., 2017). Moreover, g_s and A_N tracking overcomes one of the shortcomings of other water stress indicators widely used for scheduling irrigation, which do not consider key intrinsic processes related to fruit development (Bustan et al., 2011). Although the relationships between gas exchange measurements and fruit growth or oil accumulation are not straightforward, g_s and A_N provide more information on fruit growth than other water stress indicators. Stomata regulate the carbohydrate source and, indirectly, the incoming-outgoing fluxes in the fruit, through their effect on leaf, stem and fruit water potentials, driven in turn, by osmotic pressure and hydrodynamics (Zonia and Munnik, 2007).

3.4.2 Growth partitioning under water stress

The proposed approach is also able to predict A_N, which thus increases the value of the approach for the management of irrigation. This is due to A_N being closely related to plant growth, function, productivity and yield, in response to water deficit (Flexas et al., 2004; López-Bernal et al., 2015; Ramírez et al., 2016). As mentioned, A_N is, together with the accumulation of water, i.e. turgor, one of the determinants of fruit growth (Fishman and Génard, 1998). Our data show that reduced soil water availability, induced by SDI, modified the supply of photoassimilates through the reduction of A_N, and altered the relationships between these photoassimilates and the growth of different plant organs (Fig. 3.3). We found that fruit growth was less affected in water-stressed trees than was leaf area and the number of shoot internodes. The reduced slopes of the A_N-shoot growth relationship in 45SDI trees and the non-relationship between accumulated A_N and leaf area for that treatment, confirmed that vegetative growth in our water-stressed trees was reduced. The steeper slopes of the same relationships in well-irrigated trees indicated that growth occurred to a point suggesting that well-irrigated trees were photosynthesising enough to promote both fruit and vegetative growth. However, under conditions of water stress, 45SDI trees dedicated most of their A_N to fruit growth and oil accumulation (Fig. 3.3). Other authors working with forest and agronomical species reported

similar results (e.g., Dag et al. (2010), Müller-Haubold et al. (2013), Selås et al. (2002), Intrigliolo and Castel (2007b), Hacket-Pain et al. (2017), and Hernandez-Santana et al. (2017)), demonstrating that the competing sink relationships between vegetative growth (stem or leaves) and fruit production for newly assimilated carbon were dependent on drought. This indicates that the biological costs of reproduction increase strongly under conditions of environmental stress, penalizing vegetative growth but having no detrimental effect on vegetative growth under favourable climatic conditions (Hacket-Pain et al., 2017). Accordingly, studies on leaf-fruit water relations in olive suggest that vegetative growth is more sensitive to drought than fruit growth, and that this sensitivity can be modulated by crop load (Dell'Amico et al., 2012; Girón et al., 2015a). However, this is the first time that the hypothesis of a higher response of vegetative growth versus reproductive growth to water stress has being tested in olive. We showed that the relationship between A_N and fruit dry matter depends on the level of irrigation. Thus, in future implementations of the model, the prediction of fruit dry matter accumulation should consider the increment towards reproductive sinks under water stress conditions. In agricultural species, carbon allocation to reproductive organs is particularly important in economic terms because of its impact on fruit yield.

3.4.3 Estimation of fruit growth and oil content

Our results support the use of the described approach to simulate the impact of water management on fruit and oil yields, which are the major production targets for farmers. More work is needed, however, to achieve the objectives of predicting fruit growth and thus, crop yield, which is beyond the scope of the present study. First, predicting fruit growth in terms of fresh weight might even be more complicated because it is determined by water besides biomass accumulation, which in turn, is a consequence of changes in water flows into and out of the fruit with the parent plant and also of transpiration losses from the fruit (Greenspan et al., 1994; Greenspan et al., 1996; Matthews and Shackel, 2005). This water fruit balance has been described to change toward the end of fruit development (Matthews and Shackel, 2005). Moreover, these results may apply particularly well in olive where the water component is less important than in other species where water flows are major determinants of fruit growth such as grape (Greenspan et al., 1996), peach (Morandi et al., 2007b), pear (Morandi et al., 2014a), etc. Secondly, the relationship between A_N and yield is not so straightforward, with yield determined not only by fruit size but also by fruit number. Fruit number is highly associated with the number of leafy shoots from the previous year, and therefore, leaf area plays a key role in determining yield, as was shown for the studied orchard by Hernandez-Santana et al. (2017). Naor et al. (2013) reported that in trees with a higher crop load, fruit size decreased, suggesting a stronger competition for assimilates among

fruits. This was not the case in our study, in which the number of fruits and their size was statistically similar for all treatments. However, it is likely that under more stressful conditions, or under other conditions in which the ratio between leaf area and crop load is further reduced, we could have observed a limitation in yield produced by the number of fruits, as we did in other years in the same orchard (Fernández et al., 2013; Hernandez-Santana et al., 2017). The effect of the irrigation strategy on yield, whether regulated or sustained, is not the objective of this work and one irrigation season is not enough to evaluate the effects of an irrigation strategy on yield. Still, our study shows a remarkably tight correlation between fruit growth and accumulated A_N (Fig. 3.5). In our case, the main driving variable for A_N was D, which has a direct effect on stomatal regulation and confirms that diffusional limitations of photosynthesis are the main constraints for plant production in our environment (Flexas et al., 2014). Mechanistic models dealing with fruit growth (Lechaudel et al., 2007; Lescourret and Génard, 2005) could facilitate the calculation of yield based on gas exchange modeling.

As oil production is a key feature of olive cultivation, we also evaluated oil accumulation and observed that the final oil content in the fruit was slightly higher in water-stressed trees than in well-irrigated trees (Fig. 3.3d). Although accumulated A_N did not start from 0 (Fig. 3.3d) – because the baseline used to calculate accumulated A_N was the first day that fruit growth was measured – the dynamics of oil content accumulation in relation to A_N would have been similar if the baseline selected was different. In agreement with our results, other authors reported for olive that oil content in the fruit was less affected by water stress than shoot growth (Gómez-del-Campo, 2013), fruit size (Gómez-del-Campo et al., 2014) or yield (Dbara et al., 2016). It has been demonstrated that the amount of water in the fruit is most sensitive to decreases in irrigation supplies than is the amount of oil, which is less impacted by water deficit (Gómez-del-Campo et al., 2014). In our study, both fruit weight and oil content were expressed in dry weight terms to avoid misinterpretations due to the impact of the irrigation treatment on the fruit water content. The fruit dendrometers, however, measured the fruit diameter "in vivo", thus including the effect of changes on fruit water content. The use of fruit dendrometers is promising as these instruments work automatically and provide data with a high temporal resolution (Figs. 3.4 and 3.5). Similarly to trunk dendrometers, however, the interpretation of the signal to separate the effect of water relations from biomass accumulation is challenging (Fernández and Cuevas, 2010; Mencuccini et al., 2013; De Swaef et al., 2015). In our case, the slightly higher fruit growth in the 45SDI-2L trees, as compared to the 100C-2L trees, suggests that growth is less affected by the relatively mild atmospheric demand typical of the end of the summer (Fig. 3.2) in the smaller fruits of the 45SDI-2L. However, these results should be considered with caution because we used just two fruit dendrometers per treatment.

3.4.4 Consequences for scheduling deficit irrigation

Our findings increase the understanding of the trade-off between vegetative growth and fruit growth, and show that oil accumulation in the olive is dependent on soil water availability. A priority in dry environments, which will become even drier in the future, will be to produce more with less water. To face this challenge, irrigation management must be adapted to maximize fruit production while avoiding excessive tree growth. Excessive growth is, in fact, a major a problem in super-high-density orchards (Connor et al., 2014; León et al., 2007). Applying deficit irrigation strategies designed to optimize the carbon allocation patterns could lead to trees of reduced size, i.e., requiring less water, without severely penalizing production. Indeed, the large gain in productivity among fruit tree species is often the result of the manipulation of the carbon allocation pattern within the plant, the objective being to increase the number and size of fruits produced as a result of higher fruit competition for carbohydrates, as has been conducted in agricultural species for years (Génard et al., 2008). Deficit irrigation can extend the modification of these patterns further by enhancing fruit load and quality while controlling vegetative growth. Combined with pruning and a properly designed fertilization strategy, this approach will help to achieve the right balance between fruit and vegetative growth.

While a sustained irrigation strategy was used in the present study, regulated deficit irrigation (Chalmer et al., 1981) is often recommended for super-high-density olive orchards (Fernández et al., 2013). However, information is lacking concerning the main processes underlying crop performance to irrigation, which makes it a challenging task to design regulated deficit irrigation strategies that are pertinent to specific orchard conditions and production targets. Scheduling irrigation with a mechanistic approach as was used here could help to establish a regulated deficit irrigation strategy for each case. Although the relationships established between g_s, A_N, plant and fruit dry weight, as well as oil content, could help to establish an irrigation deficit approach based on physiological measurements, they still have to be assessed further in different olive orchards and under various environmental conditions.

3.5 Conclusions

Our results demonstrate that fruit growth can be simulated using accumulated photosynthesis, being this relation dependent on the level of irrigation. Photosynthesis is not the only determinant of growth, being the other key variable involved in fruit growth, turgor pressure, set by stem/fruit water potential gradients, also related to fruit growth via g_s, at least in a daily basis. Future efforts must be focused on studying the interrelations among leaf, stem and fruit water relations, as well as the physiological traits

determining photoassimilate partitioning between both organs. In this sense, the use of sap flow measurements for monitoring tree performance emerges as a powerful tool to understand the mechanisms involved in the dynamics of fruit growth in tree crops and their relationship with leaf gas exchange. Although sap flow monitoring can be used directly to evaluate the seasonal response to irrigation management, we used it in our approach to simulate g_s empirically. Knowing the diurnal and seasonal dynamics of g_s allows us not only to estimate transpiration with tree leaf area, but also to estimate photosynthesis. Moreover, our approach could also be used to develop process-based models of g_s, which could help us understand why crops respond differently under a given environmental condition. Mechanistic models can provide information about plant responses to increased atmospheric CO^2, providing an approach to test mechanisms by which plants can acclimate to changes in the environment. Although the use of the methodology proposed in this study should be further tested in different species and under a range of management and environmental conditions, the estimation of g_s and its use in mechanistic models emerge as the core component of the new generation of methods and tools to schedule irrigation and predict yield in the future.

3.6 Appendix: Biochemical model of photosynthesis

This appendix presents equations necessary to reproduce the model used in this study to estimate net photosynthesis rate (A_N). We estimated stomatal conductance to H_2O (g_s) from sap flow as described in the Material and Methods section, following the procedure described in Hernandez-Santana et al. (2016a) and Hernandez-Santana et al. (2016b). Then A_N was estimated following the widely used biochemical model by Farquhar et al. (1980). The supply function for net photosynthesis rate (A_s) is described by Fick's law as

$$A_s = g_{CO2,total}.(C_a - C_c) \tag{3.1}$$

where C_a is ambient CO_2, C_c is chloroplastic CO_2 and $g_{CO2,total}$ is the total conductance to CO_2 ($1/g_{CO2,total} = 1/g_{s,CO2} + 1/g_m$). In the former equation $g_{s,CO2} = g_s/1.6$.

We used the biochemical model of Farquhar et al. (1980) and the gas exchange equations of Von Caemmerer and Farquhar (1981) to simulate the demand function for net photosynthesis rate (A_d) based on the RuBP-carboxylation-limited and RuBP-regeneration-limited rates (A_c and A_q) as follows:

$$A_d = min(A_c, A_q, A_p) - R_d, \tag{3.2}$$

$$A_c = V_{cmax} \frac{C_c - \Gamma^*}{C_c + K_c \left[1 + (\frac{o_i}{K_o})\right]}, \tag{3.3}$$

$$A_q = J \frac{(C_c - \Gamma^*)}{4(C_c + 2\Gamma^*)}, \tag{3.4}$$

where V_{cmax} is the carboxylation capacity, J is the potential electron transport rate, C_c is the chloroplastic CO_2 concentration, K_c and K_o are the Michaelis constants for RuBP carboxylation and oxygenation, respectively, O is the oxygen concentration and R_d is the rate of non-photorespiratory CO_2 release.

A nonrectangular hyperbolic function (Farquhar and Wong, 1984) was used to calculate J as a function of irradiance (PPFD),

$$\theta J^2 - (\alpha PPFD + J_{max})J + \alpha PPFD J_{max} = 0 \tag{3.5}$$

where J_{max} is the maximum rate of electron transport under saturating irradiance, α is the quantum efficiency of electron transport and θ describes the degree of curvature of the function (Table 3.3).

Table 3.3: Values of carboxylation capacity (V_{cmax}), the maximum potential electron transport rate (J_{max}) and mesophyll conductance to CO_2 (g_m) used in this study. These parameters were estimated from the analysis of $A_N - C_i$ measured under field conditions as explained in Material and Methods.

	WW	WS
V_{cmax} (μmol m^2 s^{-1})	199.4 $\pm$ 19.4	162.2 $\pm$ 14.7
J_{max} (μmol m^2 s^{-1})	154.2 $\pm$ 8.4	170.5 $\pm$ 10.6
g_m (mol m^2 s^{-1})	0.341 $\pm$ 0.064	0.226 $\pm$ 0.040

Several parameters in this photosynthesis model have a high dependence on temperature. We used the following equations to describe these temperature dependencies:

$$y(T_k) = y_{25} exp(c_1 - c_3 T_k^{-1}) \left(\frac{1 + exp(c_2 - c_4 T_r^{-1})}{1 + exp(c_2 - c_4 T_k^{-1})} \right) \tag{3.6}$$

where $y(T_k)$ is the value of a parameter at a temperature T_k (kelvins); y_{25} is the parameter's value at T_k =298.15K (25°C) (for V_{cmax}, J_max and g_m those shown in Table 3.3); T_r =298.15K; and c_1, c_2, c_3 and c_4 are empirical parameters whose values used in this study for olive are suitable in Table 3.4.

At steady state the demand and supply functions are equal ($A_d = A_s$), and A_N is given by the intersection of A_s and A_d:

$$A_N = A_s \cap A_d. \tag{3.7}$$

This intersection leads to a quadratic equation whose positive root is equal to A_N.

Table 3.4: Parameter values used in this study for responses of photosynthetic parameters to temperature. Values at 25°C (y_{25}) varied across leaves, treatments and species, except that we assumed y_{25} = 272.38 Pa for K_c, 165.82 kPa for K_o and 37.43 Pa for Γ^*, based on Bernacchi et al. (2002). T_r=298.15K.

parameter y	c_1 (unitless)	c_2 (unitless)	c_3 (K)	c_4 (K)	source
K_c	32.6	0	$c_1.T_r$	0	1
K_o	9.57	0	$c_1.T_r$	0	1
Γ^*	9.87	0	$c_1.T_r$	0	1
V_{cmax}	18.7	0	$c_1.T_r$	0	2
J_{max}	19.53	43.05	$c_1.T_r$	13,608.7	2
g_m	32.27	45.87	$c_1.T_r$	13,608.7	3
R_d	18.07	0	$c_1.T_r$	0	2

Sources: (1) Bernacchi et al. (2002); (2) Diaz-Espejo et al. (2006); (3) Diaz-Espejo et al. (2007).

References

Abbas, Farhat, Ali Fares, and Samira Fares (2011). "Field calibrations of soil moisture sensors in a forested watershed". In: *Sensors* 11.6, pp. 6354–6369. DOI: 10.3390/s110606354.

Allen, R., L. S. Pereira, D. Raes, and M. Smith (1998). *Crop evapotranspiration - Guidelines for computing crop water requirements*. Rome: FAO Irrigation and Drainage, p. 15.

Berdanier, Aaron B., Chelcy F. Miniat, and James S. Clark (2016). "Predictive models for radial sap flux variation in coniferous, diffuse-porous and ring-porous temperate trees". In: *Tree physiology* 36.8, pp. 932–941. DOI: 10.1093/treephys/tpw027.

Bernacchi, C J, A R Portis, H Nakano, S Von Caemmerer, and S P Long (2002). "Temperature responses of mesophyll conductance. Implications for the determination of rubisco enzyme kinetics and for limitation to photosynthesis in vivo." In: *Plant Physiology* 130.December, pp. 1992–1998. DOI: 10.1104/pp.008250.water.

Bustan, Amnon, Avishai Avni, Shimon Lavee, Isaac Zipori, Yelena Yeselson, Arthur A. Schaffer, Joseph Riov, and Arnon Dag (2011). "Role of carbohydrate reserves in yield production of intensively cultivated oil olive (Olea europaea L.) trees". In: *Tree Physiology* 31.5, pp. 519–530. DOI: 10.1093/treephys/tpr036.

Caemmerer, S. von (2013). "Steady-state models of photosynthesis". In: *Plant, Cell & Environment* 36.9, pp. 1617–1630. DOI: 10.1111/pce.12098.

Chalmer, D.J., P.D. Mitchell, and L. van Heek (1981). "Control of peach tree growth and-productivity by regulated water supply, tree density and summer pruning". In: *J. Amer. Soc. Hort. Sci.* 106, pp. 307–312.

Connor, David J., Maria Gómez-del-Campo, M. Cecilia Rousseaux, and Peter S. Searles (2014). "Structure, management and productivity of hedgerow olive orchards: A re-

view". In: *Scientia Horticulturae* 169, pp. 71–93. DOI: 10.1016/j.scienta.2014.02.010.

Dag, Arnon, Amnon Bustan, Avishai Avni, Isaac Tzipori, Shimon Lavee, and Joseph Riov (2010). "Timing of fruit removal affects concurrent vegetative growth and subsequent return bloom and yield in olive (Olea europaea L.)" In: *Scientia Horticulturae* 123.4, pp. 469–472. DOI: 10.1016/j.scienta.2009.11.014.

David, T. S., M. O. Henriques, C. Kurz-Besson, J. Nunes, F. Valente, M. Vaz, J. S. Pereira, R. Siegwolf, M. M. Chaves, L. C. Gazarini, and J. S. David (2007). "Water-use strategies in two co-occurring Mediterranean evergreen oaks: Surviving the summer drought". In: *Tree Physiology* 27.6, pp. 793–803. DOI: 10.1093/treephys/27.6.793.

Dbara, Soumaya, Matthew Haworth, Giovani Emiliani, Mehdi Ben Mimoun, Aurelio Gómez-Cadenas, and Mauro Centritto (2016). "Partial root-zone drying of olive (olea europaea var. 'chetoui') induces reduced yield under field conditions". In: *PLoS ONE* 11.6, pp. 1–20. DOI: 10.1371/journal.pone.0157089.

De Swaef, Tom, Veerle De Schepper, Maurits W. Vandegehuchte, and Kathy Steppe (2015). "Stem diameter variations as a versatile research tool in ecophysiology". In: *Tree Physiology*. Ed. by Danielle Way, pp. 1–15. DOI: 10.1093/treephys/tpv080.

Dell'Amico, J., A. Moriana, M. Corell, I.F. F. Girón, D. Morales, A. Torrecillas, F. Moreno, J. Dell'Amico, A. Moriana, M. Corell, I.F. F. Girón, D. Morales, A. Torrecillas, F. Moreno, J. Dell'Amico, A. Moriana, M. Corell, I.F. F. Girón, D. Morales, A. Torrecillas, and F. Moreno (2012). "Low water stress conditions in table olive trees (Olea europaea L.) during pit hardening produced a different response of fruit and leaf water relations". In: *Agricultural Water Management* 114.November 2012, pp. 11–17. DOI: 10.1016/j.agwat.2012.06.004.

Diaz-Espejo, Antonio, A. S. Walcroft, José Enrique Fernández, B. Hafridi, M. J. Palomo, and I. F. Girón (2006). "Modeling photosynthesis in olive leaves under drought conditions." In: *Tree physiology* 26.11, pp. 1445–1456. DOI: 10.1093/treephys/26.11.1445.

Diaz-Espejo, Antonio, Emilio Nicolás, and José Enrique Fernández (2007). "Seasonal evolution of diffusional limitations and photosynthetic capacity in olive under drought". In: *Plant, Cell and Environment* 30.8, pp. 922–933. DOI: 10.1111/j.1365-3040.2007.001686.x.

Diaz-Espejo, Antonio, T.N. Buckley, J.S. Sperry, M.V. Cuevas, A. de Cires, S. Elsayed-Farag, M.J. Martin-Palomo, J.L. Muriel, A. Perez-Martin, C.M. Rodriguez-Dominguez, A.E. Rubio-Casal, J.M. Torres-Ruiz, and J.E. Fernández (2012). "Steps toward an improvement in process-based models of water use by fruit trees: A case study in olive". In: *Agricultural Water Management* 114, pp. 37–49. DOI: 10.1016/j.agwat.2012.06.027.

Egea, Gregorio, María M. González-Real, Alain Baille, Pedro A. Nortes, and Antonio Diaz-Espejo (2011). "Disentangling the contributions of ontogeny and water stress to photosynthetic limitations in almond trees". In: *Plant, Cell and Environment* 34.6, pp. 962–979. DOI: 10.1111/j.1365-3040.2011.02297.x.

Egea, Gregorio, Antonio Diaz-Espejo, and José E. Fernández (2016). "Soil moisture dynamics in a hedgerow olive orchard under well-watered and deficit irrigation regimes: Assessment, prediction and scenario analysis". In: *Agricultural Water Management* 164, pp. 197–211. DOI: 10.1016/j.agwat.2015.10.034.

Ethier, G. J. and N. J. Livingston (2004). "On the need to incorporate sensitivity to CO2 transfer conductance into the Farquhar-von Caemmerer-Berry leaf photosynthesis model". In: *Plant, Cell and Environment* 27.2, pp. 137–153. DOI: 10.1111/j.1365-3040.2004.01140.x.

Farquhar, G. D. (2001). "Models of Photosynthesis". In: *Plant Physiology* 125.1, pp. 42–45. DOI: 10.1104/pp.125.1.42.

Farquhar, G. D., S. von Caemmerer, and J A Berry (1980). "A biochemical model of photosynthetic CO2 assimilation in leaves of C3 species". In: *Planta* 149.1, pp. 78–90. DOI: 10.1007/BF00386231.

Farquhar, GD and SC Wong (1984). "An Empirical Model of Stomatal Conductance". In: *Australian Journal of Plant Physiology* 11.3, p. 191. DOI: 10.1071/PP9840191.

Fernández, J.E. and M.V. Cuevas (2010). "Irrigation scheduling from stem diameter variations: A review". In: *Agricultural and Forest Meteorology* 150.2, pp. 135–151. DOI: 10.1016/j.agrformet.2009.11.006.

Fernández, J.E., F. Moreno, I. F. Girón, and O. M. Blázquez (1997). "Stomatal control of water use in olive tree leaves". In: *Plant and Soil* 190.2, pp. 179–192. DOI: 10.1023/A:1004293026973.

Fernández, J.E., M. J. Palomo, Antonio Diaz-Espejo, B. E. Clothier, S. R. Green, I.F. Girón, and F. Moreno (2001). "Heat-pulse measurements of sap flow in olives for automating irrigation: Tests, root flow and diagnostics of water stress". In: *Agricultural Water Management* 51.2, pp. 99–123. DOI: 10.1016/S0378-3774(01)00119-6.

Fernández, J.E., P.J. Durán, M.J. Palomo, Antonio Diaz-Espejo, V. Chamorro, and I. F. Girón (2006). "Calibration of sap flow estimated by the compensation heat pulse method in olive, plum and orange trees: Relationships with xylem anatomy". In: *Tree Physiology* 26.6, pp. 719–728. DOI: 10.1093/treephys/26.6.719.

Fernández, J.E., Alfonso Perez-Martin, José M. Torres-Ruiz, María V. Cuevas, Celia M. Rodriguez-Dominguez, Sheren Elsayed-Farag, Ana Morales-Sillero, José M. García, Virginia Hernandez-Santana, and Antonio Diaz-Espejo (2013). "A regulated deficit irrigation strategy for hedgerow olive orchards with high plant density". In: *Plant and Soil* 372.1-2, pp. 279–295. DOI: 10.1007/s11104-013-1704-2.

Fishman, S. and M. Génard (1998). "A biophysical model of fruit growth: simulation of seasonal and dirunal dynamics of mass". In: *Plant, Cell and Environment* 21.8, pp. 739–752. DOI: 10.1046/j.1365-3040.1998.00322.x.

Flexas, J. and H. Medrano (2002). "Drought-inhibition of photosynthesis in C3 plants: Stomatal and non-stomatal limitations revisited". In: *Annals of Botany* 89.2, pp. 183–189. DOI: 10.1093/aob/mcf027.

Flexas, J., A Diaz-Espejo, J. Berry, J. Cifre, J Galmes, R. Kaldenhoff, H. Medrano, and M Ribas-Carbo (2007). "Analysis of leakage in IRGA's leaf chambers of open gas exchange systems: quantification and its effects in photosynthesis parameterization". In: *Journal of Experimental Botany* 58.6, pp. 1533–1543. DOI: 10.1093/jxb/erm027.

Flexas, J., Antonio Diaz-Espejo, J. Gago, A. Gallé, J. Galmés, J. Gulías, and H. Medrano (2014). "Photosynthetic limitations in Mediterranean plants: A review". In: *Environmental and Experimental Botany* 103, pp. 12–23. DOI: 10.1016/j.envexpbot.2013.09.002.

Flexas, Jaume, Josefina Bota, Josep Cifre, José Mariano Escalona, Jeroni Galmés, Javier Gulías, El Kadri Lefi, Sara Florinda Martínez-Cañellas, María Teresa Moreno, Miquel Ribas-Carbó, Diego Riera, Bartolomé Sampol, and Hipólito Medrano (2004). "Understanding down-regulation of photosynthesis under water stress: Future prospects and searching for physiological tools for irrigation management". In: *Annals of Applied Biology* 144.3, pp. 273–283. DOI: 10.1111/j.1744-7348.2004.tb00343.x.

Flexas, Jaume, J. Galmés, A. Gallé, J. Gulías, A. Pou, M. Ribas-Carbo, M. Tomàs, and H. Medrano (2010). "Improving water use efficiency in grapevines: Potential physiological targets for biotechnological improvement". In: *Australian Journal of Grape and Wine Research* 16.SUPPL. 1, pp. 106–121. DOI: 10.1111/j.1755-0238.2009.00057.x.

Foley, Jonathan A., Navin Ramankutty, Kate A. Brauman, Emily S. Cassidy, James S. Gerber, Matt Johnston, Nathaniel D. Mueller, Christine O'Connell, Deepak K. Ray, Paul C. West, Christian Balzer, Elena M. Bennett, Stephen R. Carpenter, Jason Hill, Chad Monfreda, Stephen Polasky, Johan Rockström, John Sheehan, Stefan Siebert, David Tilman, and David P. M. Zaks (2011). "Solutions for a cultivated planet". In: *Nature* 478.7369, pp. 337–342. DOI: 10.1038/nature10452. arXiv: 9605103 [cs].

García, J.M., M.V. Cuevas, and J.E. Fernández (2013). "Production and oil quality in 'Arbequina' olive (Olea europaea, L.) trees under two deficit irrigation strategies". In: *Irrigation Science* 31.3, pp. 359–370. DOI: 10.1007/s00271-011-0315-z.

Génard, Michel, Jean Dauzat, Nicolás Franck, Françoise Lescourret, Nicolas Moitrier, Philippe Vaast, and Gilles Vercambre (2008). "Carbon allocation in fruit trees: From theory to modelling". In: *Trees - Structure and Function* 22.3, pp. 269–282. DOI: 10.1007/s00468-007-0176-5.

Girón, I.F., M. Corell, A. Galindo, E. Torrecillas, D. Morales, J. Dell'Amico, A. Torrecillas, F. Moreno, and A. Moriana (2015a). "Changes in the physiological response between leaves and fruits during a moderate water stress in table olive trees". In: *Agricultural Water Management* 148, pp. 280–286. DOI: 10.1016/j.agwat.2014.10.024.

Goldhamer, D. A. and E. Fereres (2004). "Irrigation scheduling of almond trees with trunk diameter sensors". In: *Irrigation Science* 23.1, pp. 11–19. DOI: 10.1007/s00271-003-0088-0. arXiv: arXiv:1011.1669v3.

Gómez-del-Campo, María (2013). "Summer deficit-irrigation strategies in a hedgerow olive orchard cv. 'Arbequina': effect on fruit characteristics and yield". In: *Irrigation Science* 31.3, pp. 259–269. DOI: 10.1007/s00271-011-0299-8.

Gómez-del-Campo, María, María Ángeles Pérez-Expósito, Sofiene B.M. Hammami, Ana Centeno, and Hava F. Rapoport (2014). "Effect of varied summer deficit irrigation on components of olive fruit growth and development". In: *Agricultural Water Management* 137, pp. 84–91. DOI: 10.1016/j.agwat.2014.02.009.

Granier, A., P. Biron, and D. Lemoine (2000). "Water balance, transpiration and canopy conductance in two beech stands". In: *Agricultural and Forest Meteorology* 100.4, pp. 291–308. DOI: 10.1016/S0168-1923(99)00151-3.

Green, Steve, Brent Clothier, and Bryan Jardine (2003). "Theory and Practical Application of Heat Pulse to Measure Sap Flow". In: *Agronomy Journal* 95.6, p. 1371. DOI: 10.2134/agronj2003.1371.

Greenspan, M. D., M. A. Matthews, and K. A. Shackel (1994). "Developmental changes in the diurnal water budget of the grape berry exposed to water deficits". In: *Plant, Cell and Environment* 17.7, pp. 811–820. DOI: 10.1111/j.1365-3040.1994.tb00175.x.

Greenspan, Mark D., Hans R. Schultz, and Mark A. Matthews (1996). "Field evaluation of water transport in grape berries during water deficits". In: *Physiologia Plantarum* 97, pp. 55–62.

Greer, D. H. and M. M. Weedon (2012). "Modelling photosynthetic responses to temperature of grapevine (Vitis vinifera cv. Semillon) leaves on vines grown in a hot climate". In: *Plant, Cell & Environment* 35.6, pp. 1050–1064. DOI: 10.1111/j.1365-3040.2011.02471.x.

Hacket-Pain, Andrew J., Jonathan G.A. Lageard, and Peter A. Thomas (2017). "Drought and reproductive effort interact to control growth of a temperate broadleaved tree species (Fagus sylvatica)". In: *Tree Physiology* 37.6, pp. 744–754. DOI: 10.1093/treephys/tpx025.

Hernandez-Santana, Virginia, Adan Hernandez-Hernandez, Matthew A. Vadeboncoeur, and Heidi Asbjornsen (2015). "Scaling from single-point sap velocity measurements to stand transpiration in a multispecies deciduous forest: uncertainty sources, stand

structure effect, and future scenarios". In: *Canadian Journal of Forest Research* 45.11, pp. 1489–1497. DOI: 10.1139/cjfr-2015-0009.

Hernandez-Santana, Virginia, Celia M. Rodriguez-Dominguez, J. Enrique Fernández, and Antonio Diaz-Espejo (2016a). "Role of leaf hydraulic conductance in the regulation of stomatal conductance in almond and olive in response to water stress". In: *Tree Physiology* 36.6, pp. 725–735. DOI: 10.1093/treephys/tpv146.

Hernandez-Santana, Virginia, J.E. Fernández, Celia M. Rodriguez-Dominguez, R. Romero, and Antonio Diaz-Espejo (2016b). "The dynamics of radial sap flux density reflects changes in stomatal conductance in response to soil and air water deficit". In: *Agricultural and Forest Meteorology* 218-219, pp. 92–101. DOI: 10.1016/j.agrformet.2015.11.013.

Hernandez-Santana, Virginia, J.E. Fernández, M.V. Cuevas, Alfonso Perez-Martin, and Antonio Diaz-Espejo (2017). "Photosynthetic limitations by water deficit: Effect on fruit and olive oil yield, leaf area and trunk diameter and its potential use to control vegetative growth of super-high density olive orchards". In: *Agricultural Water Management* 184, pp. 9–18. DOI: 10.1016/j.agwat.2016.12.016.

Ho, L. C., R. I. Grange, and A. J. Picken (1987). "An analysis of the accumulation of water and dry matter in tomato fruit." In: *Plant, Cell and Environment* 10.2, pp. 157–162. DOI: 10.1111/1365-3040.ep11602110.

Hothorn, Torsten, Frank Bretz, and Peter Westfall (2008). "Simultaneous Inference in General Parametric Models". In: *Biometrical Journal* 50.3, pp. 346–363. DOI: 10.1002/bimj.200810425.

Iniesta, F., L. Testi, F. Orgaz, and F. J. Villalobos (2009). "The effects of regulated and continuous deficit irrigation on the water use, growth and yield of olive trees". In: *European Journal of Agronomy* 30.4, pp. 258–265. DOI: 10.1016/j.eja.2008.12.004.

Intrigliolo, D. S. and J. R. Castel (2007b). "Evaluation of grapevine water status from trunk diameter variations". In: *Irrigation Science* 26.1, pp. 49–59. DOI: 10.1007/s00271-007-0071-2.

Jarvis, P.G. and K.G. McNaughton (1986). "Stomatal Control of Transpiration: Scaling Up from Leaf to Region". In: *Advances in Ecological Research* 15, pp. 1–49. DOI: 10.1016/S0065-2504(08)60119-1.

Jones, H.G. and F. Tardieu (1998). "Modelling water relations of horticultural crops: a review". In: *Scientia Horticulturae* 74.1-2, pp. 21–46. DOI: 10.1016/S0304-4238(98)00081-8.

Kattge, Jens and Wolfgang Knorr (2007). "Temperature acclimation in a biochemical model of photosynthesis: a reanalysis of data from 36 species". In: *Plant, Cell & Environment* 30.9, pp. 1176–1190. DOI: 10.1111/j.1365-3040.2007.01690.x.

Kučera, Jiří, Patricia Brito, María Soledad Jiménez, and Josef Urban (2017). "Direct Penman–Monteith parameterization for estimating stomatal conductance and modeling sap flow". In: *Trees* 31.3, pp. 873–885. DOI: 10.1007/s00468-016-1513-3.

Le Roux, X, A Lacointe, A Escobar Gutierrez, S Le Dizes, X Le Roux, A Lacointe, A E Escobar-Gutiérrez, and S Le Dizès (2001). "Carbon-based models of individual tree growth: A critical appraisal". In: *Annals-of-Forest-Science. Jul-Aug 2001; 58 (5) : 469-506* 58.5, pp. 469–506. DOI: 10.1051/forest:2001140.

Lechaudel, Mathieu, Gilles Vercambre, Françoise Lescourret, Frederic Normand, and Michel Génard (2007). "An analysis of elastic and plastic fruit growth of mango in response to various assimilate supplies". In: *Tree Physiology* 27.2, pp. 219–230. DOI: 10.1093/treephys/27.2.219.

León, L., R. De La Rosa, L. Rallo, N. Guerrero, and D. Barranco (2007). "Influence of spacing on the initial production of hedgerow 'Arbequina' olive orchards". In: *Spanish Journal of Agricultural Research* 5.4, pp. 554–558.

Lescourret, Françoise and Michel Génard (2005). "A virtual peach fruit model simulating changes in fruit quality during the final stage of fruit growth". In: *Tree Physiology* 25.10, pp. 1303–1315. DOI: 10.1093/treephys/25.10.1303.

Lopez-Bernal, A., E. Alcantara, L. Testi, and F. J. Villalobos (2010). "Spatial sap flow and xylem anatomical characteristics in olive trees under different irrigation regimes". In: *Tree Physiology* 30.12, pp. 1536–1544. DOI: 10.1093/treephys/tpq095.

López-Bernal, Álvaro, Omar García-Tejera, Victorino A. Vega, Juan C. Hidalgo, Luca Testi, Francisco Orgaz, and Francisco J. Villalobos (2015). "Using sap flow measurements to estimate net assimilation in olive trees under different irrigation regimes". In: *Irrigation Science* 33.5, pp. 357–366. DOI: 10.1007/s00271-015-0471-7.

López-Bernal, Álvaro, Luca Testi, and Francisco J. Villalobos (2017). "A single-probe heat pulse method for estimating sap velocity in trees". In: *New Phytologist* 216.1, pp. 321–329. DOI: 10.1111/nph.14694.

Marcelis, L. F. M. (1996). "Sink strength as a determinant of dry matter partitioning in the whole plant". In: *Journal of Experimental Botany* 47.(Special Issue), pp. 1281–1291.

Martin-StPaul, Nicolas, Sylvain Delzon, and Hervé Cochard (2017). "Plant resistance to drought depends on timely stomatal closure". In: *Ecology Letters* 20.11. Ed. by Hafiz Maherali, pp. 1437–1447. DOI: 10.1111/ele.12851.

Matthews, Mark A. and Ken A. Shackel (2005). "Growth and Water Transport in Fleshy Fruit". In: *Vascular Transport in Plants*, pp. 181–197.

McNaughton, K. G. and P.G. Jarvis (1983). "Predicting effects of vegetation changes on transpiration and evaporation". In: *Water deficits and plant growth*, pp. 1–47.

Medrano, H. (2002). "Regulation of Photosynthesis of C3 Plants in Response to Progressive Drought: Stomatal Conductance as a Reference Parameter". In: *Annals of Botany* 89.7, pp. 895–905. DOI: 10.1093/aob/mcf079.

Mencuccini, Maurizio, Teemu Hölttä, Sanna Sevanto, and Eero Nikinmaa (2013). "Concurrent measurements of change in the bark and xylem diameters of trees reveal a phloem-generated turgor signal". In: *New Phytologist* 198.4, pp. 1143–1154. DOI: 10.1111/nph.12224.

Morandi, Brunella, Mark Rieger, and Luca Corelli-Grappadelli (2007b). "Vascular flows and transpiration affect peach (Prunus persica Batsch.) fruit daily growth". In: *Journal of Experimental Botany* 58.14, pp. 3941–3947. DOI: 10.1093/jxb/erm248.

Morandi, Brunella, Pasquale Losciale, Luigi Manfrini, Marco Zibordi, Stefano Anconelli, Fabio Galli, Emanuele Pierpaoli, and Luca Corelli Grappadelli (2014a). "Increasing water stress negatively affects pear fruit growth by reducing first its xylem and then its phloem inflow". In: *Journal of Plant Physiology* 171.16, pp. 1500–1509. DOI: 10.1016/j.jplph.2014.07.005.

Morison, J.I.L, N.R Baker, P.M Mullineaux, and W.J Davies (2008). "Improving water use in crop production". In: *Philosophical Transactions of the Royal Society B: Biological Sciences* 363.1491, pp. 639–658. DOI: 10.1098/rstb.2007.2175.

Mueller, Nathaniel D., James S. Gerber, Matt Johnston, Deepak K. Ray, Navin Ramankutty, and Jonathan A. Foley (2012). "Closing yield gaps through nutrient and water management". In: *Nature* 490.7419, pp. 254–257. DOI: 10.1038/nature11420. arXiv: NIHMS150003.

Müller-Haubold, Hilmar, Dietrich Hertel, Dominik Seidel, Florian Knutzen, and Christoph Leuschner (2013). "Climate Responses of Aboveground Productivity and Allocation in Fagus sylvatica: A Transect Study in Mature Forests". In: *Ecosystems* 16.8, pp. 1498–1516. DOI: 10.1007/s10021-013-9698-4.

Naor, A., D. Schneider, A. Ben-Gal, I. Zipori, A. Dag, Z. Kerem, R. Birger, M. Peres, and Y. Gal (2013). "The effects of crop load and irrigation rate in the oil accumulation stage on oil yield and water relations of 'Koroneiki' olives". In: *Irrigation Science* 31.4, pp. 781–791. DOI: 10.1007/s00271-012-0363-z.

Orgaz, Francisco and Elias Fereres (1997). "Riego". In: *El cultivo del olivo*. Ed. by D. Barranco, R. Fernández-Escobar, and L. Rallo. 1ª. Madrid: Grupo Mundi Prensa, pp. 251–272.

Parry, M.A.J., J. Flexas, and H. Medrano (2005). "Prospects for crop production under drought: research priorities and future directions". In: *Annals of Applied Biology* 147.3, pp. 211–226. DOI: 10.1111/j.1744-7348.2005.00032.x.

Pinheiro, José, Douglas Bates, Saikat DebRoy, Deepayan Sarkar, and R Core Team (2017). *nlme: Linear and Nonlinear Mixed Effects Models*.

R Core Team (2015). *R: A Language and Environment for Statistical Computing*. Vienna, Austria.

Ramírez, David A., Wendy Yactayo, Libby R. Rens, José L. Rolando, Susan Palacios, Felipe De Mendiburu, Víctor Mares, Carolina Barreda, Hildo Loayza, Philippe Monneveux, Lincoln Zotarelli, Awais Khan, and Roberto Quiroz (2016). "Defining biological thresholds associated to plant water status for monitoring water restriction effects: Stomatal conductance and photosynthesis recovery as key indicators in potato". In: *Agricultural Water Management* 177, pp. 369–378. DOI: 10.1016/j.agwat.2016.08.028.

Selås, Vidar, Gianluca Piovesan, Jonathan M Adams, and Mauro Bernabei (2002). "Climatic factors controlling reproduction and growth of Norway spruce in southern Norway". In: *Canadian Journal of Forest Research* 32.2, pp. 217–225. DOI: 10.1139/x01-192.

Sinclair, Thomas R. (1998). "Historical Changes in Harvest Index and Crop Nitrogen Accumulation". In: *Crop Science* 38.3, p. 638. DOI: 10.2135/cropsci1998.0011183X003800030002x.

Swanson, Robert H. (1994). "Significant historical developments in thermal methods for measuring sap flow in trees". In: *Agricultural and Forest Meteorology* 72.1-2, pp. 113–132. DOI: 10.1016/0168-1923(94)90094-9.

Troncoso, A., M. Cantos, J. Liñán, and José Enrique Fernández (2001). "Fertirrigación". In: *El cultivo del olivo*. Ed. by D. Barranco, R. Fernández-Escobar, and L. Rallo. 4th. Madrid: Coedition Mundi-Prensa and Junta de Andalucía, pp. 307–332.

Villalobos, F.J., F. Orgaz, and L. Mateos (1995). "Non-destructive measurement of leaf area in olive (Olea europaea L.) trees using a gap inversion method". In: *Agricultural and Forest Meteorology* 73.1-2, pp. 29–42. DOI: 10.1016/0168-1923(94)02175-J.

Walther, Bruno A. and Joslin L. Moore (2005). "The concepts of bias, precision and accuracy, and their use in testing the performance of species richness estimators, with a literature review of estimator performance". In: *Ecography* 28.6, pp. 815–829. DOI: 10.1111/j.2005.0906-7590.04112.x.

Zonia, Laura and Teun Munnik (2007). "Life under pressure: hydrostatic pressure in cell growth and function". In: *Trends in Plant Science* 12.3, pp. 90–97. DOI: 10.1016/j.tplants.2007.01.006.

CHAPTER 4

Effects of water stress on fruit growth and water relations between fruits and leaves in a hedgerow olive orchard.

Published as: Fernandes, Rafael Dreux Miranda, M.V. Cuevas, A. Diaz-Espejo, V. Hernandez-Santana (2018). "Effects of water stress on fruit growth and water relations between fruits and leaves in a hedgerow olive orchard". In: Agricultural Water Management 210, pp. 32–40. DOI: 10.1016/j.agwat.2018.07.028

Abstract

Yield, the final goal in agricultural systems, is highly determined by fruit growth. However, most works on deficit irrigation did not consider the physiology and dynamics of fruit growth. In this study, we explore the effect of water relations between leaves and fruits on fruit growth in well-watered (100C-1L) and water-stressed (45RDI-1L) trees in a super-high-density olive orchard (cv. Arbequina) over a full irrigation season (June–October of 2017) in southern Spain. Both leaf and fruit water potential were measured, along with pressure-volume curves. Concomitantly, fruit growth and diurnal changes in six fruits of each irrigation treatment were continuously monitored with fruit gauges, which recorded changes in the equatorial diameter of the fruit. Fruit water status and growth were greatly affected by water stress, the latter recovering markedly, following our regulated deficit irrigation strategy. The gradient between leaf and fruit water potential was positive most of the time for both irrigation treatments, and greater for 45RDI-1L than 100C-1L trees, which suggests water flow into the fruit. However, we also observed negative fruit growth in 45RDI-1L which, together with the positive gradient, suggests that water flow from the parent plant to the fruit was insufficient to balance fruit transpiration under conditions of water deficit. Although a strong correlation was found between leaf water potential and the amplitude of fruit contraction in 100C-1L trees, this relationship did not hold for 45RDI-1L trees, suggesting a progressive decoupling of fruit water status from leaves as water stress progressed. Accordingly, an osmotic adjustment as evidenced by the analyses of pressure-volume curves occurred in 45RDI-1L fruits towards the end of the season. These results indicate that leaf-fruit water potential measurements may not be sufficient to study fruit-leaf water relationships in the canopy; however, fruit gauges may serve as highly useful instruments to understand the water status and daily dynamics of fruit growth.

4.1 Introduction

The world's agricultural production needs to continue to grow to meet the increasing demand for food, challenge aggravated by climate change. Production is highly determined by fruit size, among other factors such as crop load (Naor et al., 2013) and leaf area (Hernandez-Santana et al., 2017) and thus, the study of fruit growth can provide information on final yield. Moreover, fruit growth is highly sensitive to water deficit, which decreases its carbon accumulation and tissue expansion and reduces cell number (Tardieu et al., 2011). The aforementioned characteristics make fruit growth to be a sensitive water stress indicator, directly related to plant function and yield. Specifically, the study of the water potential gradients between the parent plant and the fruit which de-

termine water flux into and out of the fruit and also of transpiration losses from the fruit (Greenspan et al., 1994; Greenspan et al., 1996), would help to understand the diurnal diameter fluctuations in fruit size.

Moreover, osmotic adjustment could also contribute to investigate fruit growth and crop yield under drought stress because it is widely recognized to have a relevant role in turgor maintenance, which plays a critical role in cell growth (Hsiao et al., 1976; Ho et al., 1987; Fishman and Génard, 1998). However, despite its relevance, osmotic adjustment in fruits has been addressed in relatively few studies (Mills et al., 1996; Pomper and Breen, 1997; Girón et al., 2015a).

Interestingly, previous studies on olive trees have shown that fruit growth has preference over vegetative growth (stem or leaves), especially under water stress conditions (Iniesta et al., 2009; Dag et al., 2010; Hernandez-Santana et al., 2017). Under such conditions, the fruit is the main sink for new carbon assimilates. Similarly, it has been reported that olive fruits are the main water sinks during water stress periods, and that this decreases in importance under conditions of no water stress (Girón et al., 2015a). However, opposite results have also been reported (Dell'Amico et al., 2012), being the different crop load in each study a possible explanation for these contrasting results (Girón et al., 2015a).

Fruit diameter has been monitored successfully with fruit gauges in different crop species such as apples (Jones and Higgs, 1982; Zibordi et al., 2009; Morandi et al., 2011c), pears (Morandi et al., 2014a), peaches (Morandi et al., 2007a; Morandi et al., 2010a), and kiwis (Morandi et al., 2011b; Morandi et al., 2011a), although studies showing their use with small fruits are less frequent (Greenspan et al., 1996) and to the best of our knowledge, they have not been used in olives. Fruit gauge measurements can provide useful information on daily growth and shrinkage and related water movement into and out of fruits (Morandi et al., 2007a; Morandi et al., 2010a; Morandi et al., 2011b; Morandi et al., 2011a; Morandi et al., 2011c). However, as for trunk dendrometers, the interpretation of data to allow the effect of water fluxes to be separated from biomass accumulation is challenging which complicates its use as a water stress index (Fernández and Cuevas, 2010; Mencuccini et al., 2013; De Swaef et al., 2015). Thus, more information on the mechanisms impacting fruit growth is needed to evaluate its use as a water stress indicator and its relation to final yield. To the best of our knowledge, this constitutes the first study of this type on the olive tree and one of the few in other species because fruit dendrometers are normally used to measure fruit growth in wet or well-irrigated orchards but they are not usually used to study fruit growth dynamics provoked by water stress.

The objective of this work is to study the effect of water stress on fruit growth dynamics of trees in a super-high-density olive orchard (cv. Arbequina) and the water potential

gradient between leaves and fruits as a possible mechanism to explain these dynamics. To fulfill this objective, we established the following aims: (i) to assess changes in fruit growth in response to water stress; (ii) to evaluate the relations between changes in fruit diameter and the gradient of water potential between leaves and fruits; and, (iii) to study osmotic adjustments in fruits as a consequence of water availability. Fruit growth was measured continuously with fruit gauges and the water potential gradient between fruits and leaves was assessed with a view to increase our understanding of the physiological mechanisms underlying fruit growth and water relations in the canopy in response to water stress. We believe this knowledge is crucial for the development in the future of new deficit irrigation methods based on process-based models focused on the improvement of crop water productivity to schedule irrigation and predict yield.

4.2 Material and Methods

4.2.1 Experimental orchard and irrigation treatments

The experiments were performed in a super-high-density olive orchard (*Olea europaea* L., cv. Arbequina), located 25 km to the south-east of Seville, Spain (37°15′N, −5°48′W). Trees were planted in a configuration of 4 m x 1.5 m (1667 trees ha-1) at the top of 0.4 m high ridges oriented N-NE to S-SW. The average annual precipitation (P) and potential evapotranspiration (ET_o) in the area are 501.2 mm and 1498.1 mm, respectively (period 2002-2016). The olive trees were 11 years old at the time of the study. Meteorological variables were recorded by a Campbell weather station (Campbell Scientific Ltd., Shepshed, UK) located in the center of the area covered by the experimental plots, with the meteorological sensors located above the canopies. The station recorded 30 min average radiation (R_s), air temperature (T_{air}), relative humidity (RH) of the air, and total P. The vapor pressure deficit (D) was calculated as a function of T_{air} and RH. The crop evapotranspiration (ET_C) was calculated from the potential evapotranspiration (ET_o) measured by the meteorological station located at Los Molares (ca. 13.5 km from the experimental plots, 37°10′34″N, 05°40′22″W). The estimation of ET_o was performed by the Penman-Monteith equation (Allen et al., 1998), with the data regarding air temperature, air relative humidity, radiation and wind speed. From the ET_o data the crop coefficient approach was used to calculate ET_C.

We applied a well-watered (100C-1L) treatment and a water-stressed (45RDI-1L) treatment. Each treatment involved three 12 m x 16 m plots in a randomized block design. Each plot had 24 trees, and measurements were made in the central 8 trees to avoid border effects. For the 100C-1L treatment, trees were irrigated daily to replace 100% of the irrigation needs (IN). IN were calculated daily based on a simplified version of the stomatal conductance (g_s) model tested for this olive orchard by Diaz-Espejo et al. (2012).

The 100C-1L treatment was assumed to have a soil water content at field capacity, i.e. a soil matric potential equal to 0. Following this model, g_s is described as a function of D, R_s and tree leaf area, the latter estimated once every two weeks for each plot during the irrigation season. Measurements were made at dawn with a LAI-2200 Plant Canopy Analyzer (Li-Cor, Inc., Lincoln, NE, USA) following the procedure described by Diaz-Espejo et al. (2012). The percentage of sunny to total leaf area was estimated to be 35% according to Diaz-Espejo et al. (2002) and Fernández et al. (2008b). Assuming a perfect coupling between canopy and atmosphere, tree water consumption (E_p) was calculated as $E_p = D \cdot (g_{s,sun} \cdot A_{sun} + g_{s,shade} \cdot A_{shade})$, where D is the vapour pressure deficit, $g_{s,sun}$ and $g_{s,shade}$ are stomatal conductance of new, sun-exposed leaves and old, shaded leaves, respectively; A_{sun} and A_{shade} are the corresponding leaf areas of sun and shade leaves, respectively. Soil evaporation (E_s) was estimated according to Orgaz et al. (2006). Finally, IN were estimated as $E_p + E_s$. We compared the g_s results calculated as described with those simulated through sap flow-related measurements (Hernandez-Santana et al., 2016a). For the 45RDI-1L treatment we applied the regulated deficit irrigation (RDI) strategy recommended by Fernández et al. (2013) for super-high-density olive orchards. This strategy considers three periods over the course of the olive growing cycle during which the crop is highly sensitive to water stress. During these periods, irrigation replaced the crop water needs. Period 1 extended from the final stages of floral development to full bloom (second fortnight of April); period 2 took place at the end of the first phase of fruit development (June); and period 3 related to a period of approximately three weeks prior to ripening, after the midsummer period of high atmospheric demand (from late August to mid-September). Between periods 2 and 3 (late June-late August), the olive tree is highly resistant to drought (Alegre et al., 2002; Moriana et al., 2003; Iniesta et al., 2009; Fernández et al., 2013), such that irrigation was only applied twice per week, amounting to a total of ca. 20% IN for that period. From the end of period 3 to harvesting (end of October) ca. 40% of IN was supplied. Further details on RDI can be found in Fernández et al. (2013) and Hernandez-Santana et al. (2016a). For the experimental period (DOY 151 – 296) the total applied irrigation was equal to 3620.95 and 1631.52 $m^3\,ha^{-1}$ for the 100C-1L and 45RDI-1L treatments, respectively. 45RDI-1L was 45% of the 100C-1L irrigation applied.

The irrigation system consisted of a single pipe per tree row with three 2 $L\,h^{-1}$ drippers per tree, spaced 0.5 m apart. To assess soil volumetric water content (θ, $m^3\,m^{-3}$) we used a Profile probe (Delta-T Devices Ltd., Cambridge, UK) calibrated in situ (Fernández and Cuevas, 2011; Fernández et al., 2011a), and two access tubes in each plot, placed 0.1 and 0.4 m from the drippers and 0.5 m from the tree trunk. Measurements were performed at the time of maximum g_s (ca. 9.00 GMT), at depths of 0.1, 0.2, 0.3, 0.4, 0.6 and 1.0 m. For the calculations of average θ for each treatment, a weighted average

was calculated for each plot with the measurements from 0.1 to 0.4 m, weighted by the percentage of roots, and then by a simple average of the averages obtained for each plot.

4.2.2 Leaf and fruit water potential

Leaf water potential (Ψ_{leaf}) and fruit water potential (Ψ_{fruit}) were measured with a Scholander-type pressure chamber (PMS Instrument Company, Albany, Oregon, USA). Measurements of Ψ_{leaf} were performed every two weeks between day of year (DOY) 151 and 296 (i.e. between May 31 and October 23). Measurements of Ψ_{fruit} were made on the same days but starting from DOY 200 (July 19). Leaves and fruits were sampled before sunrise (predawn, $\Psi_{l,pd}$ and $\Psi_{f,pd}$) and at midday (ca. 11.00 GMT, $\Psi_{l,md}$ and $\Psi_{f,md}$). Additional measurements of both $\Psi_{l,md}$ and $\Psi_{f,md}$ were performed at DOY 212, 226, 228, 243 and 256. Measurements of both $\Psi_{l,pd}$ and $\Psi_{l,md}$ were made in two leaves per plot (n = 3) sampled from current-year shoots of two central trees, from the outer part of the canopy. The leaf blade was cut to allow the insertion of the leaf petiole into the pressure chamber. For both $\Psi_{f,pd}$ and $\Psi_{f,md}$, two fruits per plot from the central trees of three plots were sampled (n = 3). The chosen fruits had a long pedicel (ca. 2 cm) to allow the use of the pressure chamber. Once the fruits and leaves were excised they were placed in a closed bag with a soaked paper in it with a saturated atmosphere of H_2O and CO_2 (to force stomata to close) and avoid transpiration to allow the water potential of the sample to equilibrate. This bag was introduced in a second zip bag which in turn was introduced in a black plastic bag inside a field fridge with ice containers. This sampling method also allowed us to collect all the samples in a very short time, reducing the variability among them due to different collecting time. Preliminary tests were conducted to test that the water potential was not changing significantly for hours. Leaf water potential and Ψ_{fruit} were measured precisely in the laboratory on the afternoon of the sampling days using magnification lens.

Fruit gauges were installed in one fruit of two representative trees per plot, totaling six monitored fruits per treatment. We used two types of fruit dendrometers; one model was the FI-XSSF from Solfranc (Solfranc Tecnologias, SL, Tarragona, Spain), and the other model was adapted using a linear potentiometer model MM(R)10-11 with internal spring return (from Megatron Elektronik GmbH & Co., Munich, Germany) coupled to a sensor holder. We had 2 of the Solfranc fruit dendrometers and four of the Megatron fruit dendrometers per treatment. The fruit dendrometers recorded fruit equatorial diameter every 5 min with the use of a datalogger (CR1000, Campbell Scientific Ltd., Shepshed, UK). From the fruit gauge measurements, we calculated cumulative fruit growth as the maximum daily diameter of the fruit minus the maximum diameter of the previous day. The fruit daily contraction was obtained by subtracting the maximum diameter from the minimum diameter of a certain day, which results in negative values. The Megatron

model was already used by Morandi et al. (2007a) to monitor apple fruit diameter, presenting useful and relevant data. A comparison was performed between the two models of fruit dendrometers, aiming at analyzing the similarity of the measured data between each model, showing very similar results(Megatron-Solfranc fruit daily variations for 100C-1L fruits: r=0.86, p <0.0001, slope=1.05 and for 45RDI-1L fruits: r=091, p <0.0001, slope=1.06).

4.2.3 Pressure-Volume Curves

On DOY 244 (September 7th), four leaves from central trees of the 45RDI-1L treatment were sampled and immediately subjected to rehydration by immersing their petioles into distilled water. These leaves were then stored in complete darkness at 2-4 °C for 24 hours for complete rehydration. Six fruits from 100C-1L plots and 11 fruits from 45RDI-1L plots were sampled from central trees by cutting the pedicel immersed in distilled water and then the fruit was left in distilled water and complete darkness at 2-4 °C for 24 hours. These measurements were conducted on four different days for 45RDI-1L trees (August 28, September 14th, October 19th and 20th) and on two different days for 100C-1L trees (September 1st and October 19th).

After rehydration, pressure-volume (PV) curves were measured by weighing the tissue (leaf or fruit) shortly before measuring its water potential (Ψ) with a Scholander-type pressure chamber (PMS Instrument Company, Albany, Oregon, USA). At the start of the curves the increase in pressure was about 0.01 MPa s^{-1}, increasing to 0.1 MPa s^{-1} for points with Ψ more negative than -1.8 MPa. After the measurement of the whole PV curve, the dry weight of the fruit or leaf was obtained by placing samples for 48 hours in a drying oven maintained at 65°C.

The PV curves for each leaf and fruit were obtained by expressing relative water content (RWC) versus the respective water potential (Ψ), where values were plotted for (100-RWC) against (-1/Ψ). Based on these plots, the turgor loss point (TLP) was obtained by the inflection point of the relation $1/\Psi$ vs. 100–RWC, providing the water potential and the relative water content at the turgor loss point (Ψ_{TLP} and RWC_{TLP}, respectively). The calculation of the osmotic potential at saturation ($\Psi_{\pi 100}$) was performed according to Nguyen et al. (2017).

4.2.4 Calculations and Statistical Analysis

We calculated the average Ψ_{leaf} and Ψ_{fruit} values for each plot and then a general average and standard error for each treatment. With the average for each plot we calculated the difference between Ψ_{leaf} and Ψ_{fruit} ($\Delta\Psi_{leaf\text{-}fruit} = \Psi_{leaf} - \Psi_{fruit}$), following which the average $\Delta\Psi_{leaf\text{-}fruit}$ value and its standard error were calculated for each treatment.

The same approach was used for data regarding soil water content. The vertical bars in graphs represent the standard error of the mean between the three plots of each treatment.

Data for soil volumetric water content, leaf and fruit water potential and the indexes calculated by the PV curves were analyzed by the Student's t-test (two independent samples). Significant differences (p <0.05) are shown with an asterisk in the graphs. All data processing and statistical analyses were performed with R 3.2.2® software (R Core Team, 2015).

4.3 Results

4.3.1 Meteorological and soil conditions

Weather conditions during the experimental period (DOY 151 to 296) were typical of the Mediterranean summer, with daily maximum temperatures (T_{max}) exceeding 30°C on 80% of days (Fig. 4.1A). Precipitation was scarce, totaling just 17.62 mm on six days during the 145-day experimental period (Fig. 4.1B). Daily crop evapotranspiration (ET_C) averaged 3.31 mm from the beginning of the experiment until DOY 230 (August 18th), and decreased thereafter, giving an overall average of 2.82 mm for the experimental period (Fig. 4.1B). Daily average of vapor pressure deficit (D) was around 2.16 kPa before DOY 240 (August 28th) and decreased slightly thereafter for an average value of 1.93 kPa for the experimental period (Fig. 4.1C). Of note is the fact that a large number of days had a maximum D of over 6 kPa, which imposed a large demand for transpiration.

Soil volumetric water content (θ, $m^3\ m^{-3}$) in the 45RDI-1L treatment was significantly lower (ca. 57% lower; p <0.05) than the 100C-1L treatment, between the pit hardening period and the irrigation recovery period (from DOY 185 to 238, i.e. from July 4th to August 26th), and also after the irrigation recovery period (Fig. 4.2).

4.3.2 Fruit growth and diameter variation

The average cumulative fruit growth for the 100C-1L treatment was relatively steady during the early part of the experiment, with a slope of 0.07 mm d^{-1} from DOY 151 until DOY 190, and decreasing thereafter (0.018 mm d^{-1}) until approximately DOY 238 (Fig. 4.3). The fruits from the 45RDI-1L treatment, on the other hand, exhibited a decrease, as evidenced by negative slopes, of cumulative fruit growth during the drought period (ca. DOY 190 to 238) and after the irrigation recovery period (ca. DOY 262 to 286). The plot of cumulative fruit growth for the 45RDI-1L treatment had a slope of 0.11 mm d^{-1} during the pit hardening period (ca. DOY 159 to 185), which was higher than the slope at the same period for the 100C-1L treatment. The 45RDI-1L treatment also exhibited a

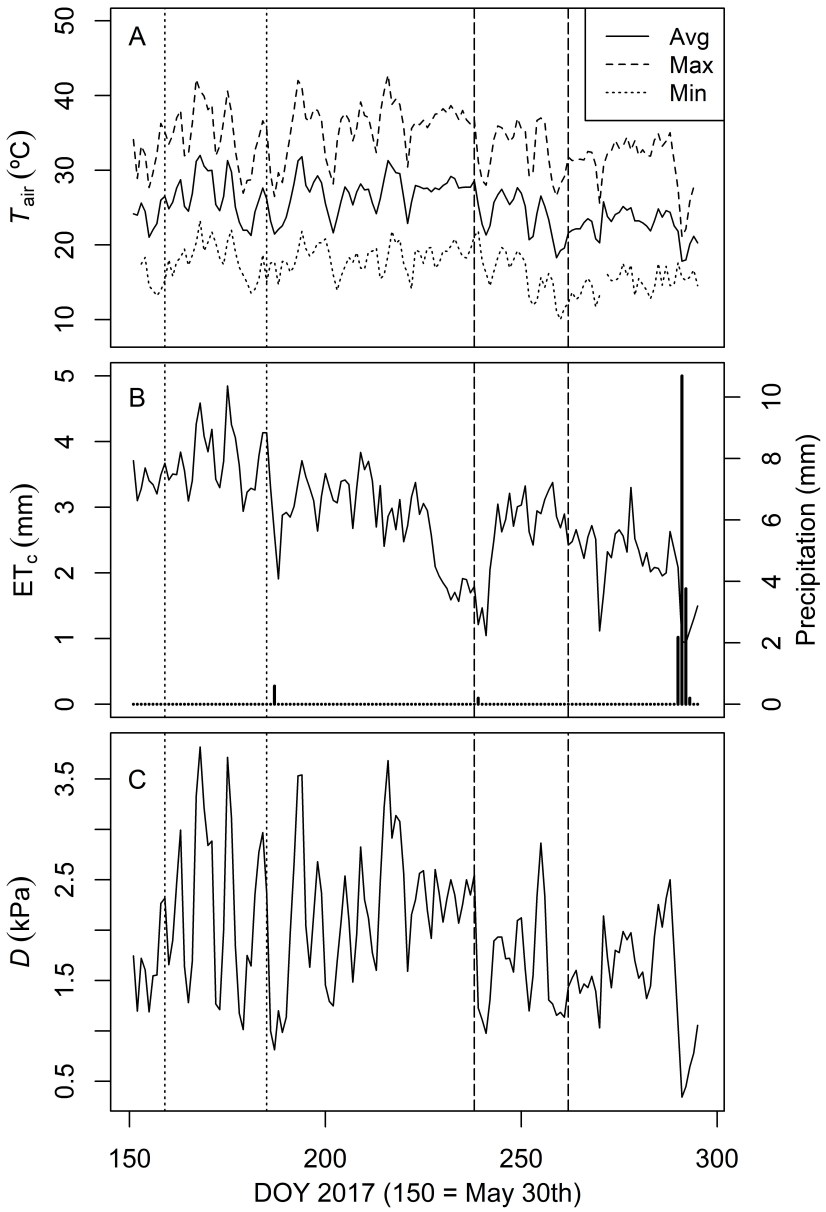

Figure 4.1: Weather conditions during the irrigation season. T_{air} - air temperature (°C); ET_C - crop evapotranspiration calculated by the Penman-Monteith equation; D - daily average vapor pressure deficit. Vertical dotted and dashed lines represent the periods when irrigation treatments were irrigated similarly.

high recovery rate at the beginning of the recovery period, with a slope of 0.23 mm d^{-1} between DOY 238 and 242, reaching a similar cumulative growth rate to that of fruits in the control irrigation treatment (100C-1L: 6.02 mm; 45RDI-1L: 5.70 mm). Fruits from both treatments grew at similar rate thereafter.

In agreement with the commented findings, a greater daily equatorial diameter contraction was observed for the 45RDI-1L treatment than for the 100C-1L treatment (Fig. 4.4). Fruits from the 45RDI-1L treatment exhibited contractions greater than –0.5 mm during most of the period when deficit irrigation was applied (ca. DOY 185 to 238). These contractions followed the irrigation frequency, which was programmed to take place twice per week, and suggest a close correlation with soil water availability. In con-

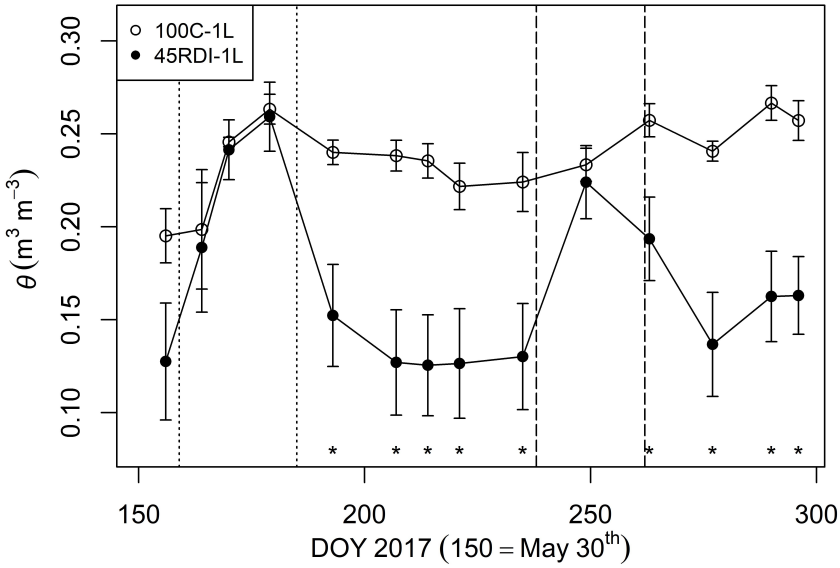

Figure 4.2: Soil water content (θ, $m^3\,m^{-3}$) for irrigation treatments. 100C-1L - well watered treatment; 45RDI-1L – water stress treatment. Each point is the average of three plots, with the vertical bars representing the standard error of the mean. The dotted and dashed lines represent the periods when irrigation treatments were irrigated similarly. Asterisks represent significant difference between treatments (p <0.05).

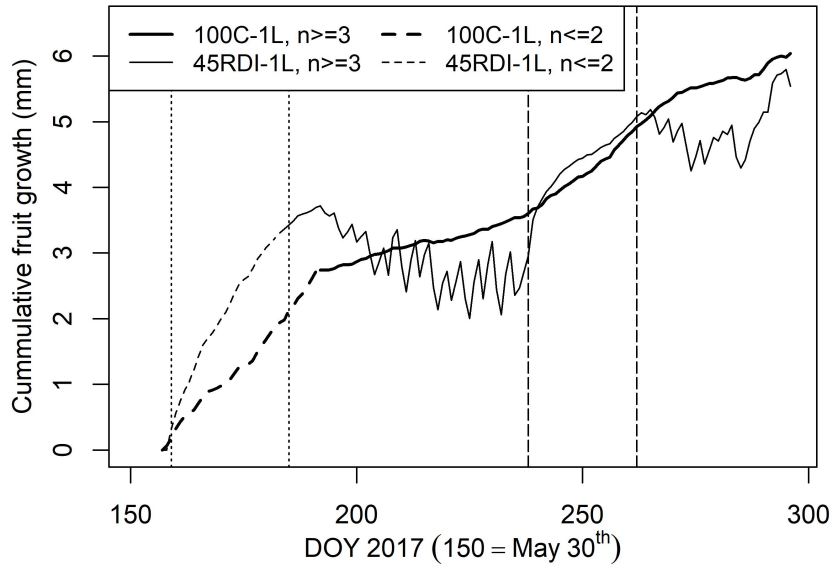

Figure 4.3: Cummulative growth in equatorial diameter of fruit (mm), where each line represents the average of three plots per treatment (100C-1L - well watered treatment; 45RDI-1L - water stress treatment). The dotted and dashed vertical lines represent the periods when irrigation treatments were irrigated similarly.

trast, fruits from the 100C-1L treatment exhibited a lower contraction due to their daily irrigation and better water status. It is also interesting to note that the contractions of fruits from the 45RDI-1L treatment were lower than those from the 100C-1L treatment during the recovery period (DOY 238 to 262).

The daily patterns (on a 24h time scale) showed that fruit contraction occurred during the day light hours (mainly during the afternoon) and its expansion and growth

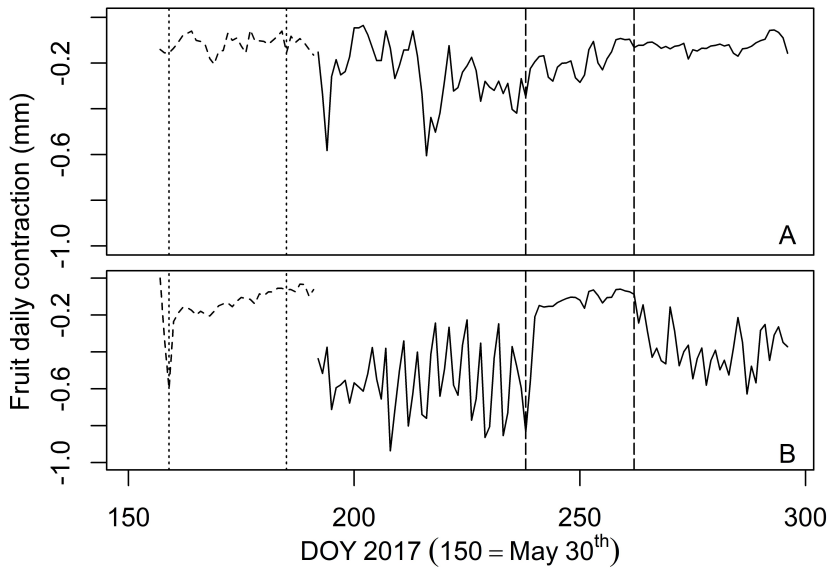

Figure 4.4: Fruit daily contraction (mm) calculated for well watered (upper, 100C-1L) and water stress treatment (lower, 45RDI-1L). Data from a period with less than three fruit dendrometers are represented as dashed lines. The dotted and dashed vertical lines represent the periods when irrigation treatments were irrigated similarly.

during the evening/night (Fig. 4.5). However, in periods of maximum stress, 45RDI-1L fruits were able to grow at night only when irrigation occurred, showing practically no contraction (Fig. 4.5B; DOY 226 and 229), being the fruit expansion the rest of the nights much smaller or not happening at all. During the recovery period (from DOY 238 onward), we observed a remarkable growth at nights in 45RDI-1L fruits (Fig. 4.5D), higher than the expansion showed by 100C-1L fruits for the same period (Fig. 4.5C).

4.3.3 Water relations between fruits and leaves

For the predawn and midday sampling times, and in the period when deficit irrigation was applied (between period 2 and 3 and after period 3), leaf water potential (Ψ_{leaf}) values for the 45RDI-1L treatment were lower than for the 100C-1L treatment, with significant differences between both treatments in a few of the measurement days within that period (p <0.05) (Figs. 4.6A and 4.6B).

Similar findings were obtained for fruit water potential (Ψ_{fruit}) (Figs. 4.6C and 4.6D) in the mentioned periods, when irrigation was lower for the 45RDI-1L treatment than for 100C-1L, and differences between the treatments were more frequently for Ψ_{fruit} than Ψ_{leaf} (p <0.05). Predawn values (Fig. 4.6C) of Ψ_{fruit} for the 100C-1L treatment were always higher than -2 MPa, with a slightly decreasing trend seen over the experimental period. Midday values of fruit water potential (Fig. 4.6D) ranged from -1 to -2 MPa for the 100C-1L treatment, and were relatively stable during the measurement period. In contrast, Ψ_{fruit} in 45RDI-1L was lower than -2MPa in predawn measurements and

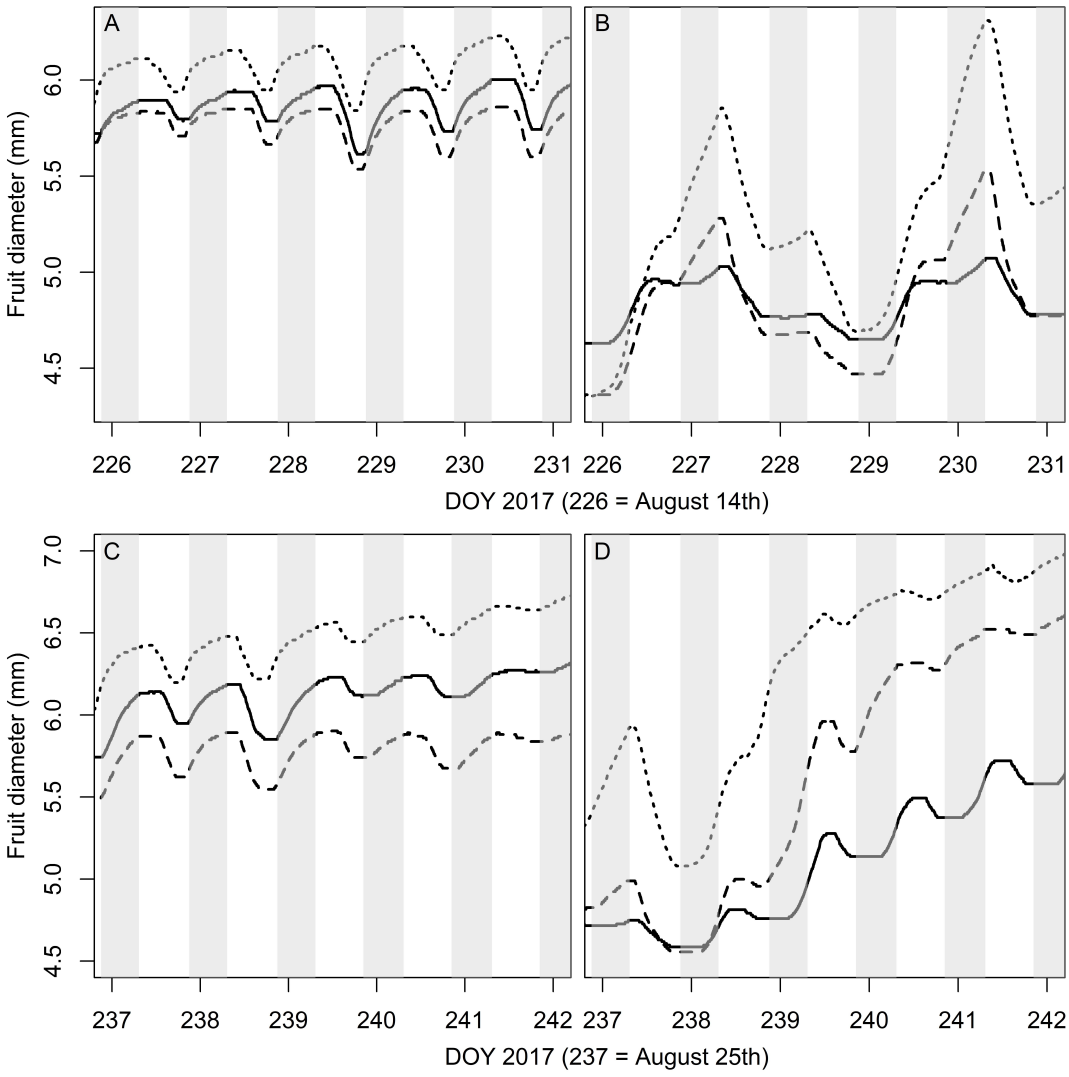

Figure 4.5: Fruit daily diameter variations from DOY 226 to 231 (A and B), a period of maximum stress and from DOY 237 to 242 (C and D), the recovery period, from the 100C-1L (well watered, A and C) and 45RDI-1L (water stress, B and D) treatments. The shaded areas represent the night hours. Each line represent data from different fruit dendrometers.

lower than -3 MPa at midday at times when olive trees were water stressed. Predawn and midday Ψ_{fruit} values during the recovery period (period 3) were similar for both treatments.

The difference between Ψ_{leaf} and Ψ_{fruit} ($\Delta\Psi_{leaf\text{-}fruit} = \Psi_{leaf} - \Psi_{fruit}$), i.e. the water potential gradient between leaves and fruits, was relatively stable and close to zero for predawn values in 100C-1L treated olive trees (Fig. 4.6E), with a slight increasing trend on the last two measurement days. In contrast, at midday these differences were positive and only close to zero after the recovery irrigation (Fig. 4.6F). On the other hand, higher values of $\Delta\Psi_{leaf\text{-}fruit}$ were more often found in 45RDI-1L trees than in 100C-1L trees.

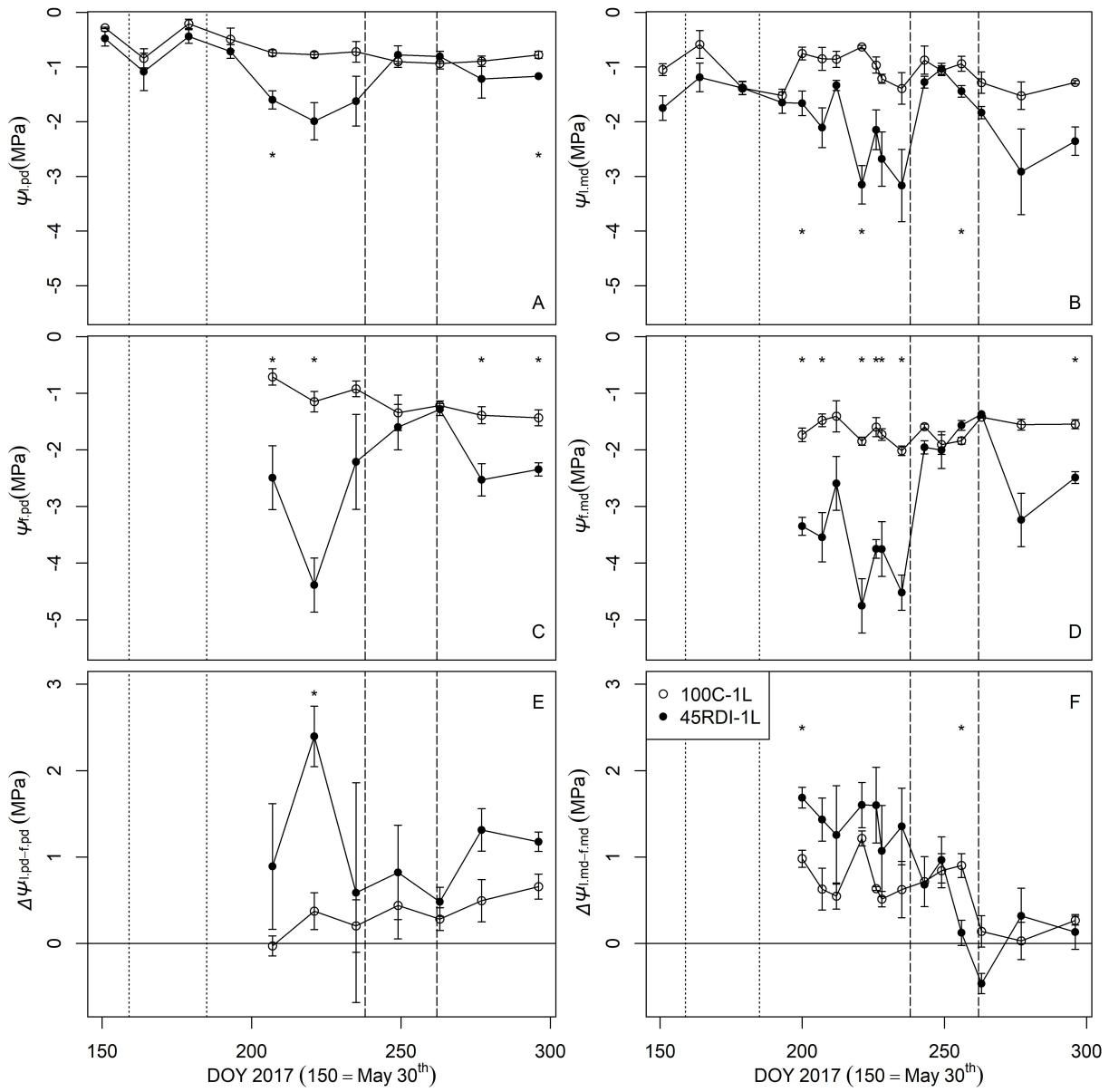

Figure 4.6: Water potential of leaves at predawn (A) and midday (B) timepoints. Water potential of fruits at predawn (C) and midday (D). Differences between leaf and fruit water potential measurements at predawn (E) and midday (F). Each point represents the mean of three plots per treatment, with the vertical bars representing the standard error of the mean. The dotted and dashed vertical lines represent the periods when irrigation treatments were irrigated similarly. Ψ_{leaf} – leaf water potential; Ψ_{fruit} – fruit water potential; $\Delta\Psi_{leaf\text{-}fruit}$ – leaf to fruit water potential gradient ($\Delta\Psi_{leaf\text{-}fruit} = \Psi_{leaf} - \Psi_{fruit}$); Asterisks represent significant difference between treatments ($p < 0.05$).

4.3.4 Fruit diameter variations and canopy water relations

Fruit contraction was significantly correlated to Ψ_{leaf} in 100C-1L treated olives (R^2= 0.48; $p < 0.001$) (Fig. 7). For the 45RDI-1L treatment, however, the Ψ_{leaf} – fruit contraction relationship was more scattered and not statistically significant ($p > 0.05$).

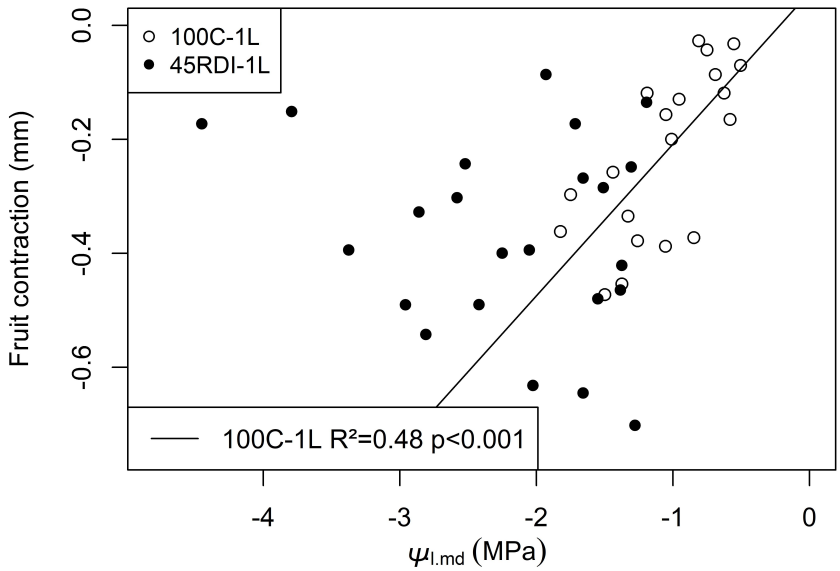

Figure 4.7: Scatterplot showing values of midday leaf water potential (Ψ_{leaf}) and fruit diameter contraction for the period when severe stress was imposed to the water stress treatment (45RDI-1L). Each point represents an individual value from each experimental plot. The line represents the linear model obtained for the well-watered treatment (100C-1L). The linear model obtained for the water stress treatment (45RDI-1L) was not significant and is therefore not shown.

4.3.5 Pressure-Volume Curves

Parameters calculated from the PV curves measured in leaves (for the 45RDI-1L treatment only) and in fruits (from both treatments) are shown in Table 4.1. $\Psi_{\pi 100}$ values for fruits from the 100C-1L treatment were higher than those seen for fruits from the 45RDI-1L treatment although no significant differences between irrigation treatments were found for $\Psi_{\pi 100}$ values in fruits. Furthermore, fruits from the 45RDI-1L treatment had significantly lower average Ψ_{TLP} values than fruits from the 100C-1L treatment, these being similar to average Ψ_{TLP} values obtained in leaves from the 45RDI-1L treatment.

Table 4.1: Parameters derived from pressure-volume curves measured in olive fruits and leaves. Data corresponds to the average ± standard error of the mean from fruits of the well-watered (100C-1L) and from the water stress treatment (45RDI-1L) and from leaves of the 45RDI-1L treatment. Different letters in the same column mean significant difference (pvalue<0.05, by the Tukey test), lowercase letters between fruits of 100C-1L and 45RDI-1L treatments and uppercase letter between fruits and leaves of the 45RDI-1L treatment. $\Psi_{\pi 100}$ – osmotic potential at saturation; Ψ_{TLP} – water potential at turgor loss point.

Tissue	Treatment	$\Psi_{\pi 100}$ (MPa)	Ψ_{TLP} (MPa)
Fruit	100C-1L	-1.615 ± 0.11a	-1.844 ± 0.08b
Fruit	45RDI-1L	-1.954 ± 0.13aA	-2.328 ± 0.09aA
Leaf	45RDI-1L	-1.488 ± 0.27A	-2.349 ± 0.34A

4.4 Discussion

4.4.1 Response of fruit growth to water stress

In this work we have studied the fruit-leaf water relations in olive trees and their influence on fruit growth. Although previous studies have extensively researched fruit development (Jones and Higgs, 1982; Lang, 1990; Higuchi and Sakuratani, 2006; Greer and Rogiers, 2009), few have focused on the interaction between water relations of fruits and leaves in the canopy under conditions of water stress (Greenspan et al., 1994; Greenspan et al., 1996; Mills et al., 1996; Pomper and Breen, 1997; Dell'Amico et al., 2012; Girón et al., 2015a).

The results presented here showed significant daily expansion and contraction of fruit diameters in response to both irrigation treatments (Fig. 4.4), with greater contraction seen for 45RDI-1L than for 100C-1L in the period when irrigation for the former was much lower than that for the latter (i.e. between period 2 and 3 and after period 3). Contractions usually happened in the afternoon and expansion at nights, except for periods of severe water stress when it did not occur (Fig. 4.5). These increased contractions reflected fluctuations in soil water content as a consequence of the irrigation scheduling used for that treatment. In contrast, fruit contraction in response to the 100C-1L treatment was mainly driven by the high vapor pressure deficit present in the study area (Fig. 4.1). These daily variations, mainly that of daily shrinkage, are usually interpreted as elastic variations in tissue volume (Lechaudel et al., 2007). Indeed, the daily changes of fleshy fruits involves a balance between supply and withdrawal of water via the vascular tissue, and losses through transpiration (Clearwater et al., 2012). The observed daily variations in fruit diameters can be interpreted as changes in water flows into and out of the fruit. The water stress caused greater fruit contraction during the day light hours within the deficit irrigated period for the 45RDI-1L treatment compared to 100C-1L, and the recovery at evening/night was not enough to increase or maintain the fruit diameter (Fig. 4.5), causing an apparent negative fruit growth (Fig. 4.3).

Under conditions of water stress, there is also a limitation of the carbon assimilated due to stomatal closure. Hernandez-Santana et al. (2018) demonstrated that cumulative fruit growth, more specifically biomass accumulation, was directly related to accumulated CO_2 assimilation. As other authors have reported (Matthews and Shackel, 2005; Génard et al., 2008) cumulative fruit growth is determined by biomass accumulation, confirming that CO_2 assimilation plays a major role in fruit growth, together with turgor maintenance. Further studies to examine the effect of water and photoassimilate relationships between fruits and leaves on fruit growth would help greatly to increase our understanding of fruit growth mechanisms. Although 45RDI-1L fruits were growing at a higher rate than 100C-1L fruits in the beginning, likely due to natural variability,

the drop in the cumulative fruit growth was relevant compared to 100C. However, even after that significant growth stop the studied 45RDI-1L trees recovered quickly, showing the daily pattern almost no contraction in some fruits during the afternoon (Fig. 4.5) such that the final fruit diameter of 45RDI-1L trees became similar to that of fruits from olive trees subjected to the 100C-1L treatment (Fig. 4.3), similar to what we found in the same orchard for several years Hernandez-Santana et al. (2017) and Hernandez-Santana et al. (2018). It is likely that the full irrigation applied during the critical stage of pit hardening, when most of the cell division and size are defined (Hammami et al., 2011), helped to reduce differences between water treatments. These results support the irrigation strategy used in this work, since water use was reduced, and a similar final fruit growth was achieved.

4.4.2 Water relations between fruits and leaves under water stress

We identified positive $\Delta\Psi_{\text{leaf-fruit}}$ values (Fig. 4.6) similar to that of Girón et al. (2015a), although they measured smaller water potential gradients. In the study by Dell'Amico et al. (2012), which was conducted in the same trees as those used by Girón et al. (2015a) (44-year-old table olive trees (cv Manzanillo)), even smaller gradients were reported and in most cases the gradient was negative (leaf water potential was lower than fruit water potential). In both studies, both leaf and fruit water potentials were higher than values measured in our study, indicating that the water stress was more severe in our study, which could explain the greater water potential gradients between leaves and fruits. Indeed, in the present work, where less stressful conditions prevailed at the end of the summer (more frequent irrigation and lower evaporative demand), the water potential gradient became smaller and closer to zero, particularly for midday measurements. They studied a different cultivar (Manzanilla) than in this study which may help to explain also these differences. The two aforementioned studies (Dell'Amico et al., 2012; Girón et al., 2015a) did not report continuous measurements of fruit growth as in our study, thus making it more difficult to interpret how $\Delta\Psi_{\text{leaf-fruit}}$ affected fruit growth. In Dell'Amico et al. (2012), fruit size was measured two times during the study, with a larger fruit size measured in stressed than in control trees. In Girón et al. (2015a), which reported results more in line with ours, fruit volume was measured regularly (13 times in 110 days), and they observed also a fruit volume decrease at the end of the water stress period. With their data they could conclude that water stress provoked that fruit was a stronger water sink than leaf. However, we demonstrated with our concomitant measurements of fruit growth dynamics (Figs. 4.3 and 4.5) and leaf-fruit water potentials (Fig. 4.6) that even according to the leaf-fruit water potentials the fruit would be a stronger water sink, the reduction of the fruit growth diameter may be explained by an imbalance in water discharge-refilling processes which in turn, may lead to a deple-

tion of water reserves in fruit exposed to water stress. This gradient towards the fruit may help olive fruits to recover growth quickly after stress compared to other temperate fruit species, where fruit have less negative water potentials than leaves (Greenspan et al., 1996; Morandi et al., 2010b; Morandi et al., 2011c). Thus, the study of water sink relationships between fruits and leaves would benefit greatly from the continuous monitoring of fruit growth, in addition to water potential measurements.

Although, this and the mentioned works (Dell'Amico et al., 2012; Girón et al., 2015a) were conducted comparing the water potentials of leaves and fruits, fruit vascular flows are driven usually by the water potential gradient between the stem and the fruit. Thus, stem water potential would be a more direct measurement influencing fruit water potential changes and their effects on fruit growth and daily shrinkage.

4.4.3 Effect of canopy water relations on fruit growth

As fruits and leaves can be considered as competing sinks for water, it has been assumed that the difference between fruit and leaf water potential determines the directionality of water exchange between the fruit and the parent plant (Matthews and Shackel, 2005). Thus, the positive $\Delta\Psi_{\text{leaf-fruit}}$ observed during maximum water stress would indicate water flow into the fruit from the parent tree. In this study, this phenomenon did take place in 100C-1L trees, but the greatest positive $\Delta\Psi_{\text{leaf-fruit}}$ measured in 45RDI-1L trees (Fig. 4.6) coincided with times of fruit contractions in these same trees (Fig. 4.3) Indeed, the greatest positive $\Delta\Psi_{\text{leaf-fruit}}$ during 45RDI-1L occurred when the highest fruit contractions were observed.

The enhanced fruit contraction along with positive $\Delta\Psi_{\text{leaf-fruit}}$ could be explained by an insufficient water flow into the fruit to balance fruit transpiration under water deficit conditions (Greenspan et al., 1994; Greenspan et al., 1996). Water entering the fruit can be used for growth, evaporation or, subsequently, a reverse flow to other tissues. The idea of sustained reverse flows from fruits to other tissues has been challenged (Clearwater et al., 2012), and it has been hypothesized that this probably occurs only as a transient morning reversal in sap flow (Higuchi and Sakuratani, 2006; Clearwater et al., 2009) or when plants undergo severe water stress (Greenspan et al., 1996; Clearwater et al., 2012). Thus, fruit transpiration together with a reduced fruit water inflow with water stress may be the most likely explanation for negative fruit growth as reported for other species (Greenspan et al., 1994; Greenspan et al., 1996; Morandi et al., 2007b; Greer and Rogiers, 2009; Clearwater et al., 2012), and especially in our case, where $\Delta\Psi_{\text{leaf-fruit}}$ was positive. The lack of correlation between leaf water potential and fruit contraction in 45RDI-1L trees (Fig. 4.7) may be considered as circumstantial evidence of a high resistance to flow from the parent tree to fruit, which could have resulted in impaired xylem water exchange in 45RDI-1L trees. In 100C-1L, however, the relationship between leaf

water status and fruit contractions was robust and significant. A change in the relative importance of xylem-phloem flows (Matthews and Shackel, 2005) as water stress develops may help to explain the lack of correlation between fruits and Ψ_{leaf} in 45RDI-1L trees as fruits would have had less influence from xylem Ψ_{leaf}. This phenomenon has also been described to occur towards the end of fruit development, as fruits become stronger sinks for water and carbohydrates (Mills et al., 1996). In addition, fruit transpiration has been reported to be relatively independent of stomatal regulation (Greenspan et al., 1994; Fishman and Génard, 1998; Montanaro et al., 2012), depending mainly on cuticular transpiration driven by vapor pressure deficit (Morandi et al., 2007b; Montanaro et al., 2012) (Morandi et al., 2007; Montanaro et al., 2012). This would result in a higher fruit transpiration on those days with remarkable a high atmospheric demand and again more independent of Ψ_{leaf} than leaf transpiration.

The greater importance of phloem compared to xylem flow could also help to explain the osmotic adjustment observed in 45RDI-1L fruits (Table 4.1) towards the end of the season (Matthews and Shackel, 2005), as this mechanism relies on the accumulation of solutes within the cells under water stress. These results indicate that leaf-fruit water potential measurements alone may not be sufficient to study competitiveness for water in the canopy. As such, fruit gauges could serve a useful role to help elucidate the water status and daily dynamics of fruit growth, and to establish deficit irrigation practices. Indeed, fruit growth is a sensitive water stress indicator as demonstrated here, with a remarkable capacity of recovery, and importantly, it is directly related to plant function and yield. These characteristics make fruit growth tracking a good candidate to schedule deficit irrigation but more work is needed before it can be used with that purpose.

4.5 Conclusions

To the best of our knowledge, this report marks the first attempt to measure fruit growth dynamics continuously in olive trees and to evaluate the role of water potential gradients between fruits and leaves on those dynamics at the same time. We confirm that olive fruit growth is sensitive to water stress and shows a remarkable capacity to recover following the irrigation strategy employed here. Our results also indicate that the study of water sink relationships between fruits and leaves would benefit greatly from the continuous monitoring of fruit growth, in addition to water potential measurements, as a progressive decoupling of fruit water status from leaves can arise as water stress progresses. We conclude that the imbalance in water discharge-refilling processes may lead to a depletion of water reserves in fruit exposed to water stress and accordingly to a net reduction in fruit diameter. Tracking fruit growth could serve as a promising approach to schedule regulated deficit irrigation, enabling determination of the level

of water stress that fruit can experience without affecting the recovery of their full size, while using less water in the process. Moreover, fruit growth is a highly relevant variable to measure because of its relationship to fruit yield. While more work is needed to fully evaluate the usefulness of fruit gauges to schedule regulated deficit irrigation, these results can be considered a first step towards achieving that purpose. The information provided by the fruit dendrometers could be integrated in increasingly used mechanistic models to schedule irrigation and predict yield for different environmental conditions, management approaches and cultivars. Future work should also consider the effect of biomass along with water accumulation and their relation to leaf water status.

4.6 References

Alegre, S., J. Marsal, M. Mata, A. Arbonés, J. Girona, and M.J. Tovar (2002). "Regulated deficit irrigation in olive trees (Olea europaea L. cv. Arbequina) for oil production". In: *Acta Horticulturae* 586, pp. 259–262. DOI: 10.17660/ActaHortic.2002.586.49.

Allen, R., L. S. Pereira, D. Raes, and M. Smith (1998). *Crop evapotranspiration - Guidelines for computing crop water requirements*. Rome: FAO Irrigation and Drainage, p. 15.

Clearwater, Michael J., Zhiwei Luo, Mariarosaria Mazzeo, and Bartolomeo Dichio (2009). "An external heat pulse method for measurement of sap flow through fruit pedicels, leaf petioles and other small-diameter stems". In: *Plant, Cell and Environment* 32.12, pp. 1652–1663. DOI: 10.1111/j.1365-3040.2009.02026.x.

Clearwater, Michael J., Zhiwei Luo, Sam Eng Chye Ong, Peter Blattmann, and T. Grant Thorp (2012). "Vascular functioning and the water balance of ripening kiwifruit (Actinidia chinensis) berries". In: *Journal of Experimental Botany* 63.5, pp. 1835–1847. DOI: 10.1093/jxb/err352.

Dag, Arnon, Amnon Bustan, Avishai Avni, Isaac Tzipori, Shimon Lavee, and Joseph Riov (2010). "Timing of fruit removal affects concurrent vegetative growth and subsequent return bloom and yield in olive (Olea europaea L.)" In: *Scientia Horticulturae* 123.4, pp. 469–472. DOI: 10.1016/j.scienta.2009.11.014.

De Swaef, Tom, Veerle De Schepper, Maurits W. Vandegehuchte, and Kathy Steppe (2015). "Stem diameter variations as a versatile research tool in ecophysiology". In: *Tree Physiology*. Ed. by Danielle Way, pp. 1–15. DOI: 10.1093/treephys/tpv080.

Dell'Amico, J., A. Moriana, M. Corell, I.F. F. Girón, D. Morales, A. Torrecillas, F. Moreno, J. Dell'Amico, A. Moriana, M. Corell, I.F. F. Girón, D. Morales, A. Torrecillas, F. Moreno, J. Dell'Amico, A. Moriana, M. Corell, I.F. F. Girón, D. Morales, A. Torrecillas, and F. Moreno (2012). "Low water stress conditions in table olive trees (Olea europaea L.) during pit hardening produced a different response of fruit and leaf

water relations". In: *Agricultural Water Management* 114.November 2012, pp. 11–17. DOI: 10.1016/j.agwat.2012.06.004.

Diaz-Espejo, Antonio, B. Hafidi, J.E. Fernandez, M.J. Palomo, and H. Sinoquet (2002). "Transpiration and photosynthesis of olive tree: a model approach". In: *Acta Horticulturae* 586, pp. 457–460. DOI: 10.17660/ActaHortic.2002.586.94.

Diaz-Espejo, Antonio, T.N. Buckley, J.S. Sperry, M.V. Cuevas, A. de Cires, S. Elsayed-Farag, M.J. Martin-Palomo, J.L. Muriel, A. Perez-Martin, C.M. Rodriguez-Dominguez, A.E. Rubio-Casal, J.M. Torres-Ruiz, and J.E. Fernández (2012). "Steps toward an improvement in process-based models of water use by fruit trees: A case study in olive". In: *Agricultural Water Management* 114, pp. 37–49. DOI: 10.1016/j.agwat.2012.06.027.

Fernández, J.E. and M.V. Cuevas (2010). "Irrigation scheduling from stem diameter variations: A review". In: *Agricultural and Forest Meteorology* 150.2, pp. 135–151. DOI: 10.1016/j.agrformet.2009.11.006.

— (2011). "Using plant-based indicators to schedule irrigation in olive". In: *Acta Horticulturae* 888, pp. 207–214. DOI: 10.17660/ActaHortic.2011.888.23.

Fernández, J.E., S.R. Green, H. W. Caspari, Antonio Diaz-Espejo, and M.V. Cuevas (2008b). "The use of sap flow measurements for scheduling irrigation in olive, apple and Asian pear trees and in grapevines". In: *Plant and Soil* 305.1-2, pp. 91–104. DOI: 10.1007/s11104-007-9348-8.

Fernández, J.E., Celia M. Rodriguez-Dominguez, Alfonso Perez-Martin, U. Zimmermann, S. Rüger, M.J. Martín-Palomo, J.M. Torres-Ruiz, M.V. Cuevas, C. Sann, W. Ehrenberger, and Antonio Diaz-Espejo (2011a). "Online-monitoring of tree water stress in a hedgerow olive orchard using the leaf patch clamp pressure probe". In: *Agricultural Water Management* 100.1, pp. 25–35. DOI: 10.1016/j.agwat.2011.08.015.

Fernández, J.E., Alfonso Perez-Martin, José M. Torres-Ruiz, María V. Cuevas, Celia M. Rodriguez-Dominguez, Sheren Elsayed-Farag, Ana Morales-Sillero, José M. García, Virginia Hernandez-Santana, and Antonio Diaz-Espejo (2013). "A regulated deficit irrigation strategy for hedgerow olive orchards with high plant density". In: *Plant and Soil* 372.1-2, pp. 279–295. DOI: 10.1007/s11104-013-1704-2.

Fishman, S. and M. Génard (1998). "A biophysical model of fruit growth: simulation of seasonal and dirunal dynamics of mass". In: *Plant, Cell and Environment* 21.8, pp. 739–752. DOI: 10.1046/j.1365-3040.1998.00322.x.

Génard, Michel, Jean Dauzat, Nicolás Franck, Françoise Lescourret, Nicolas Moitrier, Philippe Vaast, and Gilles Vercambre (2008). "Carbon allocation in fruit trees: From theory to modelling". In: *Trees - Structure and Function* 22.3, pp. 269–282. DOI: 10.1007/s00468-007-0176-5.

Girón, I.F., M. Corell, A. Galindo, E. Torrecillas, D. Morales, J. Dell'Amico, A. Torrecillas, F. Moreno, and A. Moriana (2015a). "Changes in the physiological response between leaves and fruits during a moderate water stress in table olive trees". In: *Agricultural Water Management* 148, pp. 280–286. DOI: 10.1016/j.agwat.2014.10.024.

Greenspan, M. D., M. A. Matthews, and K. A. Shackel (1994). "Developmental changes in the diurnal water budget of the grape berry exposed to water deficits". In: *Plant, Cell and Environment* 17.7, pp. 811–820. DOI: 10.1111/j.1365-3040.1994.tb00175.x.

Greenspan, Mark D., Hans R. Schultz, and Mark A. Matthews (1996). "Field evaluation of water transport in grape berries during water deficits". In: *Physiologia Plantarum* 97, pp. 55–62.

Greer, Dennis H. and Suzy Y. Rogiers (2009). "Water flux of Vitis vinifera L. cv. Shiraz Bunches throughout development and in relation to late-season weight loss". In: *American Journal of Enology and Viticulture* 60, pp. 155–163.

Hammami, Sofiene B M, Trinidad Manrique, and Hava F. Rapoport (2011). "Cultivar-based fruit size in olive depends on different tissue and cellular processes throughout growth". In: *Scientia Horticulturae* 130.2, pp. 445–451. DOI: 10.1016/j.scienta.2011.07.018.

Hernandez-Santana, Virginia, Celia M. Rodriguez-Dominguez, J. Enrique Fernández, and Antonio Diaz-Espejo (2016a). "Role of leaf hydraulic conductance in the regulation of stomatal conductance in almond and olive in response to water stress". In: *Tree Physiology* 36.6, pp. 725–735. DOI: 10.1093/treephys/tpv146.

Hernandez-Santana, Virginia, J.E. Fernández, M.V. Cuevas, Alfonso Perez-Martin, and Antonio Diaz-Espejo (2017). "Photosynthetic limitations by water deficit: Effect on fruit and olive oil yield, leaf area and trunk diameter and its potential use to control vegetative growth of super-high density olive orchards". In: *Agricultural Water Management* 184, pp. 9–18. DOI: 10.1016/j.agwat.2016.12.016.

Hernandez-Santana, Virginia, Rafael D.M. Fernandes, A. Perez-Arcoiza, J.E. Fernández, J.M. Garcia, and Antonio Diaz-Espejo (2018). "Relationships between fruit growth and oil accumulation with simulated seasonal dynamics of leaf gas exchange in the olive tree". In: *Agricultural and Forest Meteorology* 256-257.March, pp. 458–469. DOI: 10.1016/j.agrformet.2018.03.019.

Higuchi, Hirokazu and Tetsuo Sakuratani (2006). "Water Dynamics in Mango (Mangifera indica L.) Fruit during the Young and Mature Fruit Seasons as Measured by the Stem Heat Balance Method". In: *Journal of the Japanese Society for Horticultural Science* 75.1, pp. 11–19. DOI: 10.2503/jjshs.75.11.

Ho, L. C., R. I. Grange, and A. J. Picken (1987). "An analysis of the accumulation of water and dry matter in tomato fruit." In: *Plant, Cell and Environment* 10.2, pp. 157–162. DOI: 10.1111/1365-3040.ep11602110.

Hsiao, T. C., E. Acevedo, E. Fereres, and D. W. Henderson (1976). "Water Stress, Growth, and Osmotic Adjustment". In: *Philosophical Transactions of the Royal Society B: Biological Sciences* 273.927, pp. 479–500. DOI: 10.1098/rstb.1976.0026.

Iniesta, F., L. Testi, F. Orgaz, and F. J. Villalobos (2009). "The effects of regulated and continuous deficit irrigation on the water use, growth and yield of olive trees". In: *European Journal of Agronomy* 30.4, pp. 258–265. DOI: 10.1016/j.eja.2008.12.004.

Jones, H. G. and K. H. Higgs (1982). "Surface Conductance and Water Balance of Developing Apple (Malus pumila Mill.) Fruits". In: *Journal of Experimental Botany* 33.1, pp. 67–77. DOI: 10.1093/jxb/33.1.67.

Lang, Alexander (1990). "Xylem, Phloem and Transpiration Flows in Developing Apple Fruits". In: *Journal of Experimental Botany* 41.6, pp. 645–651. DOI: 10.1093/jxb/41.6.645.

Lechaudel, Mathieu, Gilles Vercambre, Françoise Lescourret, Frederic Normand, and Michel Génard (2007). "An analysis of elastic and plastic fruit growth of mango in response to various assimilate supplies". In: *Tree Physiology* 27.2, pp. 219–230. DOI: 10.1093/treephys/27.2.219.

Matthews, Mark A. and Ken A. Shackel (2005). "Growth and Water Transport in Fleshy Fruit". In: *Vascular Transport in Plants*, pp. 181–197.

Mencuccini, Maurizio, Teemu Hölttä, Sanna Sevanto, and Eero Nikinmaa (2013). "Concurrent measurements of change in the bark and xylem diameters of trees reveal a phloem-generated turgor signal". In: *New Phytologist* 198.4, pp. 1143–1154. DOI: 10.1111/nph.12224.

Mills, TM, M. H. Behboudian, and BE Clothier (1996). "Water relations, growth, and the composition ofBraeburn'apple fruit under deficit irrigation". In: *Journal of the American Society for Horticultural Science* 121.2, pp. 286–291.

Montanaro, Giuseppe, Bartolomeo Dichio, Cristos Xiloyannis, and Alexander Lang (2012). "Fruit transpiration in kiwifruit: Environmental drivers and predictive model". In: *AoB PLANTS* 2012.1, pp. 1–9. DOI: 10.1093/aobpla/pls036.

Morandi, Brunella, Luigi Manfrini, Marco Zibordi, Massimo Noferini, Giovanni Fiori, and Luca Corelli Grappadelli (2007a). "A Low-cost Device for Accurate and Continuous Measurements of Fruit Diameter". In: *HortScience* 42.6, pp. 1380–1382.

Morandi, Brunella, Mark Rieger, and Luca Corelli-Grappadelli (2007b). "Vascular flows and transpiration affect peach (Prunus persica Batsch.) fruit daily growth". In: *Journal of Experimental Botany* 58.14, pp. 3941–3947. DOI: 10.1093/jxb/erm248.

Morandi, Brunella, Luigi Manfrini, Pasquale Losciale, Marco Zibordi, and Luca Corelli Grappadelli (2010a). "Changes in vascular and transpiration flows affect the seasonal and daily growth of kiwifruit (Actinidia deliciosa) berry". In: *Annals of Botany* 105.6, pp. 913–923. DOI: 10.1093/aob/mcq070.

Morandi, Brunella, Luigi Manfrini, Pasquale Losciale, Marco Zibordi, and Luca Corelli-Grappadelli (2010b). "The positive effect of skin transpiration in peach fruit growth". In: *Journal of Plant Physiology* 167.13, pp. 1033–1037. DOI: 10.1016/j.jplph.2010.02.015.

Morandi, Brunella, Luigi Manfrini, Marco Zibordi, Pasquale Losciale, and Luca Corelli Grappadelli (2011a). "Effects of drought stress on the growth, water relations and vascular flows of young 'Summerkiwi' fruit". In: *Acta Horticulturae* 922, pp. 355–359. DOI: 10.17660/ActaHortic.2011.922.46.

Morandi, Brunella, Pasquale Losciale, Marco Zibordi, Luigi Manfrini, and Luca Corelli Grappadelli (2011b). "Leaf gas exchanges affect water flows to kiwifruit berries during the day". In: *Acta Horticulturae* 913, pp. 303–308. DOI: 10.17660/ActaHortic.2011.913.39.

Morandi, Brunella, Marco Zibordi, Pasquale Losciale, Luigi Manfrini, Emanuele Pierpaoli, and Luca Corelli-Grappadelli (2011c). "Shading decreases the growth rate of young apple fruit by reducing their phloem import". In: *Scientia Horticulturae* 127.3, pp. 347–352. DOI: 10.1016/j.scienta.2010.11.002.

Morandi, Brunella, Pasquale Losciale, Luigi Manfrini, Marco Zibordi, Stefano Anconelli, Fabio Galli, Emanuele Pierpaoli, and Luca Corelli Grappadelli (2014a). "Increasing water stress negatively affects pear fruit growth by reducing first its xylem and then its phloem inflow". In: *Journal of Plant Physiology* 171.16, pp. 1500–1509. DOI: 10.1016/j.jplph.2014.07.005.

Moriana, Alfonso, Francisco Orgaz, Miguel Pastor, and Elias Fereres (2003). "Yield responses of a mature olive orchard to water deficits". In: *Journal of the American Society for Horticultural Science* 128.3, pp. 425–431.

Naor, A., D. Schneider, A. Ben-Gal, I. Zipori, A. Dag, Z. Kerem, R. Birger, M. Peres, and Y. Gal (2013). "The effects of crop load and irrigation rate in the oil accumulation stage on oil yield and water relations of 'Koroneiki' olives". In: *Irrigation Science* 31.4, pp. 781–791. DOI: 10.1007/s00271-012-0363-z.

Nguyen, Hoa T., Patrick Meir, Joe Wolfe, Maurizio Mencuccini, and Marilyn C. Ball (2017). "Plumbing the depths: extracellular water storage in specialized leaf structures and its functional expression in a three-domain pressure –volume relationship". In: *Plant Cell and Environment* 40.7, pp. 1021–1038. DOI: 10.1111/pce.12788.

Orgaz, F., L. Testi, F.J. Villalobos, and E. Fereres (2006). "Water requirements of olive orchards–II: determination of crop coefficients for irrigation scheduling". In: *Irrigation Science* 24.2, pp. 77–84. DOI: 10.1007/s00271-005-0012-x.

Pomper, K W and P J Breen (1997). "Expansion and osmotic adjustment of strawberry fruit during water stress". In: *Journal of the American Society For Horticultural Science* 122.2, pp. 183–189.

R Core Team (2015). *R: A Language and Environment for Statistical Computing*. Vienna, Austria.

Tardieu, François, Christine Granier, and Bertrand Muller (2011). "Water deficit and growth. Co-ordinating processes without an orchestrator?" In: *Current Opinion in Plant Biology* 14.3, pp. 283–289. DOI: 10.1016/j.pbi.2011.02.002.

Zibordi, Marco, Sara Domingos, and Luca Corelli Grappadelli (2009). "Thinning apples via shading: an appraisal under field conditions". In: *The Journal of Horticultural Science and Biotechnology* 84.6, pp. 138–144. DOI: 10.1080/14620316.2009.11512611.

CHAPTER 5

Are fruit dendrometers reliable to schedule deficit irrigation in olive trees?

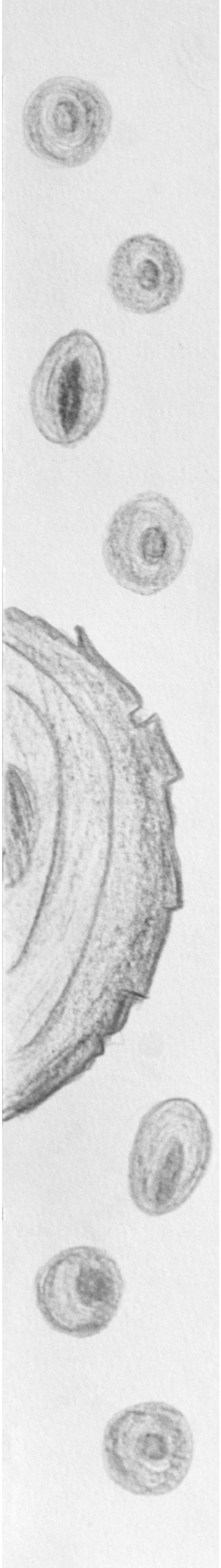

Abstract

Fruit dendrometer have been intensively used in the study of fruit crop management but rarely as a water stress indicator. This occurs despite fruit development being highly correlated to production. The objectives of this work were to evaluate the usefulness of the fruit dendrometer to assess water stress in a commercial SHD olive orchard, and to derive the best water stress index derived from the collected records and to test its potential to schedule a regulated deficit irrigation (RDI) strategy in the orchard. We compared fruit dendrometers with trunk dendrometers and ZIM probes (leaf patch clamp pressure probes), two other methods widely used with the commented purposes, as well as with physiological measurements of midday leaf water potential ($\Psi_{l,md}$), daily maximum leaf stomatal conductance ($g_{s,max}$) and daily maximum net photosynthesis rate ($A_{N,max}$). All the sensors were installed in the olive trees at the beginning of the irrigation season, in both well-watered trees (100C-1L, 100% of the crop water needs supplied) and water–stressed trees (45RDI-1L, trees under an RDI strategy supplying 45% of the crop water needs). From the indexes derived from the fruit dendrometers, the daily maximum fruit diameter (MXFD) was considered the best, because it shows the growing trend of fruit diameter and also the influence of low frequency irrigation events. For the 45RDI-1L treatment, fruit and trunk daily growth (DG_{fruit} and DG_{trunk}, respectively) showed significant correlation with $\Psi_{l,md}$, but only DG_{fruit} presented significant correlations with $g_{s,max}$ and $A_{N,max}$. On the days when irrigation was applied DG_{fruit} and the maximum output value of the ZIM probes ($P_{p,max}$) increased, but the DG_{trunk} responded only one day after irrigation was applied. We considered that the fruit dendrometer have a potential as a reliable method to schedule RDI, which is advantageous because fruits are more directly related to final yield than the other indicators to assess water stress normally used in commercial orchards. However, as fruit growth is a priority for the trees under water stress, the use of just fruit dendrometers to schedule deficit irrigation could lead to a decrease in vegetative growth, which should be considered. Still, a complementary method to schedule irrigation is required at the beginning of the irrigation season, when there are no fruits, or they are too small.

5.1 Introduction

Changes in climate, due to the global warming, are increasing the need to better manage the water use in agriculture, with the consequent need to limit irrigation in areas with low water availability. One approach to this problem is to improve performance and efficiency of the irrigation systems. But another important approach is to improve the irrigation management, mainly from effective deficit irrigation strategies (Fereres

and Soriano, 2007; Fernández et al., 2013), and from reliable and methods to schedule irrigation (Jones, 2004; Fernández, 2017).

The search for an inexpensive, easy to use and precise method to schedule irrigation has been the aim of many studies. Sensors and related systems providing sap flow (Fernández et al., 2012), trunk diameter variations (Cuevas et al., 2010; Cuevas et al., 2013) and leaf turgor related measurements (Padilla-Díaz et al., 2016; Padilla-Díaz et al., 2018) have been tested. Also, thermal images, both at the plant level (García-Tejero et al., 2017) or above the orchard (Egea et al., 2017; Gonzalez-Dugo et al., 2013; Gonzalez-Dugo et al., 2015) have been evaluated. Daily changes in fruit diameter have been studied through the use of fruit dendrometers in crops such as apple (Jones and Higgs, 1982; Zibordi et al., 2009; Morandi et al., 2011c), pear (Morandi et al., 2014a), peach (Morandi et al., 2007b; Morandi et al., 2010b), and kiwifruit (Morandi et al., 2011b; Morandi et al., 2011a), aiming at understanding the flows of water and nutrients into and out of the fruits. To our best knowledge, however, no previous studies have been published on the use of fruit dendrometers with the aim of assessing water stress in olive.

When assessing new sensors and related systems, as well as water stress indexes derived from the collected records, to schedule irrigation, authors usually compare the measurements of the new sensor with concomitant measurements with a well-known, reliable method, such as leaf water potential (Ψ_{leaf}), stem water potential (Ψ_{stem}), and daily maximum stomatal conductance ($g_{s,max}$). Padilla-Díaz et al. (2016), Padilla-Díaz et al. (2018), and Fernandes et al. (2017) used Ψ_{stem} and $g_{s,max}$ to assess the use of ZIM, or LPCP, probes in a hedgerow olive orchard with high plant density, or super high density (SHD) olive orchard, both under full irrigation and deficit irrigation. (Cuevas et al., 2013) have compared the use of sap flow and trunk diameter variation related measurements with Ψ_{stem} measurements, in different types of olive orchards, to assess the potential and limitations of each method.

Considering the lack of experiments on the use of fruit dendrometers to assess water stress in olive, this study aimed: (i) to evaluate the usefulness of the fruit dendrometer to assess water stress in a commercial SHD olive orchard, and to derive the best water stress index derived from the collected records; and (ii) to test its potential to schedule a regulated deficit irrigation (RDI) strategy in the orchard. Changes in fruit diameter were continuously recorded throughout the irrigation period of 2017 and compared with changes in trunk diameter (trunk dendrometers), leaf turgor related measurements (ZIM probes) and midday leaf water potential. Our final aim was to better understand the relations between fruit growth and plant water status, and to determine whether the first can be used to schedule irrigation in olive.

5.2 Material and Methods

5.2.1 Experimental orchard and irrigation treatments

The experiments were performed in 2017 in a super high density olive orchard, located at 25 km to the south-east of Seville, Spain (37°15′ N, −5°48′ W, 60 m a.s.l.). Trees (*Olea europaea* L., cv. Arbequina), were 11 years old at the time of the study. They were planted in a configuration of 4 m x 1.5 m (1667 trees ha^{-1}) at the top of 0.4 m high ridges oriented N-NE to S-SW. The soil has a sandy loam texture on the top 0.4 m, with a sandy clay layer below. The climate in the area is typical Mediterranean with 516.4 mm and 1528.5 mm average annual precipitation (P) and potential evapotranspiration (ET_o), respectively (period 2002-2017). Meteorological variables were recorded by a Campbell weather station (Campbell Scientific Ltd., Shepshed, UK) located in the center of the area covered by the experimental plots, with the meteorological sensors located between 1 and 3 m above the canopies. The station recorded 30 min average radiation (R_s), air temperature (T_{air}), relative humidity (RH) of the air, and P. ET_o values used to schedule irrigation with the crop coefficient approach were collected from a nearby standard weather station (37°10′N, −5°40′W) belonging to the Agroclimatic Information Network of the local government (Junta of Andalusia).

We applied a well-watered (100C-1L) treatment and a water-stressed (45RDI-1L) treatment from May 19th (day of year - DOY - 139) to October 25th (DOY 298). Each treatment was applied to four 12 m x 16 m plots in a randomized block design. Each plot had 24 trees, and measurements were made in the central eight trees to avoid border effects. The irrigation system consisted of a single pipe per tree row with three 2 $L\,h^{-1}$ drippers per tree, 0.5 m apart. An automatic controller (Agronic 2000, Sistemes electronics PROGRÉS S.A., Lleida, Spain) was used for irrigation supply. The 100C-1L trees were irrigated daily to replace 100% of the irrigation needs (IN). These IN were calculated daily with a simplified version of the stomatal conductance (g_s) model tested for our orchard by Diaz-Espejo et al. (2012), where g_s was described as a function of air vapor pressure deficit (D), R_s and tree leaf area (LA). The leaf area was estimated at dawn with a LAI-2200 Plant Canopy Analyzer (Li-Cor, Inc., Lincoln, NE, USA) once every two weeks for each plot during the irrigation season, following the procedure described by Diaz-Espejo et al. (2012). Tree leaf area was estimated as described in Section 5.2.4. The percentage of sunny to total leaf area, estimated after Diaz-Espejo et al. (2002) and Fernández et al. (2008a), was assumed to be 0.35. Vapor pressure deficit hourly values were predicted for the three following days according to the weather forecast for the studied area provided by Meteogrid (Madrid, Spain). Assuming a perfect coupling between canopy and atmosphere (the olive tree has small leaves), tree water consumption (E_p) was calculated as $E_p = D \cdot (g_{s,sun} \cdot A_{sun} + g_{s,shade} \cdot A_{shade})$, where D is the vapor pressure

deficit, $g_{s,sun}$ and $g_{s,shade}$ are stomatal conductance of new, sun-exposed leaves and old, shaded leaves, respectively; A_{sun} and A_{shade} are the corresponding leaf areas of sun and shade leaves, respectively. Soil evaporation (E_s) was estimated according to Orgaz et al. (2006). Finally, the irrigation requirements (IN) were estimated as $E_p + E_s$. Similarly, the soil water content dynamic was monitored to confirm that field capacity remained over the entire irrigation period in 100C-1L plots and therefore the IN applied had been correctly estimated. The 45RDI-1L trees were irrigated following a regulated deficit irrigation (RDI) strategy first recommended by Fernández et al. (2013) and perfected by Fernández et al. (2018b) for the orchard conditions. The RDI strategy considers three critical periods along the olive tree growing cycle, for which the plant is highly sensitive to water stress and, therefore, irrigation supplies must be equal or close to the irrigation needs. Period 1 extends from the final stages of floral development to full bloom (in our area, this usually occurs in the second fortnight of April); period 2 goes from the 6th to the 10th week after full bloom (June). This agrees with an active phase of cell division in the fruit, just before the pit offers resistance to be cut with a knife; and period 3, after the midsummer period of high atmospheric demand, when olive have a marked capacity to recover from water stress (from late August to mid-September). Between periods 2 and 3 (late June to late August) the olive tree is highly resistant to drought (Alegre et al., 2002; Moriana et al., 2003; Iniesta et al., 2009; Fernández et al., 2013). Therefore, the RDI trees were irrigated daily on periods 1 to 3 to replace the crop water needs, but in between periods 2 and 3, they were irrigated twice per week only, replacing ca. 20% IN in that period. From the end of period 3 to harvesting (end of October) ca. 40% of IN was supplied, with 2-3 irrigation events per week (see Fernández et al. (2013) and Hernandez-Santana et al. (2017) for further details). No irrigation was needed, in 2017, the experimental year, in period 1, because rainfall was enough to replace the crop water needs. The irrigation season started on DOY 139, i.e. in between period 1 and period 2. Period 2 was from June 8th to July 4th (DOY 159 to 185), and period 3 from August 26th to September 19th (DOY 238 to 262).

Two access tubes were installed in each plot, at 0.1 m and at 0.4 m from the dripper, and at 0.5 m from the tree trunk, to measure the soil volumetric water content (θ, $m^3\,m^{-3}$) with a Profile probe (Delta-T Devices Ltd., Cambridge, UK) calibrated in situ (Fernández and Cuevas, 2011). Measurements were performed at the time of maximum g_s (ca. 9.00 GMT), at depths of 0.1, 0.2, 0.3, 0.4, 0.6 and 1.0 m. A weighted θ average with the measurements from 0.1 to 0.4 m was calculated for each plot, weighted by the percentage of roots, and then by a simple average of the averages obtained in the plot. Soil volumetric water content for field capacity in the top 0-0.40 m was 0.28 $m^3\,m^{-3}$ and 0.049 $m^3\,m^{-3}$ for the permanent wilting point.

5.2.2 Plant water status and gas exchange measurements

Midday leaf water potential ($\Psi_{l,md}$) was measured at midday (ca. 11.00 GMT) every two weeks between May 31 (DOY 151) and October 23 (DOY 296) with a Scholander-type pressure chamber (PMS Instrument Company, Albany, Oregon, USA). One leave was sampled from each of two central trees per plot, in three out of the four plots, (n = 3), The leaves were young but dully developed, from near the apex of current-year shoots in the outer, sunny, part of the canopy. Leaf samples were stored in plastic bags with moist filter paper until the measurement of $\Psi_{l,md}$ were made in the laboratory, on the afternoon of the sampling days (see Fernandes et al. (2018) for further details).

On the same days and following the same criteria for sampling the leaves, maximum leaf stomatal conductance ($g_{s,max}$) and net photosynthesis ($A_{n,max}$) were measured with a Licor LI-6400 portable photosynthesis system (Li-cor, Lincoln NE, USA) with a 2 cm x 3 cm standard chamber. Two leaves from two central trees in three plots per treatment (n=3) were measured at ca. 09.00 GMT, the time for maximum daily stomatal conductance in olive tree (Fernández et al., 1997).

5.2.3 Fruit and trunk diameter variations and leaf turgor related measurements

Fruit dendrometers were installed in three out of the four plots per treatment, in one fruit of two representative trees per plot, totaling six monitored fruits per treatment. We used two types of fruit dendrometers; the FI-XSSF model from Solfranc (Solfranc Tecnologias, SL, Tarragona, Spain), installed in four fruits (two fruits per treatment); and a model adapted from a linear potentiometer MM(R)10-11 with internal spring return (from Megatron Elektronik GmbH & Co., Munich, Germany) coupled to a sensor holder, which we installed in four fruits per treatment (a total of eight fruits). All fruit dendrometers recorded fruit equatorial diameter every 5 min with the use of a datalogger (CR1000, Campbell Scientific Ltd., Shepshed, UK). The Megatron model was successfully used by Morandi et al. (2007a) to monitor apple fruit diameter. A comparison was performed between the two models of fruit dendrometers (Fernandes et al., 2018), aiming at analyzing the similarity of the measured data between each model. We found very similar results (Megatron-Solfranc fruit daily variations for 100C-1L fruits: r=0.86, p <0.0001, slope=1.05; and for 45RDI-1L fruits: r=0.91, p <0.0001, slope=1.06).

We calculated three water stress indexes from the collected records, similar to those derived from trunk diameter variations (Fernández and Cuevas, 2010). These indexes were: (i) fruit daily growth (DG_{fruit}), which is the difference between the maximum fruit diameter between two consecutive days; (ii) fruit maximum daily shrinkage (MDS_{fruit}), calculated by subtracting the minimum from the maximum diameter recorded on the

same day; and (iii) maximum fruit diameter (MXFD), i.e. the maximum diameter recorded on the day.

Trunk dendrometers (Plantsens radial dendrometer, Verdtech un Nuevo Campo S.A.; Lepe, Spain) were installed in one out of the two central trees monitored with fruit dendrometers., i.e. in three trees per treatment. Trunk dendrometers were installed at ca. 20 cm from the soil and connected to a datalogger (CR1000, Campbell Scientific Ltd., Shepshed, UK), which recorded the changes in trunk diameter every 30 minutes. From the recorded trunk diameter variations we derived the daily maximum trunk diameter (MXTD), the trunk daily growth (DG_{trunk}) and the trunk maximum daily shrinkage (MDS_{trunk}).

ZIM probes (YARA ZIM Plant Technology, Hennigsdorf, Germany) were installed in two fully expanded leaves of each tree instrumented with fruit dendrometers, totaling six leaves per treatment. They were connected to a radio transmitter, which transferred the data every five minutes to a datalogger in the orchard. Twice a day the storage data were sent via GPRS to a server of the manufacturer, for the data to be accessible through the internet. From the daily variations of P_p we derived $P_{p,max}$.

5.2.4 Calculations and statistical analysis

The daily maximum output pressure measured with the ZIM probes ($P_{p,max}$) was firstly averaged by plot, and then, the treatments' average and standard error were calculated with the average from each experimental plot.

Data regarding midday leaf water potential ($\Psi_{l,md}$), maximum stomatal conductance ($g_{s,max}$) and net photosynthesis ($A_{N,max}$) were firstly averaged by plot, then the treatments' average and standard error were calculated using the average from each experimental plot.

Comparisons of $\Psi_{l,md}$, $g_{s,max}$, $A_{N,max}$ and θ between treatments were performed by the t-Student test, as there were only two irrigation treatments, the significant differences (p <0.05) were identified with asterisks in the graphs. The data regarding DG_{fruit} and DG_{trunk} were tested individually against $\Psi_{l,md}$, $g_{s,max}$ and $A_{N,max}$ for correlation, using the Pearson's correlation coefficient (r). In the graphs, the Pearson's correlation coefficient is shown only when a significant correlation was found (p <0.05). The MDS_{fruit} and MDS_{trunk} data were also tested for correlation (Pearson's coefficient) with $P_{p,max}$, considering all the irrigation period.

5.3 Results

5.3.1 Meteorological and soil water conditions

Weather conditions during the irrigation season were typical of the Mediterranean climate in the area (Fig. 5.1). Maximum temperature exceeded 30°C on 80% of the experimental days (Fig. 5.1A). Daily potential evapotranspiration (ET_o) averaged 6.26 mm from the beginning of the experiment, on May 31st (DOY 151), to August 18th (DOY 230), with four days with peak values higher than 7.5 mm. Then decreased from mid-August to the end of the season. The average ET_o for the whole experimental period was 5.20 mm (Fig. 5.1B). Daily total solar radiation (R_s) was around 28.42 kJ m^{-2} before DOY 230 (August 18th) and decreased slightly thereafter, with an average of 24.70 kJ m^{-2} for the experimental period (Fig. 5.1C). In ca. 58% of the days, daily R_s values over 25 kJ m^{-2}. Maximum R_s and ET_o are normally recorded in July and August, but in 2017 were recorded in June.

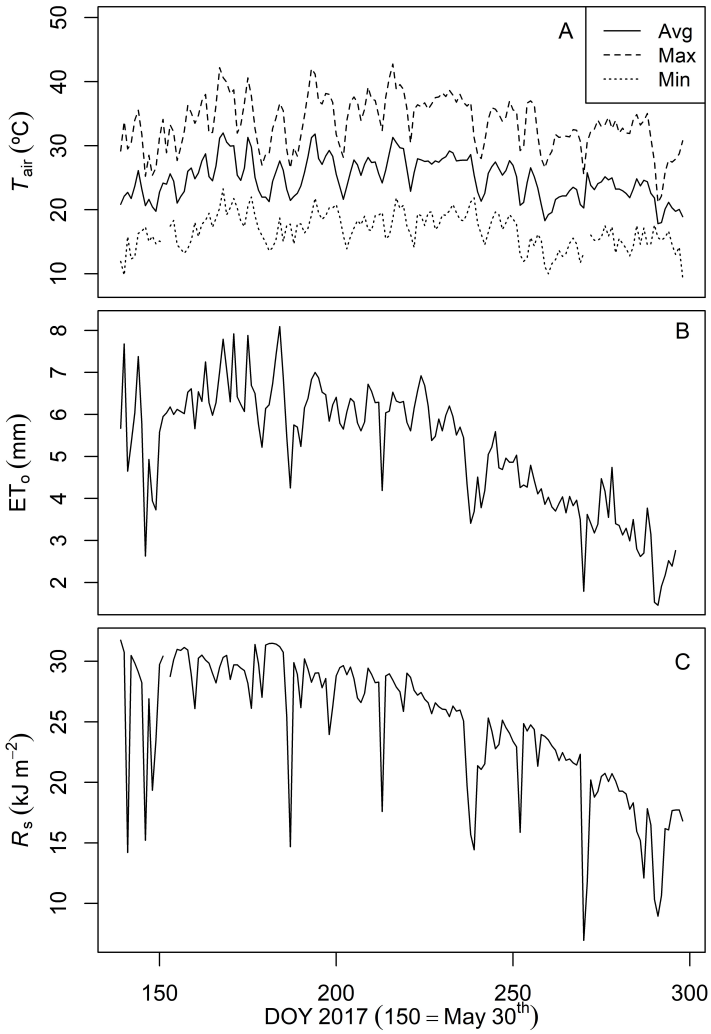

Figure 5.1: Meteorological conditions during the experimental period. (A) Air temperature (T_{air}), (B) evapotranspiration (ET_o), and (C) daily total solar radiation (R_s)

The time courses of the irrigation amounts (IA) applied in each treatment are shown in Fig. 5.2A. We calculated the IN for the experimental season with the crop coefficient approach, to compare it with the IA supplied after using the g_s approach described in Section 5.2.1 to estimate the crop water needs in the orchard. Our data show that IN estimated with the crop coefficient approach amounted to 4595.27 $m^3\,ha^{-1}$. The total IA supplied to the 100C-1L was 3748.10 $m^3\,ha^{-1}$. In other words, the IA values applied with the g_s approach were 81.6% only. The crop coefficient approach is a relatively coarse method, so this 18.4% difference does not necessarily mean that the g_s approach underestimated IN. Concerning the 45RDI-1L treatment, we applied 1689 $m^3\,ha^{-1}$, i.e. 36.8% of IN. Small amounts of precipitation occurred at the end of the irrigation season, totaling 17.62 mm on a 6-day period (Fig. 5.2A).

The impact of the water supplies on the soil water status of each treatment is shown in Fig. 5.2. On period 1, the irrigation amounts were lower in the 45RDI-1L treatment than in the 100C treatment (the adopted 45RDI irrigation strategy advices for IA to be ca. 80% of IN), but this had little effect on the averaged volumetric water contents (θ), such that no significant differences between treatments were found (Fig. 5.2B). In between periods 2 and 3, i.e. from July 4th (DOY 185) to August 26 (DOY 239), θ values in the 45RDI-1L treatment were significantly lower (ca. 57% lower; p <0.05) than in the 100C-1L treatment, in agreement with the lower IA applied to the deficit irrigation on those weeks. In period 3 the soil water content recovered, although not fully, and from the end of period 3 to the end of the irrigation season (DOY 262 to 298), they remained lower than for the 100C-1L treatment, as expected because of the lower IA applied at the end of the season (Fig. 5.2B).

5.3.2 Plant water status

Midday leaf water potential ($\Psi_{l,md}$) measurements revealed differences between 100C-1L and 45RDI-1L treatments during the deficit irrigation periods of the irrigation season (Fig. 5.3B). Measurements on periods 2 and 3 showed no differences. In the 100C-1L trees, values of $\Psi_{l,md}$ were above -1.4 MPa (a threshold for the olive water stress, according to Moriana et al. (2012)) for most of the irrigation season. The 45RDI-1L trees showed $\Psi_{l,md}$ values lower than -1.5 MPa all over the season, except in periods 2 and 3. The greater irrigation amounts supplied in those periods were enough for the trees to recover from the previous water stress. After period 3, the 45RDI-1L trees were more stressed than the 100C-1L trees. For both treatments, therefore, the time courses of $\Psi_{l,md}$ echoed those of θ, as expected.

Measurements of maximum daily leaf stomatal conductance ($g_{s,max}$) and net photosynthesis ($A_{N,max}$) also revealed a clear impact of the irrigation treatments on leaf gas exchange (Fig. 5.4). On periods 2 and 3, no differences between treatments were found,

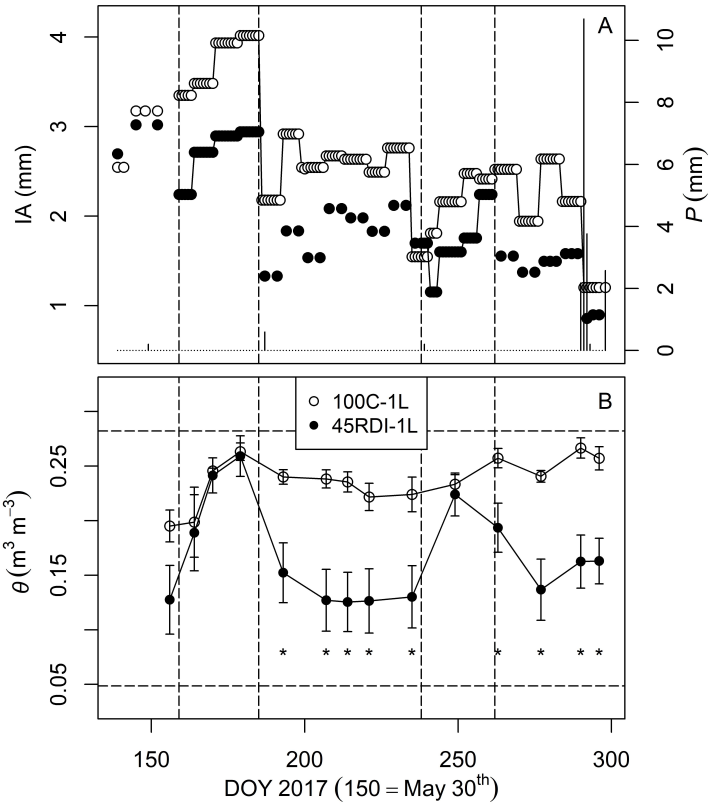

Figure 5.2: Time courses of the irrigation amounts (IA) for each treatment, precipitation collected in the orchard (A), and averaged soil volumetric water content (θ) during the 2017 irrigation season (B). For graph B, each point is the average of three plots, with the vertical bars representing the standard error of the mean. Different letters show significant differences (p <0.05). The horizontal dashed lines in graph B represent θ at field capacity and at the wilting point (0.282 and 0.049 $m^3\ m^{-3}$) respectively. Dashed vertical lines represent periods 2 and 3.

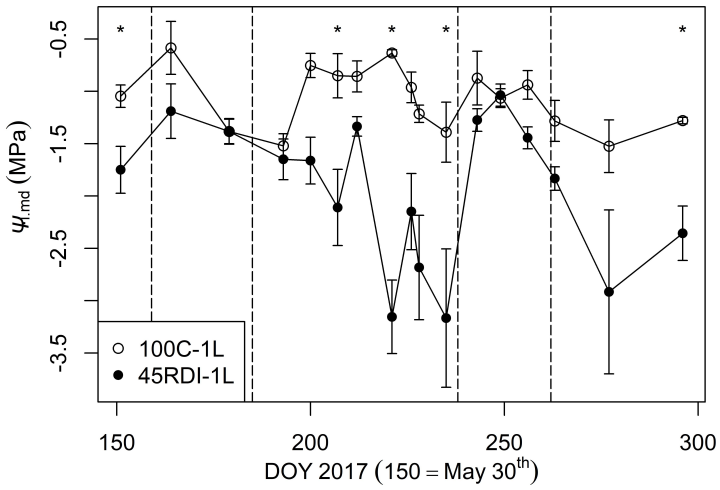

Figure 5.3: Time courses of midday leaf water potential ($\Psi_{l,md}$) for each treatment. Dashed vertical lines represent periods 2 and 3. Asterisks indicate significant difference between treatments (p <0.05). Each point is the average of two measurements in three experimental plots. Vertical bars represent the standard error of the mean between the plots.

either for $g_{s,max}$ or $A_{N,max}$. On the periods of deficit irrigation, however, both variables were lower in the 45RDI-1L trees than in the 100C-1L trees. On the first half of the season, values of both variables recorded in the control 100C-1L trees were typical of olive plants growing under non-limiting conditions. From mid-August (ca. DOY 220) to the end of the season, however, lower values of both variables were recorded. This agrees with the increase in water stress recorded in the 100C-1L trees at the end of the season (Fig. 5.3). In the 45RDI-1L trees, the lowest values of both $g_{s,max}$ and $A_{N,max}$ were recorded on the previous days to period 3 (Fig. 5.4B), i.e. at the end of the mid-summer period with high atmospheric demand and low irrigation supplies. Once again, this agrees with the dynamics of both soil water content (Fig. 5.2B) and leaf water potential (Fig. 5.3).

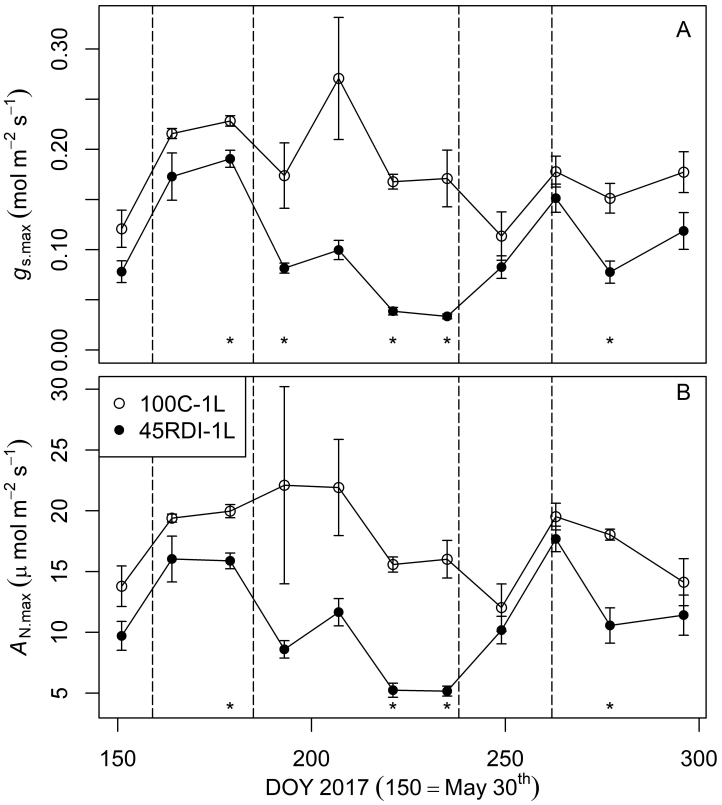

Figure 5.4: Time courses of maximum of daily maximum leaf stomatal conductance ($g_{s,max}$, A) and net photosynthesis ($A_{N,max}$, B) along the irrigation season. Dashed vertical lines represent periods 2 and 3. Asterisks indicate significant difference between treatments (p <0.05). Each point is the average of three experimental plots. Vertical bars represent the standard error of the mean between the plots.

5.3.3 Fruit dendrometer derived indexes

The DG_{fruit} values recorded in the 45RDI-1L trees present great variations from positive to negative values during the deficit irrigated periods, in agreement to the frequency of irrigation on those weeks (Fig. 5.5A). More negative DG_{fruit} values were as θ progressively decreased (Fig. 5.2B). Changes in water supplies also affected the fruit maximum

daily shrinkage (MDS_{fruit}) values of the 45RDI-1L fruits (Fig. 5.5B). Concerning those recorded in the 100C-1L, a clear effect of both weather conditions (Fig. 5.1) was also observed. This is not surprising, since both ET_o and R_s are main driving variables for olive transpiration (Fernández, 2014b). For both treatments, the time courses of the daily maximum fruit diameter (MXFD) presented a double-sigmoidal curve (Fig. 5.5C), with two periods in which the slope decreased (100C -1L trees) or even became negative (45RDI-1L trees), both in between periods 2 and 3 and after period 3. Records from the 45RDI-1L trees (Fig. 5.5C) show that his MXFD variable also responded to the intermittent irrigation supplies in between periods 2 and 3 and after period 3. The MXFD values for the 45RDI-1L trees show a greater increase in fruit diameter during period 2, in comparison to the 100C-1L fruits. We have not an explanation for that, since the rest of recorded variables on soil water content, plant water status and leaf gas exchange show similar conditions of water stress for the two irrigation treatments. Data in Fig. 5.5 shows a full recovery of fruit diameter on period 3. This illustrates the outstanding capacity of the olive tree to recover, at that time of the year, from the stress suffered in between periods 2 and 3 (Lavee et al., 1990; Moriana et al., 2007). At the end of the irrigation period, the MXFD values were similar for both irrigation treatments.

5.3.4 Water stress indexes from the other plant-based sensors

Contrary to what we expected, the trunk of the 100C-1L trees did not increase much in diameter during the experimental period. In fact, the diameter of the 45RDI-1L trees increased more than that of the fully irrigated 100C-1L trees (Fig. 5.6), with the exception of the periods of severe water stress registered in between periods 2 and 3 and after period 3 (Fig. 5.3). The MXFD values have been included in Fig. 5.6 for comparison.

Concerning the maximum output pressure ($P_{p,max}$) recorded with the ZIM probes, values recorded in the 100C-1L trees showed, in general, decreasing values in June (ca. DOY 150-180), in agreement with the increasing soil water content (θ) values (Fig. 5.2). Also, in between period 2 and 3 the $P_{p,max}$ increased, as corresponded to the decreasing θ values. At the end of the season $P_{p,max}$ values were quite low, in agreement with the high θ values. The expected inversed correlation between $P_{p,max}$ and θ was even more clear in the 45RDI-1L trees, likely because of the greater levels of water stress reached in those trees (Fig. 5.3). As for the other tested water stress indicators, the irrigation events in between period 2 and 3 markedly affected the P_p readings.

5.3.5 Impact of low frequency irrigation on MXFD, MXTD and $P_{p,max}$

To better analyze the impact of the irrigation events in the value of the tested water stress indexes, in Figure 5.7 we represent the values of MXTD, MXFD and $P_{p,max}$

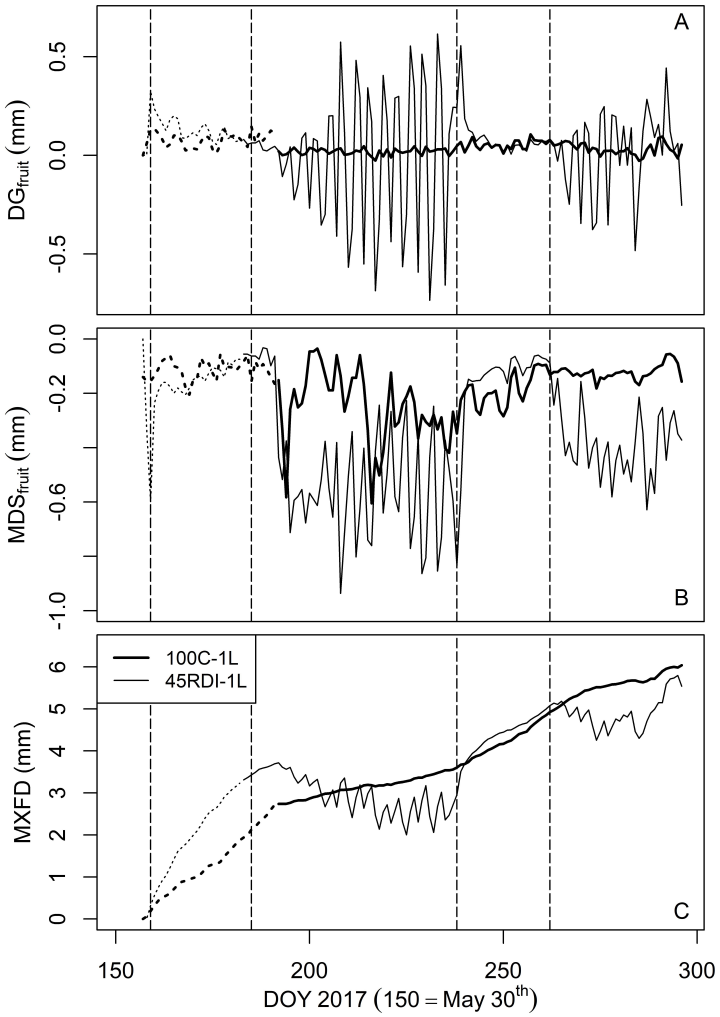

Figure 5.5: Time courses of the three water stress indexes derived from the records of the fruit dendrometers installed in trees of each treatment: daily growth (DG_{fruit}, A); maximum daily shrinkage (MDS_{fruit}, B) and maximum fruit diameter (MXFD, C). The discontinuous lines refer to the period when less than three fruit dendrometers were recording data simultaneously. Dashed vertical lines represent periods 2 and 3.

recorded in the 45RDI-1L trees in between periods 2 and 3, when irrigation was applied twice per week only. For clarity, Fig. 5.7 shows the average value only, without the error bars. All three variables behaved accordingly to the day when irrigation was applied, with an increase in MXFD and $P_{p,max}$ in these days and a decrease as water availability decreases. However, it should be noted from DOY (191) that the MXTD values increased one day after the irrigation was applied, showing a different behavior from the MXFD and $P_{p,max}$ values. It should also be noted that the fruit is the last one to accuse water stress and the first one in recovering. The trunk and leaf seem to come in and out of stress practically at the same time (from DOYs 188 y 238 respectively).

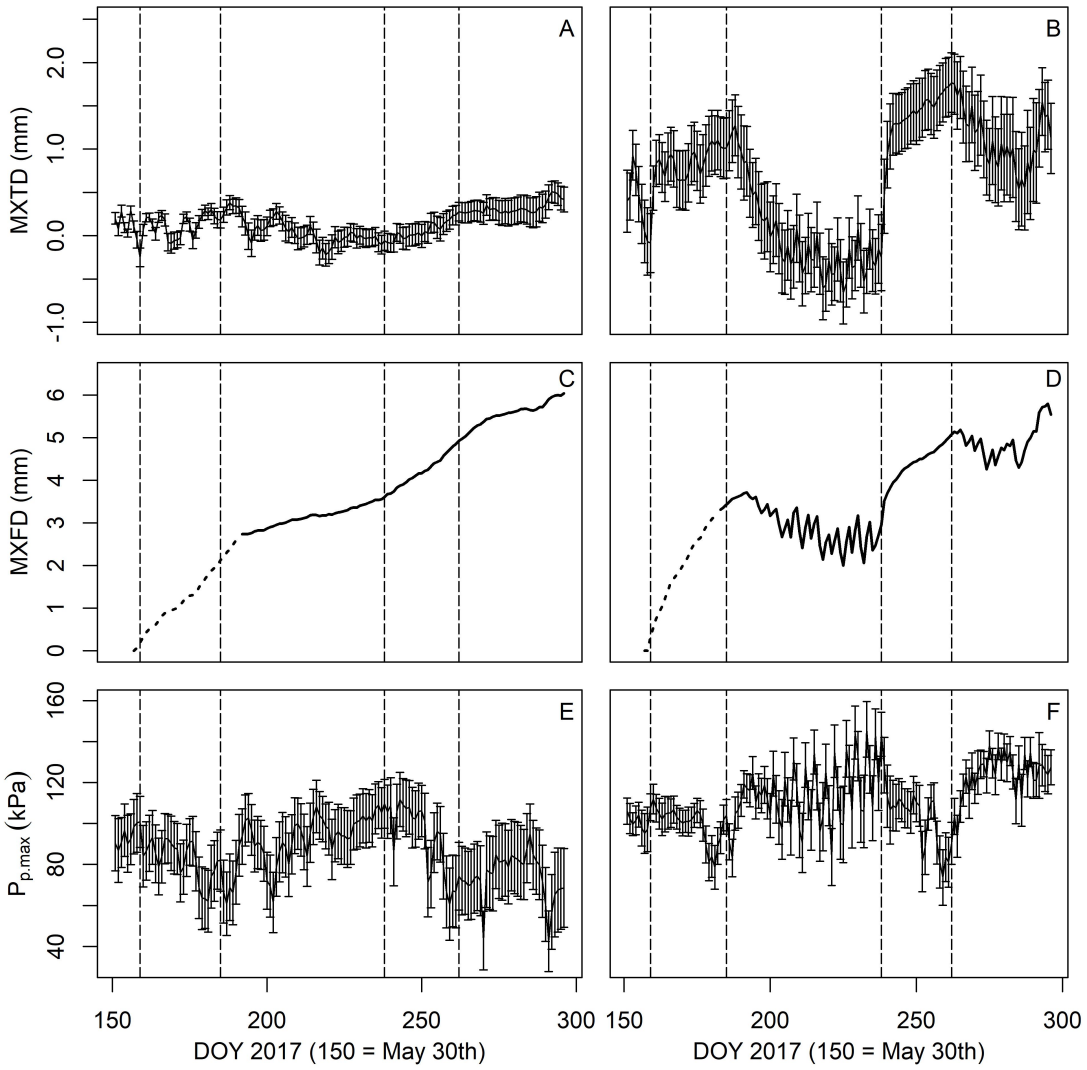

Figure 5.6: Time courses of daily maximum trunk diameter (MXTD), daily maximum fruit diameter (MXFD) and daily maximum output pressure sensed by the ZIM probe ($P_{p,max}$) for 100C-1L (A, C and E) and 45RDI-1L (B, D and F) treatments. Dashed vertical lines represent periods 2 and 3. The MXFD data (A) is presented with dashed lines when the number of functional sensors was lower than three.

5.3.6 Relations between the tested water stress indexes and main physiological parameters

In Figure 5.8 we isolated the MXFD index (derived from fruits dendrometers), and the $\Psi_{l,md}$ and $g_{s,max}$ physiological variables, both for the 100C-1L and the 45RDI-1L irrigation treatments. This allows us to evaluate the agreement between the time courses of MXFD and those of the two main physiological variables highly correlated to water stress in olive. As already commented, both $\Psi_{l,md}$ and $g_{s,max}$ values suggest low levels of water stress in the 100C trees. Accordingly, the MXFD values showed constant increase of fruit diameter, all along the irrigation season (Figs. 5.8A and C). At mid-summer, in between period 2 and 3, the slope of MXFD decreased, likely as a consequence of the harsh atmospheric conditions (high radiation and ET_o values). For the 45RDI-1L trees,

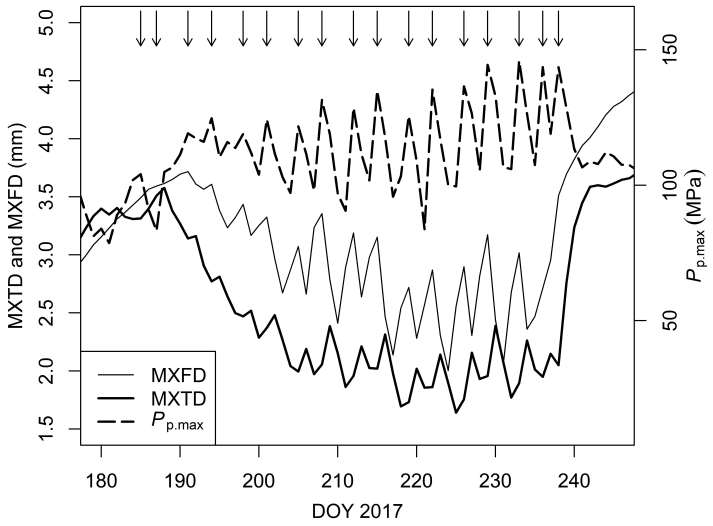

Figure 5.7: Time courses of fruit and trunk maximum diameter (MXFD and MXTD, respectively) and $P_{p,max}$ measured in 45RDI-1L trees during the deficit irrigation period in between period 2 and 3. $P_{p,max}$ - the daily maximum output pressure sensed by the ZIM probe, which is inversely proportional to the minimum leaf turgor pressure. The arrows indicate the days when irrigation was applied. Before DOY 185 and after DOY 238 irrigation was applied daily (arrows not shown).

changes in the slope of both $\Psi_{l,md}$ and $g_{s,max}$ echoed with those of MXFD. Thus during periods 2 and 3, in which the 45RDI-1L trees received enough water to avoid significant water stress, MXFD values showed a constant and marked increase in fruit diameter. In between periods 2 and 3, and after period 3, i.e. on the periods of deficit irrigation, fruit diameter was clearly affected by water stress (Figs. 5.8B and D) with negative slopes in MXFD, typical of fruit shrinking. With a great accordance between the increase in MXFD at the beginning of period 3 and the increase of $\Psi_{l,md}$ (Fig. 5.8B). Also, after period 3 MXFD values showed a slight decrease followed by an increase in its values, agreeing with both $\Psi_{l,md}$ and $g_{s,max}$ values. The relatively steady values of $\Psi_{l,md}$ and $g_{s,max}$ for the 100C-1L treatment allowed the fruits to grow continuously, with a small decrease in the slope shortly after period 2, as mentioned before (Fig. 5.8A and C).

Figures 5.5, 5.7 and 5.8 shows that, from the three water stress indexes derived from the fruit dendrometers, MXFD seems to be the most useful for the assessment of the tree water stress. The daily growth, both for the fruit and the trunk, is derived from the daily maximum diameter values so, despite of the apparent lack of response of DG_{fruit} deduced from Fig. 5.5A, we decide to plot both both DG_{fruit} and DG_{trunk} versus $\Psi_{l,md}$, maximum stomatal conductance ($g_{s,max}$), and net photosynthesis ($A_{N,max}$), to better evaluate any possible relationship (Fig. 5.9) among those water stress indicators. Values of DG_{fruit} showed significant correlation with $\Psi_{l,md}$ for the 45RDI-1L treatment (Fig. 5.9A), with a Pearson's correlation coefficient equal to 0.69 (p = 0.003). For the 100C-1L treatment the correlation between DG_{fruit} and $\Psi_{l,md}$ was not significant. Similarly, the DG_{trunk} data from the 45RDI-1L treatment had significant correlation with $\Psi_{l,md}$ (Fig. 5.9B), re-

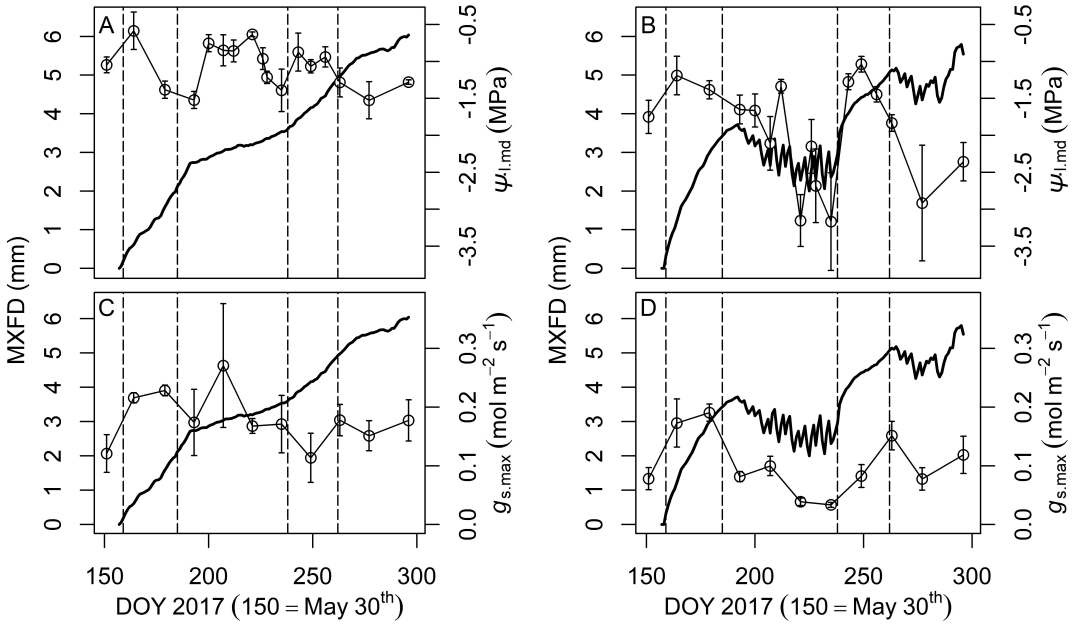

Figure 5.8: Time course of the maximum fruit diameter (MXFD) against the time courses of midday leaf water potential ($\Psi_{l,md}$, graphs A and B) and daily maximum leaf stomatal conductance ($g_{s,max}$, graphs C and D), for the 100C-1L treatment (graphs A and C) and for the 45RDI-1L treatment (graphs B and D). Vertical bars represent the standard error of the mean between the experimental plots. Dashed vertical lines represent periods 2 and 3.

sulting a Pearson's correlation coefficient of 0.59 (p = 0.017). The DG_{trunk} records from the 100C-1L treatment did not show significant correlation with those of $\Psi_{l,md}$.

For the 45RDI-1L treatment, DG_{fruit} showed significant correlation with $g_{s,max}$, with a Pearson's correlation coefficient (r) equal to 0.81 (p = 0.005), and with $A_{N,max}$ (r = 0.58, $p < 0.01$) but for the 100C-1L treatment the correlation was not significant (Fig. 5.9C, E). Additionally, the DG_{trunk} data was not significantly correlated either with $g_{s,max}$ or $A_{N,max}$, for any of the two irrigation treatments (Fig. 5.9D, F).

To further explore any possible relationship between the studied water stress indicators, we compared the fruit and trunk maximum daily shrinkage (MDS_{fruit} and MDS_{trunk}, respectively) with the daily maximum value obtained from the ZIM probes ($P_{p,max}$) (Fig. 5.10). For the 100C-1L treatment, the MDS values, both for the trunk and the fruits, showed significant correlation with $P_{p,max}$ (Fig. 5.10A and 5.10B, respectively), being necessary to use logarithm to test the correlation (i.e. Y vs. log(X)), obtaining Pearson's correlation coefficients equal to 0.82 and 0.65 for MDS_{fruit} and MDS_{trunk}, respectively ($p < 0.001$).

On the other hand, the data from the 45RDI-1L treatment only presented significant correlation for MDS_{fruit} (Fig. 5.10C), but not for MDS_{trunk} (Fig. 5.10D). The correlation was also tested by comparing the $P_{p,max}$ with the logarithm of fruit shrinking, resulting a Pearson's correlation coefficient equal to 0.44 ($p < 0.001$).

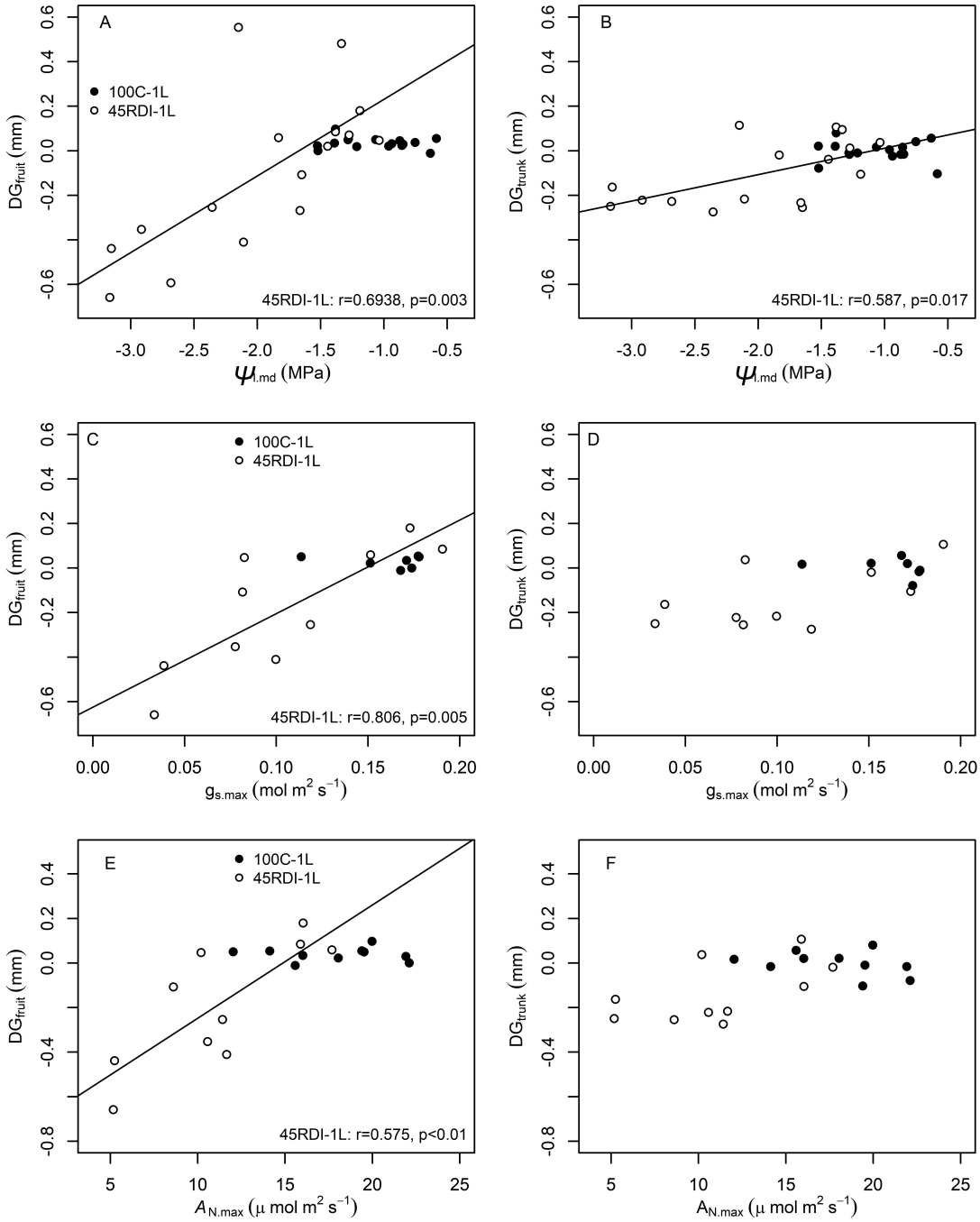

Figure 5.9: Relationships between DG_{fruit} and $\Psi_{l,md}$ (A), $g_{s,max}$ (C) and $A_{N,max}$ (E); and between DG_{trunk} and $\Psi_{l,md}$ (B), $g_{s,max}$ (D) and $A_{N,max}$ (F). DG_{fruit} = daily fruit growth; DG_{trunk} = daily trunk growth; $\Psi_{l,md}$ = midday leaf water potential; $g_{s,max}$ = maximum stomatal conductance; $A_{N,max}$ = maximum net photosynthetic.

5.4 Discussion

5.4.1 Relations between indexes derived from plant-based sensors and plant physiological parameters

The correlation lines for the 45RDI-1L treatment presented in Fig. 5.8A and 5.8B show that the correlation between DG_{fruit} and $\Psi_{l,md}$ is closer to the 1:1 line, in comparison

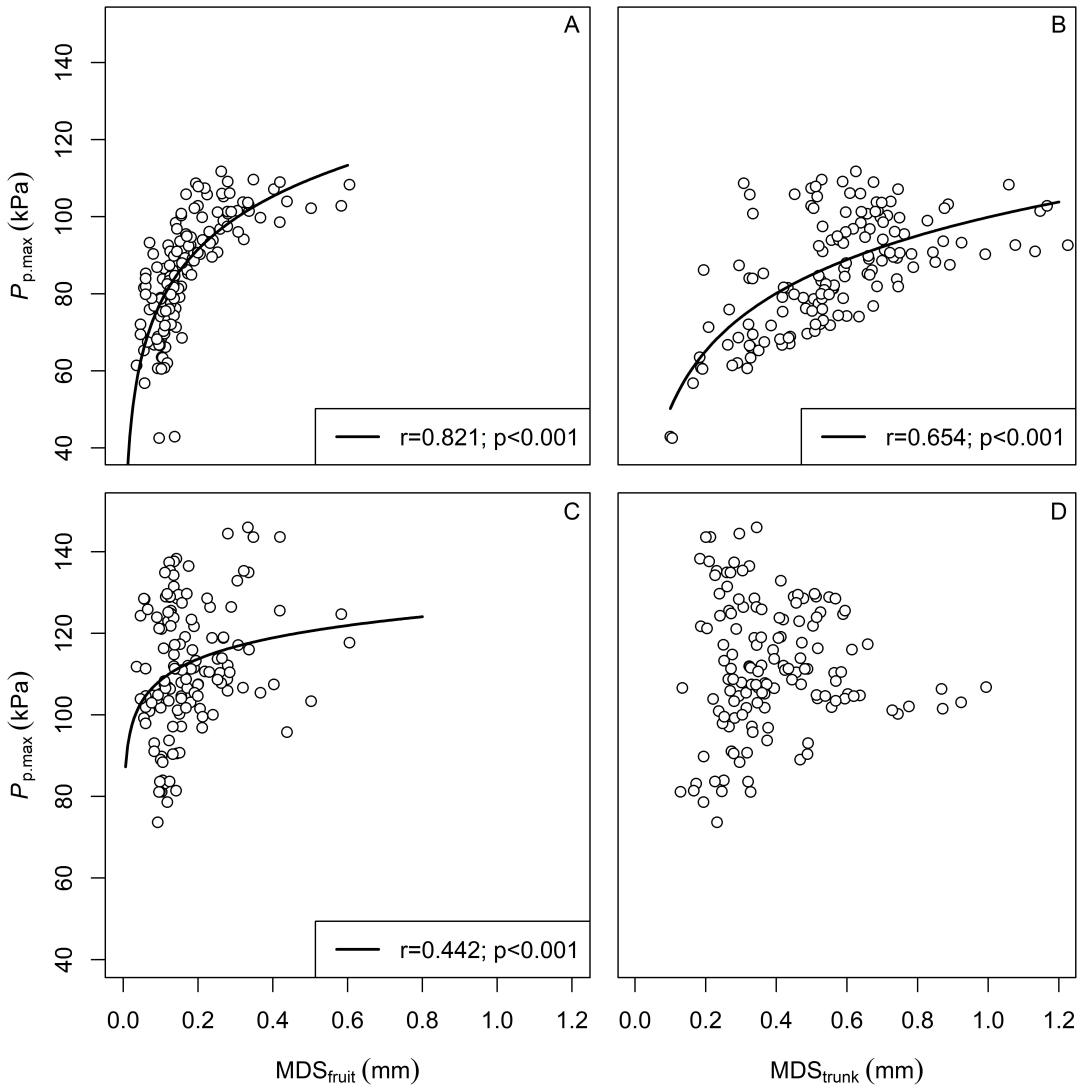

Figure 5.10: Correlation graphs between MDS_{fruit} and $P_{p,max}$ (A and C), and between MDS_{trunk} and $P_{p,max}$ (B and D), for the 100C-1L (A and B) and the 45RDI-1L (C and D) treatments. $P_{p,max}$ – daily maximum output pressure sensed by the ZIM probe, which is inversely proportional to the leaf turgor pressure; MDS_{fruit} – fruit maximum daily shrinkage; MDS_{trunk} – trunk maximum daily shrinkage.

to the correlation between DG_{trunk} and $\Psi_{l,md}$. This fact leads us to hypothesize that there is a greater hydraulic connection between fruits and leaves than between the trunk and the leaves. For the 100C-1L treatment these variables ($\Psi_{l,md}$, DG_{fruit} and DG_{trunk}) did not present significant correlation. This may be explained by the fact that the well-watered trees presented data distributed irregularly in a small range of DG_{fruit}, DG_{trunk} and $\Psi_{l,md}$, most likely being the atmospheric variables (ET_o, T_{air}, etc.) the main cause of variations in DG_{fruit} and DG_{trunk} for the 100C-1L trees.

The significant correlation found between DGG_{fruit} and $g_{s,max}$ for the 45RDI-1L treatment (Fig. 5.8C and 5.8D) and the absence of significant correlation between DG_{trunk} and $g_{s,max}$ for both treatments are additional arguments for us to believe in a greater hydraulic connection between fruits and leaves. A possible explanation for the absence of significant correlation between DG_{trunk} and $g_{s,max}$, for the 45RDI-1L treatment is that

both variables show different recovery behaviors under water stress. Thus, it may take a few days for $g_{s,max}$ to recover after rewatering stressed trees, the number depending on both the severity of the suffered water stress and the length of the previous water stress period. Thus, Perez-Martin et al. (2011) reported that $\Psi_{l,md}$ values in young 'Manzanilla' recovered from -6.0 MPa to -1.2 MPa in 36 hours. Fereres et al. (1996) reported that $\Psi_{l,md}$ recovered in about four days in mature 'Picual' trees previously stressed to $\Psi_{l,md}$ = -8.0 MPa.

The capacity of the trunk to recover from water stress was slower than that of the fruit and the leaf (Fig 5.7). The fruits, in fact, were affected later by the increasing water stress, and recovered faster under decreasing water stress conditions. This indicates that the water stored in the trunk may be consumed first on transpiration than the water stored in leaves and fruits. The fact that the MXTD responded one day after the application of the irrigation dose has already been observed previously in olive trees subjected to a RDI treatment (Cuevas et al., 2013; Fernández et al., 2011b).

Concerning the measurements related to leaf turgor, the comparisons shown in Fig. 5.9 between fruit and trunk maximum daily shrinkage (MDS_{fruit} and MDS_{trunk}, respectively), and the correlations tests, were performed with the hypothesis that the contraction of fruits and trunks occur approximately at the same time when the P_p values reach its daily maximum ($P_{p,max}$), i.e. at the daily minimum leaf turgor pressure. Our data on the Pearson's correlation coefficients obtained for the MDS_{fruit}, MDS_{trunk} and $P_{p,max}$ for the 100C-1L trees (Figs. 5.9A and 5.9B) confirms that hypothesis.

For the 45RDI-1L trees, however, data in Fig. 5.9C suggest that the fruit stop its contraction at a certain time, but $P_{p,max}$ values continue to increase (ca. $P_{p,max} > 120$ kPa). This effect was observed for lower $P_{p,max}$ values in the case of MDS_{trunk} (ca. $P_{p,max} > 100$ kPa). When testing correlation between MDS_{trunk} and $P_{p,max}$, for $P_{p,max} < 100$ kPa, we obtained a significant Pearson's correlation index (r=0.46, p=0.019). These observations support our findings, reported above, on (a) the trunk being the first water storing organ to be emptied under increasing water stress, and (b) under recovering conditions, fruits and leaves recover first than the trunk.

The fact that the same values of MXFD may occur at different moments of the irrigation season, i.e. when water deficit occurs the fruit decreased in diameter (Figs. 5.5C and 5.6D), impede the direct comparison of its values with values of physiological variables ($\Psi_{l,md}$ and $g_{s,max}$). That is why we presented the graphs shown in Figure 5.8, aiming at a merely visual comparison between MXFD values, $\Psi_{l,md}$ (Figs. 5.8A and 5.8B) and gs,max (Figs. 5.8C and 5.8D). From the visual comparison between $\Psi_{l,md}$ and $g_{s,max}$ we may infer that the relatively steady values for the 100C-1L trees (Figs. 5.8A and 5.8C, respectively) did not affect the fruit growth trend. On the other hand, the graphs from the 45RDI-1L trees (Figs. 5.8B and 5.8D) allow us to confirm that the fruit apparent nega-

tive growth occurred concomitantly with lower values of $\Psi_{l,md}$ and $g_{s,max}$, both between periods 2 and 3 and after period 3.

We hypothesize that the 100C-1L trees did not present a growing trend as the 45RDI-1L trees due to crop load, which includes fruit size but also number of fruits. Olive trees with a low crop load because of water stress may have very few fruits of big size, i.e. the size of the fruit should not necessarily reflect the accumulated water stress (Connor and Fereres, 2005; Lavee and Wodner, 2004). On the contrary, we observed that the trunks of the 45RDI-1L treatment trees did grow, despite being an RDI treatment (Fig. 5.6B). The fruit load was lower in 45RDI-1L than in 100C-1L trees (100C-1L: 12633 $\pm$ 3447 kg fruit ha^{-1}; 45RDI-1L: 7399 $\pm$ 276 kg fruit ha^{-1}), which could explain the striking results on MXTD. The greater fruit load could have responsible that negligible trunk growth in 100C-1L trees, which could have been penalized to satisfy the greater demand of water from the fruits.

To the best of our knowledge, the present study is the first to present the comparison between the correlations of physiological variables ($\Psi_{l,md}$, $g_{s,max}$, and $A_{N,max}$) and water stress indexes derived from the use of fruit dendrometers. Taking into account the complexity of the processes responsible for fruit growing, further studies are needed to collect enough knowledge required for a reliable interpretation of the water stress indexes derived from the use of fruit dendrometers.

5.4.2 Suitability of fruit dendrometers to schedule irrigation in a hedgerow olive orchard

Several works have been published in which trunk dendrometers have been used to assess tree water stress published in different types of olive groves (Corell et al., 2014; Cuevas et al., 2010; Cuevas et al., 2013; Fernández et al., 2011b; Girón et al., 2015b; Girón et al., 2015c). Basically, all these publications showed that trunk dendrometers are useful to assess water stress of woody plants in commercial orchards, with a few exceptions such as that reported by Intrigliolo and Castel (2007b) for grapevine after veraison. Studies with fruit dendrometers are scarcer (Fernández, 2017; Fernández et al., 2018a) and, as we have previously mentioned, we are not aware of any publication on the use of fruit dendrometers in olive, apart from the study by Fernandes et al. (2018), which corresponds to Chapter 4 of the present PhD. Thesis. Therefore, the comparative analysis among the water stress indexes tested in this work is new.

Our data shows that, fruit dendrometers can be useful indicators of water stress in olive, and that, from the three water stress indicators derived from the data collected by the fruit dendrometers (Fig. 5.5, 5.6 and 5.8), MXFD seems to be the best. First, deriving MXFD values requires less data processing than deriving DG_{fruit} and MDS_{fruit} values. Second, and most importantly, the user can assess the time course of plant water

stress in the orchard just by visualizing the MXFD curve. This does not apply either to DG_{fruit} or MDS_{fruit}, and it is important because any indicator of water stress suitable for being used in commercial orchards must be easy to use (Fernández, 2014a). Our conclusion on MXFD being a better indicator for water stress than DG_{fruit} and MDS_{fruit}, agree with findings reported from studies with trunk dendrometers by (Cuevas et al., 2013; Fernández et al., 2011b). The great recovery of fruit diameters from the 45RDI-1L treatment during period 3 illustrates the outstanding capacity of the olive tree to recover, at that time of the year, from the stress suffered in between periods 2 and 3 (Lavee et al., 1990; Moriana et al., 2007). At the end of the irrigation period, the MXFD values were similar for both irrigation treatments.

The use of MXFD as an indicator of water stress, coincides with that suggested by (Fernández et al., 2018b) on the use of MXTD as an indicator of trunk water stress. It was suggested as an alternative to D_{MXTD} (an indicator derived from subtracting MXTD values from concomitant measurements in reference trees), which was used by Cuevas et al. (2013) in this same plot, in a study carried out in 2010 with trees under different water treatments and in which D_{MXTD}, MXTD and MDStrunk were compared. The information provided by MXTD is reliable and it does not require the use of reference trees. Basically, our findings suggest that the grower could just visualize the time course of the MXFD values to detect the onset and severity of the tree water stress. The onset will be indicated by the slope of the MXFD curve becoming similar to zero. If the slope becomes negative, the level of water stress could be considered as severe. This is a coarse approach that must be validated for each orchard conditions, but it is validated by the close agreement we found between MXFD and both $\Psi_{l,md}$ and $g_{s,max}$, two main physiological variables closely related to water stress. The approach has also the advantages of being both sensitive and user-friendly, two useful features required for effective irrigation scheduling (Fernández, 2014a; Fernández et al., 2018b).

Still, our findings also show that the usefulness of MXFD as an indicator of water stress is curtailed by the fact that the fruit water status seems to a priority for the olive tree as compared to that of the trunk. In other words, if the user relies on MXFD as the only indicator to assess water stress, he/she can miss events where vegetative growth is penalized by water stress with no impact on fruit growth. However, this can be useful in super-high density orchards where it is highly necessary to control vegetative growth (Connor et al., 2014) and in areas where local conditions induce uncontrolled tree vigor (Correa-Tedesco et al., 2010) due to difficulties in mechanical harvesting (León et al., 2007) and a reduction of the long-term orchard productive life. Thus, fruit dendrometers may constitute a tool to manage excessive vegetative biomass and optimize fruit growth, but more information is needed.

5.5 Conclusions

Considering the results obtained in the present work, the knowledge of previous studies of trunk and fruit dendrometers, and the comparisons presented in this work, it is possible to conclude that MXFD (maximum fruit diameter) is most probably the best option among the three indexes derived from the fruit dendrometers, as it presents good visual correspondence with the increases and decreases of $\Psi_{l,md}$ and $g_{s,max}$ along the irrigation season. MXFD is also useful as it provides the fruit growing trend. It is also possible to conclude that, for physiological studies, the fruit daily growth (DG_{fruit}) may be of interest, as it possibly presents good correlation to physiological variables, depending on the plant water status. Additionally, we can also conclude that leaf turgor and fruit diameter respond faster to the irrigation events than the trunk diameter when irrigation is performed in a low frequency (2 to 3 times per week). We also conclude that fruit dendrometers are able to detect water stress in fruits, although fruits are less affected by water stress than vegetative growth. Thus, the use of the fruit dendrometers to schedule irrigation in olive trees may cause a decrease in the vegetative growth, which could be unwanted or an advantage if there is a need to control undesired excessive vegetative growth in SHD olive orchards. Further studies on the use of fruit dendrometers to schedule irrigation are needed to validate the performance of the indexes mentioned in the present study and schedule deficit irrigation based on their results.

5.6 References

Alegre, S., J. Marsal, M. Mata, A. Arbonés, J. Girona, and M.J. Tovar (2002). "Regulated deficit irrigation in olive trees (Olea europaea L. cv. Arbequina) for oil production". In: *Acta Horticulturae* 586, pp. 259–262. DOI: 10.17660/ActaHortic.2002.586.49.

Connor, David J and E. Fereres (2005). "The physiology of adaptation and yield expression in olive". In: *Horticultural reviews* 31, pp. 155–229.

Connor, David J., Maria Gómez-del-Campo, M. Cecilia Rousseaux, and Peter S. Searles (2014). "Structure, management and productivity of hedgerow olive orchards: A review". In: *Scientia Horticulturae* 169, pp. 71–93. DOI: 10.1016/j.scienta.2014.02.010.

Corell, M., I. F. Girón, A. Galindo, A. Torrecillas, R. Torres-Sánchez, A. Pérez-Pastor, F. Moreno, and A. Moriana (2014). "Using band dendrometers in irrigation scheduling. Influence of the location inside the tree and comparison with point dendrometer". In: *Agricultural Water Management* 142, pp. 29–37. DOI: 10.1016/j.agwat.2014.04.005.

Correa-Tedesco, Guillermo, M. Cecilia Rousseaux, and Peter S. Searles (2010). "Plant growth and yield responses in olive (Olea europaea) to different irrigation levels in

an arid region of Argentina". In: *Agricultural Water Management* 97.11, pp. 1829–1837. DOI: 10.1016/j.agwat.2010.06.020.

Cuevas, M.V., J. M. Torres-Ruiz, R. Álvarez, M. D. Jiménez, J. Cuerva, and J.E. Fernández (2010). "Assessment of trunk diameter variation derived indices as water stress indicators in mature olive trees". In: *Agricultural Water Management* 97.9, pp. 1293–1302. DOI: 10.1016/j.agwat.2010.03.011.

Cuevas, M.V., M.J. Martín-Palomo, Antonio Diaz-Espejo, J.M. Torres-Ruiz, C.M. Rodriguez-Dominguez, A. Perez-Martin, R. Pino-Mejías, and J.E. Fernández (2013). "Assessing water stress in a hedgerow olive orchard from sap flow and trunk diameter measurements". In: *Irrigation Science* 31.4, pp. 729–746. DOI: 10.1007/s00271-012-0357-x.

Diaz-Espejo, Antonio, B. Hafidi, J.E. Fernandez, M.J. Palomo, and H. Sinoquet (2002). "Transpiration and photosynthesis of olive tree: a model approach". In: *Acta Horticulturae* 586, pp. 457–460. DOI: 10.17660/ActaHortic.2002.586.94.

Diaz-Espejo, Antonio, T.N. Buckley, J.S. Sperry, M.V. Cuevas, A. de Cires, S. Elsayed-Farag, M.J. Martin-Palomo, J.L. Muriel, A. Perez-Martin, C.M. Rodriguez-Dominguez, A.E. Rubio-Casal, J.M. Torres-Ruiz, and J.E. Fernández (2012). "Steps toward an improvement in process-based models of water use by fruit trees: A case study in olive". In: *Agricultural Water Management* 114, pp. 37–49. DOI: 10.1016/j.agwat.2012.06.027.

Egea, Gregorio, Carmen M. Padilla-Díaz, Jorge Martinez-Guanter, José E. Fernández, and Manuel Pérez-Ruiz (2017). "Assessing a crop water stress index derived from aerial thermal imaging and infrared thermometry in super-high density olive orchards". In: *Agricultural Water Management* 187, pp. 210–221. DOI: 10.1016/j.agwat.2017.03.030.

Fereres, E, C Ruz, J Castro, JA Gómez, and M Pastor (1996). "Recuperación del olivo después de una sequía extrema". In: *Proceedings of the XIV Congreso Nacional de Riegos, Aguadulce (Almería)*, pp. 11–13.

Fereres, Elias and María Auxiliadora Soriano (2007). "Deficit irrigation for reducing agricultural water use". In: *Journal of Experimental Botany* 58.2, pp. 147–159. DOI: 10.1093/jxb/erl165.

Fernandes, Rafael Dreux Miranda, Maria Victoria Cuevas, Virginia Hernandez-Santana, Celia M. Rodriguez-Dominguez, Carmen M. Padilla-Díaz, and José Enrique Fernández (2017). "Classification models for automatic identification of daily states from leaf turgor related measurements in olive". In: *Computers and Electronics in Agriculture* 142, pp. 181–189. DOI: 10.1016/j.compag.2017.09.005.

Fernandes, Rafael Dreux Miranda, Maria Victoria Cuevas, Antonio Diaz-Espejo, and Virginia Hernandez-Santana (2018). "Effects of water stress on fruit growth and water

relations between fruits and leaves in a hedgerow olive orchard". In: *Agricultural Water Management* 210.April, pp. 32–40. DOI: 10.1016/j.agwat.2018.07.028.

Fernández, J.E. (2014a). "Plant-based sensing to monitor water stress: Applicability to commercial orchards". In: *Agricultural Water Management* 142, pp. 99–109. DOI: 10.1016/j.agwat.2014.04.017.

— (2014b). "Understanding olive adaptation to abiotic stresses as a tool to increase crop performance". In: *Environmental and Experimental Botany* 103, pp. 158–179. DOI: 10.1016/j.envexpbot.2013.12.003.

— (2017). "Plant-Based Methods for Irrigation Scheduling of Woody Crops". In: *Horticulturae* 3.2, p. 35. DOI: 10.3390/horticulturae3020035.

Fernández, J.E. and M.V. Cuevas (2010). "Irrigation scheduling from stem diameter variations: A review". In: *Agricultural and Forest Meteorology* 150.2, pp. 135–151. DOI: 10.1016/j.agrformet.2009.11.006.

— (2011). "Using plant-based indicators to schedule irrigation in olive". In: *Acta Horticulturae* 888, pp. 207–214. DOI: 10.17660/ActaHortic.2011.888.23.

Fernández, J.E., F. Moreno, I. F. Girón, and O. M. Blázquez (1997). "Stomatal control of water use in olive tree leaves". In: *Plant and Soil* 190.2, pp. 179–192. DOI: 10.1023/A:1004293026973.

Fernández, J.E., Antonio Diaz-Espejo, Riccardo D'Andria, Luca Sebastiani, and Roberto Tognetti (2008a). "Potential and limitations of improving olive orchard design and management through modelling". In: *Plant Biosystems* 142.1, pp. 130–137. DOI: 10.1080/11263500701872853.

Fernández, J.E., J.M. Torres-Ruiz, Antonio Diaz-Espejo, Antonio Montero, R. Álvarez, M.D. Jiménez, J. Cuerva, and M.V. Cuevas (2011b). "Use of maximum trunk diameter measurements to detect water stress in mature 'Arbequina' olive trees under deficit irrigation". In: *Agricultural Water Management* 98.12, pp. 1813–1821. DOI: 10.1016/j.agwat.2011.06.011.

Fernández, J.E., M.V. Cuevas, C.M. Rodriguez-Dominguez, A. Perez-Martin, J.M. Torres-Ruiz, S. Elsayed-Farag, Antonio Diaz-Espejo, and M. J. Martín-Palomo (2012). "Sap flow response to olive water stress: A comparative study with trunk diameter variations and leaf turgor pressure". In: *Acta Horticulturae* 951, pp. 101–110.

Fernández, J.E., Alfonso Perez-Martin, José M. Torres-Ruiz, María V. Cuevas, Celia M. Rodriguez-Dominguez, Sheren Elsayed-Farag, Ana Morales-Sillero, José M. García, Virginia Hernandez-Santana, and Antonio Diaz-Espejo (2013). "A regulated deficit irrigation strategy for hedgerow olive orchards with high plant density". In: *Plant and Soil* 372.1-2, pp. 279–295. DOI: 10.1007/s11104-013-1704-2.

Fernández, J.E., M.V. Cuevas, A. Perez-Martin, C.M. Rodriguez-Dominguez, V. Hernandez-Santana, R. Romero, J.M. García, A. Montero, C.M. Padilla-Díaz, G. Egea,

F. Alcon, M. Pérez Ruiz, I.F. García-Tejero, and Antonio Diaz-Espejo (2018a). "New approaches for precise irrigation in hedgerow olive orchards". In: *Acta Horticulturae* 1199, pp. 225–240. DOI: 10.17660/ActaHortic.2018.1199.36.

Fernández, J.E., A. Diaz-Espejo, Rafael Romero, Virginia Hernandez-Santana, José M. García, Carmen M. Padilla-Diaz, and M.V. Cuevas (2018b). "Precision Irrigation in Olive (Olea europaea L.) Tree Orchards". In: *Water Scarcity and Sustainable Agriculture in Semiarid Environment*. Ed. by Ivan F. García-Tejero and Victor-Hugo Durán. Elsevier. Chap. 9, pp. 179–217. DOI: 10.1016/B978-0-12-813164-0.00009-0.

García-Tejero, I. F., A. Hernández, Carmen M. Padilla-Diaz, Antonio Diaz-Espejo, and J.E. Fernández (2017). "Assessing plant water status in a hedgerow olive orchard from thermography at plant level". In: *Agricultural Water Management* 188, pp. 50–60. DOI: 10.1016/j.agwat.2017.04.004.

Girón, I.F., M. Corell, M.J. Martín-Palomo, A. Galindo, A. Torrecillas, F. Moreno, and A. Moriana (2015b). "Feasibility of trunk diameter fluctuations in the scheduling of regulated deficit irrigation for table olive trees without reference trees". In: *Agricultural Water Management* 161, pp. 114–126. DOI: 10.1016/j.agwat.2015.07.014.

— (2015c). "Limitations and usefulness of maximum daily shrinkage (MDS) and trunk growth rate (TGR) indicators in the irrigation scheduling of table olive trees". In: *Agricultural Water Management* 2010. DOI: 10.1016/j.agwat.2015.09.014.

Gonzalez-Dugo, V., P. Zarco-Tejada, E. Nicolás, P. A. Nortes, J. J. Alarcón, D. S. Intrigliolo, and E. Fereres (2013). "Using high resolution UAV thermal imagery to assess the variability in the water status of five fruit tree species within a commercial orchard". In: *Precision Agriculture* 14.6, pp. 660–678. DOI: 10.1007/s11119-013-9322-9.

Gonzalez-Dugo, V., D. Goldhamer, P. J. Zarco-Tejada, and E. Fereres (2015). "Improving the precision of irrigation in a pistachio farm using an unmanned airborne thermal system". In: *Irrigation Science* 33.1, pp. 43–52. DOI: 10.1007/s00271-014-0447-z.

Hernandez-Santana, Virginia, J.E. Fernández, M.V. Cuevas, Alfonso Perez-Martin, and Antonio Diaz-Espejo (2017). "Photosynthetic limitations by water deficit: Effect on fruit and olive oil yield, leaf area and trunk diameter and its potential use to control vegetative growth of super-high density olive orchards". In: *Agricultural Water Management* 184, pp. 9–18. DOI: 10.1016/j.agwat.2016.12.016.

Iniesta, F., L. Testi, F. Orgaz, and F. J. Villalobos (2009). "The effects of regulated and continuous deficit irrigation on the water use, growth and yield of olive trees". In: *European Journal of Agronomy* 30.4, pp. 258–265. DOI: 10.1016/j.eja.2008.12.004.

Intrigliolo, D. S. and J. R. Castel (2007b). "Evaluation of grapevine water status from trunk diameter variations". In: *Irrigation Science* 26.1, pp. 49–59. DOI: 10.1007/s00271-007-0071-2.

Jones, H. G. and K. H. Higgs (1982). "Surface Conductance and Water Balance of Developing Apple (Malus pumila Mill.) Fruits". In: *Journal of Experimental Botany* 33.1, pp. 67–77. DOI: 10.1093/jxb/33.1.67.

Jones, Hamlyn G. (2004). "Irrigation scheduling: Advantages and pitfalls of plant-based methods". In: *Journal of Experimental Botany* 55.407, pp. 2427–2436. DOI: 10.1093/jxb/erh213.

Lavee, S., M. Nashef, M. Wodner, and H. Harshemesh (1990). "The effect of complementary irrigation added to old olive trees (Olea europaea L.) cv. Souri on fruit characteristics, yield and oil production". In: *Advances in Horticultural Science* 4.3, pp. 135–138.

Lavee, Shimon and Maria Wodner (2004). "The effect of yield, harvest time and fruit size on the oil content in fruits of irrigated olive trees (Olea europaea), cvs. Barnea and Manzanillo". In: *Scientia Horticulturae* 99.3-4, pp. 267–277. DOI: 10.1016/S0304-4238(03)00100-6.

León, L., R. De La Rosa, L. Rallo, N. Guerrero, and D. Barranco (2007). "Influence of spacing on the initial production of hedgerow 'Arbequina' olive orchards". In: *Spanish Journal of Agricultural Research* 5.4, pp. 554–558.

Morandi, Brunella, Luigi Manfrini, Marco Zibordi, Massimo Noferini, Giovanni Fiori, and Luca Corelli Grappadelli (2007a). "A Low-cost Device for Accurate and Continuous Measurements of Fruit Diameter". In: *HortScience* 42.6, pp. 1380–1382.

Morandi, Brunella, Mark Rieger, and Luca Corelli-Grappadelli (2007b). "Vascular flows and transpiration affect peach (Prunus persica Batsch.) fruit daily growth". In: *Journal of Experimental Botany* 58.14, pp. 3941–3947. DOI: 10.1093/jxb/erm248.

Morandi, Brunella, Luigi Manfrini, Pasquale Losciale, Marco Zibordi, and Luca Corelli-Grappadelli (2010b). "The positive effect of skin transpiration in peach fruit growth". In: *Journal of Plant Physiology* 167.13, pp. 1033–1037. DOI: 10.1016/j.jplph.2010.02.015.

Morandi, Brunella, Luigi Manfrini, Marco Zibordi, Pasquale Losciale, and Luca Corelli Grappadelli (2011a). "Effects of drought stress on the growth, water relations and vascular flows of young 'Summerkiwi' fruit". In: *Acta Horticulturae* 922, pp. 355–359. DOI: 10.17660/ActaHortic.2011.922.46.

Morandi, Brunella, Pasquale Losciale, Marco Zibordi, Luigi Manfrini, and Luca Corelli Grappadelli (2011b). "Leaf gas exchanges affect water flows to kiwifruit berries during the day". In: *Acta Horticulturae* 913, pp. 303–308. DOI: 10.17660/ActaHortic.2011.913.39.

Morandi, Brunella, Marco Zibordi, Pasquale Losciale, Luigi Manfrini, Emanuele Pierpaoli, and Luca Corelli-Grappadelli (2011c). "Shading decreases the growth rate of

young apple fruit by reducing their phloem import". In: *Scientia Horticulturae* 127.3, pp. 347–352. DOI: 10.1016/j.scienta.2010.11.002.

Morandi, Brunella, Pasquale Losciale, Luigi Manfrini, Marco Zibordi, Stefano Anconelli, Fabio Galli, Emanuele Pierpaoli, and Luca Corelli Grappadelli (2014a). "Increasing water stress negatively affects pear fruit growth by reducing first its xylem and then its phloem inflow". In: *Journal of Plant Physiology* 171.16, pp. 1500–1509. DOI: 10.1016/j.jplph.2014.07.005.

Moriana, A., D. Pérez-López, M. H. Prieto, M. Ramírez-Santa-Pau, and J.M. Pérez-Rodriguez (2012). "Midday stem water potential as a useful tool for estimating irrigation requirements in olive trees". In: *Agricultural Water Management* 112, pp. 43–54. DOI: 10.1016/j.agwat.2012.06.003.

Moriana, Alfonso, Francisco Orgaz, Miguel Pastor, and Elias Fereres (2003). "Yield responses of a mature olive orchard to water deficits". In: *Journal of the American Society for Horticultural Science* 128.3, pp. 425–431.

Moriana, Alfonso, David Pérez-López, Aurora Gómez-Rico, María De Los Desamparados Salvador, Nicolás Olmedilla, Francisco Ribas, and Giuseppe Fregapane (2007). "Irrigation scheduling for traditional, low-density olive orchards: Water relations and influence on oil characteristics". In: *Agricultural Water Management* 87.2, pp. 171–179. DOI: 10.1016/j.agwat.2006.06.017.

Orgaz, F., L. Testi, F.J. Villalobos, and E. Fereres (2006). "Water requirements of olive orchards–II: determination of crop coefficients for irrigation scheduling". In: *Irrigation Science* 24.2, pp. 77–84. DOI: 10.1007/s00271-005-0012-x.

Padilla-Díaz, Carmen M., Celia M. Rodriguez-Dominguez, Virginia Hernandez-Santana, Alfonso Perez-Martin, Rafael D.M. Fernandes, Antonio Montero, J.M. García, and J.E. Fernández (2018). "Water status, gas exchange and crop performance in a super high density olive orchard under deficit irrigation scheduled from leaf turgor measurements". In: *Agricultural Water Management* 202.January, pp. 241–252. DOI: 10.1016/j.agwat.2018.01.011.

Padilla-Díaz, C.M., Celia M. Rodriguez-Dominguez, Virginia Hernandez-Santana, Alfonso Perez-Martin, and J.E. Fernández (2016). "Scheduling regulated deficit irrigation in a hedgerow olive orchard from leaf turgor pressure related measurements". In: *Agricultural Water Management* 164, pp. 28–37. DOI: 10.1016/j.agwat.2015.08.002.

Perez-Martin, A., J.M. Torres-Ruiz, J.E. Fernández, A. Diaz-Espejo, J. Flexas, C. Michelazzo, and L. Sebastiani (2011). "Physiological and genetic response of olive leaves to water stress and recovery: implications of mesophyll conductance and genetic expression of aquaporins and carbonic anhydrase". In: *Acta Horticulturae* 922, pp. 99–105. DOI: 10.17660/ActaHortic.2011.922.12.

Zibordi, Marco, Sara Domingos, and Luca Corelli Grappadelli (2009). "Thinning apples via shading: an appraisal under field conditions". In: *The Journal of Horticultural Science and Biotechnology* 84.6, pp. 138–144. DOI: 10.1080/14620316.2009.11512611.

CHAPTER 6 – General Discussion.

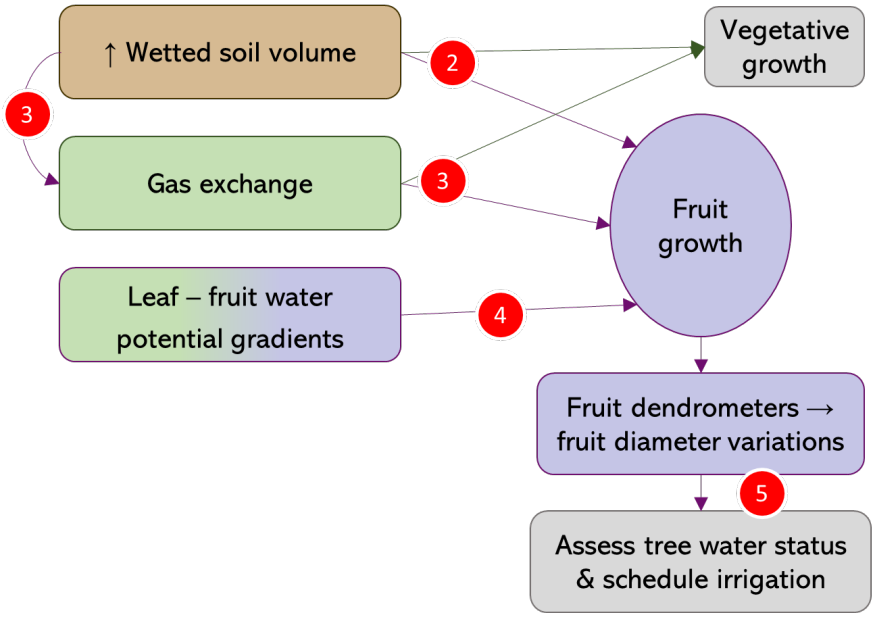

Figure 6.1: Processes and relationships studied in the different chapters of the present Thesis. The numbers shown referred to the different chapters

Fruit and olive oil yield are highly dependent on olive fruit size, among other variables. Although different studies (Gómez-del-Campo, 2013; Gucci et al., 2009; Hammami et al., 2013; Rapoport, 2004; Rapoport et al., 2013) have assessed the anatomy of fruits during their development, to the best of our knowledge, before this PhD there were no studies focusing on the physiological mechanisms explaining olive fruit growth under water stress. According to current knowledge on plant growth control (Körner, 2015; Tardieu et al., 2011) and specifically, on fruit growth (Fishman and Génard, 1998; Martre et al., 2011), growth is controlled both by the water relationships and the amount of assimilated carbon that is available for growth. Indeed, carbohydrates provide the building blocks for plant structure as well as to influence on osmotic potential while water is key to maintain plant water potential and cell turgor, required for cell expansion. Despite their critical role on growth, our understanding of the specific mechanisms and importance on controlling plant growth is still limited (Körner, 2015).

The only attempts found in olive on studying the relevance of potential gradients between the plant and fruit on fruit growth were more focused in studying the effect of water stress on the water relations in phase II of pit hardening (Dell'Amico et al., 2012; Girón et al., 2015a). However, these authors did not explain the effect of water stress on daily dynamics of fruit growth and the mechanisms controlling them. Regarding the role of carbohydrates on growth, to the best of our knowledge there is only one work, but it dealt mainly with the role of carbohydrate reserves in yield in olive trees (Bustan et al., 2011). Thus, in the present Ph.D. thesis the main focus was on evaluating fruit growth and the limiting factors under water stress such as leaf gas exchange, water potential gradient between leaves and fruits and the competition for assimilates between fruits

and vegetative growth.

We studied the water relations between leaves and fruits, to comprehend the influence of leaf to fruit water potential gradient ($\Delta\Psi_{\text{leaf-fruit}} = \Psi_{\text{leaf}} - \Psi_{\text{fruit}}$) on the fruit diameter variations and growth. We observed that fruits from water stressed trees (45RDI-1L) presented an apparent negative growth (i.e. fruit daily shrinkage greater than fruit diameter recovery) while $\Delta\Psi_{\text{leaf-fruit}}$ values were positive, presenting theoretical water flow into the fruits (Chapter 4The data on $\Delta\Psi_{\text{leaf-fruit}}$ indicate that the fruit would be a stronger water sink, therefore, the decrease in fruit diameter very likely indicates that fruit transpiration was greater than the flow into the fruits, occasioning a reduction of water reserves in the fruits. The $\Delta\Psi_{\text{leaf-fruit}}$ positive values observed probably allows olive fruits to recover growth quickly when water is again available to the tree, in comparison to other fruit species, in which fruits have less negative water potential than leaves and less capacity of water stress recovery (Greenspan et al., 1996). As far as we know, the experiment described in Chapter 4 is the first to study the effect of water relations between fruits and leaves on the fruit growth, with the continuous measurement of olive fruit diameter variations under water stress.

In addition, to study the dynamics of fruit growth, we investigated it in relation to vegetative growth (Chapters 2 and 3). We observed, in accordance to other works (Dag et al., 2010; Intrigliolo and Castel, 2007a; Hernandez-Santana et al., 2017), that the influence of water deficit was more significant on the vegetative growth (i.e. number of internodes of current-year shoots' and leaf area) than on the fruit growth (Chapters 2 and 3), likely reflecting the major sink strength of fruits compared to other organs for water and photoassimilates found in Chapters 4 and 3, respectively. The relationships between accumulated photosynthesis (A_N) and fruit dry weight and oil content were strong and highly significant for all treatments, while the relationship between accumulated A_N and leaf area was not significant for the water-stressed treatments (Chapter 3), indicating the priority of fruit over vegetative growth. Additionally, vegetative growth in terms of current-year shoots' and leaf area were influenced by the increase of wetted soil volume, including some days when data from the 45RDI-2L presented significantly similar values to those from the 100C-1L (Chapter 2). This fact could be explained by the theoretical greater water availability to the root system and a better distribution of the applied water in the soil in the two drip lines deficit irrigated treatment (45RDI-2L). However, no effect of the new drip line was observed on fruit dry weight, for both irrigation doses, calling the attention for the fact that fruits are the highest priority for the trees, in terms of water and photoassimilates. The experiment described in Chapter 2 was the first study to analyze the effect of a change in the wetted soil volume to the vegetative and fruit growth of olive trees. Most probably, the increment from one to two drip lines per tree row is not cost effective, as it mainly affected the vegetative growth,

but it did not affect the fruit growth (fruit dry weight) and yield (fruit and oil yield). In fact, our results confirm that deficit irrigation strategies could be used to control excessive vegetative growth, as fruit growth and development is a priority for the olive tree.

To conduct the mentioned experiments we developed and applied two different methods to track fruit growth. Indeed, in Chapter 3 we explained how we calibrated and validated a model to simulate A_N and relate it to fruit growth and in Chapter 4, we describe the use of fruit dendrometers. Leaf stomatal conductance (g_s) was estimated continuously throughout the irrigation season of 2016, from sap flux density measurements and data of atmospheric vapor pressure deficit. Using the Farquhar photosynthesis model (Farquhar et al., 1980) and the estimated g_s we could simulate A_N continuously. The accumulated A_N was compared to the data on vegetative (current year shoot's number of internode and leaf area) and fruit growth (fruit dry weight and oil content). Our results showed strong and highly significant relationships between A_N and fruit dry weight and oil accumulation (Chapter 3), proving the usfulness of continuously simulated A_N as a tool to study fruig growth, oil accumulation and vegetative growth in general. Although the relationships between A_N and fruit growth and yield are very complex, the results of this approach open could help to predict yield in the future. This was the first time when irrigation strategies were studied through the relationships between simulated A_N and the vegetative and fruit growth and oil content (Chapter 3).

Parallel to this approach, we also used fruit dendrometers to monitor automatically and continuously the fruit diameter variations and growth throughout the irrigation season. We used a linear potentiometer with internal spring coupled to a sensor holder and, in smaller number, a commercial sensor. The mentioned linear potentiometers were similar to those used by (Morandi et al., 2007a) in apple fruits. These sensors were capable to monitor continuously the variations in fruit diameter, with the great advantage of recording data every five minutes, with low power consumption. Another advantage is that the data obtained with the fruit dendrometers is easily handled and normalized, different from the trunk dendrometers. Fruit dendrometers are easily installed but require frequent adjustment of the offset due to its limited range of measurement.

Furthermore, the results obtained from the fruit dendrometers give us valuable information on the influence of water availability on the fruit diameter variations and growth (Chapters 4 and 5). Well-irrigated olive fruits (100C-1L treatment) presented a double sigmoidal growth curve for fruit diameter during the 2017 irrigation season (Chapters 4 and 5), accordingly to the growth pattern measured in variables such as fruit volume, fruit fresh and dry weight (Hartmann, 1949; Lavee, 1986), mesocarp width and cell size (Rallo and Rapoport, 2001). Fruits from the water-stressed treatment (45RDI-1L) presented great influence from the irrigation strategy, with great fruit shrinkage during the

days when the irrigation was not applied, and great expansion (recovery) at the days when irrigation was applied (Chapter 4). Furthermore, the results obtained through the measurements of pressure-volume curves reported in Chapter 4 reveal that osmotic adjustment actually occurs in olive fruits, being the first time in literature when this kind of measurement was performed in olive fruits. The occurrence of osmotic adjustment in olive fruits under water stress is, most probably, a strategy of the olive trees not to lose the turgor pressure in the fruits and it is a probable explanation to the fast recovery that olive fruits present when irrigation is applied.

Finally, taking into account the findings reported in Chapters 3 and 4, regarding the influence of A_N and $\Delta\Psi_{leaf\text{-}fruit}$ on fruit growth and development, and considering the noteworthy results obtained from the fruit dendrometers, there is great interest on the findings of Chapter 5 regarding the use of fruit dendrometers to assess tree water stress and schedule irrigation. We analyzed the representativeness and usefulness of the same dendrometer derived indexes standardized by (Fernández and Cuevas, 2010) for trunk, used in this PhD. thesis for the daily fruit diameter variations. The findings reported in Chapter 5 are highly relevant as the fruit dendrometer is a useful tool to automatically and continuously monitor changes in fruit diameter and fruit growth, being correlated to the final yield, and it was the first time that fruit dendrometers and its derived indexes were studied aiming at scheduling irrigation. From fruit dendrometers, the maximum fruit diameter (MXFD) was more relevant and representative compared to the other indexes, as it reflects both the accumulated growth trend and the variations of fruit diameter due to irrigation events. When compared to maximum trunk diameter (MXTD) and to LPCP probes maximum output pressure ($P_{p,max}$), the MXFD index revealed that fruits were earlier affected by the beginning of the deficit irrigated period at the 45RDI-1L trees. Also, results from Chapters 4 and 5 together call the attention to the fact that monitoring fruit diameter variations supply much more valuable information than the measurement of $\Delta\Psi_{leaf\text{-}fruit}$ alone.

Additionally, this thesis presents an appendix (Appendix A), which comprehends the first attempt to obtain classification models for the automatic identification of the water state based on the daily curves obtained from the output pressure of the LPCP probes in olive trees.

However, much is yet to be researched, future studies may focus on the flows into and out of olive fruits, and the hydraulic connections between fruits, stem and leaves. It would be interesting to perform studies about the contributions of xylem, phloem and transpiration to olive fruit diameter variations. Future studies may also focus on the direct application of the fruit dendrometer to schedule irrigation, and possibly the study of integrating the losses of water by fruits and leaves, aiming at an alternative way to estimate the whole plant transpiration. The olive fruit osmotic adjustment may

also be of interest, mainly testing other olive cultivars and at different moments along the irrigation season. A lot is still to be studied also about the relative importance of carbon and water flows in growth in general, and specifically on fruit growth. It is interesting to highlight the importance that would have the performance of an experiment with measurements of $\Delta\Psi_{stem\text{-}fruit}$ ($\Delta\Psi_{stem\text{-}fruit}$ = Ψ_{stem} - Ψ_{fruit}) at different times during the day, not only at predawn and midday, but every two hours from predawn to sunset, and at different phenological stages, for different irrigation doses. A daily cycle of $\Delta\Psi_{leaf\text{-}fruit}$ would be interesting to be able to understand what happens between leaves and fruits during the daily expansion and shrinkage processes that olive fruits present (Chapter 4). Additionally, future studies could focus on the information provided by the fruit dendrometers, from the perspective that it could be integrated in increasingly used mechanistic models to schedule irrigation and predict yield for different environmental conditions, management approaches and cultivars. The use of continuously simulated gas exchange with the proposed method of this PhD should be further tested in different species and under a range of management and environmental conditions. However, it seems that the estimation of gas exchange and its use in mechanistic models could help to improve new methods and tools to schedule irrigation and predict yield in the future.

6.1 References

Bustan, Amnon, Avishai Avni, Shimon Lavee, Isaac Zipori, Yelena Yeselson, Arthur A. Schaffer, Joseph Riov, and Arnon Dag (2011). "Role of carbohydrate reserves in yield production of intensively cultivated oil olive (Olea europaea L.) trees". In: *Tree Physiology* 31.5, pp. 519–530. DOI: 10.1093/treephys/tpr036.

Dag, Arnon, Amnon Bustan, Avishai Avni, Isaac Tzipori, Shimon Lavee, and Joseph Riov (2010). "Timing of fruit removal affects concurrent vegetative growth and subsequent return bloom and yield in olive (Olea europaea L.)" In: *Scientia Horticulturae* 123.4, pp. 469–472. DOI: 10.1016/j.scienta.2009.11.014.

Dell'Amico, J., A. Moriana, M. Corell, I.F. F. Girón, D. Morales, A. Torrecillas, F. Moreno, J. Dell'Amico, A. Moriana, M. Corell, I.F. F. Girón, D. Morales, A. Torrecillas, F. Moreno, J. Dell'Amico, A. Moriana, M. Corell, I.F. F. Girón, D. Morales, A. Torrecillas, and F. Moreno (2012). "Low water stress conditions in table olive trees (Olea europaea L.) during pit hardening produced a different response of fruit and leaf water relations". In: *Agricultural Water Management* 114.November 2012, pp. 11–17. DOI: 10.1016/j.agwat.2012.06.004.

Farquhar, G. D., S. von Caemmerer, and J A Berry (1980). "A biochemical model of photosynthetic CO2 assimilation in leaves of C3 species". In: *Planta* 149.1, pp. 78–90. DOI: 10.1007/BF00386231.

Fernández, J.E. and M.V. Cuevas (2010). "Irrigation scheduling from stem diameter variations: A review". In: *Agricultural and Forest Meteorology* 150.2, pp. 135–151. DOI: 10.1016/j.agrformet.2009.11.006.

Fishman, S. and M. Génard (1998). "A biophysical model of fruit growth: simulation of seasonal and dirunal dynamics of mass". In: *Plant, Cell and Environment* 21.8, pp. 739–752. DOI: 10.1046/j.1365-3040.1998.00322.x.

Girón, I.F., M. Corell, A. Galindo, E. Torrecillas, D. Morales, J. Dell'Amico, A. Torrecillas, F. Moreno, and A. Moriana (2015a). "Changes in the physiological response between leaves and fruits during a moderate water stress in table olive trees". In: *Agricultural Water Management* 148, pp. 280–286. DOI: 10.1016/j.agwat.2014.10.024.

Gómez-del-Campo, María (2013). "Summer deficit-irrigation strategies in a hedgerow olive orchard cv. 'Arbequina': effect on fruit characteristics and yield". In: *Irrigation Science* 31.3, pp. 259–269. DOI: 10.1007/s00271-011-0299-8.

Greenspan, Mark D., Hans R. Schultz, and Mark A. Matthews (1996). "Field evaluation of water transport in grape berries during water deficits". In: *Physiologia Plantarum* 97, pp. 55–62.

Gucci, Riccardo, Enrico M. Lodolini, and Hava F. Rapoport (2009). "Water deficit-induced changes in mesocarp cellular processes and the relationship between mesocarp and endocarp during olive fruit development". In: *Tree Physiology* 29.12, pp. 1575–1585. DOI: 10.1093/treephys/tpp086.

Hammami, Sofiene B M, Giacomo Costagli, and Hava F. Rapoport (2013). "Cell and tissue dynamics of olive endocarp sclerification vary according to water availability". In: *Physiologia Plantarum* 149.4, pp. 571–582. DOI: 10.1111/ppl.12097.

Hartmann, H. T. (1949). "Growth of the olive fruit". In: *American Society Horticultural Science* 54, pp. 86–94.

Hernandez-Santana, Virginia, J.E. Fernández, M.V. Cuevas, Alfonso Perez-Martin, and Antonio Diaz-Espejo (2017). "Photosynthetic limitations by water deficit: Effect on fruit and olive oil yield, leaf area and trunk diameter and its potential use to control vegetative growth of super-high density olive orchards". In: *Agricultural Water Management* 184, pp. 9–18. DOI: 10.1016/j.agwat.2016.12.016.

Intrigliolo, D S and J R Castel (2007a). "Crop load affects maximum daily trunk shrinkage of plum trees." In: *Tree physiology* 27.1, pp. 89–96.

Körner, Christian (2015). "Paradigm shift in plant growth control". In: *Current Opinion in Plant Biology* 25, pp. 107–114. DOI: 10.1016/j.pbi.2015.05.003.

Lavee, Shimon (1986). "Olive". In: *Handbook of fruit set and development*. Ed. by S. P. Monselise. 1st. Boca Raton, Florida, USA: CRC Press Inc., pp. 261–276.

Martre, Pierre, Nadia Bertin, Christophe Salon, and Michel Génard (2011). "Modelling the size and composition of fruit, grain and seed by process-based simulation mod-

els". In: *New Phytologist* 191.3, pp. 601–618. DOI: 10.1111/j.1469-8137.2011.03747.x.

Morandi, Brunella, Luigi Manfrini, Marco Zibordi, Massimo Noferini, Giovanni Fiori, and Luca Corelli Grappadelli (2007a). "A Low-cost Device for Accurate and Continuous Measurements of Fruit Diameter". In: *HortScience* 42.6, pp. 1380–1382.

Rallo, Pilar and Hava Rapoport (2001). "Early growth and development of the olive fruit mesocarp". In: *The Journal of Horticultural Science and Biotechnology* 76.4, pp. 408–412. DOI: 10.1080/14620316.2001.11511385.

Rapoport, H. F. (2004). "The effect of water deficit during early fruit development on olive fruit morphogenesis". In: *Journal of the American Society for Horticultural Science* 129.1, pp. 121–127.

Rapoport, H. F., D. Pérez-López, S. B M Hammami, J. Agüera, and A. Moriana (2013). "Fruit pit hardening: Physical measurement during olive fruit growth". In: *Annals of Applied Biology* 163.2, pp. 200–208. DOI: 10.1111/aab.12046.

Tardieu, François, Christine Granier, and Bertrand Muller (2011). "Water deficit and growth. Co-ordinating processes without an orchestrator?" In: *Current Opinion in Plant Biology* 14.3, pp. 283–289. DOI: 10.1016/j.pbi.2011.02.002.

CHAPTER 7 - Conclusions.

- The increment of an extra drip line per tree row influenced positively the root growth closer to the new wetted soil volume, on both root length density (L_v) and root surface area per unit volume (S_v), mainly in the deficit irrigated treatments.
- The greater L_v and S_v values, together with the greater fraction of the soil wetted by irrigation, contributed to a slightly lower water stress levels in the two drip line treatments as compared to the one drip line treatments, especially under the deficit irrigation approaches tested.
- The addition of the second drip line increased the vegetative growth, but no benefit was observed in fruit growth.
- The simulation of the diurnal and seasonal dynamics of stomatal conductance through sap flow related measurements allows the estimation of accumulated photosynthesis, which in turn can be used as a tool to study fruit and vegetative growth in response to water stress.
- The study of water sink relationships between fruits and leaves would benefit greatly from the continuous monitoring of fruit growth, in addition to water potential measurements. As a progressive decoupling of fruit water status from leaves can arise as water stress progresses, the measurement of the water potential gradient alone may not be enough to understand the water relations between fruits and leaves.
- The imbalance in water discharge-refilling processes may lead to a depletion of water reserves in fruit exposed to water stress and accordingly to a net reduction in fruit diameter.
- Fruit osmotic adjustment was confirmed by the data obtained from the pressure-volume curves. Fruits from the deficit irrigated treatment presented greater resistance to lose turgor pressure, in comparison to the full irrigated treatment.
- Fruit growth is the first priority to olive trees under water stress, regarding competition with the vegetative growth for photoassimilates and for water.
- Our results confirmed that olive fruit growth is sensitive to water stress but has a remarkable capacity to recover following a regulated deficit irrigation strategy, as the one employed in this research. With this, and the former conclusion, we confirmed the usefulness of a regulated deficit irrigation strategy to control unwanted vegetative growth without penalizing severely fruit growth.

- Maximum fruit diameter (MXFD) is most probably the best option among the three indexes derived from the fruit dendrometers, as it presents good visual correspondence with the increases and decreases of $\Psi_{l,md}$ and $g_{s,max}$ along the irrigation season. MXFD is also useful as it provides the fruit growing trend.
- For physiological studies, the fruit daily growth (DG_{fruit}) may be of interest, as it possibly presents good correlation to physiological variables, depending on the plant water status.
- Leaf turgor and fruit diameter respond faster to the irrigation events than the trunk diameter when irrigation is performed in a low frequency (2 to 3 times per week).

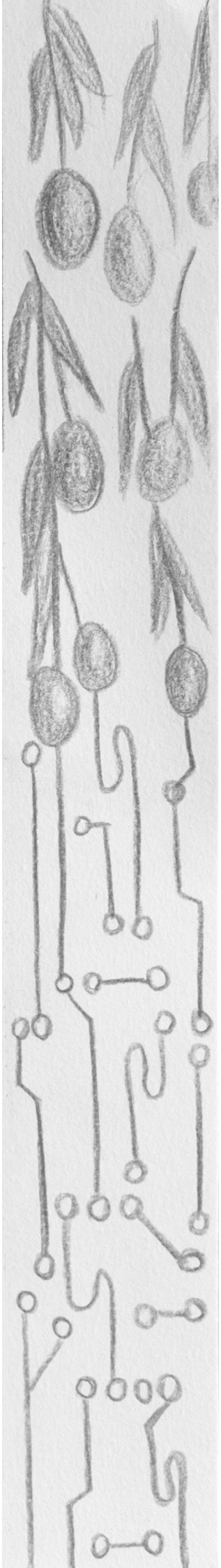

APPENDIX A

Classification models for automatic identification of daily states from leaf turgor related measurements in olive.

Published as: Fernandes, Rafael Dreux Miranda, M.V. Cuevas, V. Hernandez-Santana, C.M. Rodriguez-Dominguez, C.M. Padilla-Díaz, J.E. Fernández (2017). "Classification models for automatic identification of daily states from leaf turgor related measurements in olive.
In: Computers and Electronics in Agriculture 142, pp. 181-189.
DOI: 10.1016/j.compag.2017.09.005

Abstract

The leaf patch clamp pressure (LPCP) probe is being used to remotely assess leaf turgor pressure. Recently, different shapes of the LPCP daily curves have been suggested as potential water stress indicators for irrigation scheduling. These curves shapes, called states, have been studied and related to different water stress levels for olives. To our knowledge, the only way to differentiate these curves shapes or states is through the visual observation of the dynamics of the LPCP records during the day, which is highly time-consuming and reduces its potential to automatically schedule irrigation. The aims of this study were: (i) to obtain a random forest model to automatically identify the states from daily LPCP curves recorded in olive trees, by using visually identified states to train the model; (ii) to improve the identification of state II through a second random forest model, relating this state to the midday stem water potential, and; (iii) to obtain a random forest model to identify the states based on ranges of stem water potential. We used LPCP daily curves collected in a commercial olive orchard from 2011 to 2015. The states were visually identified for the days on which concomitant measurements of stem water potential and leaf stomatal conductance were made. We had a data set of 307 LPCP daily curves, being 157 curves in state I, 78 in state II and 71 in state III. The two biggest inflection points of the LPCP curves were used to adjust the models through the use of the R package "randomForest", using the Leave-p-Out Cross-Validation method. With the first model, which was obtained from the whole dataset, its data regarding the inflection points and the visually identified states, we obtained an overall accuracy of 94.37%. With the second model, obtained with the use of the data regarding curves visually identified as state II only, the overall accuracy was of 88.64%. This model was adjusted to be used after the first model, to narrow the stem water potential range of state II curves. Finally, the third model was obtained using the whole dataset and the states established from ranges of stem water potential. This last model did not consider the visual identification, and yielded an overall accuracy of 88.08%. Our results facilitate the use of LPCP probes, since it allows for the automatic identification of the states related to leaf turgor pressure, a key information to schedule irrigation.

A.1 Introduction

Deficit irrigation (DI) is applied in fruit tree orchards to ensure production in areas with low irrigation water availability. A reliable monitoring of the tree water status has been suggested as an appropriate option to sustainable manage DI strategies. This is definitely necessary in regulated deficit irrigation (RDI), one of the most effective strategies for fruit orchards, in which severe water stress is avoided with enough irrigation

during phases of the growing period sensitive to water stress (Fernández, 2014b), while water supplies are reduced on periods when the crop is less sensitive to drought.

A variety of methods based on plant measurements have been successfully used to monitor water status in olive trees (Cuevas et al., 2013; Fernández et al., 2013; Girón et al., 2015a; Padilla-Díaz et al., 2016), apple and pear trees (**Fernandez2008**), and vineyards (Rüger et al., 2011), among other woody crops. However, the use of these methods is still very limited in commercial orchards, mainly because they are expensive and both their installation and data interpretation require training (Fernández, 2014a). One of these methods relies on the use of the leaf patch clamp pressure (LPCP) probe (Zimmermann et al., 2008). This is a userfriendly method suitable to monitor water stress and to schedule irrigation in commercial orchards (Fernández et al., 2011a; Padilla-Díaz et al., 2016). The LPCP probe contains a miniaturized pressure sensor integrated into a small metal piece. After being clamped in a leaf, the LPCP probe measures the attenuated pressure (P_p) response of the leaf patch upon the application of a constant clamped pressure (P_{clamp}). Values of P_p are inversely proportional to the leaf turgor pressure, P_c (Ehrenberger et al., 2012). A commercial version of the probe, called ZIM probe (YARA ZIM Plant Technology, Hennigsdorf, Germany) uses a magnet, instead of a clamp, to apply P_{clamp} on the leaf.

From the shape of the daily P_p curves recorded with LPCP probes in olive trees under different water status, Fernández et al. (2011a) and Ehrenberger et al. (2012) described three different states, related to the water stress level of the monitored trees: state I accounted for low water stress, state II for moderate water stress, and state III for severe water stress. They both reported that state I corresponded, for olive, to $\Psi_{stem} > 1.2$ MPa (being Ψ_{stem} the midday stem water potential), state II to $1.2 > \Psi_{stem} > 1.7$ MPa and state III to $\Psi_{stem} < 1.7$ MPa. These Ψ_{stem} ranges for States I to III may be different in orchards with different cultivars and locations (Marino et al., 2016). Findings by Fernández et al. (2011a) and Ehrenberger et al. (2012), and a recent work by Padilla-Díaz et al. (2016), confirm that the ranges reported above are valid for 'Arbequina' trees and for our orchard conditions.

Both Fernández et al. (2011a) and Ehrenberger et al. (2012), and also Padilla-Díaz et al. (2016), analyzed the correlation between the state determined from a visual analysis of the daily Pp curves and the stem water potential (Ψ_{stem}) measured with a Scholander-type pressure chamber. Padilla-Díaz et al. (2016) used the biggest data set and found that 68.3% of the trees in state I showed $\Psi_{stem} > 1.2$ MPa and that 81.8% of those days in state III presented $\Psi_{stem} < 1.7$ MPa. However, only 32.8% of the trees in state II days showed values of Ψ_{stem} between 1.2 and 1.7 MPa. Their results agree with findings already stated by Fernández et al. (2011a), in the sense that states I and III are easily defined from a visual analysis of the curves, and that both states are reasonably well correlated to Ψ_{stem}.

The correlation of state II with Ψ_{stem}, however, is low, which could be partly explained by this state being more difficult to be visually identified by the user. A proper identification of state II, however, is important when using the LPCP probes for scheduling irrigation, as it represents a moderate stress level between state I and III. Thus, the appearance of state II may advice for modifying the irrigation dose or irrigation frequency (Fernández et al., 2011a; Padilla-Díaz et al., 2016).

An option to improve the identification of states is to use classification methods usually applied for automatic sensed data. Among them, decision tree classification techniques have substantial advantages for automatically sensed data classification problems because of their flexibility, intuitive simplicity and computational efficiency (Fayyad and Irani, 1992; Hampson and Volper, 1986). Moreover, decision trees are strictly non-parametric and do not require assumptions regarding the distribution of the input data. In addition, decision trees handle nonlinear relations between features and classes, allow missing data and are capable of handling both numeric and categorical inputs in a natural fashion (Fayyad and Irani, 1992; Hampson and Volper, 1986). To improve the prediction accuracy, random forests have been used as a classification method because they are based on a specific algorithm that uses hundreds of decision trees to achieve a better prediction. Thus, we hypothesize that the identification of states from daily P_p curves can be substantially improved using the random forest classification method. Other classification methods imply some assumptions, such as data normality, and some even require that independent variables are identically distributed. The linear discriminant analysis (LDA), support vector machine (SVM) and artificial neural networks (ANNs) could also be used but they imply relevant assumptions and this curtails their applicability.

This work had three main objectives: (i) to adjust a random forest model to automatically identify the daily states from P_p daily curves recorded in a commercial olive orchard; (ii) to improve the identification of state II curves through a second random forest model; and (iii) to adjust a random forest model to identify the states based on Ψ_{stem} ranges only, without any visual identification. We used a large data set of P_p daily curves collected along five years from the olive orchard in which Fernández et al. (2011a) and Padilla-Díaz et al. (2016) worked, and identified characteristic points and tendencies of the P_p variations during the day as predictors to train the model, together with the states visually identified.

A.2 Material and Methods

A.2.1 Experimental orchard and irrigation treatments

Measurements were made by Fernández et al. (2011a) and Padilla-Díaz et al. (2016) in a super-high-density olive orchard (Olea europaea L., cv. Arbequina), located at 25 km

to the southeast of Seville (37° 15′ N, 5° 48′ W). It had trees planted at 4m x 1.5 m (1667 trees ha^{-1}), at the top of 0.4 m high ridges oriented N–NE to S–SW. The annual average precipitation (P) and potential evapotranspiration (ET_o) in the area are 501.2 mm and 1498.1 mm, respectively (period 2002–2016). The olive trees were five years old in 2011, when the experiments started.

In 2011 and 2012 the olive trees were submitted to three irrigation treatments: (i) full irrigation (FI), in which trees were irrigated for the whole irrigation season to replace 100% of the irrigation needs (IN); (ii) 60% regulated deficit irrigation (60RDI), in which the trees were irrigated with 60% of the total IN, varying depending on the phenological phase water requirements, and; (iii) 30% regulated deficit irrigation (30RDI), in which the trees were irrigated with 30% of the total IN, varying depending on the phenological phase water requirements.

From the results of 2011 and 2012, Fernández (2014a) concluded that the best irrigation strategy should be between 30 and 60% of the IN. Therefore, from 2013 there were two treatments: (i) full irrigation (FI), in which trees were daily irrigated for the whole irrigation season to replace 100% of the irrigation needs (IN), and; (ii) a regulated deficit irrigation treatment ($45RDI_{CC}$), in which the total water supplied along the season was aimed to replace 45% of IN. Both treatments were scheduled with the crop coefficient approach (Allen et al., 1998). See Fernández (2014a) for details. In 2014 and 2015, the olives were also submitted to FI and to $45RDI_{CC}$, but in addition we had a $45RDI_{TP}$ treatment, for which we also used the 45RDI strategy but scheduled from leaf turgor pressure related measurements, i.e. from the outputs of LPCP probes. See Padilla-Díaz et al. (2016) for details.

The treatments were distributed in a randomized block design with four 12 m x 16 m plots per treatment. Each plot contained eight central trees surrounded by 24 border trees. All measurements were taken in the central trees of each plot. The irrigation seasons lasted from May until the end of October or mid-November (see next section for details).

A.2.2 Plant water status assessment

During the five experimental irrigation seasons, one leaf per tree from two representative trees in three plots per irrigation treatment (n = 8) were sampled for measurements of midday stem water potential (Ψ_{stem}). The leaves, close to a main branch of tree, were covered with aluminum foil ca. 2h before measurement with the Scholander-type pressure chamber (PMS Instrument Company, Albany, Oregon, USA) at 12.00–13.00 h (GMT). These measurements were taken all along the irrigation seasons (May to October): from DOY 165 to 293 in 2011; from DOY 130 to 292 in 2012; from DOY 133 to 301 in 2013; from DOY 116 to 324 in 2014, and; from DOY 98 to 298 in 2015.

Maximum leaf stomatal conductance ($g_{s,max}$) was measured in one leaf per tree from two representative trees in four plots per irrigation treatment (n = 8). The leaves sampled were the 4th or 5th leaf from the apex of current-year shoots, from the outer part of the canopy, facing S–E at ca. 1.5 m above ground. We used an open flow single pass gas exchange system with a standard 2 x 3 cm chamber (Li-6400, Li-Cor Inc., Lincoln, NE, USA), at 8.00–9.00 h (GMT) which, according to Fernández et al. (1997) is the hour of $g_{s,max}$. The measurements were made in the same days than those of Ψ_{stem}.

The measurements of both Ψ_{stem} and $g_{s,max}$ were performed in trees considered representative of those in each plot in terms of canopy size, leaf area, water status and gas exchange. For both variables (Ψ_{stem} and $g_{s,max}$) the average value of the two leaves was considered.

One tree in three plots per irrigation treatment was monitored with LPCP probes to monitor the state. As mentioned before, the output of these probes was used to schedule irrigation during the 2014 and 2015 irrigation periods. To monitor water status with the LPCP probes, one central tree was chosen, being representative to the plot, regarding size, leaf area, water status and gas exchange. In the chosen trees, a fully expanded leaf was chosen from a current-year branch at an approximate height of 1.5 m above ground at the east side of the canopy. The LPCP probes were installed at DOY 153, 103, 115, 97 and 126 for the years of 2011, 2012, 2013, 2014 and 2015, respectively. In total, there were nine LPCP probes in 2011, 2014 and 2015; eight probes in 2012 and six probes in 2013.

From the irrigation periods of the five experimental years, we obtained 307 P_p daily curves corresponding to the days of concomitant measurements of LPCP probes (P_p), Ψ_{stem} and $g_{s,max}$. The 307 P_p daily curves collected along the five irrigation seasons were observed to identify the state, according to Fernández et al. (2011a) and Ehrenberger et al. (2012). Typical P_p curves for each state are shown in Fig. A.1. As stated by Fernández et al. (2011a) and Ehrenberger et al. (2012), state I corresponds to a P_p curve with maximum values at then central hours of the day and minimum values during the night (Fig. A.1a). State II is characterized by a P_p curve (Fig. A.1b) with a decrease in P_p values by early afternoon and an increase in late afternoon, i.e. with two peaks during the day. This curve is also known as half-inverted curve. And state III is characterized by a fully inverted curve, with higher values during the night and minimum values during the day (Fig. A.1c). To obtain the random forest models we have provided the known state for each day, i.e. the state identified by visual observation of the P_p daily curves. This was necessary because random forest models are obtained through a type of analysis known as supervised classification or supervised machine learning, which requires teaching the model the pattern to be predicted or imitated.

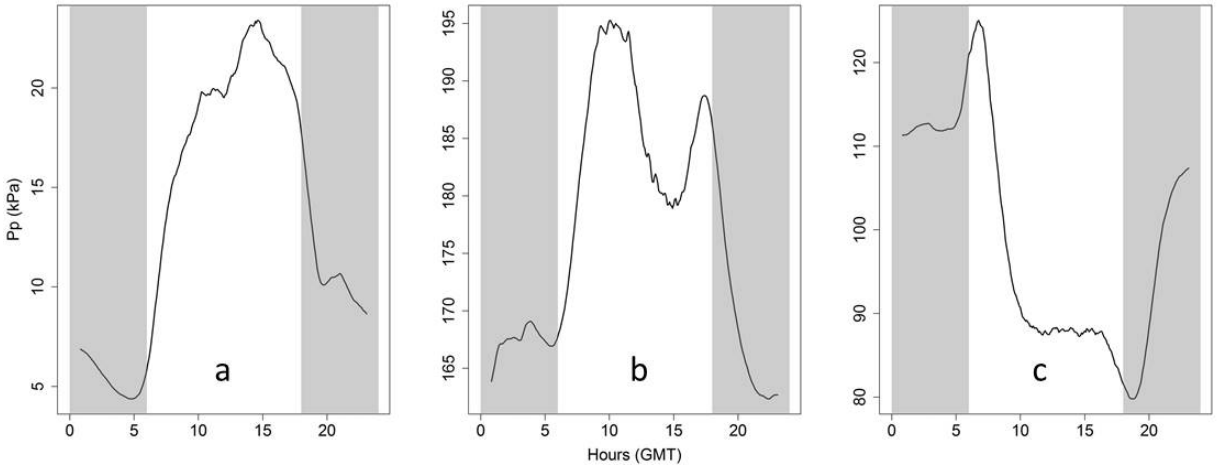

Figure A.1: Typical daily P_p curves for each state: (a) state I (low water stress); (b) state II (moderate water stress) and; (c) state III (severe water stress). The gray areas represent the night. P_p - the output pressure sensed by the LPCP probe, which is inversely proportional to the leaf turgor pressure

A.2.3 P_p daily curves analysis

Through the observance of daily P_p curves for each state, we identified different indicators that could be used to characterize and differentiate the state. These indicators allowed us to derive numbers from the Pp curves, which could be used as predictors of the random forest models. The indicators, represented in Fig. A.2, were: (i) the slope of the linear regression of the values between the maximum and minimum P_p (slope1); (ii) the slope of the linear regression of the P_p values between 16.15 GMT and the end of the day (slope2) which comprehends the afternoon hours when vapor pressure deficit (D_a) decreases and the leaves recover its turgor pressure. This time was established by observing the overall behavior of the curves, in most cases, the change in the slope of the curve corresponding to the last part of the day occurred around that time, and 16.15 GMT was the closest to the actual average value; (iii) the moment of the day when started the biggest fall of P_p value (max1); (iv) the duration of the fall starting at max1 (pmax1); (v) the ratio between the beginning and the end of the fall of P_p values starting at max1 and lasting pmax1 (rat1); (vi) the moment of the day when started the second biggest fall of P_p value (max2); (vii) the duration of the fall starting at max2 (pmax2), and; (viii) ratio between the beginning and the end of the fall on P_p values starting at max2 and lasting pmax2 (rat2).

A.2.4 Statistical analysis

For each day, the data from the LPCP probes were filtered using the moving average method (Wei, 2006), with the use of 20 data points, ten before and ten after, for the calculation of each moving average. For all data mining and statistical procedures the R 3.2.2 (R Core Team, 2015) was used. The R package randomForest (Liaw and Wiener,

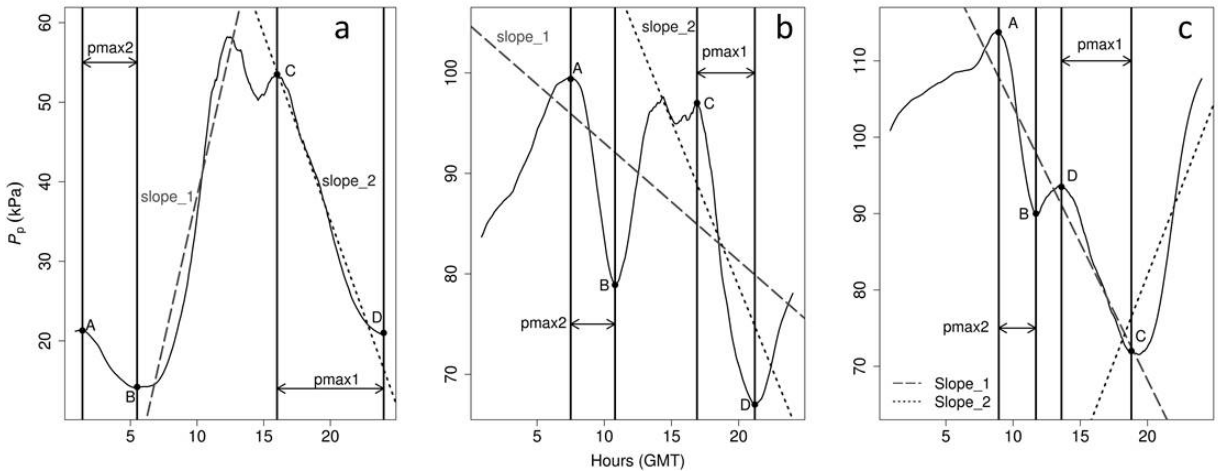

Figure A.2: Graphical representation of predictors for the use in random forest models, as usually seen in state I (a), state II (b) and state III (c) P_p daily curves. The tangents of the dashed and dotted lines represent slope1 and slope2, respectively; points A and C represent the beginning of the inflection ('max'); pmax is the horizontal distance between points A and B and between C and D, and; the ratio between Pp values in A and B and between C and D is 'rat', i.e. the ratio between the P_p value at the beginning and at the end of the inflection. P_p – the output pressure sensed by the LPCP probe, which is inversely proportional to the leaf turgor pressure.

2002) was used to adjust the random forest models, using 1000 trees for each Random Forest model obtained.

To fulfill the three objectives of this study and obtain the best model, the Leave-p-Out Cross Validation method (LpO CV, Arlot and Celisse (2010) and Shao (1993)) was used. This method consists on randomly dividing the data set into three sets (1, 2 and 3), using two of them to obtain a model and the third one to validate it. This procedure was repeated for three times, each with a different pair of sets of data (1 and 2; 2 and 3, and 1 and 3). From the resulting three models we chose the one with the best overall accuracy and tested it against the whole dataset.

The LpO CV was used with all the 307 P_p daily curves, its predictors (Fig. A.2) and the state visually identified, in order to obtain a random forest model capable of identifying the states in an automatic way, as similar to the visual identification as possible. The chosen model in this part will be named as "rf1", to facilitate future explanation of results.

Secondly, the LpO CV was used to adjust a random forest model specifically for the Pp daily curves that were visually identified as state II. Some of these curves presented physiological characteristics (Ψ_{stem} and $g_{s,max}$) typical of state I or III. We wanted to obtain a random forest model able to clearly differentiate state II curves with Ψ_{stem} and $g_{s,max}$ values typical of that state, from the rest of state II curves with Ψ_{stem} and $g_{s,max}$ values normally found in curves of states I or III. For this, the data of state II days was separated into three groups: (i) group II.1 with $\Psi_{stem} > 1.5$ MPa and $g_{s,max} > 0.2$ mol m^{-2} s^{-1}, which physiologically should correspond to state I but were visually identi-

fied as state II; (ii) group II.2 with Ψ_{stem} between 1 and 2 MPa and $g_{s,max}$ between 0.1 and 0.2 mol m^{-2} s^{-1}, which physiologically should correspond to state II and were indeed visually identified as state II, and; (iii) group II.3 with $\Psi_{stem} < 3$ MPa and $g_{s,max} <$ 0.1 mol m^{-2} s^{-1}, which physiologically should correspond to state III but were visually identified as state II. The total data obtained in these three groups were 44 curves, 17 from group II.1, 18 from group II.2 and nine from group II.3. The Ψ_{stem} and $g_{s,max}$ ranges used to split state II were used as a trial to narrow the variety of curves in each group, this is why they are different from the ranges mentioned by Ehrenberger et al. (2012) and Fernández et al. (2011a). The same predictors that were used for rf1 (Fig. A.2) were also used to obtain this random forest model. The model with higher overall accuracy was chosen, being named "rf2". Both rf1 and rf2 were then used together, first rf1 was applied to all the data and following rf2 was applied for the curves predicted as state II by rf1.

Finally, we applied the LpO CV method to the whole dataset, not using the states visually identified but with the states being established as ranges of Ψ_{stem}. The Ψ_{stem} ranges to establish the states were: (i) State I $\Psi_{stem} > 1.2$; (ii) State II Ψ_{stem} between 1.2 and 1.7 MPa, and; (iii) State III $\Psi_{stem} < 1.7$ MPa. For this we used the whole data set of 307 curves, the same used for rf1, using the same predictors as for rf1 and rf2 (Fig. A.2). We obtained 121 curves with Ψ_{stem} in the range characteristic of state I, 67 in the range of state II and 118 in the range of state III. These Ψ_{stem} ranges were used to follow the results and conclusions obtained by Ehrenberger et al. (2012) and Fernández et al. (2011a) as mentioned before. The obtained model was used to predict states for the same data set, and then plotted its Ψ_{stem} and $g_{s,max}$ with different colors for each state. The chosen model will be named "rfp". In Fig. A.3 there is a graphical representation of the rf1, rf2 and rfp models as a workflow of these three random forest models.

From the dataset of physiological variables we have plotted Ψ_{stem} versus $g_{s,max}$ in different symbols according to the state visually identified and predicted both by rf1 and rf2 used together and by rfp. These plots helped us to calculate what we called as percentage of agreement for each model, i.e. how each random forest model was able to match the states and its characteristic Ψ_{stem} ranges (Ehrenberger et al., 2012; Fernández et al., 2011a).

A.3 Results

A.3.1 States and physiological variables

The Ψ_{stem} vs. $g_{s,max}$ values, measured on days with different states visually identified, are shown in Fig. A.4.

From the analysis of the Ψ_{stem} ranges for each state (Fig. A.4) we obtained that 57.3%

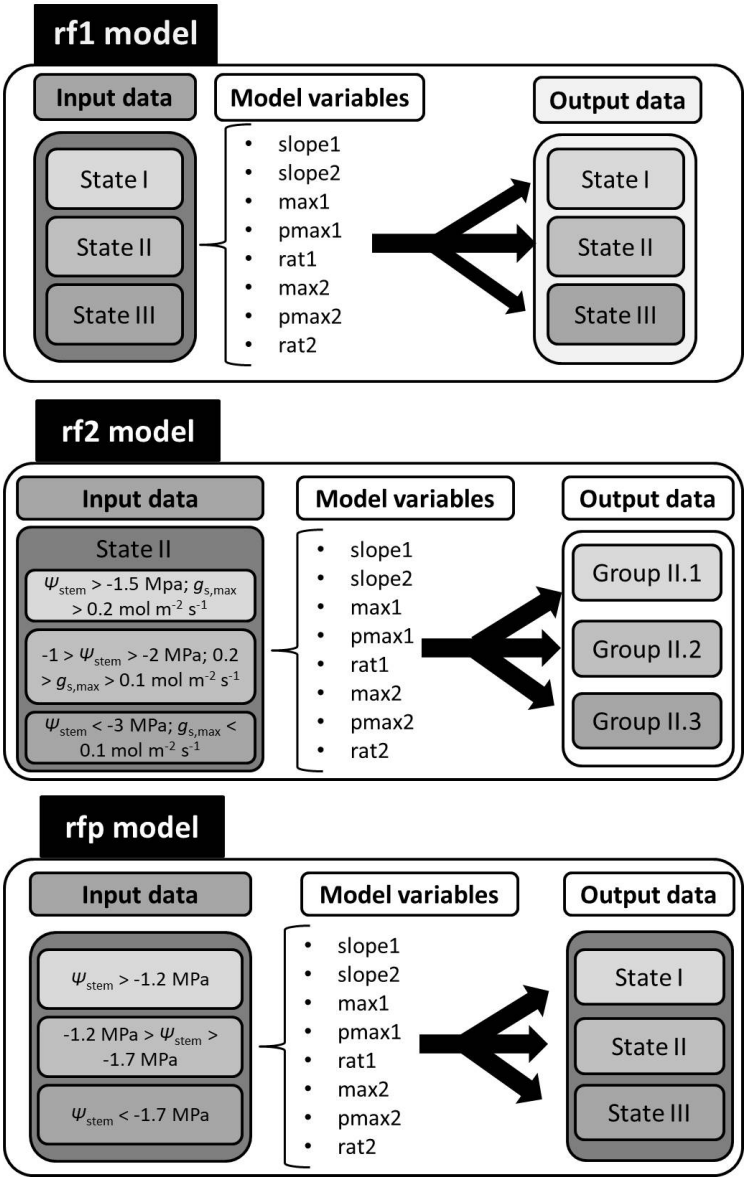

Figure A.3: Representation of the rf1, rf2 and rfp models as workflows. The input data are the data supplied to obtain the model, the output data is the data (states or groups) predicted by each model. Ψ_{stem} – stem water potential; $g_{s,max}$ – maximum leaf stomatal conductance (mol m^{-2} s^{-1}); slope1 – the slope of a linear regression line between the maximum and minimum P_p value of each day; slope2 – the slope of a linear regression line between the P_p values from 16.15 GMT and the end of the day; max1 and max2 – the points where the two biggest inflection points in each day begin; pmax1 and pmax2 – the duration of the inflections which started at max1 and max2 (respectively); rat1 and rat2 – the ratio between the P_p values between the beginning and the end of the inflections starting at max1 and max2 (respectively). Group II.1 constituted by P_p daily curves identified as state II but with physiological values characteristic of state I. Group II.2 is constituted by P_p daily curves identified as state II and with physiological values characteristic of state II curves. And group II.3 is constituted by P_p daily curves identified as state II but with physiological values characteristic of state III curves. P_p – the output pressure sensed by the LPCP probe, which is inversely proportional to the leaf turgor pressure.

of the state I curves correspond to $\Psi_{stem} > 1.2$ MPa, 24.4% of the state II curves correspond to Ψ_{stem} in the range from 1.2 to 1.7 MPa, and 87.3% of the state III curves correspond to $\Psi_{stem} < 1.7$ MPa. The average of these percentages weighted by the number of

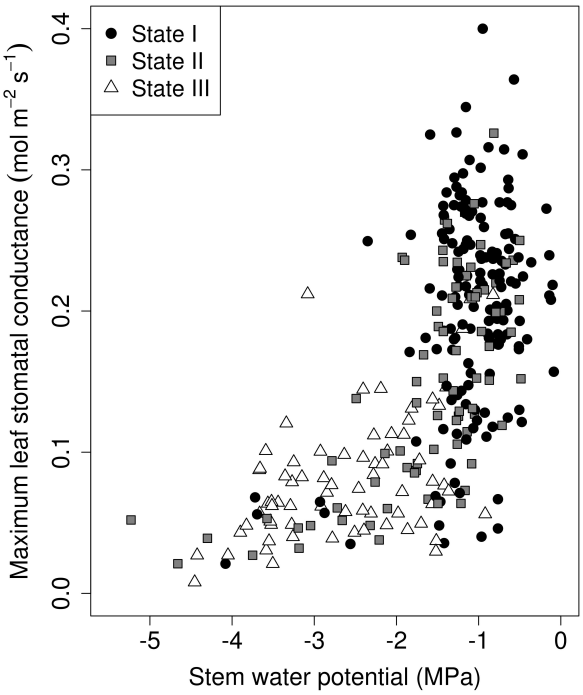

Figure A.4: Scatter plot between stem water potential and maximum leaf stomatal conductance according to the states visually identified through the P_p daily curves. State I curves as black dots, state II as gray squares and state III as white triangles. P_p – the output pressure sensed by the LPCP probe, which is inversely proportional to the leaf turgor pressure.

curves of each state was 55.9%. This number could be considered as an indicator of the accuracy of the states' visual identification.

A.3.2 Random forest model based on visual identification of the states

We used the predictors of the 307 curves and the visual identification of the states to obtain a random forest model (rf1 model) through the LpO CV method. The rf1 model, when used with the whole dataset resulted in the confusion matrix shown in Table A.1.

The rf1 model presented an overall accuracy of 94.4% (Table A.2), with accuracies of 97.4, 92.2, and 89.9% for states I, II and III, respectively (Table A.1). For the three states the rf1 model presented a high accuracy level, approximately 90%.

A.3.3 Random forest model for the state II curves

The confusion matrix of the rf2 model obtained with the data from state II splitted into II.1, II.2 and II.3 groups when tested with the data of the three groups is shown in Table A.3.

The rf2 model presents an overall accuracy of 88.6% (Table A.2), and accuracies of 100, 77.8 and 88.9% for the groups II.1, II.2 and II.3, respectively (Table A.3). It is evident that the model presented better accuracy for the groups II.1 and II.3 than for group II.2.

Table A.1: Confusion matrix and accuracies, for each state, for the rf1 model when tested against the whole data set of the 307 P_p daily curves from the experimental trees. Data in the table show the number of curves in which the state determined through visual analysis (Reference) agreed with the state predicted by the model (Prediction) as well as the number of curves in disagreement between Reference and Prediction.

	Reference		
Prediction	I	II	III
I	152	3	0
II	3	71	7
III	1	3	62
Accuracies	97.4%	92.2%	89.9%

Table A.2: Random forest models' datasets, overall accuracies, error rates and percentages of agreement. In the case of the percentage of agreement shown for model rf2, it was obtained with the joint use of models rf1 and rf2 together.

Model	Dataset	overall accuracy (%)	Error rate (%)	% of agreement
rf1	307 P_p daily curves	94.4	5.6	55.9
rf2	44 P_p daily curves	88.6	11.4	61.9
rfp	307 P_p daily curves	88.1	11.9	84.4

Actually it showed no error for the group II.1 (Table A.3).

The states predicted by rf2 and its corresponding Ψ_{stem} and $g_{s,max}$ values were plotted in Fig. A.5a. We have also applied the rf2 model to all the state II data, regardless of the range of Ψ_{stem} and $g_{s,max}$ (Fig. A.5b).

The data predicted by the rf2 model agreed with the expected results: points from group II.1 corresponds the highest Ψ_{stem} and $g_{s,max}$ values; points from group II.2 were in the central area of the plot and points from group II.3 corresponded to the lowest Ψ_{stem} and $g_{s,max}$ values.

The rf2 model was then applied for the curves identified as state II by the rf1 model (Fig. A.6). Fig. A.6b shows the same data than Fig. A.6a, but after grouping the results from the rf1 and rf2 models, i.e. after considering the points from group II.1 as state I and those from group II.3 as state III. The points from group II.2 are represented as state II.

The use of both rf1 and rf2 (Fig. A.6) enabled a better Ψ_{stem} and $g_{s,max}$ range definition for the three turgor states than the visual identification (Fig. A.3) or the use of rf1 alone. Data from group II.1 and II.3 (predicted by the rf2 model) were close to the ranges of state I and state III, respectively (Fig. A.5a). Most of the data identified as state II by the use of both rf1 and rf2 are in a range of Ψ_{stem} from 1 to 3 MPa, and correspond to $g_{s,max}$ values below 0.2 mol m^{-2} s^{-1} (Fig. A.5b). It is a considerable improvement of the range

Table A.3: Confusion matrix and overall accuracy for the rf2 model. The II.1 to II.3 groups are the groups in which the state II curves were split to obtain the model. A total of 44 curves were considered in the analysis. Data in the table show the number of curves in which the group determined according to the Ψ_{stem} and $g_{s,max}$ values (Reference) agreed with the group predicted by the model (Prediction), as well as the number of curves in disagreement between Reference and Prediction.

	Reference		
Prediction	II.1	II.2	II.3
II.1	17	2	0
II.2	0	14	1
II.3	0	2	8
Accuracies	100%	77.8%	89.9%

of the physiological variables of state II when compared to the visual identification (Fig. A.4).

Through comparison between results from Fig. A.6 (predicted by the rf2 model) and the Ψ_{stem} measurements, we obtained that 56.0% of the state I curves corresponded to $\Psi_{stem} > 1.2$ MPa, 31.4% of the state II curves corresponded to Ψ_{stem} in the range from 1.2 to 1.7 MPa, and 80.9% of the state III curves had $\Psi_{stem} < 1.7$ MPa. Calculating the average of these percentages weighted by the number of curves of each state we obtained an overall percentage of agreement of 61.9%, from the joint use of rf1 and rf2.

It is important to remember that the rf1 model was trained based on the visual identification of the states. The groups used to train rf2 were split according to the Ψ_{stem} of the curves that were visually identified as state II.

A.3.4 Random forest model based on states as Ψ_{stem} ranges

The model obtained by the use the states defined by ranges of Ψ_{stem} (rfp) resulted in the confusion matrix shown in Table A.4. The rfp model presented a better performance for states I and III (90.8 and 95.7%, respectively), than for state II (69.2%).

Fig. A.7 shows the scatter plot between Ψ_{stem} and $g_{s,max}$ with different icons to the states as predicted by the rfp model. As shown in Tables A.2 and A.4, the overall accuracy was 88.1%, with accuracies of 90.8, 69.2 and 95.7% for the states I, II and III, respectively.

The analysis of Fig. A.7 showed that 81.1% of the state I curves correspond to $\Psi_{stem} > 1.2$ MPa, 85.5% of the state II curves correspond to Ψ_{stem} in the range from 1.2 to 1.7 MPa, and 87.4% of the state III curves have $\Psi_{stem} < 1.7$ MPa. Calculating the average of these percentages weighted by the number of curves of each state we obtained 84.4% as an overall percentage of agreement of the rfp model. These percentages of agreement were greater than those obtained by the rf1 model alone (Fig. A.4, Table A.2), and than

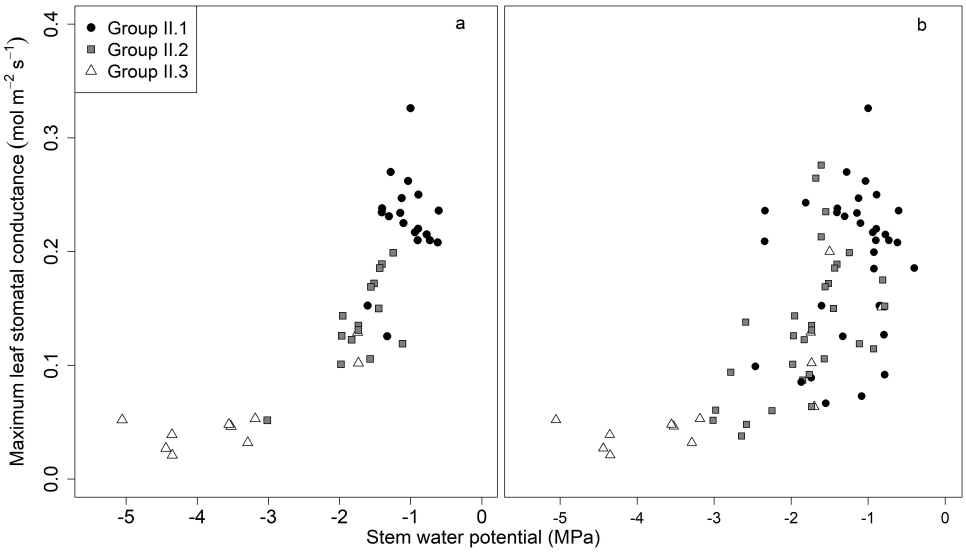

Figure A.5: Scatter plot between stem water potential and maximum leaf stomatal conductance obtained with data predicted by the random forest model trained with the state II data. (a) Regarding the data about the groups II.1, II.2 and II.3; (b) regarding all state II data. Being group II.1 constituted by P_p daily curves identified as state II but with physiological values characteristic of state I (black dots). Group II.2 is constituted by P_p daily curves identified as state II and with physiological values characteristic of state II curves (gray squares). And group II.3 is constituted by P_p daily curves identified as state II but with physiological values characteristic of state III curves (white triangles). P_p – the output pressure sensed by the LPCP probe, which is inversely proportional to the leaf turgor pressure.

Table A.4: Confusion matrix and accuracies for the rfp model. Data in the table show the number of curves in which the state determined according to the Ψ_{stem} values (Reference) agreed with the group predicted by the model (Prediction), as well as the number of curves in disagreement between Reference and Prediction. A total of 307 curves were considered in the analysis.

	Reference		
Prediction	I	II	III
I	109	15	4
II	5	45	1
III	6	5	112
Accuracy	90.8%	69.2%	95.7%

those obtained with the joint use of the rf1 and rf2 models (Fig. A.5b, Table A.2). The percentages of agreement were also better than the ones from the visual analysis of the daily P_p curves (Fig. A.3).

The results obtained by the rfp model helped us to understand how well this model is capable of restricting the range of Ψ_{stem} for each state.

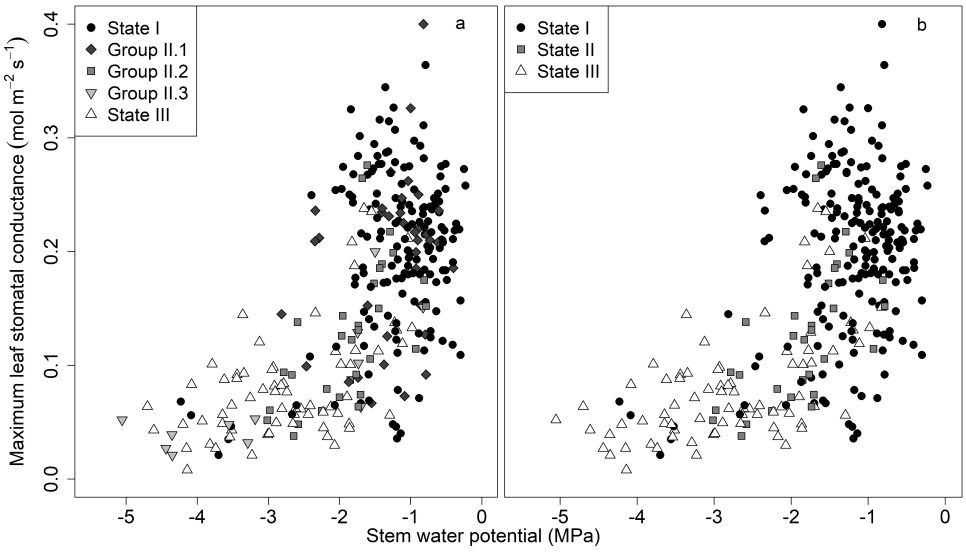

Figure A.6: Stem water potential and maximum leaf stomatal conductance according to the states predicted by the two random forest models (rf1 and rf2): (a) splitting state II into three groups, state I as black dots, group II.1 represented as diamonds, group II.2 as gray squares, group II.3 as gray inverted triangles and state III represented as white triangles; (b) representing group II.1 as state I (black dots), group II.3 as state III (white triangles), and group II.2 as state II (gray squares). Being group II.1 constituted by P_p daily curves identified as state II but with physiological values characteristic of state I curves. Group II.2 is constituted by P_p daily curves identified as state II and with physiological values characteristic of state II curves. And group II.3 is constituted by P_p daily curves identified as state II but with physiological values characteristic of state III curves. P_p – the output pressure sensed by the LPCP probe, which is inversely proportional to the leaf turgor pressure.

A.4 Discussion

The LPCP probes and related system may be useful for both assessing plant water status and scheduling irrigation in an automatic, continuous and remote way. This is based on the close relation between the states and the level of water stress suffered by the instrumented plant. As already mentioned, however, identifying the state of the curve from visual analysis is subjected to uncertainties. In the present study we have obtained random forest models that allow the automatic identification of the state related to the leaf turgor pressure. Our approach therefore, avoid the visual analysis of the daily P_p curves, which reduces time, effort and uncertainties and, consequently, increases the potential for the LPCP probes and related system to be used with the purposes mentioned above.

The results on the visual identification of the states (Fig. A.3) are slightly different from those reported by Padilla-Díaz et al. (2016) regarding the amount of data in the ranges of Ψ_{stem} suggested by Fernández et al. (2011a) and Ehrenberger et al. (2012) for each state (Fig. A.4 and Section 5.3.1). Padilla-Díaz et al. (2016) reported that 68.3, 32.8 and 81.8% of the daily P_p curves identified as states I, II and III (respectively) were in

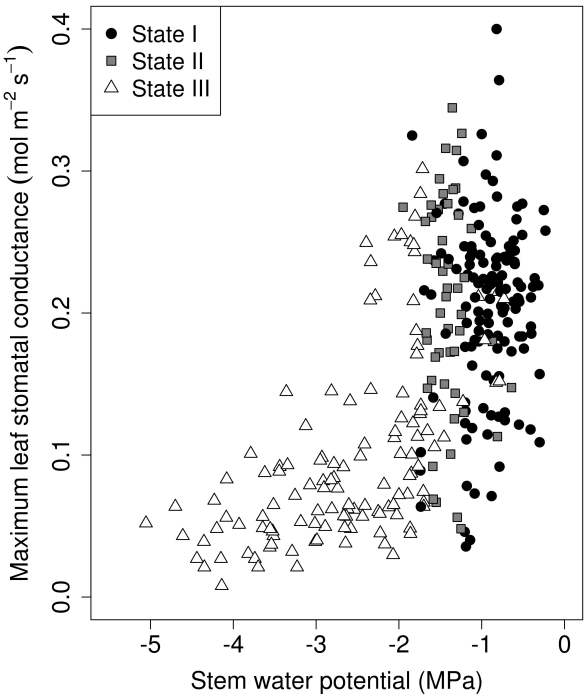

Figure A.7: Stem water potential and maximum leaf stomatal conductance of the states as predicted by rfp model. State I is represented as black dots, state II as gray squares and state III as white triangles.

the corresponding Ψ_{stem} ranges. However, we have obtained 57.3, 24.4 and 87.3% for the states I, II and III (respectively), i.e. lower percentages for states I and II and a higher percentage for state III. These differences found between the present study and the results reported by Padilla-Díaz et al. (2016) are likely due to the period analyzed in each study. We have analyzed data from 2011 through 2015 (including both years), while Padilla-Díaz et al. (2016) considered the 2010–2014 period. The relation found between $g_{s,max}$ and Ψ_{stem} (Fig. A.4) has also been reported by Erel et al. (2014) in olive trees, with a greater range of $g_{s,max}$ when Ψ_{stem} is above 1.5 MPa (approximately) and with a significant decrease when Ψ_{stem} is lower than 1.5 MPa.

The rf1 model, obtained based in the states visually identification, was able to imitate the data from the visual identification, being an automatic and fast way to predict the states, predicting similar results than those obtained by visual identification, with an overall accuracy of 94,4% (Table A.2). Therefore, there was a high correlation between the shape of the Pp curves and the states predicted by the model since it was taught to imitate the visual patterns of the states. It also means that the percentages of data inside the respective Ψ_{stem} ranges would also be predicted by the model, i.e., the low correlation between each state and its Ψ_{stem} range will be reproduced by the model. However, the rf1 model is still an alternative for automatic identification of the states, being faster and more user-friendly than the visual identification.

Differently from rf1, the rf2 model was obtained with the use of only state II Pp daily curves splitted by ranges of Ψ_{stem} and $g_{s,max}$ values. The joint use of rf1 and rf2 increased

in 6% the data from the states in its respective Ψ_{stem} ranges in comparison to the isolated use of rf1 model and also to the visual identification. Therefore, the joint use of both rf1 and rf2 is recommended as a way to obtain an identification of the states with an increased correspondence with the ranges of Ψ_{stem}. It is important to consider that the states predicted by the joint use of the rf1 and rf2 models may not be so correlated to the shape of curves as the use of the rf1 model, as splitting the data into three groups was performed regardless of the shapes of the curves.

The rfp model, as mentioned, was obtained with the states defined by Ψ_{stem} ranges, as suggested by Fernández et al. (2011a) and Ehrenberger et al. (2012). In other words, the rfp model was obtained by trying to get the best relation between the P_p daily curves' predictors and Ψ_{stem} ranges. In contrast to the rf1 model, the rfp model predicts the states differently from the visual identification. The percentage of agreement for the rfp model was 27.1 and 22.5% higher (Table A.2) than the isolated use of rf1 and the joint use of rf1 and rf2 (respectively). It was able to find characteristics of the P_p daily curves' predictors that are related to the ranges of Wstem values correspondent to each state. Thereby, the data predicted by the rfp model does not necessarily correspond to the visual aspects that would be considered in the visual identification; however, it presented the highest percentage of agreement (84.4% – Table A.2) among the states identification models obtained in the present study. Caution must be taken when assessing States I to III from the measured Ψ_{stem} values before using the rf2 and rfp models, since there are evidence on the Ψ_{stem} ranges corresponding to States I to III since being cultivar and location dependent (Fernández et al., 2011a; Marino et al., 2016).

As mentioned, the isolated use of rf1 and rfp models and the joint use of rf1 and rf2 are different approaches to the issue of identifying the states from P_p daily curves. The isolated use of rf1 is recommended when aiming at predicting the states as similar to the visual identification as possible, with a high correspondence between the shapes of P_p daily curves and the predicted states. It is important to consider that the same mistakes or errors that a user would commit will occur in the states predicted by rf1. The joint use of rf1 and rf2 models and the use of the rfp model is recommended when higher importance is given to the relation between the states and Ψ_{stem} ranges. The difference between the joint use of rf1 and rf2 and the use of rfp is that the former identifies state I and III similarly to the visual identification, using the Ψ_{stem} ranges just for the state II identification, however the rfp model uses the Ψ_{stem} ranges for all the states. As a general consideration, all three models (rf1, rf1 + rf2 and rfp) are unbiased mathematical methods to predict the states from P_p daily curves, which are much faster than the visual identification, being able to process big datasets in a matter of seconds.

The random forest methodology was suitable to handle both nonparametric data and data from different ranges of scales. Their capacity to consider a big number of

input variables, as that used in the present study, and the lack of requirements for any assumption on the data distribution, probed to be useful features to shorten and facilitate the data analysis.

A.5 Conclusions

The adjusted rf1 random forest model proved to be reliable for the analysis and automatic identification of the state of daily P_p curves in leaves of olive trees from a super high density orchard A total of 307 curves were considered in the analysis. Moreover, the obtained rf2 model was successful on relating the shape of state II P_p curves and the corresponding Ψ_{stem} and $g_{s,max}$ ranges. Finally, the rfp model trained for the Ψ_{stem} ranges was capable of a robust identification of the state of daily P_p curves. The good performance of the three models was due, to a high extent, to their ability to handle non-parametric and non-normalized data. Despite of being rarely use in plant physiological studies, our findings suggest a great potential of the use of random forest models to better assess plant water stress. The results obtained in this study are relevant for the use of LPCP probes for irrigation scheduling of commercial farms and orchards, since it allows the automatic identification of the state of daily P_p curves. This eliminates the uncertainty derived from the visual analysis of the P_p curves by the user, with automatic data processing a matter of seconds.

A.6 References

Allen, R., L. S. Pereira, D. Raes, and M. Smith (1998). *Crop evapotranspiration - Guidelines for computing crop water requirements*. Rome: FAO Irrigation and Drainage, p. 15.

Arlot, Sylvain and Alain Celisse (2010). "A survey of cross-validation procedures for model selection". In: *Statistics Surveys* 4, pp. 40–79. DOI: 10.1214/09-SS054. arXiv: 0907.4728.

Cuevas, M.V., M.J. Martín-Palomo, Antonio Diaz-Espejo, J.M. Torres-Ruiz, C.M. Rodriguez-Dominguez, A. Perez-Martin, R. Pino-Mejías, and J.E. Fernández (2013). "Assessing water stress in a hedgerow olive orchard from sap flow and trunk diameter measurements". In: *Irrigation Science* 31.4, pp. 729–746. DOI: 10.1007/s00271-012-0357-x.

Ehrenberger, W., S. Rüger, C.M. Rodriguez-Dominguez, Antonio Diaz-Espejo, J.E. Fernández, J. Moreno, D. Zimmermann, V. L. Sukhorukov, and U. Zimmermann (2012). "Leaf patch clamp pressure probe measurements on olive leaves in a nearly turgorless state". In: *Plant Biology* 14.4, pp. 666–674. DOI: 10.1111/j.1438-8677.2011.00545.x.

Fayyad, Usama M. and Keki B. Irani (1992). "On the Handling of Continuous-Valued Attributes in Decision Tree Generation". In: *Machine Learning* 8.1, pp. 87–102. DOI: 10.1023/A:1022638503176.

Fernández, J.E. (2014a). "Plant-based sensing to monitor water stress: Applicability to commercial orchards". In: *Agricultural Water Management* 142, pp. 99–109. DOI: 10.1016/j.agwat.2014.04.017.

— (2014b). "Understanding olive adaptation to abiotic stresses as a tool to increase crop performance". In: *Environmental and Experimental Botany* 103, pp. 158–179. DOI: 10.1016/j.envexpbot.2013.12.003.

Fernández, J.E., F. Moreno, I. F. Girón, and O. M. Blázquez (1997). "Stomatal control of water use in olive tree leaves". In: *Plant and Soil* 190.2, pp. 179–192. DOI: 10.1023/A:1004293026973.

Fernández, J.E., Celia M. Rodriguez-Dominguez, Alfonso Perez-Martin, U. Zimmermann, S. Rüger, M.J. Martín-Palomo, J.M. Torres-Ruiz, M.V. Cuevas, C. Sann, W. Ehrenberger, and Antonio Diaz-Espejo (2011a). "Online-monitoring of tree water stress in a hedgerow olive orchard using the leaf patch clamp pressure probe". In: *Agricultural Water Management* 100.1, pp. 25–35. DOI: 10.1016/j.agwat.2011.08.015.

Fernández, J.E., Alfonso Perez-Martin, José M. Torres-Ruiz, María V. Cuevas, Celia M. Rodriguez-Dominguez, Sheren Elsayed-Farag, Ana Morales-Sillero, José M. García, Virginia Hernandez-Santana, and Antonio Diaz-Espejo (2013). "A regulated deficit irrigation strategy for hedgerow olive orchards with high plant density". In: *Plant and Soil* 372.1-2, pp. 279–295. DOI: 10.1007/s11104-013-1704-2.

Girón, I.F., M. Corell, A. Galindo, E. Torrecillas, D. Morales, J. Dell'Amico, A. Torrecillas, F. Moreno, and A. Moriana (2015a). "Changes in the physiological response between leaves and fruits during a moderate water stress in table olive trees". In: *Agricultural Water Management* 148, pp. 280–286. DOI: 10.1016/j.agwat.2014.10.024.

Hampson, S E and D J Volper (1986). "Linear function neurons: structure and training". In: *Biol Cybern* 53.4, pp. 203–217.

Liaw, Andy and Matthew Wiener (2002). "Classification and Regression by randomForest". In: *R News* 2.3, pp. 18–22.

Marino, Giulia, Fulvio Pernice, Francesco Paolo Marra, and Tiziano Caruso (2016). "Validation of an online system for the continuous monitoring of tree water status for sustainable irrigation managements in olive (Olea europaea L.)" In: *Agricultural Water Management* 177, pp. 298–307. DOI: 10.1016/j.agwat.2016.08.010.

Padilla-Díaz, C.M., Celia M. Rodriguez-Dominguez, Virginia Hernandez-Santana, Alfonso Perez-Martin, and J.E. Fernández (2016). "Scheduling regulated deficit irrigation in a hedgerow olive orchard from leaf turgor pressure related measurements".

In: *Agricultural Water Management* 164, pp. 28–37. DOI: 10.1016/j.agwat.2015.08.002.

R Core Team (2015). *R: A Language and Environment for Statistical Computing*. Vienna, Austria.

Rüger, S., W. Ehrenberger, Ulrich Zimmermann, A. Ben-Gal, N. Agam, and D. Kool (2011). "The leaf patch clamp pressure probe: a new tool for irrigation scheduling and deeper insight into olive drought stress physiology". In: *Acta Horticulturae* 888, pp. 223–230. DOI: 10.17660/ActaHortic.2011.888.25.

Shao, Jun (1993). "Linear Model Selection by Cross-validation". In: *Journal of the American Statistical Association* 88.422, pp. 486–494. DOI: 10.1080/01621459.1993.10476299.

Wei, William Wu-Shyong (2006). *Time Series Analysis - Univariate and Multivariate Methods*. 2nd. Boston: Pearson Addison Wesley, p. 614.

Zimmermann, D., R. Reuss, M. Westhoff, P. Geßner, W. Bauer, E. Bamberg, F. W. Bentrup, and U. Zimmermann (2008). "A novel, non-invasive, online-monitoring, versatile and easy plant-based probe for measuring leaf water status". In: *Journal of Experimental Botany* 59.11, pp. 3157–3167. DOI: 10.1093/jxb/ern171.